Mechanistic investigations of DNA reactive carcinogens at low dose, through analysis of DNA adducts, mutations and DNA repair.

Thomas, Adam David

Mechanistic Investigations Of DNA Reactive Carcinogens At Low Dose, Through Analysis Of DNA Adducts, Mutations And DNA Repair.

Adam David Thomas BSc (Hons).

Submitted to Swansea University in fulfilment of the requirements for the degree of Doctor of Philosophy.

2012

Acknowledgements.

I am indebted to many people for their help and support during my PhD studies. I would like to thank every member of the DNA damage group and my fellow PhD colleagues for creating such a stimulating and encouraging work environment. In particular, Dr James Davies, Dr Elizabeth McAdam and Dr Thomas Cushion, as well as, Mrs Margaret Clatworthy, Dr Shareen Doak and Dr Paul Lewis for their technical proficiency, Professor Gareth Jenkins for continued feedback and energising discussions and my primary supervisor, Dr George Johnson, for my studentship and creating multiple opportunities to further my skills and enhance my research experience. My gratitude is also extended to visiting Professor Anupam Chaterjee for his insightful discussions. I would like to thank committee members of UKEMS (in particular Dr Karen Brown) and EEMS for granting me funding and allowing me to present my work as posters and oral talks at national and international conferences. I am very grateful to Dr Rajinder Singh for sharing his expertise on mass spectrometry, during my time at Leicester University. I am hugely appreciative of the efforts of Professor Bernd Kaina and Mr Karl-Heinz Tomaszowski in our collaboration featured in Chapter 6.

Special thanks are extended to my parents, my brother Allyn and my grams for all that they have done and my girlfriend, Laura for her patience and support throughout, the challenge would have been much greater otherwise.

Summary.

Genetic toxicology assesses the genotoxic potential of chemicals in consumer products, pharmaceuticals and from agricultural and industrial processes. Such assessment is integral in hazard identification and risk assessment to prevent unnecessary human exposure and limit cancer risk. Human risk assessments for genotoxic alkylating agents were based upon linear dose-response models where genotoxicity accrues proportionally with dose. Evidence is accumulating to support a non-linear dose-response at low doses of ethyl methanesulfonate (EMS), a model alkylating agent. For acceptance of non-linear dose responses, a strong explanatory mechanism of action needs to be elucidated. In the following work, low dose mutagenic effects of methyl nitorosurea (MNU), the most potent alkylating agent, have been examined in AHH-1 human lymphoblastoid cells using the HPRT assay. An increase in mutant frequency was not observed until 0.01μg/ml MNU (LOGEL, Lowest Observed Genotoxic Effect Level) with a No-Observed Genotoxic Effect Level (NOGEL) at 0.0075μg/ml MNU. Of interest, is the apparent hormesis induced at 0.0025μg/ml MNU. The principle adduct responsible for MNU mutagenesis is O^6Methylguanine (O^6MeG) that miscodes during replication and becomes fixed as GC→AT transitions. Accordingly, the non-linear increase in mutant frequency is accompanied by a non-linear increase in GC→AT transitions. Furthermore, evidence is provided that implicates methlyguanine methyltransferase (MGMT) in protecting DNA from MNU induced mutagenesis by repairing O^6MeG at low doses, thereby creating the NOGEL. AHH-1 cells treated with O^6Benzylguanine (O^6BG), to inactivate MGMT, were hypersensitive to low dose MNU mutagenesis. At 0.0075μg/ml MNU, there was a three-fold increase in mutant frequency and an increase in proportion of GC→AT transitions, from 28% to 48% in MGMT inactivated cells. This thesis presents a non-linear dose-response for MNU with a strong biological mechanism of action involving DNA repair.

Table of contents

Chapter 2

Chapter 3

Chapter 4

Chapter 5

Chapter 7

Appendices

List of Tables and Figures

Chapter 1

Chapter 2

Chapter 3

Chapter 4

Chapter 5

Chapter 6

Chapter 7

Abbreviations.

MNU-Methyl nitrosourea

ENU-Ethyl nitrosourea

MMS-Methyl methanesulfonate

EMS-Ethyl methanesulfonate

O^6MeG-O^6Methylguanine

N7MeG-N7-Methylguanine

MGMT-Methylguanine methyltransferase

O^6BG-O^6Benzylguanine

MMR-Mismatch repair

DNA-Deoxyribonucleic acid

RNA-Ribonucleic acid

HPRT-Hypoxanthine phosphoribosyltransferase

NO(G)EL-No observed (genotixc) effect level

LO(G)EL-Lowest observed (genotoxic) effect level

BMD-Benchmark dose

Td-Threshold dose

G-Guanine

A-Adenine

C-Cytosine

T-Thymidine

WOE-Weight of evidence

Chapter 1.

General Introduction.

Introduction To Genetic Toxicology.

1.1. The need for genotoxicology testing: chemicals cause mutations, mutations cause cancer.

The deoxyribonucleic acid (DNA) sequence within genes and their arrangement within chromosomes in the genome are often evolutionary conserved. Permanent changes to DNA sequence or structure (mutation) can have catastrophic consequences to the organism or its offspring (if the changes occur in germline cells). Heritable mutations in the germline are required for genetic diversity and evolutionary success of a species. However, mutations in critical genes such as tumour suppressor genes or proto-oncogenes of somatic cells lead to unregulated cell division and cancer (Loeb and Loeb, 2000). Mutations arise through indirect DNA damage (e.g. perturbations in the spindle apparatus during nuclear division) or directly by, for example, unavoidable mistakes by the replication machinery during DNA replication, or induced by pre-mutagenic adducts. Adducts are chemical groups covalently added to nucleophilic centres within cellular macromolecules (e.g. DNA and proteins) by electrophiles. In DNA, adducts can be efficiently repaired. However, replication of unrepaired adducts "fixes" the damage into mutations (Miller and Miller, 1971). Mutations can be grouped into micro-mutations to the sequence of a gene or macro-mutations affecting chromosome structure or number.

1.1.2. Micro-mutations affecting DNA sequence.

There are three classes of mutations that affect the sequence of DNA. These are:

1. **Point mutations**, of which there are three types:
    - *Silent (synonymous)*. Due to the redundancy of the genetic code, a nucleotide, often the third (wobble) base of the triplet codon, can be substituted for another without changing the amino acid and with no consequence to the phenotype.
    - *Missense*. A base is substituted for another that subsequently changes the amino acid upon transcription then eventual translation. If the amino acids have similar chemical properties there may be no effect. Protein function can be altered if a chemically different amino acid is coded for, leading to loss of protein function or gain of an abnormal function either to the benefit or, often, detriment to the cell/organism.

- *Nonsense*. A base substitution that changes the triplet codon to a stop codon leading to a non-functional truncated protein.

2. **Insertions**, The insertion of one or more nucleotides into DNA is often the result of polymerase slippage in repeated sequences (microsatellites), integration of viral genomes or insertion of transposable elements. Frameshift insertions alter the open reading frame (ORF) thereby changing all amino acids in the polypeptide.
3. **Deletions,** deletion of DNA through, for example, exon skipping during mRNA maturation that results in the loss of information for protein translation, could also cause frameshifts resulting in disruption to the ORF.

Gene mutations are well documented as cancer initiating events (Knudson, 1971).

1.1.3. Macro-mutations affecting chromosomes.

Chromosomal mutations can change the ploidy of loci that alters gene dosage. There are two types:

Changes to chromosome number (Aneuploidy). Gain/loss of an entire chromosome. Aneuploidy (the failure of the chromosomes to separate equally into the daughter cells) results from non-disjunction during meiosis in gametocytes and during mitosis in somatic cells. Additionally, exposure to indirect genotoxins (aneugens) disrupts the spindle apparatus leading to improper chromosome segregation resulting in the loss or gain of chromosome in the daughter cell. This imbalance of genetic information is a well-documented cause of reproductive failure (Boué, Boué and Lazer, 1975), cancer (Boveri, 1914) and hereditary genetic defects (Korenberg, 1991) such as Down's syndrome, largely caused by the gain of chromosome 21 (trisomy 21). To regain balance of gene expression, cells modify the epigenome, which may cause dysregulation (Scheid *et al*, 1996).

Changes to chromosome structure. Gain/loss or alteration of fragment of a chromosome. There are many types of structural rearrangements, the most notable being:

- **Deletion**- A portion of the chromosome is lost causing haploinsufficiency at an affected locus, whereby the single, remaining functional allele is insufficient for normal function (**Figure 1.1A**).

- **Duplication**- During mitosis, misaligned homologous chromosomes are at risk of unequal crossover. A chromosomal fragment is removed from one chromosome and given to the other. This duplicates the fragment in the second chromosome (**Figure 1.1B**).
- **Inversion**-A fragment of chromosome is reversed in orientation (**Figure 1.1C**).
- **Translocation**-A portion of a chromosome is exchanged for another. A well-documented mechanism is the reciprocal translocation. This occurs, for example, in formation of the Philadelphia chromosome. Part of chromosome 9 is translocated to chromosome 22, forming a fusion gene (bcr/abl) at the chromosome 22/chromosome 9 junction. This has shown to be a cause of chronic myelogenous leukaemia (Daley, Van Etten and Baltimore, 1990) (**Figure 1.1D**).

Structural aberrations result in a multitude of diseases depending on the genes in the fragment.

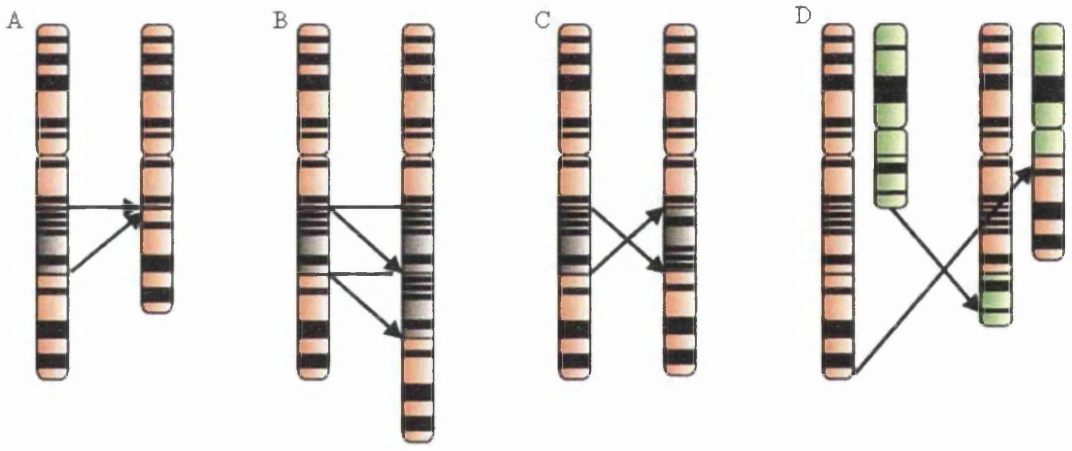

Figure 1.1. Macro-mutations affecting chromosome structure including deletion (A), duplication (B), inversion (C) and translocation (D). Taken from http://www.bioscience.org/2012/v4s/af/302/fulltext.asp?bframe=figures.htm&doi=yes

Point mutations are causal events in tumourigenesis responsible for creating a "mutator phenotype" that has increased propensity for genome instability and cell cycle dysregulation (Loeb, 1991; Shibata and Lieber, 2010; Fox *et al*, 2010). However, it is uncertain whether aneuploidy is a cause or consequence of genome instability and tumorigenesis (Ganem, Storchova and Pellman, 2007). Surprisingly,

Weaver *et al* (2007) note the role of anueploidy as a tumour suppressor. However, aneuploid cells are found in an array of malignancies (Dey, 2004) and was found in 65% of patients with non-small-cell lung cancer (Choma *et al*, 2001).

The realisation that environmental or occupational chemicals cause point mutations and chromosome damage through adducts (Hemminki, 1983) or aneuploidy through perturbation of the cell division machinery, served as the impetus to develop genetic toxicology. This field of study aims to test chemicals for their genotoxic, mutagenic and carcinogenic potential in order to limit human risk (Ames, 1979).

1.2. Genetic toxicology in hazard identification/characterisation.

Genetic toxicology in mammalian cells (*in vitro*) and in animal models (*in vivo*) is used in hazard identification and characterisation. The exposure scenario is then extrapolated to the human condition forming a four-step risk assessment framework detailed below:

1. **Hazard identification.** Identifies the nature of adverse effects through an increase in genotoxic end-points such as DNA lesions, mutation and chromosomal anomalies in genotoxicity assays. Often merged with hazard characterisation.
2. **Hazard characterisation.** Quantifies consequences of exposure (response) to molecular dosimetry in a dose-response relationship, used to inform mechanism and mode of action. This is of importance in the following work and will be discussed further under section 1.3.
3. **Exposure assessment.** Estimates the level of hazard in the external environment through direct measurement of concentration. This can be at the source of exposure and also the internal or biologically effective dose following exposure by determining levels of macromolecular adducts as biomarkers of exposure (this is further detailed in chapter 4).
4. **Risk characterisation**. The summation of all available data to predict likelihood and consequence of human exposure.

Unregulated exposure to known or potential carcinogens represents a significant cancer risk (National Cancer Institute at the U.S. Department of Health and Human Services, 2010). Before the realisation of endogenous damage, exogenous agents were

thought to account for 85% of human cancers (Wood, 1969). Occupational hazards represent a significant risk because workers are exposed to higher than normal levels of hazardous substances for prolonged periods of time. Since the discovery of other carcinogens such as viruses and endogenous processes, Boffetta and Kogevinas (1999) more accurately estimate that occupational exposures account for 13-18% of lung cancers, 2 to 10% of bladder cancers and 2-8% of laryngeal cancers. Early epidemiological observations of exposed individuals highlighted the risk of exposure to hazardous substances. For example, Percivall Pott noted the increase in scrotal cancers in chimney sweeps following exposure to soot in 1775 (Androutsos, 2006). Whereas soot is a complex mixture of chemicals, contemporary studies in hazard identification and characterisation aim to identify carcinogenic potential and mode of action (Sonich-Mullin *et al*, 2001) of each chemical on a case-by-case basis through controlled dosimetry studies in cell culture and animal models. Nevertheless, epidemiology still plays an important part in hazard identification and characterisation (Wogan *et al*, 2004). If available epidemiological and mode of action data (EPA, 2005) suggest that exposure to a certain chemical will increase incidence of human cancer, it is categorised by the International Agency for Research on Cancer (IARC) as group 1-carcinogenic to humans. Other categories are:

- Group 2A-Probably carcinogenic to humans
- Group 2B-Possibly carcinogenic to humans
- Group 3-Not classifiable as to its carcinogenicity to humans
- Group 4-Probably not carcinogenic to humans

IARC's monographs are used here as an example, monographs published by other agencies exist and their robustness can be debated (Dr Paul Fowler, personal communication). These monographs detail the risk of a variety of chemicals including those in pesticides, diet, lifestyle factors (smoking and tanning devices), pharmaceuticals, general environment (plant extracts) and industry as well as the carcinogenicity of viruses (Hepatitis B virus, group 1), bacteria (*Helicobacter pylori*, group 1), radiation (Gamma, group 1) and surgical implants (cardiac pacemakers, group 3). With legislative action, exposure to group 1 carcinogens can be limited to better public health. Such exposure limitation is crucial in preventing an increase cancer risk over the pre-existing, natural level of cancer incidence.

1.3. Hazard identification and characterisation.

Hazard identification and characterisation requires *in vitro* bacterial and mammalian cell based assays and *in vivo* studies to assess genotoxicity, and 2-year bioassays in animal models to assess carcinogenicity. The following work discusses genotoxicity tests and so carcinogenicity bioassays will not be considered. Carcinogens cause cancer through either direct DNA interaction (genotoxins e.g. alkylating agents) or through interaction with other cellular components via a non-genotoxic mode of action (MOA). Aneugens and topoisomerase inhibitors are the exception as they are *indirect* genotoxins because they cause mutations (aneuploidy and double strand breaks, respectively) through interaction with the DNA replication machinery and not directly with DNA. It is understood that aneugens have an adverse effect threshold, whereby a sufficiently high concentration of chemical is needed to cause adverse effects (Kirsch-Volders, Aardema and Elhajouji, 2000) this is further discussed under section 1.5.4.1. Genotoxins, however, are thought not to have a threshold and are damaging at low levels, although this is under contention (Jenkins *et al*, 2005; Doak *et al*, 2007; Gocke and Muller, 2009). Therefore, distinguishing the mode of carcinogenic action has important implications in risk assessment. A number of genotoxicity assays are employed to distinguish MOA as genotoxic or non-genotoxic by assessment of numerous endpoints:

1. **DNA adducts** through highly sensitive physical chemistry methods like mass spectrometry (positive for DNA reactive genotoxins)
2. **Point mutations** that cause loss of function of an easily assayable protein (positive for mutagens)
3. **Aberrations in chromosomal structure** as examined under microscopy (positive for clastogens and agents with other MOA such as cytostatic drugs)
4. **Changes in chromosome number** under fluorescence microscopy using pan centromeric probes (positive for aneugens such as nocodazole)

A positive result is defined as a statistically significant increase in endpoint over respective solvent control. If all endpoints are negative it is assumed that the carcinogen is not genotoxic but causes cancer by other methods such as increased cell proliferation in hormone-induced carcinogenesis (Liehr, 2000a). However, in this instance, caution is urged as the chemical may show tissue specificity or require metabolic activation into a mutagenic product before genotoxicity can be seen.

1.4. Regulatory genotoxicity.

Specific guidelines are used in genotoxicity testing to ensure the standardisation of assay methodology. During drug development, pharmaceutical companies adhere to guidelines proposed by the International Conference on Harmonisation of Technical Requirements for Registration of Pharmaceuticals for Human Use (ICH). Their mission statement is "to achieve greater harmonisation to ensure that safe, effective, and high quality medicines are developed and registered in the most resource-efficient manner." Genotoxicity testing for other purposes, such as the regulation of food by European Food Standards Agency (EFSA), consults strategy documents (e.g. COM, 2011) proposed by Committee of Mutagenicity in Food, Consumer Products and the Environment. This advisory panel of experts from scientific societies reference guidelines from the Organisation for Economic Cooperation and Development (OECD) for well-established and validated genotoxicity tests. Genotoxicity assays performed at Swansea University adhere and contribute to these guidelines for inter-laboratory comparisons (Johnson *et al*, 2010) necessary for the global standardisation of assays.

1.4.1. Regulatory genotoxicity testing strategies.

There is a general consensus that the strategy for testing consists of stage 1; basic *in vitro* genotoxicity tests and stage 2 follow up *in vivo* genotoxicity tests on equivocal or positive stage 1 findings (COM, 2000). COM 2011 guidelines also state a stage 0. This involves prior consideration of physico-chemical properties of the test chemical with emphasis on solvent/vehicle interactions (Fischer *et al*, 2008), solubility, stability and volatility as well as consideration for possible artifactual positive results through cell stress by pH changes in cell culture media. For the assessment of genotoxic impurities, recent validations permit the *in silico* evaluation of quantitative structure activity relationships (QSAR) (Benigni and Bossa *et al*, 2008). Designated as computational toxiocology, programs like DEREK (Cariello *et al*, 2002) are used to identify structural moieties responsible for the chemical's mutagenicity (Ashby and Paton, 1993). COM 2011 also recommends the use of high throughput pre-screens such as GADD45-GFP assay (Walmsley, 2008).

1.4.2. Stage 1; a battery of *in vitro* genotoxicity tests.

A number of OECD validated *in vitro* assays are available, with debate as to the most suitable (Kirkland *et al*, 2005). Since there are a number of genotoxic endpoints that need to be assessed, a battery of assays is required. Due to the research by Kirkland *et al* (2005), the guidelines recommend that a battery of two "core" assays are used to detect mutagenicity, clastogenicity and aneugenicity. The authors found that sensitivity and predictability of three commonly used assays (Ames, *in vitro* micronucleus assay (MNvit) and chromosome aberration) were highest when used in combination to identify rodent carcinogens. Although, the assays had poor specificity; the rate of false positives (known non-carcinogens to be wrongly classified as positive genotoxins) was high (75-95%). Addition of more assays to the battery reduced specificity and caused more misleading false positives. COM 2011 suggests the use of Ames in combination with MNvit, since MNvit (coupled with kinetochore staining) can more accurately detect aneuploidy than chromosome aberration tests (Lorge *et al*, 2007). Of relevance to this thesis is the hypoxanthine phosphoribosyltransferase (HPRT) gene mutation assay (chapter 3), which is used as a stage 1 test to assess a chemical's ability to cause small DNA sequence changes, predominantly point mutations. The HPRT assay can also be used as an *in vivo* mutation sensor. According to OECD, for full evaluation, the tests should be performed under a variety of exposure concentrations and times and in the absence and presence of metabolic activating enzymes provided by rat liver extracts, S9, to identify any mutagenic products. However, S9 is a potent inducer of mutagenic reactive oxygen species (ROS). Tweats *et al* (2007) identified a number of chemicals positive *in vivo* but not *in vitro*. Although the majority of chemicals show the same response, meaning that *in vitro* models are highly predictive of *in vivo* genotoxicity (Tennant, 1987). If stage 1 negative results agree with published literature and QSAR analysis, the chemical is considered not mutagenic, only requiring *in vivo* testing if prolonged human exposure is anticipated. Positive results in any stage 1 assay are further investigated in stage 2 *in vivo* tests although the biological relevance of *in vitro* positives must be considered before stage 2 tests are performed (Kirkland and Muller, 2000).

1.4.3. Stage 2: *in vivo* testing.

Stage 2 evaluates *in vivo* genotoxicity of a given chemical that shows *in vitro* genotoxicity in stage 1. This includes; germ cell genotoxicity for heritable genetic effects, site of exposure genotoxicity and tissue specificity. Testing strategy is decided on a case-by-case basis, depending on, for example, the genotoxic mode of action identified in stage 1 and SAR information (Thybaud *et al*, 2007). COM (2011) recommends the use of three assays. These being; rodent bone marrow chromosome aberration assay for clastogenicity, transgenic rodent mutation (TGR) assay for gene mutations and a rodent comet assay able to detect a wide range of low level DNA damage such as strand breaks, cross links and repair induced alkali labile sites. A small number of positive *in vitro* mutagens are negative *in vivo*. The question exists as to whether it is a false (*in vitro*) positive or true (*in vivo*) negative. A lack of absorption, rapid elimination or detoxification *in vivo* (true negative) or physiologically irrelevant testing conditions *in vitro* (false positive) could cause this disparity. Distinguishing false positives, due to non-physiological conditions *in vitro*, from true *in vivo* negatives relies on a WOE approach (Kirkland *et al*, 2005; Kirkland *et al*, 2007) often requiring more animal tests. The complete process is shown in **Figure 1.2**.

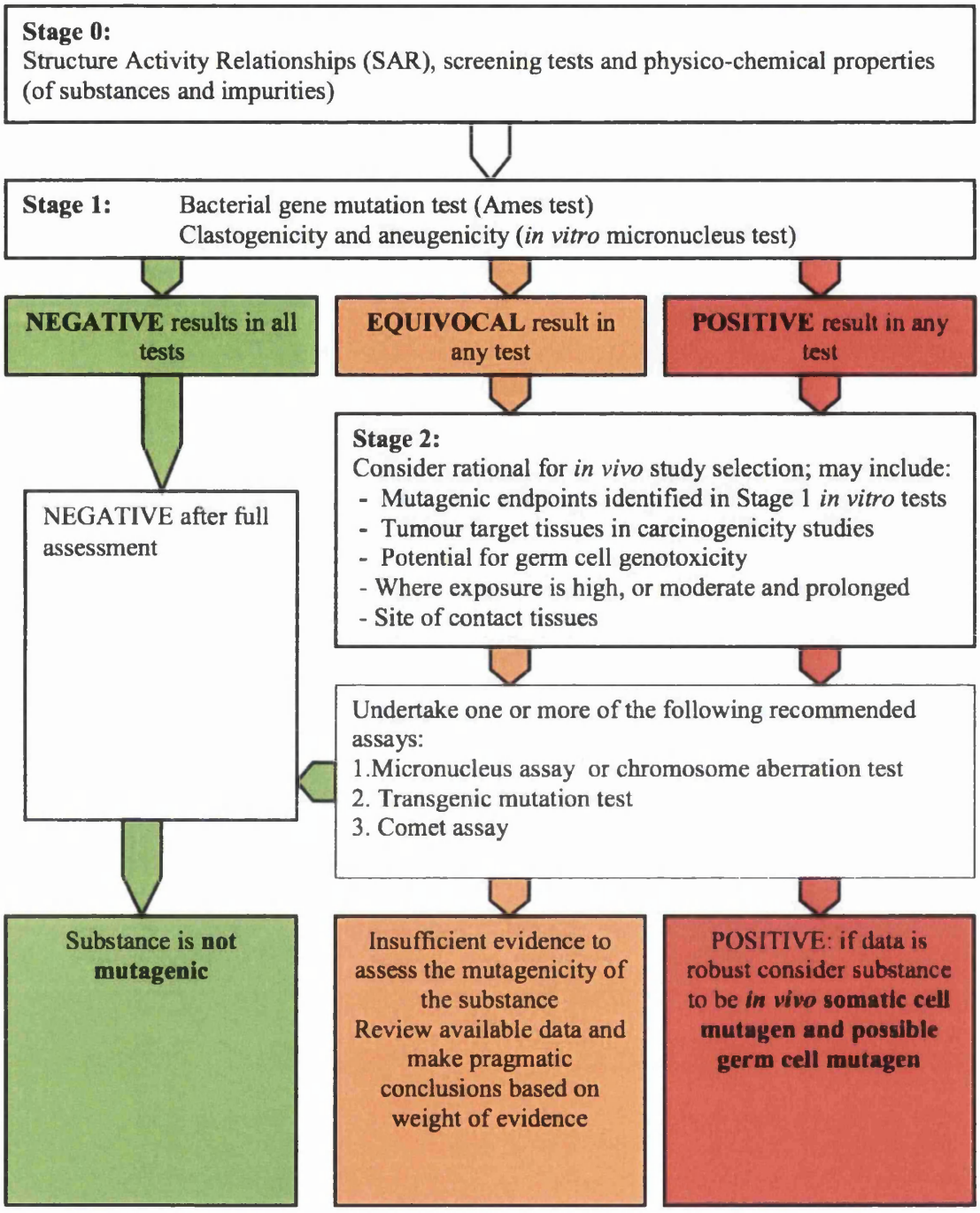

Figure 1.2. The process of current genotoxicity testing to identify and characterise chemical hazards. Image taken from COM (2011).

1.4.4. Reduce, refine and replace animal usage in genotoxicology.

The use of animals in genotoxicity testing is contentious. The European Union (EU) 7th Amendment to the Cosmetics Directive in March 2009 banned the testing of

cosmetics on animals in the EU, so efforts are in place to improve *in vitro* tests to reduce, refine and replace animals in research. Increasing the reliability of *in vitro* methods would reduce the high level of false positives and reduce the need for stage 2 follow up testing in animals. Cosmetics Europe, formerly the EU Cosmetics Association (COLIPA), has funded research into improving *in vitro* methodology to reduce false positive results. Sources of false positives were highlighted by Kirkland *et al* (2007) and Blakey *et al* (2008) which included; unstable or sensitive (e.g. p53 deficient) mammalian cell lines; CHO, CHL and V79 (Pfuhler *et al*, 2011; Fowler *et al*, 2012a), unnecessarily high (10mM, OECD) top concentrations (Kirkland and Fowler, 2010) and cytotoxicity assessment methods (relative population doubling (RPD), relative increase in cell counts (RICC), relative cell counts (RCC), and cytokinesis-blocked proliferation index (CBPI)) that underestimate toxicity leading to selection of an unnecessarily high LD_{50}, a dose to give 50% toxicity, that subsequently gives misleading positive genotoxicity data (Johnson *et al*, 2010; Whitwell *et al*, 2010; Fowler *et al*, 2012). Another avenue of COLIPA funded research is to develop other *in vitro* assays (Pfuhler *et al*, 2010) such as the development of the Epiderm™ 3D human skin based micronucleus assay (Aardema *et al*, 2010). The advantage of such assays, over existing *in vitro* assays, is that the route of exposure is considered. Reader is directed to www.alttox.org for further information.

1.4.5. *In vitro* to *in vivo*, high dose to low dose and animal to human extrapolation.

Predicting the genotoxic and carcinogenic response in humans relies on cell culture and animal models. Therefore, risk assessment relies on inter-species extrapolation. Extrapolating risk from inbred laboratory animals to a genetically diverse human population is difficult as some individuals are more susceptible than others. Genetic polymorphisms in genes encoding phase I and phase II metabolic enzymes involved in absorption, distribution, metabolism and excretion of carcinogens coupled with variations in dietary detoxifying agents have been shown to alter individual cancer risk (Ratnasinghe *et al*, 2000). These unknowns exist due to a deficiency in data and are known as uncertainty factors (UF) (WHO, 2001; IGHRC, 2003). UF's introduce a

10- to 100-fold safety margin around a "safe dose" of chemical (Lehman and Fitzhugh, 1953). Obtaining a "safe dose" requires extrapolation from high doses, which are required to achieve a statistically significant increase in measured endpoint over background levels. Methods of extrapolation depend on genotoxic potency of the given carcinogen (Bolt *et al*, 2004). Non-genotoxic carcinogens and those observing thresholds (aneugens, discussed later under section 1.5.5.1) are perceived as less potent than direct genotoxins (Perera, 1991). For non-genotoxic carcinogens, animal carcinogenicity assays determine a threshold dose at which no adverse effects are seen, i.e. there is no increase in tumours at a particular dose of carcinogen. No observed effect level NOEL, or the more robust, benchmark dose (BMD) models are used to extrapolate this dose to a lower level applicable to human exposure (Guess, Crump and Peto, 1977). On the other hand, genotoxic carcinogens are perceived to be mutagenic at all doses. Therefore, without evidence of a threshold, it is precautionary to assume a linear extrapolation from high to low doses (USEPA, 2000). This assumption of low dose linearity is challenged in this thesis and will be discussed under section 1.5.5.2. Under a linear hypothesis, the mathematical models used to determine a safe level are more cautionary (Bolt, 2004). Models include threshold of toxicological concern (TTC) or a more conservative risk assessment; as low as reasonably practicable (ALARP), to limit the concentration of chemical to as low as reasonably possible. The reader is referred to Muller *et al* (2009) for an example of risk assessment of likely exposure to the genotoxic impurity, ethyl methanesulfonate (EMS), in Viracept®. It can be said that *in vivo* studies are useful for dose extrapolations to humans. However, dosage extrapolations from *in vitro* toxicology are seldom used (Bernauer *et al*, 2005). Recently, there is interest in *in vitro* (and *in vivo*) dose-response relationships at *low* doses to establish potency (Pottenger and Gollapudi, 2009) and biological relevance (Kirkland and Muller, 2000) at low dose, mechanism of action and to better inform risk assessments if linear high dose to low dose extrapolation is assumed correctly for genotoxins (Lutz, 1990).

1.5. Dose-response relationships for genotoxicity.

The dose-response quantifies a given genotoxic endpoint at increasing doses of chemical, thus giving an idea of potency. The shape of the dose-response has implications in safety assessment. A variety of dose-response models are postulated for different genotoxic endpoints (Lutz, 1990).

These are:

1. Supralinear and Sublinear
2. J-shaped
3. Linear
4. Threshold

Each model is shown in **Figure 1.3**. It may be imprudent to assume a linear extrapolation from high to low doses (Lutz, 1998) if an alternative dose-response can be sufficiently supported. Each dose-response will be explained in turn with emphasis on J-shaped, linear and threshold.

A).

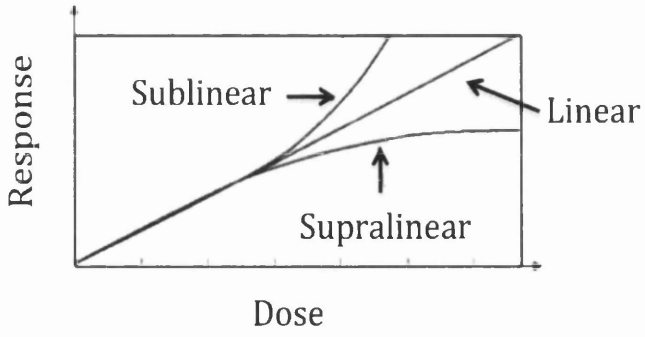

B).

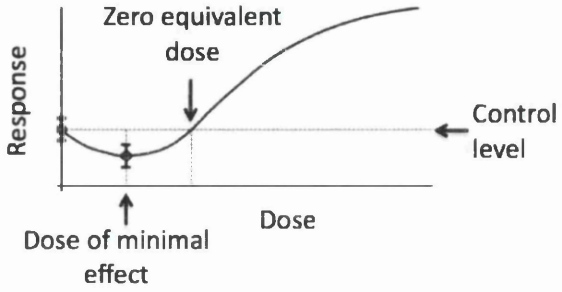

C).

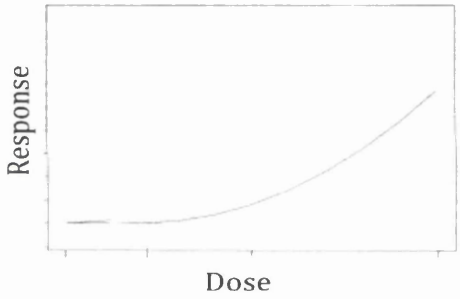

Figure 1.3. Theoretical dose-response models. (A) Sublinear, linear and supralinear taken from Swenberg *et al* (2008). (B) Hormesis/J-shaped model taken from Gaylor, Lutz and Connolly (2004). (C) Threshold dose-response taken from Lovell (2000).

1.5.1. Supralinear and sublinear dose responses.

Supralinearity and sublinearity occur towards higher doses of chemical, with linearity assumed at low doses. These models have been shown for various DNA adducts (Swenberg *et al*, 1987). A supralinear dose-response can be explained by saturation of metabolic enzymes necessary for pro-carcinogen activation into a DNA reactive electrophile, capable of adduct formation. This would limit activated carcinogen and as a result would limit adduct formation. For example, a supralinear dose-response was observed for O^6-methylguanine (O^6MeG) adducts present in DNA of rodent respiratory mucosa following increasing doses of tobacco-specific, 4-

(methylnitrosamino)-1-(3-pyridyl)-1-butanone (NNK). Higher concentrations were less effective at causing O^6MeG adducts (Swenberg *et al*, 1995). Although, it could be postulated that repair of adducts at these concentrations is upregulated and improves the removal of adducts, this hypothesis has yet to be substantiated. At higher concentrations, the effect of toxicity cannot be ignored. Cell death is an effective way of removing heavily damaged and mutated cells from the population and could account for a plateau in dose-response. Sublinear dose-responses, in contrast, show disproportionally higher potency for adduct and mutation at higher doses. This is hypothesised to occur following saturation of protective mechanisms such as detoxification and DNA repair. Sublinearity has been shown for DNA-protein cross links following increasing concentrations of formaldehyde, the result of intracellular glutathione depletion (Casanova *et al*, 1987). Mutations have been hypothesised to show sublinearity due to increased adduct fixation caused by regenerative hyperplasia (increased cell division following neighbouring cell death) in response to cytotoxic doses of genotoxin (Lutz, 1990).

1.5.2. J-shaped dose-response.

The J-shaped relationship is an example of hormesis, a biphasic dose-response ubiquitous in biomedical literature (Calabrese, 2006). In most instances, hormesis refers to an inverted-U shaped dose-response, depicting low dose stimulation and high dose inhibition of for example, growth or cell proliferation. In toxicology, hormesis is illustrated by a J-shaped curve, referring to "low dose reduction and high dose enhancement" of endpoint such as cancer incidence (Calabrese, 2009), which may reflect low dose stimulation and high dose inhibition of cytoprotective mechanisms. Hormesis states that low doses of substances can be beneficial. Rozman (2005) insists that *all* substances are beneficial at low doses. The hormesis hypothesis was used to explain low dose stimulatory effects on cell division following radiation exposure in algae as early as 1898. Since then, evidence of radiation hormesis has accumulated (Calabrese and Baldwin, 2000). However, stimulatory effects were not reproducible or considered true, but the result of overcompensation following insult (Calabrese, 2005). Further criticism came from prominent statisticians, including R.A. Fischer, who dismissed hormetic effects as variation in data. Many US regulatory bodies

maintain that radiation hormesis has not been proven in humans. As a result, the hormetic dose-response was overlooked in favour of linear models (Calabrese, 2009). Recently, robust data showing hormesis, has increased interest in its predictability of low dose effects in toxicology. Calabrese and Baldwin (2001) report that citations of hormesis have increased from 1 in 1945-1954 to 485 citations in 1995-2004 with publications in respected scientific journals including Nature (Calabrese, 2004) and Science (Kaiser, 2003). Publications by US department of agriculture (USDA) refer to hormesis and have incorporated the model into risk assessments but not for human health. Calabrese (2006; 2007), Scott (2008) and Tubiana *et al* (2009) suggest that hormesis better predicts low dose effects than threshold and linear models, particularly for radiation exposure. For chemical agents, the hormetic concept has been described for many carcinogenic endpoints such as tumour incidence, glutathione *S*-transferase (GST-P) hepatic foci and bladder hyperplasia (Calabrese, 2005) and for many non-genotoxic carcinogens including phenobarbitol, a tumour promoter that inhibited tumour promotion in low concentration (Kinoshita *et al*, 2003). A report by Calabrese and Baldwin (2001) showed that 1600 dose-response relationships for toxicity endpoints displayed hormesis in microbial, plant and animal systems. Hormesis has also been observed for genotoxicity endpoints in response to direct acting genotoxins such as MNNG. Conolly and Lutz (2004) proposed a mechanism to explain hormesis for adducts. They postulate that exogenous adducts formed from exposure to genotoxin, can activate or upregulate expression of genes whose products remove endogenously and exogenously generated adducts. The authors also postulate that low dose genotoxin causes a low level of adducts that slow cell cycle progression allowing sufficient time for repair. Both mechanisms support low dose linearity that is well accepted for exogenous adducts (Zito, 2001; Swenberg *et al,* 2008). Calabrese and Baldwin (2001) recognise that hormesis is dependent on time, as time increases the hormetic effect becomes more pronounced, potentially owing to the time to upregulate DNA repair proteins. Since changes to the DNA repair transcriptome are rapid, we can hypothesise that hormesis would be evident by 24 hours (Sandrini *et al*, 2009). Analogies have been made between hormesis and the adaptive response to environmental changes, which has been a long known event in bacteria in response to alkylating agents which relies on upregulation of DNA repair enzymes through expression of inducible promoters (Lindahl *et al*, 1988). The adaptive response "pre-conditions" the cell to better withstand higher doses in future

exposures (Calabrese *et al*, 2009) and so hormesis may be more evident in chronic exposures and repeated dosing regimes.

1.5.3. Linear dose-response.

As previously mentioned, regulatory bodies favoured the linear (no threshold) model as a default prediction of low dose adverse effects in response to genotoxic carcinogens. One of the advantages of the linear model was that it could be generally applied to all chemical and physical genotoxins, however, it does not apply to aneugens or non-genotoxic carcinogens (Calabrese, 2009). The "additivity to background" hypothesis (Crump *et al*, 1976) gave justification for this assumption of linear low dose extrapolation. It states that if a carcinogen adds to a naturally occurring carcinogenic process, responsible for spontaneous tumour incidence, then only linearity could be accepted. Considering that DNA damage is unavoidable (Gupta and Lutz, 1999), exposure to exogenous genotoxins would add to the already formed damage. Therefore, all genotoxins, until recent publications, were assumed to be linear. This assumption was substantiated by the "single hit-single target" theory based on historical work with ionising radiation (UNSCEAR, United Nations Scientific Committee on the Effects of Atomic Radiation, 1958). The theory supposes that a single hit (damage) to DNA is sufficient to cause a mutation and subsequently cancer (Knudson, 1971). It is now known that not all DNA damage is fixed as mutations (Swenberg *et al*, 2008). However, there are some instances where mutagenicity is proportional to DNA damage induced in cases of poor adduct repair or its increased mispairing potential during DNA replication e.g. Aflatoxin B1 (Morris *et al*, 1999). Where data to support other dose-response relationships is lacking, low dose linearity is the most appropriate hypothesis for the protection of public health (USEPA, 2000). However, this model is likely to overestimate risk. Therefore, Conolly and Lutz (2004) conclude that "cost compliance…may be greater than is actually needed" for protection. Through the use of assays with ever increasing sensitivity the true low dose effect can be established.

1.5.4. Threshold dose-response.

Thresholds are well known in toxicology (Cox, 1987). A threshold dose-response, referring to Paracelsus "the dose makes the poison," states that there is *no increase* in adverse effects at low doses compared to the untreated control. This differs from hormesis, which states low doses *reduces* endpoint to below the background level. Current opinion states that threshold dose-responses for genotoxic endpoints are accepted but need to be proven on a case-by-case basis (COM, 2011). The International Commission for Protection against Environmental Mutagens and Carcinogens define thresholds as "a range of sub-critical doses incapable of producing the specific response; as dose increases, the minimal dose that can elicit the response is the threshold dose" (ICPEMC, 1983). A threshold may be the result of poor assay resolution, which imparts an artificially high background level, meaning the assay is insensitive to increases in specific response until sufficiently high number of events have occurred. There are many definitions of a threshold dose (reviewed in Kirsch-Volders *et al*, 2003; Slob, 1999) as a result; thresholds in genotoxicology are confused by "semantic ambiguity" (Zito, 2001). The differences in absolute and pragmatic threshold are given in **Figure 1.4**.

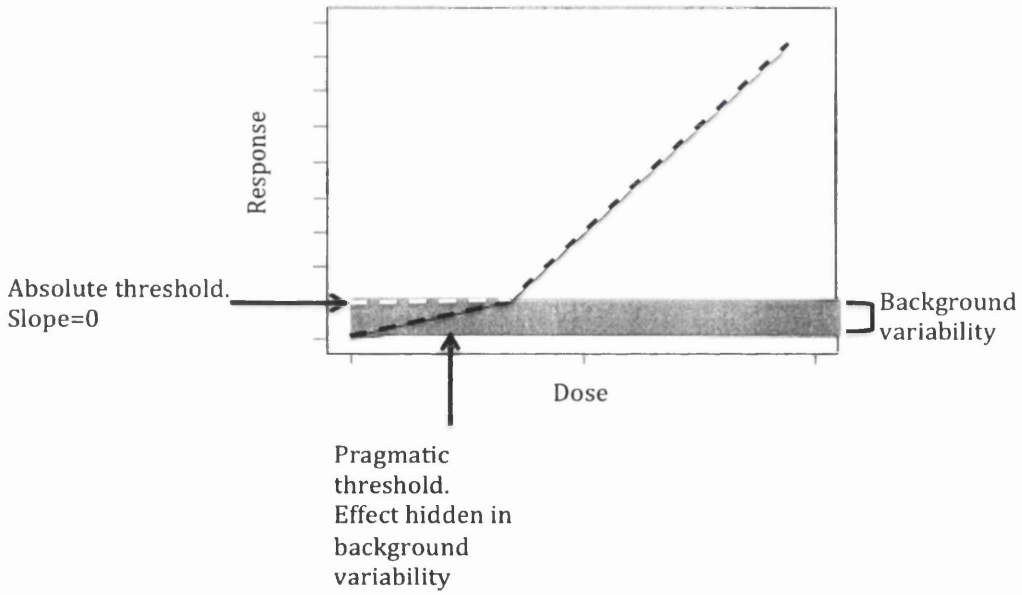

Figure 1.4. The differences in threshold definitions (pragmatic v absolute) as defined by COM (2009). Image adapted from Lovell (2000) based on definitions by Kirsch-Vodlers *et al* (2000).

The European Centre for Ecotoxicology and Toxicology of Chemicals (ECETOC) defines an absolute threshold as a concentration that does not interact with cellular machinery, the point in the dose response where slope 0 changes to slope >0 (Lutz, 1998). Experimentally determining an absolute threshold dose is difficult (Schneiderman *et al*, 1979). Therefore, of interest here are pragmatic thresholds, where low dose linearity is hidden within the background variability of the untreated control (Lutz, 1998). To define a pragmatic threshold, the use of statistics identifies a No Observed Effect Level (NOEL) defined as the highest concentration that is not statistically significantly different from the control and Lowest Observed Effect Level (LOEL) defined as the lowest concentration that produces a statistically significant increase in the endpoint in a well designed experiment (Waddell, 2005) with sufficient statistical power (Lovell, 2000). NO(G)ELs and LO(G)ELs are determined by *a priori* Dunnets and *post hoc* analysis of variance (ANOVA) (Doak *et al*, 2007). A more robust stepwise approach as recommended by Gocke and Wall (2009) are now employed. This involves:

1. Comparison of untreated and solvent controls by one-way ANOVA
2. Best of fit modeling between the null hypothesis of linearity and quadratic, the simplest non-linear curve over the entire dose-range (Johnson *et al*, 2009)
3. Determining the NOEL and LOEL using post hoc Dunnett's
4. Linear vs quadratic curve estimation at below NOEL doses
5. Application of "Broken stick" model to determine the threshold dose (td) (Lutz and Lutz, 2009) defined as an inflection point where the curve departs from slope 0 to a slope greater than 0 (**Figure 1.5**).

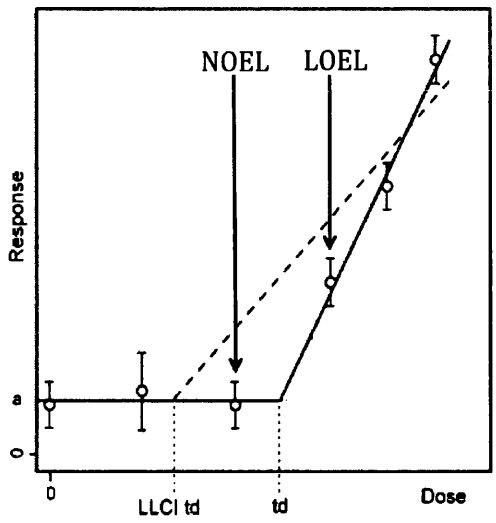

Figure 1.5. Representation of the "broken stick" statistical modelling of non-linear threshold dose-response to determine the threshold dose (td) with NOEL and LOEL identified. LLCI td=lower confidence interval of the td. Image adapted from Lutz and Lutz (2009) and Johnson *et al* (2009).

The acceptance of thresholds depends on statistical inference and "sound theoretical understanding" of the underlying biological mechanism of genotoxicity (ICPEMC, 1983). Thresholds have been observed in genotoxiciology to explain false positive *in vitro* results that may not be relevant *in vivo*, if the LOEL dose has not been exceeded *in vivo* (Henderson, Albertini and Aardema, 2000). Threshold identification relies upon:

1. The number of (redundant) targets
2. The mode of interaction with target
3. The type and sensitivity of endpoint e.g adduct versus mutation detection
4. Physiological cytoprotective mechanisms that prevent observable adverse effects at low dose (Speit *et al*, 2000; Kirsch-Volders *et al*, 2000).

According to the above criteria, thresholds have been accepted for aneugens, topoisomerase and polymerase inhibitors.

1.5.4.1. Genotoxic thresholds for indirect genotoxins.

The one hit theory has been applied to genotoxins targeting a *single* target, i.e. DNA and linearity has been assumed. For non-DNA targeting carcinogens, effect is

observed once *multiple* targets have been hit. The multiple target theory is generalised across all genotoxins and forms the theory behind the threshold dose-response for indirect genotoxins. The chemical must be in sufficient concentrations to interact with and damage all (or majority of) targets before an adverse effect is seen. A threshold has been shown for induction of indirect clastogenicity by topoisomerse II inhibitors, e.g. etoposide (Lynch *et al*, 2003) and induction of aneuploidy by spindle poisons (Parry, Fielder and McDonald, 1994; Elhajouji *et al*, 1995). For aneugens, since alterations in chromosome number are the first observable endpoint, a lack of sensitivity in being able to detect initial damage to individual spindles (referring to point 3 on the previous page) may account for the threshold. Damage to spindle apparatus may be linear; this is the emerging case with genotoxins when adducts are assessed as the genotoxic endpoint, a question of assay resolution (discussed in the following section).

1.5.4.2. Genotoxic thresholds for direct genotoxins.

Arguing that a threshold dose-response is more predictive than the favoured linear model is difficult for genotoxic carcinogens (Gehring and Blau, 1978). Genotoxic carcinogens are said to abide by the "one hit" theory, which has been interpreted to mean that there is no safe level of DNA damage, thereby assuming a linear dose response. With recent advancements in assay sensitivity, low dose effects can be ascertained. Increasing evidence challenges the "one hit" theory particularly when mutations are measured as the genotoxic endpoint; stipulating that one hit does not necessarily cause one mutation. Koana *et al* (2004) showed a threshold for mutation induction by ionising radiation attributed to protection by DNA repair mechanisms. Ever increasing evidence substantiates NOELs for mutation and chromosome break induction by direct acting genotoxins. *In vitro* and *in vivo* data by Doak *et al* (2007), Pottenger *et al* (2009), Gocke *et al* (2009), Lutz (2009), Bryce *et al*, (2010) and Lynch *et al* (2011) provide evidence in support of NOELs for mutagenic and clastogenic alkylating agents; methyl-*N*-nitrosourea (MNU), methyl methanesulfonate (MMS), ethyl methanesulfonate (EMS) and ethyl-*N*-nitrosourea (ENU). NOEL's have also been found for induction of hepatocarcinogensis by food-derived genotoxins, 2-amino-3,8-dimethylimidazo[4,5-*f*]quinoxaline (MeIQx) and *N*-nitrosodiethylamine

(Fukushima *et al*, 2002; Waddell, Fukushima and Williams, 2006). This is logical given the "number of targets" criteria (specified on page 21) and the multistage progression of cancer. The shape of the dose-response for genotoxins depends on the genotoxic endpoint being assessed. This is in support of Waddell *et al* (2006) and Fukushima *et al* (2002) where, "different NOELs may exist for different parameters" (**Figure 1.6**).

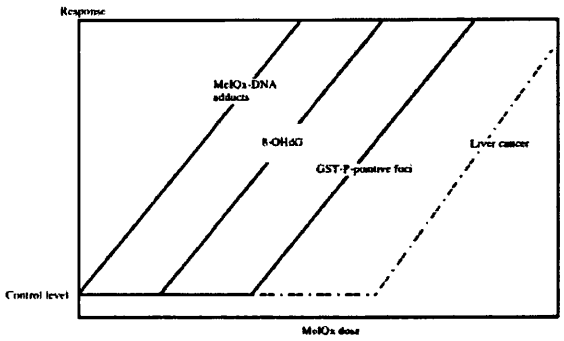

Figure 1.6. Conclusions drawn from analysis of genotoxic endpoints in the carcinogenesis caused by MeIQx. Taken from Fukushima *et al* (2002).

For example, quantifying adducts as the genotoxic endpoint reveals a linear dose-response at low doses of exogenous chemical suggesting that all doses are capable of adduct formation whereas mutation curves observe thresholds (Perera, 1988; Swenberg *et al*, 2008). It is reasonable to hypothesise a NOEL for adducts at extremely low doses where the chemical fails to interact with DNA either through detoxification or cellular membrane/nuclear envelope exclusion (Speit *et al*, 2000). The discrepancy in dose-response shapes for mutations and adducts could reflect the enhanced sensitivity of methods used in adduct quantitation (Jenkins *et al*, 2005). Mutational assays typically detect one non-synonymous mutation in $10^5/10^6$ nucleotides (Rossiter and Caskey, 1990). Quantitative adduct detection is capable of detecting 1 adduct in $10^{10}/10^{11}$ nucleotides with the advent of accelerator mass spectrometry (Swenberg *et al*, 2000; Farmer, 2004). Swenberg *et al* (2008) concludes that adducts can be detected at doses below the mutagenic NOEL, thus questioning the biological relevance of adducts if not all are fixed as mutations and questioning the "one-hit" postulations (Jenkins *et al*, 2005). The resulting NOEL for mutation will depend upon the adduct's propensity for mutation. Highly mutagenic adducts will

shift the NOEL to the left, in some instances eliciting a linear mutation dose-response. This reflects:

- Half-life of the adduct depending upon proficiency of its repair process.
- Miscoding potential during replication.
- Location for adducts within the genome. Adducts in exons are likely to disrupt protein sequence if they are converted into missense/nonsense(non-synonymous) mutations, since it will only be non-synonymous changes that will be detected in mutation assays.

This is exemplified by Doak *et al* (2007). The authors report mutational NOELs for alkylsulfonates (MMS and EMS) but not for alkylnitrosoureas (MNU and ENU). The alkylnitrosoureas are 20 times more mutagenic than alkylsulfonates due to a higher level of O^6alkylguanine (O^6AlkG) induced which has a high propensity for miscoding (Beranek, 1990). Lower doses of alkylnitrosoureas would be required to determine NOELs (Pottenger *et al*, 2009). The presence of adducts at doses which do not cause mutations implicate DNA repair as a potential mechanism behind mutation induction curves observed for DNA damaging genotoxins, i.e the NOEL must involve a post-adduct mechanism of action as found for ENU (Zair *et al*, 2011).

1.5.4.3. Potential mechanisms behind threshold dose response to genotoxins.

Many authors recognise the possible contribution of cytoprotective mechanisms behind the threshold dose-response for mutation induction by genotoxins (Speit *et al*, 2000). These include:

- Plasma membrane exclusion from cells and/or nuclear envelope exclusion from nucleus
- Metabolic inactivation of xenobiotics
- DNA repair of induced lesions
- Removal of heavily damaged cells by apoptosis and/or necrosis

These are shown in **Figure 1.7**.

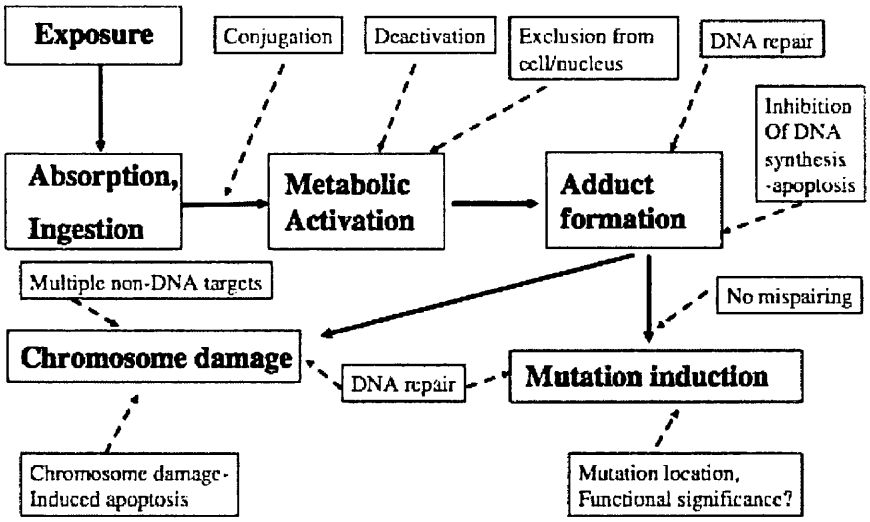

Figure 1.7. The process of mutagenesis from chemical exposure (solid lines) and cytoprotective mechanisms (dashed lines) that would account for a NOEL. Taken from Jenkins *et al* (2005)

Of interest to the following work is the hypothesised role of DNA repair in the removal of pre-mutagenic adducts prior to DNA replication in creating a NOEL for mutation induction. DNA repair deficiency sensitises cells to mutagenic and cytotoxic effects of high dose alkylating agents, highlighting the protective effect of DNA repair (Glassner *et al*, 1999) even in reducing the efficacy of alkylating agent chemotherapy (Shiraishi, Sakumi and Sekiguchi, 2000; Frosina 2009). If the linear hypothesis holds true, alkylating chemotherapy would be damaging at all doses. This is not the case. Furthermore, there is an established correlation between DNA repair gene expression and low dose genotoxin exposure. This has been shown for upregulation of O^6-methylguanine-DNA methyltransferase (MGMT) 4 hours post low dose MMS treatment (Doak *et al*, 2008) and immediate upregulation of N-methylpurine-DNA glycosylase (MPG) following EMS treatment (Zair *et al,* 2011). The upregulation did not reduce the level of adverse effects below the control level and so it is not considered as hormesis. The role of DNA repair in protection of low dose clastogen has been determined by Zair *et al* (2011). By utilising cells deficient in N7-Ethylguanine repair (MPG deficient cells), the authors have removed the NOEL for clastogenicity caused by EMS induced N7-Ethylguanine or N3-Ethyladenine adducts giving a linear dose-response. Additionally, there was no change to the dose-response of mutation induction by EMS in MPG deficient cells, since N7-

Ethylguanine is not a major miscoding adduct and inducer of point mutations. Therefore, the authors clarified that NOELs are mechanism of action specific and so these experiments can help generalise thresholds to genotoxins of similar mechanisms. Polymorphisms within DNA repair genes that exist in a human population would influence the shape of the dose-response. Susceptible individuals may be less tolerant to low level genotoxins and may not display a NOEL. Risk estimates to a population would be difficult (Jenkins, 2010).

1.5.4.4. Implications of thresholds in risk assessment of genotoxic impurities.

Throughout the manufacturing of pharmaceuticals, substances can be contaminated with genotoxic impurities. McGovern and Jacobson-Kram (2007) suggest that genotoxic impurities "carry only risk" and that pharmaceuticals should "strive to achieve the lowest levels of genotoxic impurities that are technically feasible or that carry no significant increase in cancer risk." While this is logical for a positive chemical assumed to be under the linear hypothesis of no safe level, if substantial evidence suggests an impurity causes no appreciable risk, precautionary measures would be an unnecessary cost. In situations where it is not possible to remove the genotoxic impurity, the Food and Drug Administration's (FDA) Centre for Drug Evaluation and Research (CDER) guidelines permit the re-evaluation of genotoxic potential of positive impurities (FDA, 2006). If a lack of genotoxic hazard can be concluded, using a WOE approach and mechanism of action data, "clinical studies could proceed" without need for further evaluation. The European Medicines Agency (EMEA) published guidelines on the limit of genotoxic impurities (EMEA, 2006). The guidelines state the calculation of a permitted daily exposure (PDE) from the experimentally determined NOEL. Whereas, without sufficient threshold data, levels should be controlled according to ALARP or threshold of toxicological concern (TTC). Therefore the determination of NOELs have implications in risk assessment but require substantial experimental evidence for justification.

1.6. Methyl-*N*-nitrosourea (MNU), a potent mutagen.

This thesis examines the low dose effects of MNU. The structure is shown in **Figure 1.8**. The monofunctional alkylating agent, MNU (Cas No; 684 93 5), is a direct acting

genotoxin that adds methyl groups (-CH_3) to nucleic acids and proteins. In DNA, methyl adducts show propensity for mutation but can be efficiently repaired without consequence. MNU is classified by IARC as a "group 2A probable carcinogen". MNU is used widely in mutagenesis research as a model alkylating agent, most extensively for the induction of rat mammary tumours, although MNU has broad tissue specificity (Tsubura *et al*, 2011). Compared to other alkylating agents, MNU is a potent transplacental mutagen (Donovan and Smith, 2010) and at equitoxic doses, MNU is more proficient at inducing *HPRT* mutants in V79 cells (Suter *et al*, 1980). This is attributed to the higher level of O^6-methylguanine (O^6MeG) induced by MNU (Beranek, 1990). Due to this, at the doses tested, MNU is linear for mutation induction (Doak *et al*, 2007).

A). B). C).

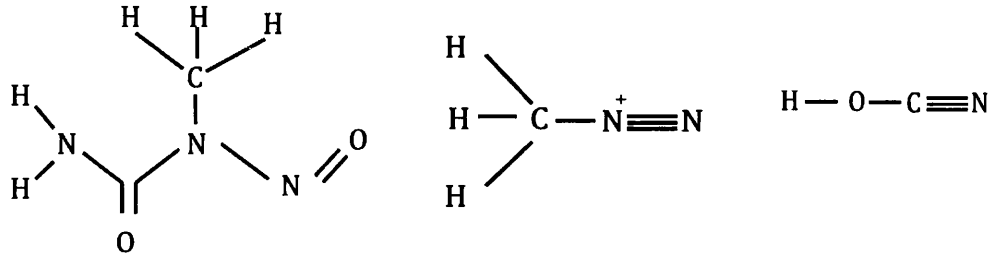

Figure 1.8. Structure of MNU (A), which decomposes into a DNA reactive methyldiazonium ion (B) and cyanic acid (C) and a hydroxide ion in aqueous solution. Details from (Golding *et al*, 1997).

1.7. MNU induced carcinogenesis.

Given the multistage model of cancer progression (Kirsch-volders *et al*, 2003), MNU is a tumour initiator in skin tumourigenesis (Brown, Buchmann and Balmain, 1990; Mukhtar *et al*, 1988) and also in thyroid tumours (Ohshima and Ward, 1986), in both situations requiring application of a tumour promoter. However, a single dose of 1 milligram (mg) MNU was sufficient to cause murine epidermal tumours by regenerative hyperplasia after 38 weeks (Kirkhus, Hilmar and Kristensen, 1987). Additionally, administration of a single high dose or multiple low dose of MNU caused murine lymphomas after a 4-week latency period, which was accelerated by female hormones (Romach *et al*, 1994). Swenberg *et al* (1975) conclude that various tissues are susceptible to MNU induced oncogenic transformation particularly at the

site of exposure. The authors also note differential tissue sensitivity to the effects of MNU. It seems that MNU alone is sufficient to initiate tumorigenesis.

1.8. Mode of carcinogenic action.

Evidence for DNA reactivity came from Swann and Magee (1968). The authors detected DNA methylation in various tissues following administration of radioactively labeled MNU. The critical initiating event seems to be MNU induced transformation of *ras* proto-oncogenes (Newcomb, Bayona and Pisharody, 1995). Of the three *Ras* genes (*H-ras, K-ras* and *N-ras*) a point mutation at codon 12, 13 or 61 of any of the isoforms is a known initiating mutation in carcinogenesis (Bos, 1989). MNU induced mutations have been found in all codons (Mariyama *et al*, 1989; Sukumar, 1989). It is well established that MNU induces a GC→AT transition at the middle base of codon 12 (GGA→GAA) of the *ras* proto-oncogenes resulting in an aspartic acid to glutamic acid change sufficient for oncogenic transformation (Jacoby *et al*, 1992). Methylation of O^6Guanine by MNU forms O^6-methylguanine (O^6MeG), which has miscoding potential during replication resulting in the GC→AT transition. O^6MeG is removed by MGMT however at codon 12 of *K-ras*, MGMT's activity is hindered, increasing the probability of mutation, which accounts for this mutation hotspot (Engelbergs, Thomale and Rajewsky, 2000). As will be discussed, O^6MeG causes double strand breaks (DSBs) through mismatch repair (MMR) processing, forming a substrate for recombination. This can lead to chromosome aberrations and oncogene activation (Jackson, 2002). O^6MeG can also be converted into a toxic lesion capable of killing the cell, however, in a tissue this would cause neighbouring cells with sub-lethal damage to undergo regenerative hyperplasia contributing to tumourigenesis; a common carcinogenic MOA of many toxic chemicals.

1.9. Reaction with DNA; mode of genotoxic action.

The intracellular biochemistry of MNU under physiological conditions is complex (Anderson and Burdon, 1970). There is greater extent of DNA alkylation at higher intracellular thiol (glutathione) concentration due to increased decomposition of MNU into its DNA reactive metabolite, methyldiazonium ion (Lawley and Thatcher, 1970)

(**Figure 1.8B**). The rate of MNU decomposition is solvent and pH dependent and this influences the genotoxic potential of MNU (McCalla, Reuvers and Kitai, 1968; Golding *et al*, 1997). Nevertheless, MNU induced DNA alkylation is well understood. According to Ingold's concept of nucleophilic substitution (Spratt *et al*, 1997), alkylating agents abide by either S_N1 or S_N2 reaction kinetics upon reaction with DNA. MNU is a S_N1 alkylating agent, which shows first order kinetics, and the rate of reaction depends on the degradation into a carbocation intermediate (methyldiazonium for MNU). MMS, for example, is a S_N2 alklyating agent (**Figure 1.9**). Sega, Wolfe and Owens (1981) report that DNA was 1.5 times more methylated after 4 hr MNU treatment than following MMS treatment showing a faster rate of reaction for S_N1 alkylating agents.

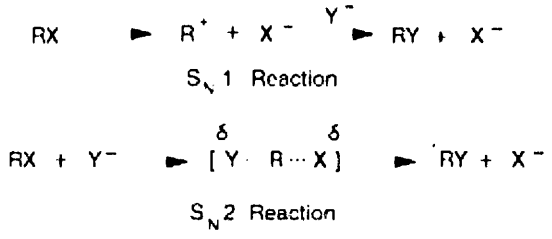

Figure 1.9. Schematic representation of S_N1 and S_N2 reaction mechanisms. R=methyl group, X=leaving group, Y=DNA. Taken from Colvin (2000).

A number of nucleophilic sites are susceptible to alkylation. The location and proportion of alkyl adducts in DNA, termed adduct spectra, is determined by the agents' electrophilic potential, governed by the swain-scott constant (*s* value) (Swain and Scott, 1953). MNU has a low *s* value of 0.42. Due to this it is able to methylate sites of low nucleophilicity such as O^6G. MMS and agents with higher *s* values, approaching 1 of methylbromide, react with sites of higher nucleophilicty such as N7guanine (N7G), to a greater extent, forming a larger proportion of N7Methylguanine (N7MeG) (Beranek, Weis and Swenson, 1980). Each adduct in the spectra can theoretically contribute to the biological effect of exposure. However, the consequences of O^6MeG and N7MeG have been well characterised. O^6MeG is a highly mutagenic adduct due to its propensity for miscoding during replication. N7MeG, is relatively innocuous since it is present at naturally high levels in genomic

DNA. However, it can cause point mutations and chromosome breaks due to spontaneous depurination and erroneous repair. The ratio of O^6alkylG:N7alkylG is predictive of an alkylator's mutagenic potential. Referring to the adduct spectra of MNU, O^6MeG constitutes 5.9-8.2% and 65.0-70.0% N7MeG. MMS, however forms only 0.3% O^6MeG (high *s* value) and 81.0-83.0% N7MeG. MNU therefore has a higher ratio of Θ^6alkylG:N7alkylG and is more mutagenic.

1.10. The biological relevance of N7MeG.

N7MeG, the major adduct upon exogenous DNA alkylation, does not have miscoding properties but its formation weakens the glycosidic bond leaving an apurinic site following spontaneous depurination or removal by its repair enzyme (MPG). Processing of the apurinic site by error prone base excision repair (BER) and bypass translesion synthesis (TLS) renders the lesion mutagenic (Boiteux and Guillet, 2004). If left unrepaired, apurinic sites can cause eventual chromosome breaks and is the hypothesised lesion responsible for the induction of micronuclei (Zair *et al*, 2011). The apurinic site can also lead to point mutations. Due to the "A-rule" (Ide *et al*, 1995), the preferential incorporation of adenine opposite the apurinic site may result in a GC→TA transversion. It is postulated that TLS polymerases and MMR may incorporate a variety of bases opposite an abasic site to account for the high level of GC→AT transitions and other transversions seen following treatment of MMS that are not compatible with its adduct spectra (Glaab *et al*, 1998; Glaab, Tindall and Skopek, 1999; Kokoska, McCulloch and Kunkel, 2003).

1.10.1. The biological relevance of O^6MeG.

The biological relevance of O^6MeG in carcinogenicity, cytotoxicity and mutagenicity was first noted by Loveless (1969) who noted the predominance of GC→AT transitions following exposure of bacteriophages to O^6-methylating agents. Methylation of exocyclic oxygen in O^6MeG disrupts a hydrogen bond held with exocyclic nitrogen at the fourth position of cytosine so that only two groups capable of hydrogen bonding remain on guanine. The structure of O^6MeG therefore resembles adenine and has significant miscoding potential (Baranek, 1983). Upon replication,

the polymerase inserts a thymine opposite O^6MeG forming O^6MeG:Thymine mispair in the first post-treatment cell cycle. During the second cell cycle, there are two eventualities:

1. Repair of O^6MeG in the mispair leaving a G/T mispair. MMR can either insert an adenine opposite the thymine causing the GC→AT transition or it can incorporate cytosine opposite guanine restoring the original DNA sequence (Kaina *et al*, 2007).
2. O^6MeG is not repaired and remains in the mispair. MMR processing of O^6MeG:Thymine mispair can cause DSBs and in turn initiate apoptosis, this is regarded as the mechanism for O^6MeG cytotoxicity (Discussed under section 1.13).

O^6MeG is therefore not only mutagenic but can be clastogenic and cytotoxic in MMR proficient cells (Shiravstav, Li and Essigman, 2010). To a lesser extent, mutations are caused by other MNU induced methyl adducts. Another miscoding lesion is O^4Methylthymine (O^4MeT) that constitutes 0.1-0.7% of total alkylation events by MNU (Baranek, 1990). O^4MeT causes TA→CG transitions (Klein *et al*, 1994). O^6MeG and O^4MeT adducts have been shown to cause transitions *in vitro* and *in vivo* (Singer *et al*, 1985; Singer *et al*, 1989). Palombo *et al* (1991) found 20 GC→AT transitions and 1 TA→CG transitions at the human *gpt* gene following MNU exposure, attributable to O^6MeG and O^4MeT, respectively. Furthermore, GC→AT transitions account for 98% of mutations induced by MNU (Sledziewska-Gojska and Torzewska, 1997). Even though a number of mutagenic adducts are produced, it is recognised that O^6MeG is the most mutagenic as it is readily mispaired. This is further discussed in chapter 5.

1.11. Repair of O^6MeG by MGMT prevents GC→AT transitions.

MGMT efficiently repairs O^6MeG, restoring guanine without consequence to DNA (**Figure 1.10**). The protective effects are evident in studies which show a reduction in MNU induced thymomas and skin carcinogenesis in transgenic murine models expressing human MGMT (Dumenco *et al*, 1993), MGMT mediated inhibition of MNU induced malignant progression (Becker *et al*, 2003), resistance of CHO cells over-expressing MGMT to the genotoxic and cytotoxic effects of O^6-methylating

agents (Kaina *et al*, 1991), perturbation of skin tumour initiation in transgenic mice (Becker *et al*, 1996) and increased sensitivity to alkylating agent induced mutagenesis and cytotoxicity in MGMT deficient cells (termed Mer-/Mex-) (Fritz and Kaina, 1992; Tsuzuki *et al*, 1996). Despite the importance of MGMT to DNA repair, little is known about transcriptional regulation and protein turnover within human cells, which is the current topic of interest (Professor Bernd Kaina, personal communication). Ishibashi *et al* (1994) provide immunohistochemical evidence to suggest that the majority of MGMT molecules reside in the cytoplasm and are actively transported into the nucleus to replace inactivated nuclear molecules. The signalling pathway responsible has not been identified. However, the mechanisms of removal of O^6MeG by MGMT are well understood.

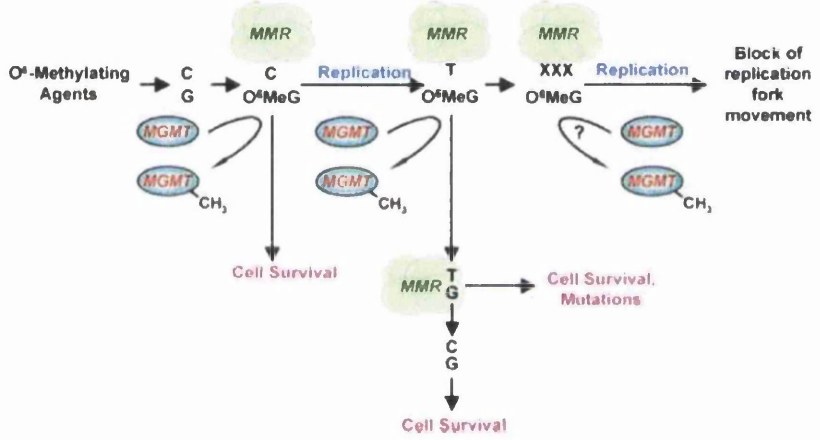

Figure 1.10. Repair of O^6-methylguanine (O^6MeG) by O^6-methylguanine-DNA methyltransferase (MGMT) prevents mutagenesis by O^6-methylating agents. MMR=mismatch repair. Image taken from Kaina *et al* (2007).

In a suicide reaction that inactivates MGMT, the methyl adduct is irreversibly transferred to an internal cysteine residue in the active site of the protein. The reaction is stoichiometric i.e the number of adducts that can be repaired is equal to the number of active MGMT molecules, which has been shown to differ between cell types. Therefore the cell has limited capacity to repair O^6MeG, depending on basal levels of MGMT, which can be depleted (reviewed by Pegg and Byers, 1992). Depletion of MGMT leaves the cell sensitive to alkylation damage (Hirose *et al*, 2003). The rate of MGMT regeneration is cell type specific. Repletion occurred faster in mitogen

stimulated T cells (Gerson, 1988) suggesting that cell division is important (Sklar *et al*, 1981).

1.12 Transcriptional regulation of MGMT.

It is well established that in rats, MGMT has an expression induction system in response to alkylation and X-ray induced damage (Fritz *et al*, 1991; Grombacher, Mitra and Kaina 1996). The mechanics are not well understood, possibly involving p53 and transcription factors (Activator Protein-1, AP-1 and Specificity Protein-1, SP1 (Rafferty *et al*, 1996; Grombacher, Eichhorn and Kaina, 1998) although this is controversial (Harris *et al*, 1996). There is very little evidence for the same induction system in humans in response to genotoxins (Doak *et al,* 2008). However, upregulation has been observed following treatment with corticosteroids, phorbol-12-myristate-13-acetate (TPA) and other Protein Kinase C activators in HeLa S3 cells (Boldogh *et al*, 1998; Grombacher, Mitra and Kaina, 1996). Humans have a higher level of basal MGMT activity than rodent cells (Dunn *et al*. 1986). Bacteria have MGMT at two loci. The *ogt* gene shows a constitutive basal level of MGMT expression, and upon insult, a second gene, *ada*, is expressed. This is the well-documented adaptive response that seems to be lacking in humans. Due to its unique inactivation reaction with O^6MeG, structural analogues such as O^6Benzylguanine (O^6BG) have been used to inactivate MGMT as a knockout strategy in chemotherapy to sensitise MGMT proficient gliomas and other malignancies to alkylating chemotherapy. The point of the cell cycle where damage is induced is important in allowing sufficient time for O^6MeG to be repaired by MGMT (Meikrantz *et al*, 1998). Tong, Fazio and Williams (1980) concluded that cells in S phase are most sensitive to alkylation damage given the increased mutant frequency of cells exposed when in S phase. Replication of O^6MeG adducts that have failed to be repaired in the first cell cycle cause O^6MeG/Thymine mispairs during S phase that enter the second cell cycle. Here, MMR processing of mispairs cause second cell cycle delay by G2 arrest with possible apoptosis.

1.13. Cellular processing of O^6MeG:Thymine mispairs.

O^6MeG:Thymine mispairs are formed during the first S phase and are substrate for MMR processing which can cause a variety of mutations and eventual cytotoxicity (**Figure 1.11**). "Methylation tolerant" cells are defective in MMR proteins, most commonly; MutSα (composed of MSH2 and MSH6) or MutLα (composed of MLH 1 and PMS2). They are resistant to alkylation-induced cytotoxicity at the expense of O^6MeG mediated GC→AT point mutations and a high cancer incidence. Conversely, there are reports of MMR deficiency *causing* cytotoxicity following alkylation damage (Aquilina *et al*, 1998). This was attributable to increased genomic instability like that observed in MMR deficient human non-polyposis colorectal cancer (HNPCC) (Fishel *et al*, 1993). It is recognised that MMR is essential for converting O^6MeG into a clastogenic lesion and is essential for O^6MeG induced chromosomal aberrations (Galloway *et al*, 1995), sister chromatid exchanges (SCE's) (Vernole, Pepponi and D'Atri, 2003) and apoptosis (Morris *et al* 1994) in the second cell cycle. Triggering apoptosis is achieved by direct MMR signalling or from MMR induced secondary lesions (O'Brien and Brown, 2006). Yoshioka, Yoshioka and Hsieh (2006) provide evidence that MMR directly initiates apoptosis by interaction with ATR (ataxia telangiectasia related) upon recognition of O^6MeG:Thymine mispairs. ATR is a phosphoinositide 3-kinase related kinase (PIKK) DNA damage sensor that relays the DNA damage signal to eventual effector molecules such as p53 to bring about cell cycle arrest for DNA repair or apoptosis. Hickman and Samson (1999) suggest that MMR can also activate apoptosis independent of p53 following p53 independent G2 arrest, where a decision to enter mitosis or apoptosis is made (McNamee and Brodsky, 2009). Chromatin associated MMR proteins can also cause direct apoptosis by triggering S phase arrest immediately after the formation of O^6MeG/Thymine mispairs (Schroering *et al*, 2009). Another method of apoptosis is through secondary DNA lesions caused by MMR processing of mispairs. Futile cycling produces single strand gaps in DNA that are too small to attract recombinogenic foci (RAD51) and fail to trigger checkpoints (Mojas, Lopes and Jiricny, 2007). They enter the second S phase leading to DSBs that can either be repaired by Brca2/Xrcc2 dependent homologous recombination giving SCE's (Roos *et al*, 2009) or lead to second cell cycle G2 arrest and apoptosis by ATR/ATM (ataxia telangiectasia mutated) mediated

recognition of the lesion or resulting stalled replication forks (Bohgaki, Bohgaki and Hakem, 2010; Quiros, Ross and Kaina, 2010). This would trigger the observed upregulation of p53 and Fas/CD95/Apo-1, triggering the death response in T cells (Roos, Baumgartner and Kaina, 2004). Additionally, Hirose *et al* (2003) provide a link between MMR and G2 arrest via p38, possibly representing another pathway of O^6MeG induced G2 arrest. Schroering *et al* (2009) investigated cell cycle effects following alkylation exposure in MGMT deficient/MMR proficient HeLa MR cells. The authors show a lack of second cell cycle delay, the cells traverse into the third cell cycle with high level of DSBs that result in multinucleation, which serves as a trigger for apoptosis. In mutation assays, cells that undergo apoptosis as a result of MMR processing in the first few post-treatment cell cycles will not be recovered. However, the mutational event will persist since GC→AT transitions would occur in half of the viable daughter cells upon replication of thymine and not O^6MeG in the template strand, unless the damage at other sites trigger apoptosis (Morris *et al*, 1994). Therefore, with the "dilution of O^6MeG during cell cycle (divisions), a decline in the level of cell kill is to be expected" (Quiros, Roos and Kaina *et al*, 2010). These investigations are important in alkylating chemotherapy to distinguish methods of sensitising alkylation-resistant tumours (Heacock *et al*, 2010).

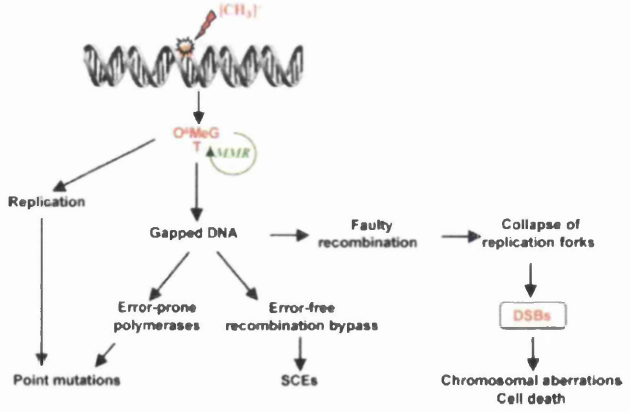

Figure 1.11. The current model of processing O^6MeG:Thymine mispairs to explain the various mutations observed following treatment with MNU and other O^{6-} methylating agents. Taken from Kaina *et al* (2007).

1.14. Mutation spectra of MNU.

The mutation spectrum identifies the frequency and location of mutations across a locus to identify non-random mutational hotspots. Hotspots are useful "to infer mechanisms of mutagenesis contributing to tumourigenesis" (Glazko *et al*, 2006).
Since GC→AT transitions constitute the majority of MNU induced point mutations, sequence specificity has only been considered for this transition. It is noted that guanines preceded by a purine (5'-PuG-3') are particularly susceptible to mutation in *E.coli* (Glickman *et al*, 1987) and mammalian cells (Palombo, Bignami and Dogliotti, 1992). Glickman *et al* (1987) state "the distribution of the initial DNA damage" is responsible. The nearest neighbour effect of the flanking purine enhances the molecular electrostatic potential of the O^6 site for alkylation (Pullman and Pullman, 1981). This explains why it is the second guanine of GGA (codon 12 of *K-ras*) that is methylated by MNU. Another explanation would be reduced adduct repair by MGMT at sites preceded by a purine (Dolan, Oplinger and Pegg, 1988) and chemical involvement in alkylation by the preceding purine (Horsfall *et al*, 1990). Palombo *et al* (1992) demonstrated that MNU induced mutations predominantly occurred on the non-transcribed strand, and was independent of transcriptional status. The mutation spectra therefore, cannot be attributed to transcription-coupled repair. This could reflect the accessibility of DNA within the nucleus. Furthermore, Jack and Brooks (1981) state that DNA damage is heterogeneous throughout the genome, predominantly occurring at sites that are accessible to the genotoxin. *In vitro* mutation spectra for alkylating agents used a mutation sensor gene such as *HPRT* on an extra-chromosomal vector (Dogliotti *et al*, 1991) and so may not reflect mutational patterns on genomic DNA. Mutation spectra can identify hotspots, with additional multivariate statistical analysis; the mutation spectra can identify commonalities between treatments or treatment groups. It is a reliable tool for analysis of mutation spectra to understand mutation induction by alkylating agents (Benigni, Palombo and Dogliotti, 1992). The authors found that S_N1 agents have markedly different spectra than S_N2 agents. Two such methods of multivariate statistics are principle component analysis (PCA) and cluster analysis (CA) (Lewis and Parry 2002). At the *HPRT* locus, Bouwens-Rombouts *et al* (1993) identified two hotspots of exon 3 these being a GC→AT transition at 16676 and a GC→TA transversion at 16680 one in each of two

families. These were also sites for mutation following MMS treatment (Jenkins *et al*, 2005). Furthermore, Tomita-Mitchell *et al* (2003) state that the mutation spectra determined following alkylation exposure *in vitro* is reflective of the mutational pathways *in vivo*.

1.15. MNU dose-response for mutation induction.

Linearity has long been assumed for MNU induced mutations at low doses. Doak *et al* (2007) found that MNU elicited chromosomal aberrations and gene mutations in proportion to dose. However, the authors postulate that a threshold could exist at doses lower than those tested. This has been substantiated by Pottenger *et al* (2009). The authors report a NOEL of 0.69μM (0.71μg/ml) MNU at the thymidine kinase (*TK*) locus in L5178Y mouse lymphoma cells. It is clarified that the dose-response curve does not correlate to N7MeG levels which is not mutagenic. Since O^6MeG is the major mutagenic adduct, a potential threshold would be dependent upon repair of this adduct by MGMT. It is possible that previously tested doses have caused sufficient O^6MeG to saturate the repair enzyme, inhibiting the cell's ability to prevent mutations. Doak *et al* (2007) found a linear low dose-response but attributed the linearity to other adducts and mutations that result from MNU exposure and erroneous repair mechanisms such as translesion synthesis. The following work further tests the repair mediated threshold hypothesis by using a dose range 10-fold lower than that of Doak *et al* (2007).

1.16. Thesis aims and objectives.

A study by Zair *et al* (2011) that characterised a biological mechanism behind the mutagenic NOEL of EMS is emulated in the following work to assess the role of MGMT in the prevention of GC→AT point mutations at low doses of MNU. This study has critical importance because:

1. MNU is the most mutagenic of the four alkylators discussed previously (MNU, ENU, EMS and MMS), therefore, describing low dose effects for MNU sets precedence for lesser mutagenic alkylating agents.

2. Point mutations have a better defined role in carcinogenesis than chromosomal aberrations. Therefore, there is real impetus for defining the mechanism of mutation induction.

This evidence together with *in vivo* substantiation will provide a strong biological WOE for low dose protection to alkylating agents, which may be applicable to genotoxins of similar mechanisms of action. This thesis is an all-encompassing report into the characterisation of low dose MNU from dose-response modelling, adduct detection, mutation analysis and DNA repair. The layout of the results chapters are shown in **Figure 1.12**.

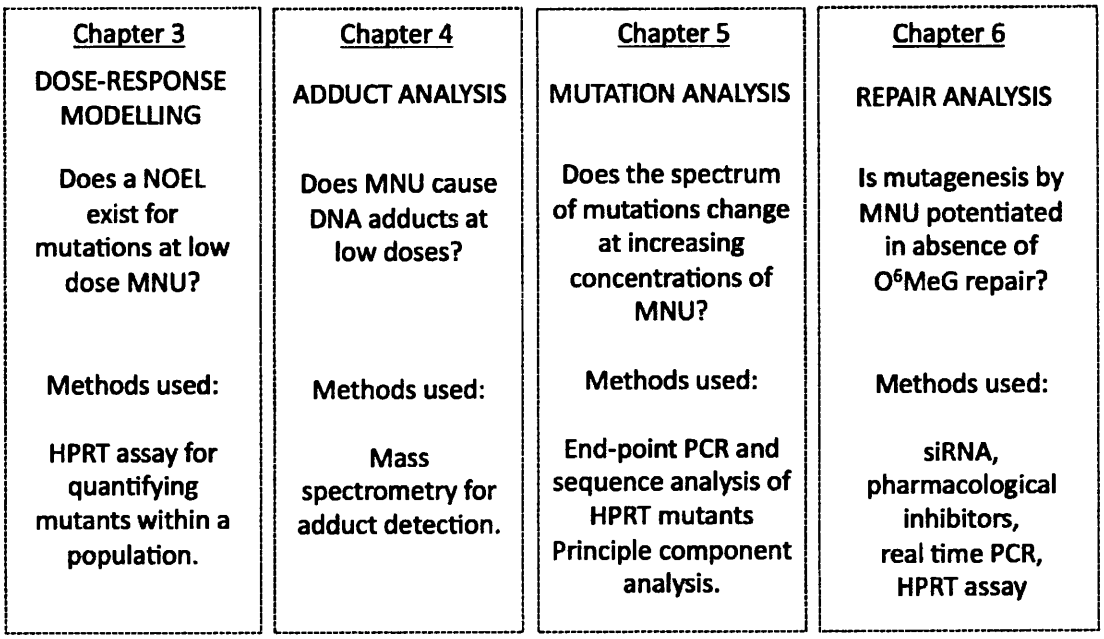

Figure 1.12. Layout of the results chapters in this thesis.

Chapter 2.

General Materials And Methods.

2.1. General materials and methods.

The following account is of the materials and methods that are common to at least two results chapters.

2.2. AHH-1 cell culture.

AHH-1 (*TK*+/-) cells were purchased from American Type Culture Collection (ATCC) (Middlesex, UK). AHH-1 cells are Epstein-Barr virus transformed human B lymphoblastoid cells expressing cytochrome p4501A1 (Crespi and Thilly, 1984). Originally derived from RPMI-1788, AHH-1 also has aryl hydrocarbon hydroxylase (AHH) activity (Freedman *et al*, 1979) for xenobiotic metabolism. Corso and Parry (2004) showed that AHH-1 maintained a stable karyotype for five weeks in culture. AHH-1 cells harbour a heterozygous mutation at codon 282 (CGG→TGG) of *p53*. This is a hotspot for spontaneous 5'methylcytosine deamination in *p53* gene (Guest and Parry, 1999). It may act in a dominant negative way to cause the loss of G1 arrest (Morris *et al*, 1996) but AHH-1 are capable of apoptosis (Zair *et al*, 2011) and G2 arrest (Morris *et al*, 1996; Guest and Parry, 1999) in response to alkylating agent exposure.

2.2.1 Cell culture procedure.

All cell culture was performed using aseptic techniques in Scanlaf Mars Pro class 2 hoods pre-cleaned with 70% ethanol with routine UV sterilisation. All centrifugation steps were performed in an Eppendorf 5810r centrifuge with a radius of 173mm unless otherwise stated.

2.2.2 AHH-1 growth media.

AHH-1 cells were grown, mycoplasma free, in growth media composed of RPMI 1640 (GIBCO, Paisley, UK) supplemented with 10% horse serum (BioSer, Sussex, UK) and 1% L-Glutamine (GIBCO, Paisley, UK) in humidified atmosphere at 37°C,

5% CO_2. Mycoplasma testing was carried out routinely using MycoAlert® mycoplasma detection kit (Lonza, Slough, UK). Between experiments, cells were maintained at $1.25x10^5$cells/ml in 50ml cultures and sub-cultured every 2 days (at confluency) with microscopic examination under x100 objective on a Ziess Axiovert 25 light microscope.

2.2.3 Cell freezing for storage.

25ml of 50ml confluent culture was centrifuged at 1500rpm for 3 minutes (min), the supernatant discarded and the pellet re-suspended in 1ml freeze down media (12% DMSO in horse serum). The cells were left to cool at -80°C overnight at a rate of 1°C/min in a Nunclon cell freezer. After this time, the cells were transferred to liquid nitrogen for long-term storage. Upon resurrection cells were thawed rapidly at 37°C and transferred to 50ml growth media.

2.2.4 Dilution of cells.

For an experiment, the appropriate concentration of cells was obtained by using **equation 2.1**:

Equation 2.1 $$V_2 = \frac{(C_1 x V_1)}{C_2}$$

Derived from, $C_1 x V_1 = C_2 x V_2$

Where;

C_1=Concentration needed (cell/ml)

V_1=Volume needed (ml)

C_2=Concentration of culture (cells/ml)

V_2=Volume of stock required (ml).

For example; diluting a cell stock of $1.5x10^6$ cells/ml to 50ml at $1.25x10^5$cells/ml.

$$V_2 = \frac{(1.25x10^5 x 50)}{1.5x10^6}$$

V_2=4.2. Therefore 4.2ml+45.8ml growth media (50-4.2) will give 50ml at $1.25x10^5$cells/ml.

All calculations were checked using **equation 2.2**.

Equation 2.2 $(C_2/C_1)xV_2=V_1$

2.3. Preparation of chemical stocks for testing.

Chemical handling took place inside Scanlaf Mars Pro class 2 hoods under aseptic techniques with the necessary safety precautions. All equipment was sterilised by UV. To prevent leaching of plastics, stocks were diluted in glass vials (Sigma, Gillingham, UK) with appropriate solvents (**Table 2.1**).

Table 2.1. Preparation of chemical stocks.

Chemical name	Cas number	Solvent	Reconstituted stock concentration (µg/ml)	Final concentration in media (µg/ml)	Storage temperature of powder (°C)	Storage once reconstituted (°C)
Methyl-*N*-nitrosourea (MNU)	684-93-5	DMSO	1000	Refer to **Table 2.2**	4	Discarded after use
O^6-benzylguanine (O^6BG)	19916-73-5	100% Methanol	10	2.4	26	Discarded after use
6-thioguanine (6-TG)	154-42-7	1M sodium hydroxide (NaOH)	1.5	0.6	4	-20

2.3.1. MNU.

Pottenger *et al* (2009) reported the purity of MNU (Sigma Aldrich, USA) as 69%. We have used an alternative product (MNU ISOPAC®, Cat number: N1517 Sigma-Adrich, Gillingham, UK), which has previously been used to induce mammary tumours in rodents (Bhat and Lacroix, 1989). Unfortunately the manufacturers do not

state purity, the specification sheet presented as appendix 1. For each replicate and treatment with MNU a new stock was ordered. 10ml DMSO reconstituted MNU to 0.1g/ml. 1µl of this was added to 10ml DMSO in a 1/10000 dilution to give a 0.01mg/ml stock. 200µl of 0.01mg/ml stock was further diluted 1/10 in 1.8ml DMSO to yield a stock of 0.001mg/ml. These stocks were further diluted to the desired concentration using **equation 2.1** (**Table 2.2**).

Table 2.2. Dilution series for low dose MNU treatments.

	Volume (µl)		
Final	**DMSO**	**0.001mg/ml**	**0.01mg/ml**
0.00075	185	15	-
0.001	180	20	-
0.0025	150	50	-
0.005	100	100	-
0.0075	185	-	15
0.01	180	-	20
0.025	150	-	50
0.05	100	-	100
0.075	50	-	150

100µl of MNU at appropriate concentration was added to 10ml cell culture; this x100 dilution factor was accounted for. These concentrations were nominal without exact purity of MNU and should only be compared to studies of the same methodology. Experimental determination of dose is achievable according to the solvent extraction method of Mirvish and Chu (1973). However, this was not undertaken. The manufacturers estimate that 13% of MNU ISOPAC® is made up of water and acetic acid necessary to maintain stability of MNU. It must be noted that when comparing to studies that use MNU of 100% purity, the concentrations shown here should be adjusted.

2.3.2. 6-thioguanine.

To minimise freeze/thaw cycles, 5ml single use working stocks at 0.15mg/ml (1x) were prepared. 1x stock was prepared from a 30x stock of 6-thioguanine (6-TG, 4.5mg/ml) by addition of 29ml 0.1M sodium hydroxide (NaOH) to 1ml 30x 6-TG, filter sterilized by use of 0.2µM filters and kept at -20°C for storage. Dissolving 1g NaOH (Sigma, Gillingham, UK) in 250ml distilled water gave 0.1M NaOH, which

was autoclaved. For every 25ml of culture media, addition of 100µl 1x 6-TG gave a final concentration of 0.6µg/ml. One stock of 6-TG was used through all HPRT assays. The quality of stock was checked by determining the absorbance ratio of 320/260nm (Fenwick, 1985). A ratio >2.5 is a reliable stock. The stock used here had a ratio of 4.8 (0.708/0.149).

2.4. Cytotoxicity assessment using relative population doubling (RPD).

Toxicity of MNU+/-O^6BG was determined by counting the number of cells before and after treatment, used to calculate relative population doubling (RPD). $1.5x10^5$AHH-1 cells/ml were set up as 10ml cultures per dose of MNU and incubated for 24hr at 37°C, 5% CO_2. Five additional 10ml cultures were established, for pre-treatment (baseline) counts. After 24hr, the baseline flasks were gently shaken and 100µl sampled and mixed with 10ml Isoton (Beckman) and cell number counted using a Beckman coulter counter set to count cells between 5-17µM. These counts were averaged and used for calculating relative population doubling (RPD) in **equation 2.3**. 100µl of MNU at the appropriate dose was added to the treatment flasks and incubated for 24hr at 37°C, 5% CO_2. At this time, the flasks were washed twice in phosphate buffered saline (PBS. Lonzo, Blackley, UK) and re-suspended in 10ml growth media. 100µl was sampled and counted to obtain 24hr post treatment counts. The flasks were incubated for a further 24hr and sampled to obtain 48hr post treatment counts.

Equation 2.3

$$\text{RPD} = \frac{\text{number of population doubling (PD) in treated cultures}}{\text{number of population doubling (PD) in control cultures}}$$

Where,

$$\text{PD} = \frac{[\log(\text{24 or 48hr post-treatment cell number/baseline counts})]}{\log 2}$$

Taken from Fellows *et al* (2008).

2.5. HPRT Forward mutation assay.

2.5.1. Mutant purification; establishing a HPRT mutant free stock.

To purify AHH-1 cell populations of existing hypoxanthine phosphoribosyltransferase (HPRT) mutants, $5x10^5$ AHH-1 cells/ml were grown in a 50ml culture for 3 days in hypoxanthine, aminopterin and thymidine (HAT) supplemented growth media. 1ml 50x HAT supplement (Invitrogen, Paisley, UK) was added to 49ml growth media. The final concentration was $2x10^{-4}$mol/L hypoxanthine, $8x10^{-7}$mol/L aminopterin and $3.5x10^{-5}$mol/L thymidine. After this time, the cells were centrifuged at 1500rpm for 3min washed with PBS and re-suspended in 100ml HT supplemented media (HAT media without aminopterin) for appropriate cell sub culturing. 2ml 50x HT supplement (Invitrogen, Paisley, UK) was added to 98ml growth media. Cells were grown in presence of HT for 24hr washed with PBS and re-suspended in 200ml normal growth media to culture for 2 days. Cells were then frozen according to method outlined in section 2.2.3.

2.5.2. Treatment protocol.

Following mutant purification, AHH-1 cells were revived and grown in normal growth media for 2 days. 10ml culture was established at a concentration of $5x10^5$ AHH-1 cells/ml and exposed to:

- 100µl of the appropriate dose of MNU
- 100µl DMSO (final concentration of 0.1% DMSO) for solvent control
- 100µl growth media for the untreated control
- 0.075µg/ml MNU as the positive control (LOEL in Doak *et al*, 2007)

For 24hr at 37°C, 5% CO_2. Cells were then washed in PBS and re-suspended in 50ml growth media for a total of 13 days to remove residual wildtype HPRT activity and allow expression of a mutant HPRT phenotype. Treatment wash off was counted as day 0 and sub-culturing, as described, took place on days 1,3,5,7,9,11. Due to the high number of 96 well plates needed for statistical power on day 13, incubator space was limited. To overcome this, all doses were frozen during the mutant expression period on day 7 and 2 doses were revived at a time. Upon revival, cells were designated day 7 and sub-cultured 2 days later (day 9). To account for the effect of freezing/thawing

on recovery of wildtype and mutant cells, a control culture should have been removed from storage at the same time as dosed cultures. This was not performed as the positive control gave the expected increase in mutant frequency, indicating that the assay was working. On day 9, cells were sub-cultured to $1.25x10^5$ cells/ml in 80ml. Upon day 11, 80ml was divided into 4 x $125cm^2$ flasks with the addition of 60ml growth media for sufficient number of cells on day 13. On day 13, 96 well plates were loaded with 100µl of AHH-1 cells at $4x10^5$ cells/ml ($4x10^4$ cells/well) in selective 6-thioguanine (6-TG) supplemented media (100µl 0.15mg/ml 6-TG stock per 25ml of media) at a final concentration of 0.6µg/ml 6-TG. This caused efficient removal of HPRT wildtype cells but allowed sensitive selection of HPRT mutants. For threshold analysis, 10000 wells were required per dose. In addition, 60 plates per dose containing 200cells/ml (20 cells/well) in non-selective media were used for measurements of colony forming ability (plating efficiency). All plates were incubated at 37°C, 5% CO_2 for 14 days and the number of wells with colonies scored. 60 wells per plate were scored and the perimeter wells were excluded because the media partially evaporated. Colonies were identified as being <20 cells in diameter and were light in colour.

2.5.3. Calculating Mutant frequency.

Equation 2.4 Percentage Plating Efficiency (% PE) = $-\text{Ln}\,(X_o/N_o) \times 100$

Equation 2.5 Cell Viability (%) = $\dfrac{\text{PE}}{\text{PE of control}} \times 100$

Equation 2.6 Mutant frequency (MF) = $\dfrac{-\text{Ln}\,(X_s/N_s)}{-\text{Ln}\,(X_o/N_o)} \times \text{DF}$

DF = Dilution factor = $\left[\dfrac{\text{(No. of initial cells per well) Non-selective conditions}}{\text{(No. of initial cells per well) Selective conditions}}\right]$

X_s= No. of wells without colonies
N_s = Total no. of wells
} Selective conditions

X_o= No. of wells without colonies
N_o = Total no. of wells
} Non-selective conditions

2.5.4. Enumeration of mutant colonies for sufficient RNA yields.

At the end of the HPRT assay, colonies were aspirated and transferred to a 24 well plate (Nunc, ThermoScientific, Loughborough, UK) containing 2ml of growth media per well and left to grow at 37°C, 5% CO_2. After 5 days, cells were carefully aspirated using a 300µl pipette and mixed with 5 volumes (1.5ml) RNA protect® cell reagent (Qiagen, Sussex, UK) and stored at -20°C for RNA extraction.

2.6. RNA extraction.

Total RNA extraction was performed using RNeasy kit® (Qiagen, Sussex, UK). All centrifugation took place at 25°C for 15sec at 10000rpm in Heraeus Biofuge Fresco centrifuge with a radius of 85mm. Surfaces and equipment were wiped with RNAzap® (Applied Biosystems, Warrington, UK) to remove RNAses. Cells in RNA protect® cell reagent were defrosted at room temperature and pelleted by centrifuging at 1800rpm for 3mins and re-suspended in 350µl RLT cell lysis buffer. Cells were homogenised by passing through a narrow gauge needle. To help bind RNA to the spin column, equal volume (350µl) of 70% ethanol was added, mixed thoroughly and applied to the spin column. To bind RNA, the column was centrifuged and the flow through discarded. The column was washed with 350µl wash buffer RW1 with repeat centrifugation. Genomic DNA was digested using RNase-free DNA set (Qiagen, Sussex, UK). For each column, 80µl DNase mix (10µl DNase+70µl RDD buffer) was applied and incubated at room temperature for 15mins. 350µl of wash buffer RW1 was added and centrifuged. 500µl buffer RPE was added and centrifuged. This was repeated but centrifuged for 2min to dry the column of ethanol present in buffer RPE. 30µl of water was applied directly to the column, incubated at room temperature for 10mins and centrifuged for 1min to elute RNA. RNA was kept on ice once eluted. The concentration was determined by use of nanodrop 1000 spectrophotometer. The samples were divided into two aliquots and stored at -80°C. For endpoint PCR and sequencing in mutation detection, the first RNA aliquot was used to find mutations and the process repeated with the second aliquot to confirm mutations.

2.7. cDNA synthesis for end-point PCR.

cDNA synthesis reactions were set-up on ice using RETROscript® (Applied Biosystems, Warrington, UK) in a purifier vertical clean bench (Labconco, USA) pre-cleaned with RNAzap®. Volumes of reagents are given in (**Table 2.3**). Oligo (dT) primers were used over random decamers to preferentially target mRNA from other RNA species (tRNA and rRNA). The reaction ran at 44°C for 60min followed by 10min at 90°C to inactivate reverse transcriptase enzymes using an icycler (Biorad, Hemel Hempstead, UK). 2µl of completed reaction mixture was immediately used in each master mix for end-point PCR.

Table 2.3. Components (per sample) for cDNA synthesis.

Reagent	Volume (µl)
Buffer	1
Oligo (dT)	1
dNTP	2
RNase inhibitor	0.5
MMLV-reverse transcriptase enzyme	0.5
RNA template	1000ng
Nuclease-free water	=5-volume of RNA
Total	**10**

2.8. Calculation of 1µg RNA for use in cDNA synthesis.

Equation 2.7 Volume (µl) of sample to give 1µg. $1\mu g\ RNA = \frac{1000(ng)}{\text{Amount of RNA (ng) per } \mu l}$

For example, for a RNA sample of 250ng/µl, 4µl of sample would give 1µg for cDNA synthesis.

The use of Oligo(dT) primers targeted all mRNA transcripts from the total RNA extracted from cells. β-actin is an abundant target with optimised primers. Therefore, β-actin primers were used to amplify β-actin mRNA to clarify the success of the cDNA reaction. The reaction was set-up according to **Table 2.4**.

Table 2.4. Components of the master mix for amplifying β-actin mRNA to clarify the success of each cDNA reaction.

Reagent	Volume in β-actin master mix	Final
5x Buffer	5	1X
10mM dNTP mix	0.5	0.2mM each
25mM Magnesium Chloride	1.5	2mM
β-actin forward primer	0.5	0.2μM
β-actin reverse primer	0.5	0.2μM
Go*Taq* DNA polymerase (5u/μl)	0.15	1.5U
cDNA template	1	-
Water	15.85	-
Total	25	-

2.9. End-point PCR.

HPRT mRNA was amplified by use of two pairs of overlapping primers (D and K) to obtain 83% gene coverage. The oligonucleotide sequence for each primer is shown in **Table 2.5.** The location of each primer is shown in **Figure 2.1**.

Table 2.5. Sequences of the primers used for successful amplification of HPRT cDNA.

Primer Name	Sequence
D Forward	5'-GAACCTCTCGGCTTTCCC-3'
D Reverse	5'-TGCCAGTGTCAATTATATCTTCC-3'
K Forward	5'-GATGATCTCTCAACTTTAACTGG-3'
K Reverse	5'-CTTACTTTTCTAACACACGGTGG-3'

GGCGGGGCCTGCTTCTCCTCAGCTTCAGGCGGCTGCGACGAGCCCTCAGG
CGAACCTCTCGGCTTTCCCGCGCGGCGCCGCCTCTTGCTGCGCCTCCGCCT
CCTCCTCTGCTCCGCCACCGGCTTCCTCCTCCTGAGCAGTCAGCCCGCGCG
CCGGCCGGCTCCGTTATGGCGACCCGCAGCCCTGGCGTCGTGATTAGTGA
TGATGAACCAGGTTATGACCTTGATTTATTTTGCATACCTAATCATTATGC
TGAGGATTTGGAAAGGGTGTTTATTCCTCATGGACTAATTATGGACAGGA
CTGAACGTCTTGCTCGAGATGTGATGAAGGAGATGGGAGGCCATCACATT
GTAGCCCTCTGTGTGCTCAAGGGGGGCTATAAATTCTTTGCTGACCTGCTG
GATTACATCAAAGCACTGAATAGAAATAGTGATAGATCCATTCCTATGAC
TGTAGATTTTATCAGACTGAAGAGCTATTGTAATGACCAGTCAACAGGGG
ACATAAAAGTAATTGGTGGA**GATGATCTCTCAACTTTAACTGG**AAAGAA
TGTCTTGATTGTGGAAGATATAATTGACACTGGCAAAACAATGCAGACTT
TGCTTTCCTTGGTCAGGCAGTATAATCCAAAGATGGTCAAGGTCGCAAGC
TTGCTGGTGAAAAGGACCCCACGAAGTGTTGGATATAAGCCAGACTTTGT
TGGATTTGAAATTCCAGACAAGTTTGTTGTAGGATATGCCCTTGACTATAA
TGAATACTTCAGGGATTTGAATCATGTTTGTGTCATTAGTGAAACTGGAAA
AGCAAAATACAAAGCCTAAGATGAGAGTTCAAGTTGAGTTTGGAAACATC
TGGAGTCCTATTGACATCGCCAGTAAAATTATCAATGTTCTAGTTCTGTGG
CCATCTGCTTAGTAGAGCTTTTTGCATGTATCTTCTAAGAATTTTATCTGTT
TTGTACTTTAGAAATGTCAGTTGCTGCATTCCTAAACTGTTTATTTGCACT
ATGAGCCTATAGACTATCAGTTCCCTTTGGGCGGATTGTTGTTTAACTTGT
AAATGAAAAAATTCTCTTAAACCACAGCACTATTGAGTGAAACATTGAAC
TCATATCTGTAAGAAATAAAGAGAAGATATATTAGTTTTTTAATTGGTATT
TTAATTTTTATATATGCAGGAAAGAATAGAAGTGATTGAATATTGTTAATT
AT**ACCACCGTGTGTTAGAAAAGTAAG**AAGCAGTCAATTTTCACATCAAA
GACAGCATCTAAGAAGTTTTGTTCTGTCCTGGAATTATTTTAGTAGTGTTT
CAGTAATGTTGACTGTATTTTCCAACTTGTTCAAATTATTACCAGTGAATC
TTTGTCAGCAGTTCCCTTTTAAATGCAAATCAATAAATTCCCAAAAATTTA
AAAAAAAAAAAAAAAAAAAAA

Figure 2.1. Sequence of HPRT mRNA and the locations of D primers (underlined) and K primers (bold).

Primers were designed using Beacon 2 software (Premier Biosoft) and synthesised by MWG Eurofins (Germany) with instructions for reconstitution of lyophilized primers to 100μM (pmol/μl) in nuclease free water. This master stock was further diluted 1:10 to 10μM working stock in nuclease free water and frozen as single use (10μl) aliquots. To prevent primer dimers, two master mixes (designated D and K) were established for each primer pair, according to the volumes in **Table 2.6**.

Table 2.6. Constituents of each master mix to amplify HPRT mRNA.

		D Master mix	K Master mix	
Reagent	**Supplier**	**Volume (µl)**	**Volume (µl)**	**Final concentration**
5x Buffer	Promega, Southampton, UK	10	10	1X
10mM dNTP mix	Promega, Southampton, UK	1	1	0.2mM each dNTP
25mM Magnesium Chloride	Promega, Southampton, UK	4	4	2mM
D forward primer	MWG Eurofins, Germany	1	0	0.2µM
D reverse primer	MWG Eurofins, Germany	1	0	0.2µM
K Forward primer	MWG Eurofins, Germany	0	1	0.2µM
K reverse primer	MWG Eurofins, Germany	0	1	0.2µM
Go*Taq* DNA polymerase (5u/µl)	Promega, Southampton, UK	0.3	0.3	1.5U
cDNA template	-	2	2	-
Water	-	30.7	30.7	-
Total	-	**50**	**50**	-

Both master mixes ran simultaneously under the conditions given in **Table 2.7** using an icycler (Biorad, Hemel Hempstead, UK). Upon reaction completion, samples were stored at -20°C awaiting purification for DNA sequencing.

Table 2.7. The conditions for amplification with D and K master mixes. The numbers in brackets specify conditions used to amplify β-actin mRNA.

Stage	Temperature (°C)	Time (sec)	Number of cycles
Initial denaturation	93	120	1
Denaturation	93	10	40 (25)
Annealing	52.6 (60)	20	
Extension	72	10	
Preservation	4	Infinity	1

2.10. 6% PAGE.

To verify the success of PCR amplification, 10µl aliquot of reaction mixture was loaded onto vertical 6% PAGE (polyacrylamide gel electrophoresis) gels. The constituents and respective volumes used for 6% PAGE are given in **Table 2.8** which are sufficient for two 7.5cm x 9cm gels.

Table 2.8. Reagents of 6% PAGE gels.

Reagent	Supplier	Volume
Distilled water	-	16ml
10x TBE (Tris/Borate/EDTA)	-	2.3ml
10% APS (ammonium per sulphate)	Sigma	110µl
30% Acrylamide/Bis acrylamide	Biorad	4ml
N,N,N',N'-Tetramethylethylenediamine (TEMED)	Sigma	22.5µl

For 1L of 10x TBE; 108g of Tris (Sigma, Gillingham, UK), 55g boric acid (Sigma, Gillingham, UK), and 40ml of 0.5M EDTA (ethyldiamine tetraacetic acid). For 500ml 0.5M EDTA, 93.05g of EDTA (Sigma, Gillingham, UK) was dissolved in 400ml of water, the pH adjusted with 2M sodium hydroxide and the final volume increased to 500ml with water. Gel construction was as follows; 1.5mm glass plates (Biorad, Hemel Hempstead, UK) were washed with 70% ethanol and assembled in the casting stand supplied. The reagents in **Table 2.8** were premixed and added to the cast. A 15 well comb was inserted and the gel allowed to polymerise for 30min at room temperature. Following successful polymerisation, the comb was removed and the samples pipetted into the wells. 10µl of each sample was premixed with 2µl loading dye supplied with the RETROscript® cDNA syntheis kit. 1µl of 100 base pair (bp) DNA ladder (Promega, Southampton, UK) was mixed with 2µl loading dye and ran on the gel. The gel ran at 170V for 30min using a mini protean® 3 cell kit and a power pac 300 (Biorad, Hemel Hempstead, UK). D primers gave a product of 537bp and K primers gave a product of 715bp. The product bands were visualised by silver nitrate staining.

2.11. Silver nitrate staining.

The stain and developing solution were made up according to **Table 2.9**. Gels were immersed in silver nitrate for 8mins at room temperature, washed twice with distilled water and incubated at room temperature in developing solution with gentle agitation until the bands were visible. A photographic record was kept using a Biorad universal hood II (Biorad).

Table 2.9. Volumes of silver stain reagents used to visualize PCR products on PAGE gels.

	Reagent	Amount	Supplier
Silver stain	0.1% Silver nitrate ($AgNO_3$)	1g	Sigma
	Distilled water	1L	-
Developer	Sodium hydroxide (NaOH)	13.5g	Sigma
	37% formaldehyde (CH_2O)	3.6µl	Sigma
	Distilled water	0.9L	-

2.12. Preparation of samples for sequencing.

The remaining 40µl of PCR product (50µl-10µl for gel analysis) was purified using PCR purification kit® (Qiagen, Sussex, UK). 5x volume (200µl) of buffer PE, with pH indicator, was added to the reaction mixture. None of the samples needed pH adjustments. The solutions were applied to the provided Qiaquick spin columns and centrifuged for 1min at 13000rpm in a Heraeus Biofuge Fresco centrifuge with a radius of 85mm and the flow through discarded. 750µl of wash buffer was added with repeat centrifugation and the flow through discarded. The columns were centrifuged to remove ethanol, present in the wash buffer. 30µl of nuclease free water was added, incubated for 1min at room temperature and eluted by centrifugation. The samples were sent to Genome Enterprise Limited (Norwich, UK) for sequencing. To prevent DNA contamination, all equipment used to package samples were wiped with

DNAaway™ wipes (Molecular Bioproducts, USA). Under the instruction of Genome Enterprise Limited, 20µl of each sample was put into PCR tubes (Fisher Scientific, Loughborough, UK) in supplied sequencing boxes for shipment. 1.5µM D forward and K forward primers were also included in separate tubes in sufficient volume for 5µl per sequencing reaction. Sequencing data were analysed using mutation surveyor 3.3. Any mutations found were confirmed by repeat processing of the second aliquot of RNA.

2.13. Construction of mutation spectrum.

Mutation spectra were constructed using iMARS software, kindly provided by Dr Paul Lewis at Swansea University (Morgan and Lewis, 2006).

2.14. Two step real time PCR.

2.14.1. cDNA synthesis for real time PCR.

cDNA synthesis was performed under the same precautions used in end-point PCR. 1µg of RNA was used in cDNA synthesis using Quantitect reverse transcription kit (Qiagen, Sussex, UK) according to manufacturers instructions. Firstly, RNA was subject to genomic DNA (gDNA) elimination using the reagents in **Table 2.10**.

Table 2.10. Constituent reagents for elimination of genomic DNA from RNA samples.

Reagent	Volume per sample (µl)
gDNA elimination buffer	2
RNA	1000ng
Nuclease-free water	Make up to total volume
Total	**14**

The reagents were vortexed and centrifuged and incubated on an icycle (Biorad, Hemel Hempstead, UK) at 42°C for 2mins, then returned to ice. 6µl of the reverse transcription master mix was added (**Table 2.11**), the tube vortexed, centrifuged briefly and incubated for 15mins and at 42°C.

Table 2.11. cDNA synthesis reaction mixture for real time PCR.

Reagent	Volume per sample (µl)
Reverse transcriptase enzyme	1
Quantiscript buffer	4
Primer mix	1
gDNA elimination step	14
Total	**20**

2µl of the completed reaction mixture was added to one well of the real time PCR plate. Note, **equation 2.8** was used in scaling up the reverse transcription master mix.

Equation 2.8. Volume of reagent = (n+1) (where n=number of samples).

2.14.2. Real time PCR.

Real time PCR was performed immediately after cDNA synthesis under the same laboratory practice. Expression analysis was performed using QuantiFast Probe PCR +ROX Vial Kit (Qiagen, Sussex, UK) and inventoried FAM conjugated Taqman® gene expression assays (Applied Biosystems, Warrington, UK) for MGMT (assay ID; Hs01037698_m1), TBP (assay ID; Hs00427620_m1); an appropriate house keeping gene and GAPDH (assay ID; Hs99999905_m1) for siRNA validation (Chapter 6). The reaction was set up according to instructions provided in the QuantiFast kit. The volumes of reagents in the master mix are given in **Table 2.12**.

Table 2.12. Components of each well of a 96 well plate for real time PCR.

Reagent	Volume per sample well (µl)
Taqman probe	1
QuantiFast buffer	10
Nuclease-free water	7
cDNA sample	2
Total	**20**

To scale the reaction, **equation 2.9** was used.

Equation 2.9. Volume of reagent (n+5) (where n=number of samples).

Real time PCR for each cDNA template was performed in triplicate in separate wells.

To minimise pipetting errors between triplicates, 59.4µl of the master mix was premixed with 6.6µl cDNA sample (allowing 10% excess), vortexed and centrifuged, 20µl was then pipetted into each of three wells. The plates were sealed using microseal B film (Biorad Hemel Hempstead, UK), centrifuged and placed in a MY iQ icycler single colour real time PCR detection system. Thermocycling conditions are shown in **Table 2.13**.

Table 2.13. Conditions for two step real time PCR using Taqman® probes.

Stage	Temperature (°C)	Time (sec)	Number of cycles
PCR initial activation step	95	180	1
Denaturation	95	3	40
Combined annealing/extension	60	30	

2.15. Protein extraction.

A total of $1x10^6$ AHH-1 cells gave approximately 1mg/ml protein yield using RIPA buffer (Sigma, Gillingham, UK). Upon harvest, cells were centrifuged at 1500rpm for 5mins at room temperature, washed twice in PBS to remove inhibitory media components and the pellet re-suspended in 200µl RIPA buffer by brief vortex. The sample was incubated on ice for 5min, vortexed briefly and frozen at -80°C for long term storage. Once defrosted, the samples were centrifuged at 8000rpm for 10min at 4°C in a Heraeus Biofuge Fresco centrifuge, the supernatant was carefully removed and the pelleted insoluble aggregate discarded. The samples were then quantified by use of the Bicinchoninic acid (BCA) assay.

2.16. Protein quantitation.

The BCA assay is colorimetric, measuring absorbance at 562nm (blue/purple), which signifies the reduction of Cu^{2+} to Cu^{+} in the presence of alkaline proteins. A standard curve was constructed (**Table 2.14**) for determination of protein concentration. The maximum concentration of bovine serum albumin (BSA) supplied was 1mg/ml, therefore, dilutions of samples in RIPA buffer were sometimes necessary to fit onto the standard curve. The BCA working reagent was made up of 1ml Reagent A mixed

with 20µl Reagent B until precipitate dissolved. 160µl of the BCA working reagent was added to 20µl sample or 20µl standard per well of a 96 well plate (Nunc, ThermoScientifc, Loughborough, UK).

Table 2.14. Dilution of BSA protein standard.

Concentration of BSA standard (µg/ml)	Volume of protein standard (µl)	Volume of RIPA buffer (µl)
1000	20	0
800	16	4
600	12	8
400	8	12
200	4	16
0	0	20

The plate was sealed using nescofilm and incubated at 37°C for 30min. Absorbance was measured using a polarstar luminometer. The concentration of protein in each sample was determined from the standard curve using **equation 2.10**.

Equation 2.10 y=mx+c re-arranged for x, x=(y-c)/m

Where,
y=absorbance of sample
m=gradient of graph
x=concentration of sample (µg/ml)
c=y-axis intersect.

2.17. Western blotting.

Investigations into MGMT protein levels were made by western blot. All antibodies were purchased from Abcam (Cambridge, UK). These were;

- Mouse monoclonal antibody to MGMT (ab39253)
- Mouse monoclonal antibody to β-actin loading control (mAbcam 8226)
- Rabbit polyclonal secondary antibody to mouse IgG-HRP (horse radish peroxidsase) conjugated (ab6728).

2.18. SDS-PAGE.

1.5mm glass plates were washed with 70% ethanol and assembled vertically in a casting stand. The constituents of the resolving gel (**Table 2.15**) were premixed and added to the cast leaving ~2cm for the stacking gel. 1ml of propan-2-ol (ThermoScientific, Loughborough, UK) was added immediately to the top of the resolving gel and left to polymerise at room temperature for 30mins. The layer of propan-2-ol was removed and the stacking gel applied (**Table 2.15**). A 10 well comb was inserted and the gel left to polymerise for 30min at room temperature. After which time, the comb was removed and the gel removed from the casting stand and assembled in the electrode assembly kit filled with running buffer at 4°C. The optimum amount of protein loaded per well was found to be 40µg. The volume of sample required for 40µg protein was mixed in a 1:1 ratio with Laemmli buffer (Sigma, Gillingham, UK), vortexed, centrifuged and incubated at 95°C for 5min using heatblock. 5µl Western C molecular weight marker (Biorad, Hemel Hempstead, UK) was added to the first lane, 10µl Dual Colour standard (Biorad, Hemel Hempstead, UK) was added to the second and tenth lane. 40µg of protein was added to respective wells and the gel run at 120V for 90min at 4°C.

Table 2.15. Constituents of SDS-PAGE for separation of extracted protein.

	Volume (ml)	
Reagent	**Stacking Gel**	**10% Resolving Gel**
30% Acrylamide	0.65	5
Distilled water	3	6
1.5M Tris (pH8.8)	-	3.75
1M Tris (pH6.8)	1.25	-
10% sodiumdodecylsulfate (SDS)	0.05	0.15
10% ammonium persulfate (APS)	0.025	0.075
N,N,N',N'-Tetramethylethylenediamine (TEMED)	0.005	0.015

2.19. Protein blotting.

Proteins separated by SDS-Page were transferred to Immuno-blot Polyvinylidene fluoride (PVDF) membrane (Biorad, Hemel Hempstead,UK) pre-soaked in 100%

methanol (ThermoScientific, Loughborough,UK). The stacking gel was separated from the resolving gel and discarded. The gel, PVDF membrane, 2x fibre pads and 2x blot paper were soaked in transfer buffer pre-cooled to 4°C. The transfer cassette was assembled ensuring there were no air bubbles between the gel and membrane. The cassette was put into the electrode assembly and run at 400mA for 90min at 4°C. Upon completion, the membrane was washed in TBS/T buffer (see section 2.22) and the membrane cut to separate the Western C ladder in the first lane for separate antibody incubations. The membrane was cut according to the bands of Dual colour standard. MGMT has a molecular mass of 22KDa and so the membrane was cut either side of 10KDa and ~30KDa. β-actin is 44 KDa and the membrane was cut either side of 37KDa and 75KDa.

2.20. Membrane blocking and antibody dilutions.

To reduce background noise, 0.5% milk in TBS/T was used as the blocking buffer. Membranes were immersed in blocking buffer and left for 1hr at room temperature with gentle agitation. Blocking buffer was removed and membranes probed with 1:1000 of respective primary antibody in dilution blocking buffer. The Western C membrane remained in blocking buffer. The membranes were left overnight at 4°C with gentle agitation. The primary antibody was removed and the membranes washed four times with vigorous shaking for 5min in TBS/T. HRP-conjugated secondary antibody, diluted 1:1000 in blocking buffer, was added to MGMT and β-actin sample membranes and incubated with gentle shaking for 1hr at room temperature. Western C membranes were incubated under the same conditions with StrepTactin-HRP (Biorad, Hemel Hempstead, UK) conjugate diluted in blocking buffer. The secondary antibody was removed following repeated washing with TBS/T as described.

2.21. Protein detection.

Protein bands were detected using Immun-Star Western C chemiluminescent kit (Biorad, Hemel Hempstead) according to manufacturers instructions. Luminol/enhancer solution was mixed with equal volume of peroxide buffer and kept

out of light. The membranes were immersed for 1min with vigorous shaking, the excess removed and visualised using a ChemiDoc XRS (Biorad, Hemel, Hempstead, UK). On manual exposure, 2sec was sufficient to detect β-actin whereas MGMT required up to 3min.

2.22. Western blot reagents.

10% (W/V) Ammonium persulfate (APS)-1g APS diluted in 8ml distilled H_2O, volume adjusted to 10ml by addition of dH_2O.

10%(w/v) sodium dodecylsulfate (SDS)-25g SDS dissolved in 200ml dH_2O and the volume increased to 250ml by distilled H_2O.

1.5M Tris (pH 8.8)-45.4g Tris dissolved in 150ml water adjusted to pH 8.8 by addition of 10M hydrochloric acid (HCl) and the volume increased to 250ml by distilled H_2O.

1M Tris (pH 6.8)-30.3g Tris dissolved in 150ml water adjusted to pH 6.8 by addition of 10M HCl and the volume increased to 250ml by distilled H_2O.

10x Running buffer-30.3g Tris, 144.1g Glycine, 100ml 10% (w/v) SDS in 800ml water adjusted to 1L by addition of distilled H_2O.

1x running buffer-100ml of 10x buffer and 900ml distilled H_2O.

Transfer buffer-100ml 10x running buffer, 200ml 100% methanol, 700ml distilled H_2O.

10x TBS-24.2g Tris, 80.1g NaCl dissolved in 800ml dH_2O, pH adjusted to 7.6 by 10M HCl and volume increased to 1L by distilled H_2O.

TBS/T wash buffer-100ml 10x TBS, 10ml 10% (v/v) Tween20 and distilled H_2O to 1L.

0.5% milk blocking buffer-0.5g Semi skimmed milk powder dissolved in 80ml TBS/T adjusted to 100ml once dissolved.

Chapter 3.

Dose-response Modeling.

Dose-response For Mutation Induction By Low Dose MNU In Human Cells.

3.1. Introduction.

The following chapter highlights the hypoxanthine (guanine) phosphoribosyl transferase [H(G)PRT] forward mutation assay as an important sensitive test system used for assessing mutation induction at low doses of exposure to mutagens. The HPRT assay has well-established guidelines (OECD 476, 1997). The end result of the assay is the mutant frequency (MF), which dictates the frequency of HPRT mutants in a population of cells. A mutagen gives a positive result, which is observed as a statistically significant increase in MF over the untreated and solvent control (OECD 476, 1997). The assay is specific enough to correctly identify a wide range of mutagens. The assay can identify agents that cause base substitutions or small deletions at the HPRT gene, whereas major changes in the X chromosome, where HPRT gene is located, are lethal and cannot be detected. The assay can be run in a number of mammalian cell lines including hamster V79 and CHO cells. However, with considerable impetus for the use of human cell lines as a model of hazard identification in human populations (Hawksworth, 1994), the HPRT assay is used in human cell lines such as TK6 and AHH-1 and in isolated lymphocytes in bio-monitoring studies. Fowler *et al* (2012a) provide impetus for using human cell lines for specific and sensitive assessment of genotoxic potential over rodent cell lines.

3.1.1. HPRT as a mutation sensor.

Located on the X chromosome in mammalian cells, Xq26-27 (Pai *et al*, 1980), the *HPRT* gene is hemizygous; it is present as only one allelic copy in male cells, whereas in female cells, due to imprinted silencing of the second X chromosome (Ahn and Lee, 2008), only one *functional* copy exists. Therefore, it is designated HPRT+/o. This means that, unlike autosomal genes, a second allele does not compensate for recessive changes in the first allele. As a result, this locus is more sensitive to phenotypic alteration. The *HPRT* locus has been used as a surrogate mutation sensor for other important loci like p53 (Dobrovolsky, Shaddock and Heflich, 2005). Caution is urged as different loci may have different mutation rates (Hodgkinson and Eyre-Walker, 2011). Impaired HPRT protein function, through non-synonymous mutations within the protein coding region, will confer resistance to a toxic agent (a toxic

analogue of guanine). This means HPRT mutants gain a growth advantage (DeMarini *et al,* 1989). Therefore, use of simple selective media allows the differentiation of HPRT deficient (-/o) from HPRT proficient (+/o) cells and vice versa. An inherent disadvantage of this and other mutation assays, which select for loss of protein function, is that synonymous/silent mutations that change DNA sequence but not protein function will be missed.

3.1.2. HPRT function in wildtype cells.

Functional HPRT is a housekeeping enzyme (EC 2.4.2.8) found in the cytoplasm where it contributes to the salvage pathway, one of two biosynthetic pathways that produce purines for RNA and DNA biosynthesis. The pathways are;

1. *De novo* synthesis (synthesis from simple molecules)-A metabolically expensive, 10 enzyme pathway that synthesises purines from the sugar 5'phosphoribosyl-1-pyrophosphate (PRPP).
2. Salvage pathway-HPRT recycles degraded DNA bases into usable purine nucleotides. 90% of free purines in mammalian cells are recycled (Rossiter and Caskey, 1995). The salvage pathway is the main purine biosynthetic pathway in erythrocytes because they are deficient in the *de novo* pathway for synthesis of purines, such as adenosine triphosphate, ATP used as an energy source (Fontelle and Henderson, 1969).

3.1.2.1 Intracellular purine biochemistry: the salvage pathway involves HPRT.

The role of HPRT in the condensation of PRPP and guanine or hypoxanthine into guanosine monophosphate (GMP) and inosine monophosphate (IMP) is shown in **Figure 3.1**. The reaction, featuring the ribosylation of guanine where PRPP acts as a ribosyl donor, is influenced by magnesium (Mg^{2+}). HPRT binds to PRPP and then guanine or hypoxanthine, forming a temporary intermediate. Following the transfer of phosphoribosyl to guanine; pyrophosphate is released as a by-product, giving IMP or GMP for DNA or RNA synthesis.

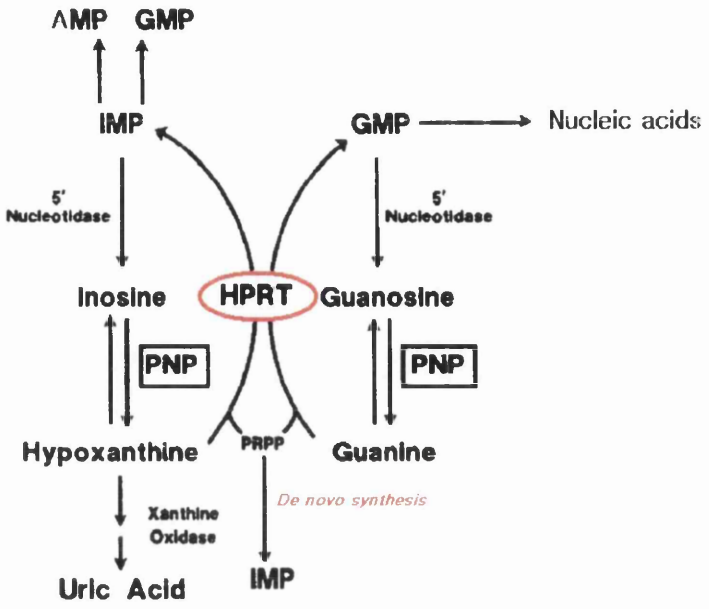

Figure 3.1. Purine recycling through the salvage pathway, HPRT (Hypoxanthine phosphoribosyl transferase) is circled. Adapted from Stout and Caskey (1985).

3.1.2.2. *De novo* purine synthesis.

PRPP serves as the starting point for the main purine biosynthetic *de novo* pathway. This involves 10 steps, culminating in the production of IMP that can form adenosine monophosphate (AMP) or GMP (**Figure 3.2**). This is the default pathway in most mammalian cells but it is energetically expensive. The salvage pathway compensates when the *de novo* synthesis pathway is inhibited (see section 3.1.4.1). Purine metabolism and its influence on DNA synthesis is a target for chemotherapy (Riscoe *et al*, 1989).

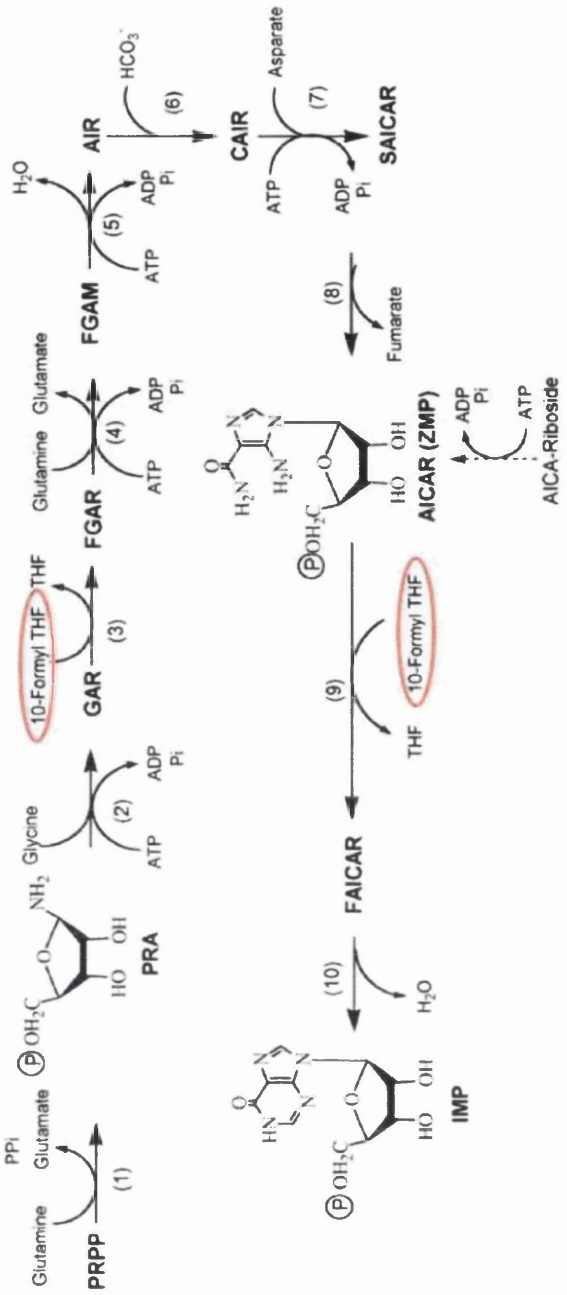

Figure 3.2. Purine biosynthesis via the de novo pathway. PRPP, the ribosyl donor in the salvage pathway initiates the process. Increased PRPP concentration in HPRT deficiency syndromes increases de novo throughput. 10-formyltetrahydrofolate (circled in red) acts as a formyl (CHO) donor for two reactions. Without this donor this pathway does not function. This forms the basis of selection for HPRT+/o cells that use the salvage pathway to overcome loss of nucleotide synthesis through de novo pathway. Image manipulated from Ashihara and Suzuki (2004).

3.1.3. Exploiting HPRT for mutation analysis.

The use of readily available media supplements can distinguish HPRT mutants from wildtype cells allowing easy quantitation of mutant frequency and mutagenic potency. Commonly used supplements are;

1. HAT, a combination of Hypoxanthine, Aminopterin and Thymidine that allows HPRT+/o wildtype cells to survive. Used to remove existing mutants from the population at the start of the assay
2. 6-Thioguanine, a toxic purine analogue that allows HPRT-/o cells to survive.

3.1.4. Selection procedures for isolation of mutant or wildtype HPRT.

3.1.4.1. Using HAT supplement to select for HPRT+/o wildtype cells.

Media supplemented with HAT will block *de novo* purine synthesis (**Figures 3.2** and **3.3**). This forces cells to use the salvage pathway to provide purines for DNA synthesis. Cells deficient in HPRT (through loss of heterozygosity (LOH) mutations) will be unable to synthesise purines, when grown in HAT media and undergo apoptosis through an unknown mechanism possibly involving *c-myc* proto-oncogene expression (Chung *et al*, 2001). At the start of the HPRT assay HPRT mutants are removed, increasing the sensitivity of the assay to chemical mutagenesis, an advantage held over other loci such as *lacI* in transgenic mice (Skopek, Kort and Marino, 1995). Aminopterin, present in HAT supplement, was used as an antileukemic drug (Farber and Diamond 1948). Like other chemotherapeutic antimetabolites such as methotrexate (Kinsella, Smith and Pickard, 1997), it targets enzymes to inhibit synthesis of DNA building blocks thereby limiting a cell's capacity to divide. Aminopterin competes with folic acid for the active site of dihydrofolate reductase (DHFR, **Figure 3.3**), an enzyme that converts folic acid into cofactors essential for enzymes in *de novo* biosynthesis (Huennekens *et al*, 1963). Once bound to the active site, aminopterin will inhibit this enzyme and deplete intracellular pools of nucleotides, affecting DNA strand synthesis during S phase of the cell cycle, ultimately limiting cell division (Tsurusawa *et al*, 1990). The end product is 10-formyltetrahydrofolate that serves as a formyl (CHO) donor at two steps of the 10 steps of the *de novo* synthesis pathway (**Figure 3.2**). Without 10-formyltetrahydrofolate, *de novo* synthesis shuts down and only cells proficient in

HPRT will be able to synthesise nucleotides and proliferate. DHFR inhibition also leads to the loss of thymidine/deoxythymine, a pyrimidine nucleotide whose loss is toxic to all cells. This is provided in HAT as thymidine. Incidentally hypoxanthine in HAT is supplied as a substrate for HPRT mediated purine synthesis. Both additives maintain the growth of HPRT+/o cells.

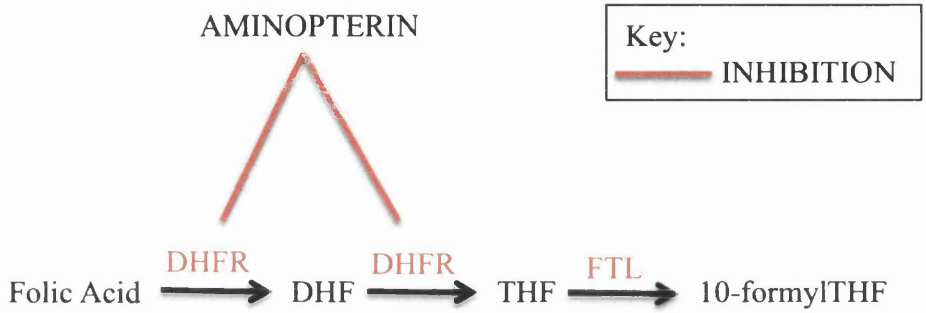

Figure 3.3. Part of the human folate metabolism pathway. The enzyme DHFR (dihydrofolate reductase) is inhibited by aminopterin. The end product, 10-formylTHF donates formyl (CHO) groups to intermediates of the *de novo* purine biosynthetic pathway (**Figure 3.2**). Without this, purine biosynthesis can only occur through HPRT and the salvage pathway. DHF; dihydrofolate, THF; tetrahydrofolate, FTL; formate-tetrahydrofolate ligase. Constructed from Lightfoot *et al* (2005) and Vickers *et al* (2009).

3.1.4.2. Counter selection; toxic analogues are used to select for HPRT -/o mutants.

A particular attraction to this locus is the ability to select for HPRT mutants as well as wildtype cells, as previously discussed. When selecting for mutants, only cells deficient in HPRT will survive. This is achieved through use of a guanine analogue; it is converted into a toxin only if HPRT is functional, thereby killing wildtype cells. 8-azaguanine was commonly used as a guanine analogue for selecting HPRT mutants (Arlett *et al*, 1975). However, van Diggelen *et al* (1979) report that 8-azaguanine is a poor substrate for HPRT. Wildtype HPRT shows higher affinity for 6-TG over 8-azaguanine (Cellela *et al*, 1983) offering a more stringent mutant selection. Therefore,

the assay featured in the following work uses 6-thioguanine (6-TG) as the most stringent selective agent.

3.1.5. Mechanism of 6-Thioguanine toxicity in wildtype HPRT cells.

Once 6-TG enters the cell it is firstly converted to 6-thioguanine monophosphate (6-TGMP), which inhibits purine biosynthesis by;

1. Pseudo feedback inhibition of amidophosphoribosyl transferase, the first enzyme of *de novo* purine biosynthesis
2. IMP dehydrogenase inhibition.

These effects shutdown all sources of purine nucleotides, meaning a higher probability that 6-TGMP will be incorporated into nucleic acids. 6-TGMP is then phosphorylated and is incorporated into DNA (Nelson *et al*, 1975) (**Figure 3.4**). Ling *et al* (1992) propose that the presence of 6-TG in the template strand of DNA blocks polymerase extension. Balajee and Geard (2004) identified Replication protein A (RPA) and γ-H2AX foci at the site of replication blockage. These proteins are involved in the repair of double stranded breaks (DSBs), a highly cytotoxic lesion. Therefore, it is possible that their presence as foci indicates that DSBs are a possible outcome of replication blockage by 6-TG. In addition to DSBs as a method of cell killing by 6-TG; Yan *et al* (2003) propose that mismatch repair (MMR) has a role. The authors questioned the role of futile MMR processing in introducing persistent single stranded breaks, which lead to G2-M triggered apoptosis. The authors found significant increases in ssDNA breaks occurred in MMR+ cells than in MMR- following treatment of 6-TG. This model of 6-TG toxicity has important implications. This agent would only suffice as a selective agent if the host cell was proficient in MMR and G2-M checkpoint control. The ability to counter select for wildtype or HPRT mutant strains has allowed investigators to calculate reversion rates at this locus (Yang *et al*, 1988), however this hasn't been determined in AHH-1 cells. Selection strategies are summarised in **Figure 3.5**.

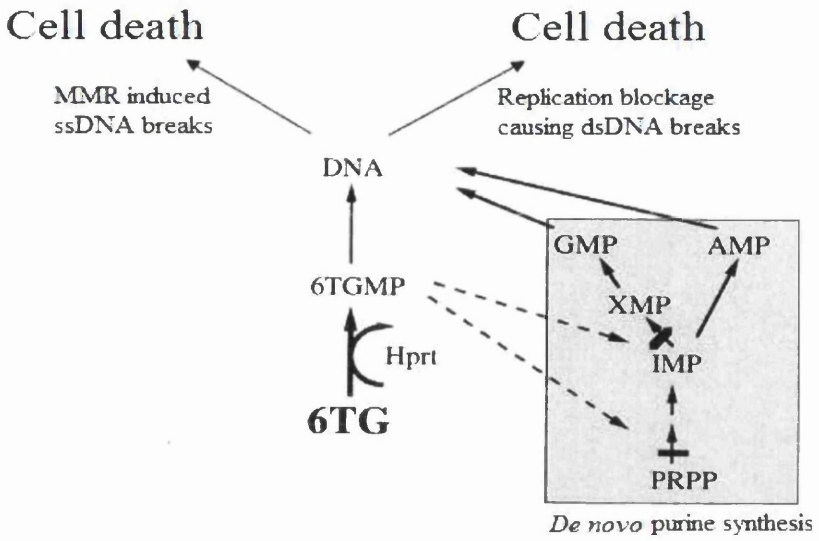

Figure 3.4. Metabolism of 6-thioguanine (6-TG) in HPRT wildtype cells. 6-TG is converted into its monophosphate form, 6-TGMP, that inhibits *de novo* purine synthesis and is incorporated into DNA leading to cell death. Cells deficient in HPRT will not metabolise 6-TG and will survive. Modified from Aubrecht *et al* (1997).

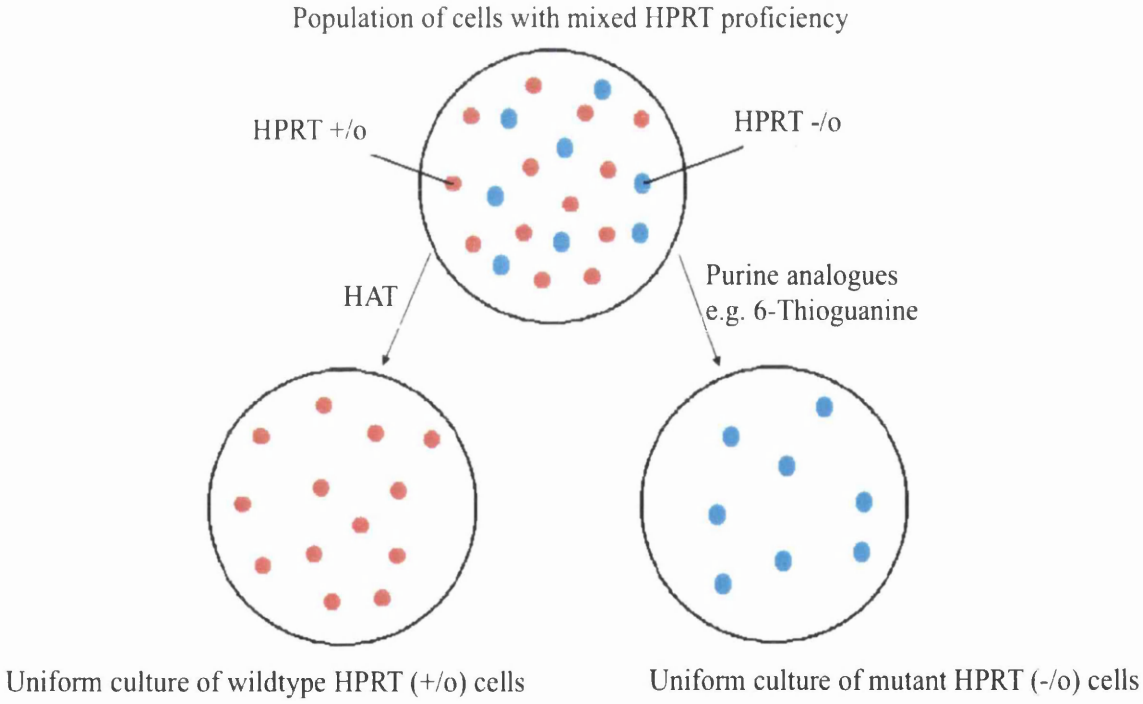

Figure 3.5. A schematic of the selective agents used to unify a population based on the cell's HPRT proficiencies.

3.1.6. Alternative HPRT proficiency selection strategies.

Supplemented media is the easiest and most effective way of HPRT selection. However, other methods exist. Dorman *et al* (1978) report the positive selection through autoradiographic analysis following tritium labelled hypoxanthine ([^{3}H]hypoxanthine) incorporation into cells proficient in HPRT.

3.1.7. Outline of HPRT assay methodology.

The HPRT assay has been described in AHH-1 cells by Crespi and Thilly (1984). The assay has three important stages; mutant cleansing, treatment with test article, followed by selection for mutants and quantitation. A schematic is shown in **Figure 3.6**.

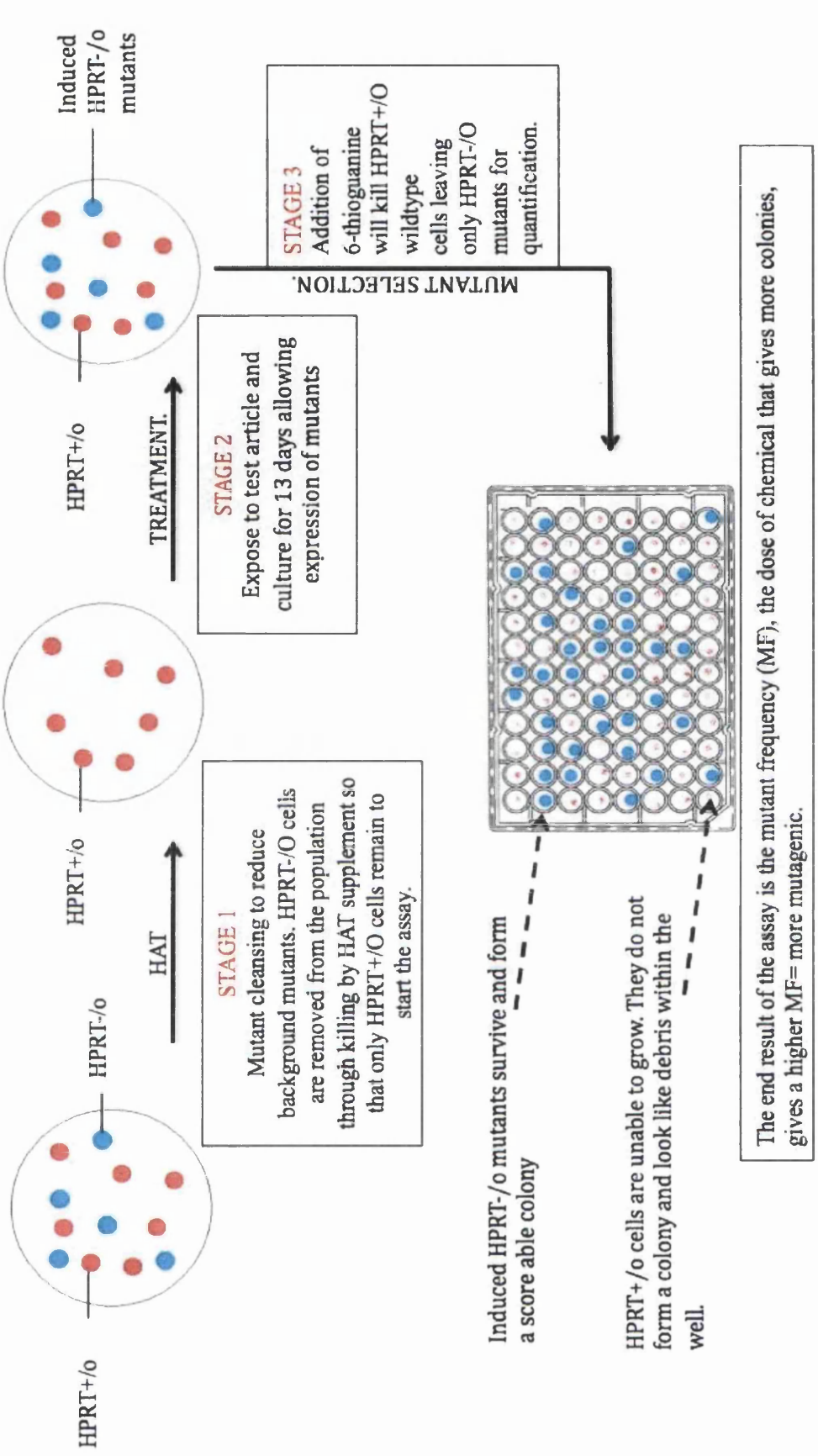

Figure 3.6. Representation of the method employed in the HPRT assay to quantify the mutagenic potential of a test article based on frequency of HPRT mutants in a treated population.

3.1.7.1. Stage 1-Mutant cleansing, Reducing the background HPRT-/o mutants.

The mutagenic potential of a test article is only realised once the mutant frequency (MF) at a certain dose is compared to that of the untreated control, as previously stated. The untreated control is vitally important. It infers the background level of MF that occurs, the result of spontaneous DNA damage, under the conditions of the assay. If the background is high then an increase in MF may not be significant and a mutagen could be misclassified. It is therefore essential that the assay has a low and stable background level. This is achieved through use of HAT supplemented media. See section 3.1.4.1. Only cells capable of salvage synthesis of purines (HPRT+/o) will survive, mutant cells (HPRT-/o) cannot survive. This lowers the existing level of mutants, lowering the background to 1-100 mutant cells in a population of 10^5 cells (this is further discussed in section 3.3.1). Thus, increasing the sensitivity of the assay. Cells are then given four days growth under normal conditions to ensure sufficient cell numbers for treatment.

3.1.7.2. Stage 2-Treatment with test article and sub-culturing.

Cells are diluted and exposed to a range of concentrations of the test article under the instructions given in OECD guideline 476 (1997). These being;

1. Concentrations should not be more than 2 to $\sqrt{10}$ units to a maximum of 5000mM, solubility limit or 50% cytotoxicity (LD_{50}) measured by replicative plating efficiency (RPE) for the HPRT assay
2. An appropriate diluent (solvent) as given in the Merck index or in the manufacturer's recommendations. The solvent used must; "be compatible with the survival of the cells," not induce mutations giving an increase in MF over the spontaneous MF and it must not react with the test article
3. Cells are left in the presence of test article for up to 24hr. Shorter exposure strategies are adopted if an enzyme/rat liver (S9) mix is used. This mix is highly mutagenic after 4hr but it is necessary for metabolism of the test article into its respective end products for testing. Genetically modified cell lines like MCL-5, a derivative of AHH-1, possess limited metabolism to overcome the use of S9.

Following removal of the test article after the appropriate exposure strategy, the cells are cultured for 13 days. The initial cell divisions fix the resulting DNA damage into permanent mutations if not repaired prior to cell division, possibly changing the structure and/or function of the resulting HPRT protein. The remainder of the 13 days gives time for the mutant non functional HPRT to replace the wildtype HPRT within the cell, effectively becoming HPRT-/o. Diamond *et al* (1982) identified an optimal expression period of 4-5 days post treatment only in Syrian hamster embryo cells. Grosovsky and Little (1983) state that a maximum mutation frequency was reached 9 days post treatment, which remained stable up until 17 days. At alternating days the cells are diluted in fresh media, to replenish the nutrients, giving a cell concentration that will repopulate but not outgrow the culture.

3.1.7.3. Stage 3-Selection for mutants and quantitation.

The population at this stage contains wildtype (HPRT+/o) and mutant (HPRT-/o) cells, resulting from spontaneous mutagenesis and induced damage following genotoxin exposure. The next process is to isolate HPRT-/o cells for propagation and colony counting. This is achieved through use of 6-TG that becomes toxic when catalysed by HPRT in HPRT+/o cells. (See section 3.1.4.2). Cells are diluted and pipetted into 96 well plates in the presence of 6-thioguanine. Each well represents an independent observation. Increasing the number of observations greatly increases the statistical power required for threshold analysis (Doak *et al*, 2007). A colony represents a HPRT-/o cell as one colony is derived from one cell and only HPRT-/o mutant cells will grow.

3.1.8. Why use the HPRT assay?

3.1.8.1. Alternative *in vitro* mutation assays.

There are a number of mutation assays that quantify MF at different loci. Consequently, each has a unique way of distinguishing mutant from wildtype cells. Sensitivity and specificity depend on the stability of the host cell genome. In a report by Kirkland *et al* (2005), the bacteria based mutation assay (Ames assay) is only

sensitive enough to detect 58.8% of known genotoxins, far inferior to a combination of three mammalian cell based assays (73.2%). However the reverse is true if specificity of the assay is examined. The Ames assay correctly identified 73.9% of non-carcinogens as negative compared to 39% in mammalian cell based assays. Therefore one test does not give sufficiently robust sensitivity and specificity. A battery of three assays is used to predict genotoxicity by regulatory bodies. However, in our mechanistic studies only one assay needs to be used because the results will not be used to predict genotoxicity in a regulatory sense (Kirkland, *et al*, 2007). **Table 3.1** highlights the most popular alternatives to the HPRT assay and their relative advantages and disadvantages.

Table 3.1. Some alternative assays to the HPRT assay available for genotoxicity testing.

Assay	Description	Advantages	Disadvantages
Ames	A bacteria-based assay that measures reversion mutations that restores the host's ability to synthesise certain amino acids, which are lacking from the culture media.	Included in the battery of *in vitro* tests used. **Has a well-defined OECD guideline.**	**Only applicable in bacterial hosts.** Can only evaluate base substitutions or frameshifts. **Cannot mimic genomic organisation or metabolism found in eukaryotes.**
Pig-a	Fluorescently labeled antibodies identify wildtype cells as GPI linked surface marker (CD58) positive. Knockout mutants cannot synthesise CD58 and do not fluoresce.	Rapid screening by flow cytometry. **Rapid turnaround of results.** Can be used *ex vivo*.	**Not yet OECD validated.** Source of PigA mutants have not been identified (point mutations, deletions etc).
Tk Assay	Same principle as the HPRT assay but at the thymidine kinase (TK) locus involved in pyrimidine biosynthesis. Trifluorothymidine (TFT) is used for mutant selection in an analogous way to 6-thioguanine.	**Detects larger effects such as recombination, nondisjunction and large deletions.** Can be used *ex vivo*.	**Higher background than HPRT assay in our laboratory (Doak *et al*, 2007).**

3.1.9. HPRT assay in mutation research.

Simple and effective procedures to discriminate and quantify HPRT mutants from HPRT wildtype cells have lead to the assay being employed in mutation research. Three features of HPRT biology have attracted scientists for its use in mutation quantification. These being;

1. The gene is present as only one true or functional copy in males or females, respectively, making this locus sensitive to recessive mutagenesis.
2. It is a non-essential enzyme in cell culture as purines can be provided through *de novo* synthesis meaning cells can survive with both HPRT copies lost.

The HPRT assay is able to quantify point mutations and small deletions or insertions at the *HPRT* locus. More drastic changes to the X chromosome are lethal and mutants will not be recovered. However, only missense or nonsense point mutations that cause amino acid substitutions to adversely affect HPRT function will be detected. Methyl nitrosourea (MNU), used in this thesis, induces pre-mutagenic adducts including O^6MeG a miscoding lesion that leads to GC→AT point mutations that will be detected in the HPRT assay if it alters HPRT function. Silent mutations will not be recovered, a commonality between all mutation assays that rely on phenotypic alterations. This is acceptable because silent mutations are not biologically relevant

Biomonitoring and long exposure studies have used *HPRT* in human blood cells as an *in vivo* sensor for mutations, predicting cancer and genetic disease (Albertini *et al*, 1993).

The *HPRT* locus has proved useful in identifying mutations arising;

- Spontaneously and between individuals (Lichtenauer-Kaligis *et al*, 1995)
- Over many population doublings in various cell lines with varying proficiency of MMR (Glaab and Tindall, 1997)
- From occupational/environmental exposure (da Cruz and Glickman, 1997) and lifestyle factors such as smoking (Curry *et al*, 1999)
- Following disasters such as the Chernobyl incident (Moore *et al*, 1997)
- As a side effect of cancer treatment (Dempsey, Seshadri and Morley, 1985; Ammenheuser *et al*, 1991)
- During leukaemogenesis (Finette *et al*, 2001)
- From exposure to test chemicals in stage 1 and stage 2 genotoxicity tests.

Lymphocytes isolated from blood sampled from individuals are models for the *in vivo* condition. They are easy to isolate but are short lived *in vitro*. To overcome this problem, scientists use the clonal assay whereby cells are stimulated to divide by an appropriate mitogen such as phytohaemagglutinin (PHA) that stimulates T cell mitosis (Pistoia *et al*, 1982). This has been useful in biomonitoring studies but not so useful in stage 1 genotoxicity testing, where the demand for cells would exceed supply. Here, the use of continually growing immortal cell lines is required. It is advantageous to carry out *in vitro* work using cell lines of human origin (Hawksworth, 1994). For this reason human lymphoblastoid cell lines such as AHH-1 and TK6 are used in the HPRT assay.

3.1.10. HPRT assay has been used to determine the dose-response of alkylating agents.

Methyl-*N*-nitrosourea (MNU), ethyl methanesulfonate (EMS) methyl methanesulfonate (MMS) and ethyl nitrosourea (ENU) are four representative alkylating agents in use to elucidate low dose genotoxoicity. Alkylating agents are mutagenic by adding alkyl groups to a variety of nucleophilic centres in DNA (nitrogen and oxygen of the bases and phosphate of the backbone). Thus, producing an array of alkyl adducts (adduct spectra). The predominant adducts are O^6-methylguanine (O^6MeG), N7-methylguanine (N7MeG) and N3-methyladenine (N3MeA). Each adduct has different consequences to DNA. For example, a O^6MeG has miscoding potential and causes GC→AT transitions unless repaired by MGMT. Whereas N7MeG and N3MeA, are clastogenic and responsible for EMS induced low dose micronuclei frequencies (Zair *et al*, 2011). The proportion of each adduct in the adduct spectra is determined by the electrophilic potential of the alkylating agent and is indicative of the likely mode of action (mutagenic or clastogenic). MNU used in this study, produces 20 times more O^6MeG than MMS and is consequently, 20 times more mutagenic (Singer, 1980).

It was previously thought that alkylating agents elicited a linear dose-response even at low doses since they abide by the "one-hit" hypothesis as discussed in Chapter 1. Recently, with the contamination of Viracept® with low levels of EMS (Gerber and Toelle, 2009), there has been renewed impetus for strong scientific evidence to establish low dose effects of model alkylating agents as representatives of structurally

and mechanistically similar genotoxic impurities (Muller *et al*, 2006). Although, currently, each chemical is assessed on a case-by-case basis. Concluding a safe-level of exposure requires substantial data, robust statistical modeling and evidence of an underlying biological mechanism. The work conducted at Swansea University by Doak *et al* (2007) established an *in vitro* NOEL for EMS for mutation and micronuclei induction. A further study by Zair *et al* (2011) identified DNA repair as the potential mechanism behind the NOEL. This data, together with necessary *in vivo* evidence has been used to clarify an acceptable level of EMS exposure with no/negligible risk (Gocke and Muller, 2009;Gocke *et al*, 2009;Pozniak *et al*, 2009;Muller *et al*, 2009;Gocke and Wall, 2009). The aim of this study is to assess the low dose effects of MNU, to elucidate a NOGEL at concentrations 10-fold lower than previously tested in the laboratory (Doak *et al*, 2007). *In vitro* work alone is not appropriate to justify safe exposure levels, due to the uncertainty factors from *in vitro* to *in vivo* extrapolation. However, *in vitro* studies can provide:

- Initial characterisation of the dose-response prior to *in vivo* work
- Invaluable mechanistic data to determine the mechanism of genotoxic action of carcinogens.

It is hoped that with ever-increasing evidence from *in vivo* studies (Lynch *et al*, 2011) the true low dose effect of MNU exposure can be ascertained, which would have implications in assessing risk to direct-acting genotoxins of similar chemistry to MNU.

3.2. Results.

The HPRT assay was performed in AHH-1 cells to examine low dose effects of MNU at 10-fold lower concentrations than previously tested by Doak *et al* (2007). The dose-response was constructed and the shape determined by sophisticated statistical modelling described by Johnson *et al* (2009) and Gocke and Wall (2009).

3.2.1. MNU dose-response.

Plating efficiency (PE) of treated cultures normalised to control was used as the standard measure of toxicity in the HPRT assay (Duthie *et al*, 1995; Kulling *et al*, 1997) based on colony forming ability of cells when inoculated into a 96 well plate without 6-thioguanine (non-selective conditions). The dose-range utilised here, was

limited by the dose of chemical that caused 50%+/-5% reduction in cell viability compared to the negative control. The highest concentration of 0.075μg/ml MNU induced 40+/-5% toxicity (**Figure 3.7**). This is within the acceptable range for testing, as dictated in the OECD guideline 486 (OECD, 1997). A two-tailed t-test compared PE of each dose to PE of solvent control. The only statistically significant difference was a decrease in PE at 0.075μg/ml (p=0.007), which was expected.

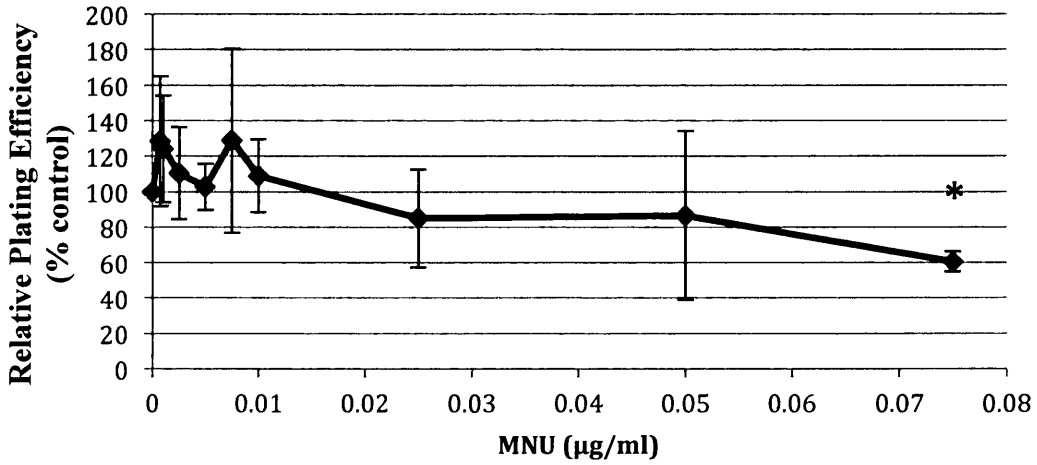

Figure 3.7. Plating efficiency relative to control was used to assess the ability of cells to grow in 96 well plates alongside plates to assess mutant frequency. The solvent control (DMSO) is shown here. In comparison, the untreated control showed 92.3+/-18.2% PE. Therefore, DMSO had no great effect on PE. n=3, error bars signify standard deviation (SD), * p=<0.01.

The frequencies of HPRT mutants were plotted against increasing concentrations of MNU (**Figure 3.8**). It was noted that the mutant frequency (MF) of the solvent control is indistinguishable from the untreated control. The MF being; $1.4x10^{-5}$+/-$1.8x10^{-6}$ (Mean +/-standard deviation) and $1.4x10^{-5}$+/-$3.2x10^{-6}$, respectively. A One-Way ANOVA revealed that they were not significantly different (p=0.952). Since DMSO is not known to be mutagenic, they both represent the spontaneous HPRT MF in a wildtype AHH-1 population.

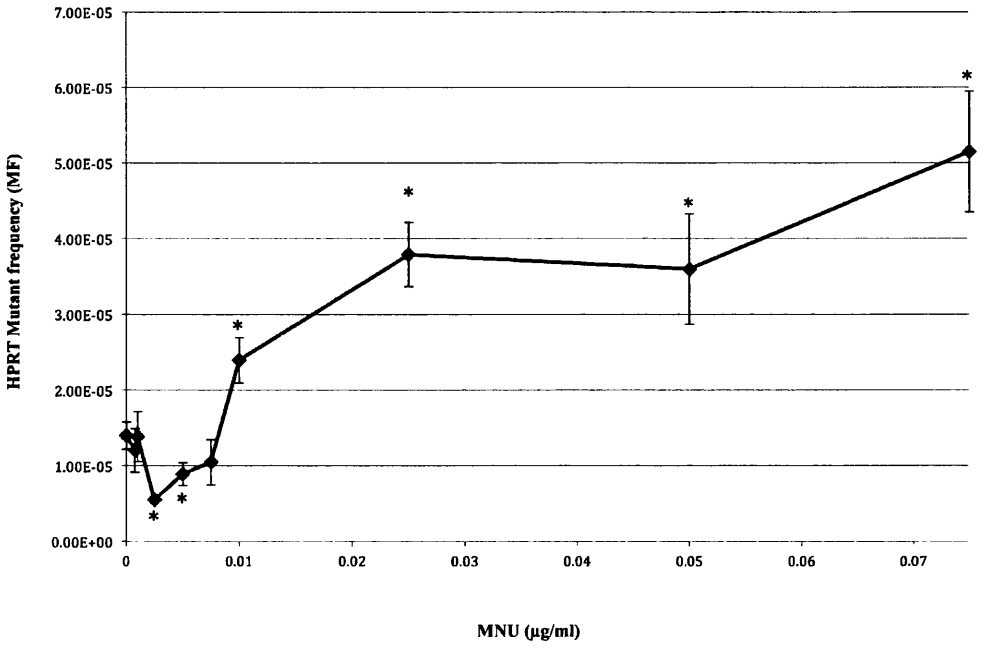

Figure 3.8. Non-linear dose-response of MNU in AHH-1 cells quantified through the HPRT assay (solid line). n=3, error bars indicate SD, *p=<0.001.

The dose-response (**Figure 3.8**) resembles that of a J-shaped curve, indicative of hormesis where the lowest doses have the opposite effect to higher doses (Davis and Svendsgaard, 1990). The MF remains constant up to 0.001µg/ml MNU, but is significantly lower at 0.0025µg/ml, an average of $5.52x10^{-6}$+/-$2.1x10^{-7}$ of three replicates. This was significantly lower than the spontaneous level (p=0.003) using the t-test as recommended by Gaylor, Lutz and Conolly (2004). Using the author's terminology, 0.0025µg/ml MNU is the dose showing minimum response (d_m). Square root transformation of the data accounted for the heterogeneity of the variance, which became normally distributed under the Kolmogorov-Smirnov test. A two-sided Dunnett's test on transformed data revealed that 0.0025g/ml (p=0.005) and 0.005µg/ml (p=0.000) were significantly lower than the solvent control. The MF increases to the zero equivalent dose at approximately 0.0075µg/ml. At 0.01µg/ml and above, there are statistically significant increases in MF over the spontaneous frequency at higher doses of MNU.

3.2.2. Statistical analysis.

Calculation of the MF is based upon the assumption that the variance in number of colonies between replicate plates is equal to the mean, thus conforming to a poisson distribution (Luria and Delbruck, 1943; Leonhardt *et al*, 1999) and statistical analysis was performed accordingly. On guidance from Johnson *et al* (2009), the raw data across the entire dose response was tested for best of fit between linear (null hypothesis) and quadratic (alternative hypothesis), the simplest non-linear model. The output of SPSS is shown in **Figure 3.9**. Comparing the goodness of fit values for both models using the F-distribution (See appendix 3 for detailed instructions), the null hypothesis of linearity could not be rejected (p=0.58). However, the dose-response did not appear linear in **Figure 3.8**. It is possible that the decrease in MF at 0.0025μg/ml obscures regression analysis. The statistical approach was originally developed for analysis of threshold dose-responses not J-shaped curves and so the approach by Gocke and Wall (2009) was modified for the current analysis.

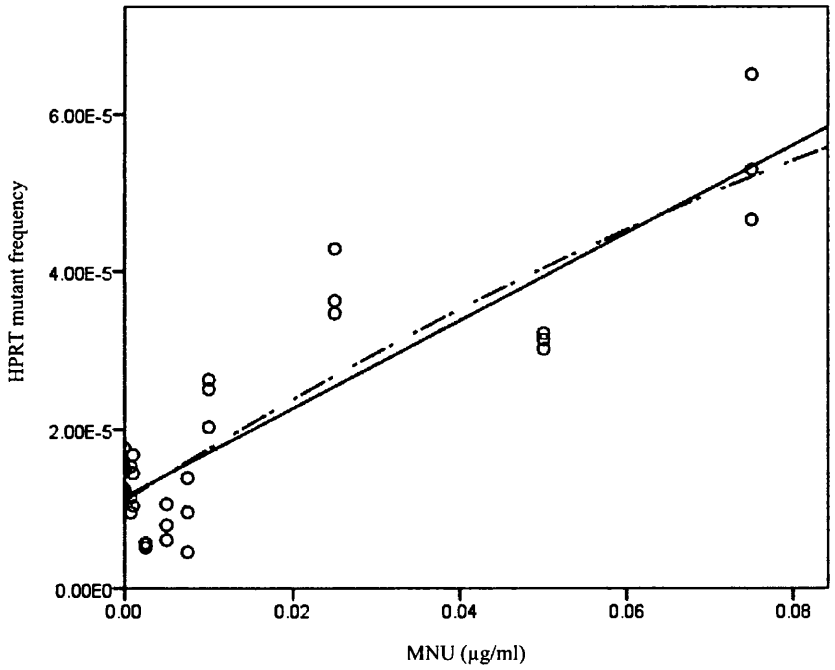

Figure 3.9. Initial regression analysis of HPRT full data set (0.00075μg/ml to 0.075μg/ml MNU) suggested a linear dose-response. Open circles=observed data, solid line=linear fit and broken line=quadratic fit.

Due to this, attempts to identify the no observed and lowest observed genotoxic effect levels (NOGEL and LOGEL) were made as described by Doak *et al* (2007). A *post*

hoc Dunnett's analysis was performed on the raw data to compare all treatment MF with control (DMSO and untreated). It was found that the NOGEL was 0.0075μg/ml (p=0.99) and the LOGEL being 0.01μg/ml (p=0.001). Log transformation of the data and re-analysis confirmed this. For further confidence, a two-tailed t-test was used to determine significance by comparing individual treatments to control values, which would overcome confusion caused by the initial decline in MF at lower doses of MNU. Under the t-test the conclusions were the same (NOGEL=0.0075μg/ml, p=0.19 and LOGEL=0.01μg/ml, p=0.01). Gocke and Wall (2009) recommended regression analysis on the dose-response at doses below the statistical NOGEL of 0.0075μg/ml MNU. The data has a negative linear relationship substantiating the decrease in MF at lower doses of MNU. The gradient of the slope shown (**Figure 3.10**) is -0.00075 (to 5d.p) with 95% confidence limits of -0.00133 to -0.00017 (calculated in the appendix). A true NOGEL that supports a broken stick dose-response would have a gradient of 0 (Lutz and Lutz, 2009).

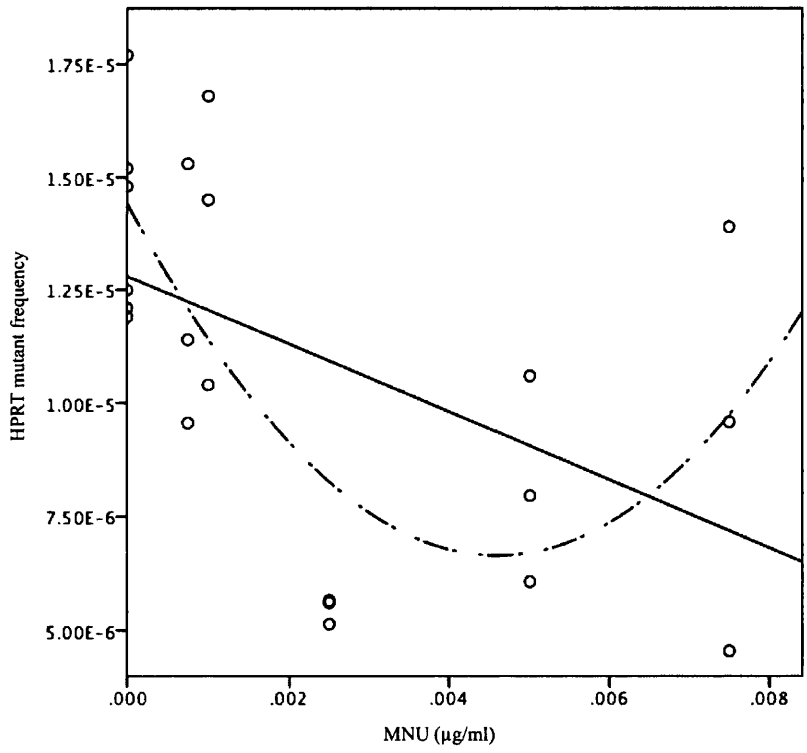

Figure 3.10. The dose-response up to the NOGEL (0.0075μg/ml MNU) shows a quadratic relationship. The gradient of the slope is negative, indicative of hormesis. Open circles=observed data, solid line=linear fit and broken line=quadratic fit.

From **Figure 3.10**, it is evident that the dose response below NOGEL doses of MNU fit a quadratic model (p=0.01), substantiating the appearance of a J-shaped dose-response.

3.3. Discussion.

The aim of this chapter was to elucidate the dose-response relationship of mutation induction by MNU. Previous studies in our group have shown a linear dose response for MNU induced mutations in AHH-1 cells, but this may have been due to the higher doses tested (Doak *et al*, 2007). Therefore, we have used 10-fold lower concentrations using the same standardised methodology and cell line as Doak *et al* (2007). I have used the following term "no observed *genotoxic* effect level" (NOGEL) to discriminate from the opposite "effect" observed at 0.0025μg/ml MNU.

3.3.1. HPRT assay methodology.

The methodology for HPRT assay has standardised OECD guidelines for testing of chemicals (number 486, OECD, 1997), which have been followed here (with the exception of freezing cultures during the expression period) and in previous publications by our research group (Doak *et al*, 2007). However, there is some debate as to the optimum HPRT methodology and the variation and uncertainty it can cause in determining mutant frequencies. For example, the density of cells within the wells when plating up under selective conditions, will manipulate the ratio of cells: nutrients: selective agent. Thus, impacting on the recovery of clones resistant to the selective agent (6-TG). There is some debate as to what effects high cell densities have on the MF in the HPRT assay. If a high density of wildtype cells exist in a well, it may negatively impact the growth of mutant cells by depleting nutrients in the initial few days before 6TG is metabolised into a toxin (Khaidakov and Glickman, 1996). However, a higher cell density may more rapidly deplete 6-TG and enhance survival of cells, which would overestimate MF. Wildtype cells may also metabolise 6-TG and leak the genotoxic metabolite into the media, potentially affecting HPRT mutant cells. Hallahan *et al* (1989) state that with the eventual 6-TG induced death of wildtype cells, debris from dead cells may impact on the survival of mutants leading to an underestimation of MF. Many studies have incorporated 12-O-

tetradecanoylphorbol-13-acetate (TPA) to prevent metabolic cross talk between mutant and wildtype cells (Raveh and Huberman, 1983) by inhibiting intercellular gap-junctions (Walder and Lutzelschwab, 1984). However, TPA is a tumour-promoting agent with published clastogenic abilities (Emerit and Cerutti, 1983). The HPRT assay shares similarities with the TK assay, which served as validation when establishing the HPRT assay in our laboratory (Doak *et al*, 2007). One difference it holds is that HPRT occupies a larger region of the genome, approximately 40Kb whereas the TK gene is 13Kb. Therefore, the HPRT loci could be considered more representative of global genomic mutation frequencies and would serve as a more sensitive mutation sensor. Additionally, Chen *et al* (2002) concluded that both loci were similar in their response to ENU. Monroe *et al* (1998) compared *HPRT*, *LacI* and *cII/cI* as mutational sensors in Big Blue B6C3F1 mice and found that *HPRT* offered superior sensitivity due to the low background mutant frequency at this loci, making it an appropriate reporter gene for low dose mutagenicity studies. Dr George Johnson and Dr Shareen Doak have optimised the methodology used here, with careful consideration of aforementioned caveats. Comparison of mutant frequencies in response to increasing concentrations of MMS gave identical responses at both HPRT and TK loci (Doak *et al*, 2007). Thus, the HPRT assay has been validated against the TK assay and provides a sensitive method for detecting mutagenic events at low doses of genotoxin. Such a testing strategy, based on low dose exposures is accumulating more credence given the caveats of high dose to low dose extrapolations in predicting risk of likely human exposures (Pottenger and Gollapudi, 2009). For sufficient confidence in the results, 10080 wells were scored in total for each dose. The inner 60 wells of each of 56 plates were scored (60x56=3360 per replicate). The perimeter wells were omitted for fear of confounding effects due to evaporation of media. Such numbers gave sufficient sample size for 80% power for a significance level of p=0.05. Under the conditions specified in Chapter 2, the spontaneous mutant frequency was inferred from the solvent and untreated control, being an average of 1.4×10^{-6}. This is comparable to published mutant frequencies at the HPRT locus in a range of cell types (**Table 3.2**).

Table 3.2. Frequency of spontaneous HPRT mutants in various populations of cells at the HPRT locus. The spontaneous values reported in this study are more comparable to other studies than previously reported frequencies from our laboratory.

HPRT MF ($x10^{-6}$)	Source population	Reference
2+/-0.6 (SE)	Big Blue B6C3F1 mice	Monroe *et al* (1998)
6+/-0.41 (SD)	Adult T lymphocytes	McGinniss *et al* (1990)
0.6+/-0.1 (SD)	T lymphocytes Male 129/ola and C57B1/6 normal mice	Bol *et al* (1998)
3.6+/-1.1 (SD) 5.2+/-1.5 (SD)	TK6 1 TK6 3	Steen, Meyer and Recio (1997)
3.78	TK6 lymphoblastoid cells	Sussman *et al* (1999)
2-10.8	H2EI (derivative of AHH-1 lymphoblastoid cells)	Chiang *et al* (1997)
1.4+/-1.8(SD)	AHH-1 in this study	-

3.3.2. MNU treatment strategy.

Cells were treated by 100µl addition of MNU in DMSO, at the appropriate working concentration; to 10ml culture of AHH-1 asynchronous cells and incubated for 24hr. This method mimicked that of Doak *et al* (2007) for direct comparison. It was felt that the use of asynchronous cells would better reflect cycling cells *in vivo* (Cheshier *et al*, 1999) than would a synchronised population created by cell cycle arrest, such as serum starvation and inhibition of DNA replication (Pedrali-Noy *et al*, 1980). The half-life of MNU shows considerable variation between studies owing to the differences in buffer pH and temperature. For example, Druckery *et al* (1967) report a half-life of 1.2hr at 37°C pH 7, compared to 0.35 s in aqueous buffer at pH 4. Reaction with DNA is thought to occur rapidly after administration. However, Baker and Topal (1983) showed the formation of methyladenine products from the *in vitro* reaction of MNU and dATP (deoxyribose adenine triphosphate) nucleotide continued for 24hr increasing from 43% yield at 2hr to 77% at 24hr without MNU becoming

limited. It should be noted that adenine is a lesser-targeted nucleophilic centre than guanine and so reaction with DNA *in situ* may be shorter than 24hr. Nevertheless, exposure to MNU for 24hr maximises the likelihood for DNA reaction.

3.3.3. MNU dose-response.

Doak *et al* (2007) report that, at the doses tested, MNU did not exhibit a NOGEL and every dose caused an appreciable level of DNA damage, with significance achieved at 0.0075μg/ml (the LOGEL). This finding was confirmed as a linear dose-response by Johnson *et al* (2009), using the statistical model by Lutz and Lutz (2009). The authors postulated the appearance of a NOGEL for mutation induction at lower doses, since MNU is 20 times more mutagenic than MMS (Beranek, 1990), an alkylating agent which the authors showed to have a NOGEL. However, many reports provide evidence of a NOGEL for mutation induction by MNU in various assays. Pottenger *et al* (2009) demonstrate a NOGEL of 0.69μM (0.071μg/ml) of MNU using Dunnetts test on log transformed data, which was confirmed as the threshold dose (td) using broken stick modelling (Lutz and Lutz, 2009). A study by Lynch *et al* (2011) examined MNU induced mutagenesis *in vivo* at the *Pig-a* locus in primary rodent reticulocytes. There is evidence of a threshold like dose response for gene mutations after a 28 day repeat dosing chronic study. This substantiated the findings of Pottenger *et al* (2009). Both data sets are currently being analysed using the statistical framework of Gocke and Wall (2009) by Dr George Johnson, which is of interest to the ILSI-HESI working group to better inform on the quantitative relationship of low dose exposure and human risk. The reader is referred to http://www.hesiglobal.org/files/public/Factsheets/2010/IVGT_2010.pdf. Such datasets, as produced in this chapter, have important implications in human exposure risk assessment. Additionally, a threshold dose for MNU induced chromosomal aberrations has been found in TK6 cells in the *in vitro* micronucleus assay (MNvit) at 0.75μg/ml (Bryce *et al*, 2010). Similarly, Doak *et al* (2007) found a NOGEL of 0.1μg/ml MNU in AHH-1 cells using MNvit assay, although the dose-response was found to be linear using the broken stick model. The discrepancy potentially highlights differential sensitivities of endpoint; differential repair capacities between cell lines or differences in methodology (manual vs automated scoring). MNU is considered more mutagenic than clastogenic, which explains the –fold increase in

concentrations at the NOGEL for chromosome break endpoints. However, MNU has been found to be a potent inducer of chromosomal aberrations (Lynch *et al*, 2011). However, these studies were over a protracted length of time where chromosomal aberrations were possibly caused by MMR processing of O^6MeG and not just depurination of N7MeG or N3MeA, the predominant cause of chromosomal aberrations up to 24hr after a single acute exposure (Zair *et al*, 2011).

3.3.4. Hormetic dose-response for MNU.

This study correlates with those discussed that have found a NOGEL for MNU induced gene mutations. However, in this study, using sufficient sample size for 80% power for p=0.05, the doses below the NOGEL (0.00075μg/ml to 0.0075μg/ml) showed a negative slope with confidence limits that do not pass 0. Therefore the MF values were not randomly distributed around the negative control values, as would be expected of a true no effect level. The data presented here, showed a reduction in mutant frequency compared to the negative (spontaneous) level, contrary to previous work by Doak *et al* (2007) and Pottenger *et al* (2009). Data presented in this chapter reported a background MF of $1.4x10^{-5}$, this is 6.8-fold lower than in L1587Y mouse lymphoma cells used in Pottenger *et al* (2009). A higher background MF may compromise the assay's sensitivity to detect a decrease in MF at sub-NOGEL doses of MNU. The identified NOGEL by Pottenger *et al* (2009) of 0.69μM (0.071μg/ml) MNU at the TK locus in L1578Y mouse lymphoma cells is 9.5-fold higher than the NOGEL reported in this study (0.0075μg/ml). Within a cell type, the TK and HPRT loci are concordant in the shape of the dose-response (Doak *et al,* 2007) and mutational spectra in response to a similar alkylator, ENU (Chen, Harrington-Brock and Moore, 2002). The increased sensitivity to MNU in AHH-1 human cells may reflect differences in DNA repair capacities between the cell populations or a function of differential MNU purity used in the experiments. The most likely repair protein is MGMT shown to be important in mutagenic thresholds (Gocke, Tang and Singer, in press). The quadratic shape to the sub-NOGEL dose-response (**Figure 3.10**) further emphasises a hormesis dose-response. Gocke and Wall (2009) have also concluded this after statistical analysis of micronuclei frequency in the bone marrow of EMS treated mice, however, this was likely due to an outliar in the data set (Gocke *et al*,

2009). For further emphasis of low dose benefit, a two-tailed t-test revealed a statistically significant decrease in MF compared to controls at 0.0025μg/ml ($p=0.003$) and 0.005μg/ml MNU ($p=0.034$), an appropriate method to identify hormesis (Calabrese, Stanek and Nascarella, 2011). Further statistical analysis revealed two doses that were significantly lower than the control, substantiating the argument that the observed reduction in MF is a true effect. It must be noted that the present experiments were not designed to identify hormesis (Conolly and Lutz, 2004) and so caution should be urged in promulgating this finding. However, the data does satisfy the concerns of Calabrese (2008), which states "There does not appear to be a means to prove, in an absolute sense, that hormesis has occurred in a specific case. Firm, statistically based conclusions, however, can be drawn that hormesis has occurred if the studies are well designed, with adequate numbers of doses, proper dose spacing, and sufficient statistical power and replication of findings."

3.3.5. Biology behind hormesis.

There are many manifestations of hormesis across many disciplines (Calabrese, 2008). In toxicology, a J-shaped or hormesis dose-response has been shown for a number of endpoints, such as glutathione-s-transferase (GST)-positive foci in hepatic carcinogenesis (Fukushima *et al*, 2005). In toxicity studies, low dose beneficial effects are attributed to overcompensation to restore the balance in homeostasis (Calabrese and Baldwin, 2001). When mutations are the measured endpoint, hormesis (non-monotonic dose-response) has been attributed to the stimulation of DNA repair processes (Feinendegen, 2003) or removal of cells with damaged/mutated DNA by apoptosis (Feinendegen, 2005). Hormesis is usually applied in the adaptive response to chemical and physical mutagens (Calabrese and Blain, 2005). Ugazio, Koch and Recknagel (1972) provide an early example of adaptation to environmental carcinogens where a small ("priming") dose is given prior to treatment with damaging concentrations of the same agent (challenging dose). This has been well-established in *E.coli*, which harbours two MGMT genes (*ogt* and *ada*), in response to O^6-methylating agents, such as N-methyl-N-nitroso-guanidine (MNNG). The priming dose increased expression of MGMT at a second, inducible locus (*ada*), and increased the number of MGMT proteins from a basal level of 13-60 MGMT molecules per cell (from the constitutive *ogt* gene), to 3000 per cell (Mitra *et al*, 1982). This conferred a

6000-fold increase in resistance to future challenging doses (Cairns, 1980). The adaptive response also occurs in V79 rodent cells, reducing the sum toxicity and aberration frequencies from priming and challenging doses of MNU or MNNG (Kaina, 1982). The adaptive response has also been shown under the same conditions using the HPRT assay (Kaina, 1983), where a priming dose of MNNG protected against MNU or MMS clastogenicity. However, it didn't adapt V79 cells to their mutagenic potential. Therefore, multiple adaptive response pathways may exist (Kaina, 1983). Despite the evidence of an adaptive response in V79 cells to O^6-methylating agents, they were shown to have no detectable MGMT in northern blot hybridisation studies (Fritz *et al*, 1991). This study needs to be revised using real time PCR that offers superior sensitivity. Alternatively, the adaptive response could be mediated by another repair process. The adaptive response to O^6-methylating agents is hypothetically mediated by an upregulation of MGMT as seen in *E.coli*. However, induction in mammalian cells is cell type specific. In cells where it has been identified (rodent cells), upregulation occurs to a lesser extent than in microbial hosts (Fritz *et al*, 1991). Doak *et al* (2008) provide evidence that MGMT is induced in AHH-1 human lymphoblastoid cells upon genotoxin exposure but other examples in humans are lacking. However, the results reported couldn't be categorised as an adaptive response of AHH-1 cells to MNU because only a single acute dose of MNU was administered rather than a chronic exposure strategy (Gocke *et al*, 2009) or a priming dose to adapt a cell to future exposures. Data showing hormesis following acute exposures to ionising radiation and chemicals exist (Professor Edward Calabrese, personal communication).

3.3.6. Hypothesised mechanism to explain hormesis.

The reduction in MF observed at 0.0025μg/ml maybe an artefact of the calculation of MF. The PE is included in the calculation of MF (equation 2.6, Chapter 2) and has an inverse effect, whereby a higher PE lowers the MF. This could account for the observed reduction in MF. However, the dose showing minimum response (d_m) (0.0025μg/ml) causes significantly fewer HPRT mutants as compared to solvent control ($p=0.01$) (**Figure 3.11**).

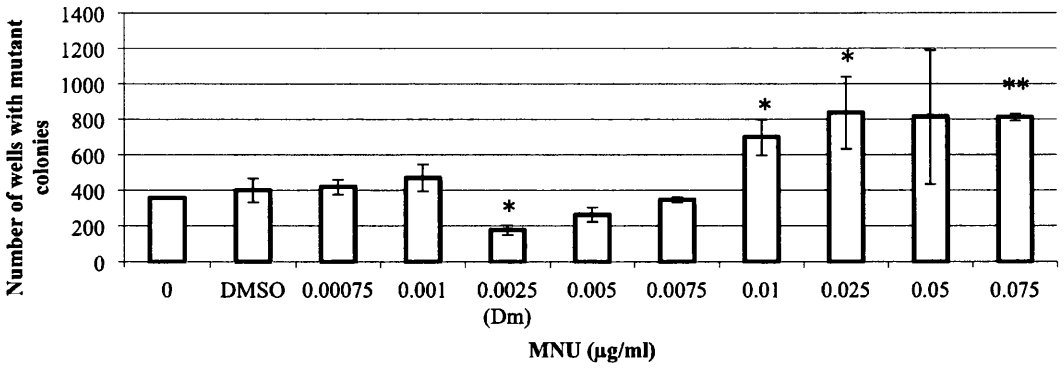

Figure 3.11. A reduction in the number of HPRT mutant colonies was observed at 0.0025µg/ml MNU (d_m). n=3. Error bars=SD. * p=<0.05, ** p=<0.001 as compared to solvent (DMSO) control.

The PE of each replicate at 0.0025µg/ml was substituted for the PE of each replicate of the solvent control and the MF calculated. The actual MF at 0.0025µg/ml was $5.52x10^{-6}$+/-$2.1x10^{-7}$. This changed to an average of $6.11x10^{-6}$ +/-$1.6x10^{-6}$, which still remained significantly lower than the control (p=0.005). Therefore, it is likely that the increased PE did not cause the decrease in MF at 0.0025µg/ml. Since the hormetic response is not dose-dependent it seems likely that this is not a true reduction in the MF and may be an artefact of poor mutant recovery following freezing/thawing cultures during the expression period. Nevertheless, It is interesting to speculate that there is a biological mechanism responsible for the reduction in MF. Toxicity assessment over the treatment period suggests that sub-NOGEL doses of MNU do not cause cell death, which is a mechanism to reduce the number of mutants within a population. Conolly and Lutz (2004) postulate a number of explanations to account for the reduction in spontaneous MF following genotoxin exposure. Assuming that;

1. Endogenous (background) adducts are formed at a zero-order rate
2. MNU ellicits adducts proportional to dose (linear dose-response as shown by Swenberg *et al*, 2008). This is tested in Chapter 4.
3. A basal level of DNA repair is upregulated by exogenous MNU
4. Exogenous adducts by MNU are capable of saturating repair mechanisms at higher concentrations (hypothesis of this thesis)
5. Repair capacities act on exogenous MNU adducts and background adducts,

It could be hypothesised that 0.0025µg/ml causes an upregulation of DNA repair capacities or detoxification mechanisms that remove or prevents damage from MNU

and endogenously generated genotoxins (e.g. from mitochondrial processes). p53 may play a role as it is implicated in reducing mutant frequency (Morris, 2002), but there is no evidence showing upregulation by MNU. Base excision repair (BER) is a known inducible repair mechanism to protect against spontaneously occurring oxidative damage induced mutations (Cabelof *et al*, 2002).

Hormesis is recognised to have a temporal component; therefore, the extent of reduction in spontaneous mutation frequency would depend upon the efficiency of induction of DNA repair mechanisms (may explain the lack of reduction in MF at doses below 0.0025μg/ml), the speed of repair and even duration of the upregulation (Conolly and Lutz, 2004). The data presented here suggest that 24hr exposure to MNU upregulates DNA repair, presumably within the treatment period (Doak *et al*, 2008). However, it is difficult to determine when the reduction in MF occurred in the inherent post-treatment incubation periods of the HPRT assay. To give more confidence, MF should be measured at different post-treatment incubation periods but this cannot be performed in the HPRT assay.

3.3.7. MNU mechanism of action (MOA).

Point mutation induction by MNU has been attributed to O^6Methlyguanine (O^6MeG). This adduct constitutes 5.9-8.2% of the adduct spectra of MNU, approximately 20-fold more than the adduct spectra of MMS (Beranek, 1990). Suter *et al* (1980) found that MNU was 20-fold more mutagenic than MMS in V79 cells. Therefore, one would expect a MNU LOGEL to exist at a 20-fold lower concentration than MMS. Pottenger *et al* (2009) found the LOGEL of MNU to be only 2.5-fold lower than the LOGEL for MMS in L1578Y mouse lymphoma cells. In this study, the LOGEL for MNU is 0.01μg/ml (0.097μM), which is 117-fold lower than the LOGEL of MMS (1.25μg/ml, 11.35μM) (Doak *et al*, 2007).

This drastic difference emphasises;

1. Other mutagenic MNU adducts to which AHH-1 cells are sensitive
2. Increased sensitivity to O^6MeG in AHH-1 cells compared to V79 and L1578Y rodent cells
3. Differences in adduct spectra at lower doses compared to the higher doses used to obtain adduct spectra in Beranek (1990).

The mutability of each MNU adduct has been established. It is well known that O^6MeG is the main cause of MNU mutagenesis, causing GC→AT transitions. The following chapters aim to determine the mechanism of mutation induction by MNU and the cytoprotective mechanism responsible for the NOGEL observed in this chapter. We hypothesise that DNA repair by MGMT is responsible for low dose protection by removing O^6MeG before replication, when it becomes fixed as GC→AT mutations. The following chapter examines the formation of MNU adducts at increasing concentrations of MNU, to highlight the role of post-adduct DNA repair in the protection of DNA from mutation induction at doses below the NOGEL.

Chapter 4.

Adduct Analysis.

Assessment of DNA Damage Following Low Dose MNU Treatment Through Mass Spectrometry.

4.1. Introduction.

The following chapter examines the biological importance of adducts and their use in genetic toxicology as biomarkers of exposure to DNA damaging carcinogens (genotoxins).

4.1.1. Adduct formation is a critical carcinogenic event.

Adducts are chemical groups covalently added to cellular macromolecules such as DNA and proteins by electrophiles. In the following work, the term adduct refers to DNA adducts unless otherwise stated. All direct acting genotoxins are electrophiles capable of adduct formation, either as administered or through metabolic activation (Miller and Miller, 1971). Adduct formation is non-random occurring at nucleophilic (electron rich) centres such as oxygen and nitrogen of the bases and phosphate of the DNA backbone (Nehls and Rajewsky, 1985). Electron loving electrophiles (Lewis acids) accept an electron pair donated from the nucleophilic centre (Lewis base) forming a covalent Lewis adduct by sharing the electron pair in a reversible covalent bond as defined by International Union of Pure and Applied Chemistry (IUPAC). Adducts are pre-mutagenic lesions that, if not efficiently repaired, persist through replication, where they are fixed as permanent genetic mutations. Of interest to the current work are adducts caused by methyl nitrosourea, MNU a methylating agent that is classed as an alkylating agent, a group of genotoxins that add alkyl adducts to DNA (**Figure 4.1**).

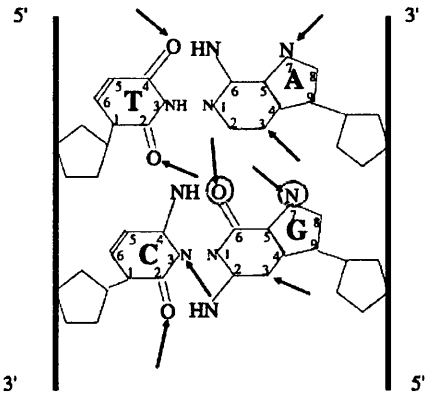

Figure 4.1. Sites of alkylation in double stranded DNA. Of importance to this study is methylation at Oxygen and Nitrogen (O^6Methlyguanine (O^6MeG) N7-Methylguanine (N7MeG), respectively), circled in red. Adapted from Jenkins *et al* (2005).

4.1.2. Electrophile chemistry.

Adducts differ in location and structure owing to the chemical properties of the parent electrophile. Consequently, different adducts pose different mutagenic threats to the DNA. Alkylating agents have a defined DNA reaction mechanism and produce a spectrum of adducts shown (**Table 4.1**). Adduct formation is determined by;

1. The electrophilic potential of the agent, which is governed by the Swain Scott constant (*s* value) (Swain and Scott, 1953)
2. Reaction kinetics, S_N1 v S_N2.
3. Steric hindrance and nearest neighbour effects of the local nucleotide sequence within the double helix (Swenson and Lawley, 1978;Glickman *et al*, 1987;Mathison, Said and Shank, 1993).

MNU shows a low *s*-value, which is associated with a S_N1 reaction mechanism. Conversely, MMS has a higher *s*-value, which is associated with a S_N2 mechanism. This difference in electrophilic potential leads to the differences in adduct spectra. However, it is likely that these were determined at high doses of alkylating agent and the distribution could be different at low doses should the kinetics of DNA reaction depend upon concentration. The most abundant adducts are O^6-methylguanine (O^6MeG), N7-methylguanine (N7MeG) and N3-methyladenine (N3MeA). The critical differences are in the proportions of methylation at O^6G and N7G (**Table 4.1**). MNU produces more O^6MeG that has miscoding properties through replication and causes GC→AT transitions. As a result, MNU is considered to be more mutagenic than agents that have a lower O^6MeG:N7MeG ratio. Additionally, methylating agents are more DNA reactive than their ethylating equivalents (*ethyl*- nitrosourea, *E*NU) but are subject to better repair (Singer, 1985).

Table 4.1. Comparative adduct spectra between two model methylating agents. A low *s* value (e.g. MNU) shows higher propensity for alkylation at exocyclic oxygen of guanine (O^6G), forming a potent miscoding adduct responsible for GC→AT transitions. Taken from Beranek (1990).

	Proportions of adduct spectra (%)	
Adduct site	**MMS**	**MNU**
s-value	>0.83	0.42
N7G	**81-83**	**65-70**
O^6G	**0.3**	**5.9-8.2**
N3A	10.4-11.3	8-9
N3G	0.6	0.6-1.9
N7A	1.8	0.8-2
N3C	<1	0.06-0.6
O^2C	Nd	0.1
N3T	0.1	0.1-0.3
O^2T	Nd	0.1-0.3
O^4T	Nd	0.1-0.7

4.1.3. Some genotoxins require activation into an electrophile to cause DNA damage.

There are many examples where genotoxic carcinogens require "bioactivation" into an electrophile that is capable of reacting with DNA and forming adducts (Guengerich, 1992). Cytochrome P450s (CYPs) typically perform reduction or oxidation reactions converting the pro-carcinogen into an electrophile in a redox reaction dependent on nicotinamide adenine dinucleotide phosphate (NADPH) generating systems, hence the use of enzyme extracts such as S9 in *in vitro* toxicology (Maack *et al*, 1986). Chesis *et al* (1984) provide a role for flavoenzymes such as NADPH-cytochrome P450 reductase in activating quinones (an environmental carcinogen). Stern *et al* (1993) and Degawa *et al* (1994) identify the role of CYPs 2C, 3A4 and 1A1 enzymes in polyaromatic hydrocarbon (PAH) activation to produce

adducts identified in laryngeal tumours of smokers. Conversely, the cell is also equipped with detoxifying metabolism to rid the cell of potentially damaging agents. These include, glutathione S-transferase (GST), which conjugates pro-carcinogens and endogenously generated DNA reactive species to glutathione, a biosynthetic defensive antioxidant, to detoxify the cell and protect from mutagenesis. Shupe and Sell (2004) substantiate this by showing increased adduction by aflatoxin B1 in cells with low GST concentration. However, an increased intracellular thiol concentration *increases* adduction by alkylating agents (Lawley and Thatcher, 1970). Metabolism of aromatic and heterocyclic amines by arylamine *N*-acetyltransferases (NATs) can either serve to detoxify or promote their metabolic activation into DNA damaging agents (Hein, 2002). The balance of these processes determines risk of DNA damage and carcinogenesis (Androutsopoulos *et al*, 2009). The potency of pro-carcinogens can be enhanced;

- By inter-individual polymorphisms within the CYP encoding genes that improves pro-carcinogen activation (Bartsch *et al,* 2000; Katoh, 1995)
- In tissues showing over-expression of activating enzymes (Perin-Roussel *et al*, 1997).
- By an imbalance in detoxification mechanisms
- Polymorphisms within GST that reduces its detoxifying capacity (Mohr *et al*, 2003).

The risk of damage from pro-carcinogens is dependent on the phenotype of the cell or individual. MNU used in this study does not require metabolic activation. Nevertheless, extrapolating safe levels of exposure to genotoxins across a heterogeneous human population requires careful consideration of polymorphisms in detoxifying and activating pathways, which has been correlated to cancer susceptibility (Coles *et al*, 2003).

4.1.4. Endogenous electrophiles cause adducts that contribute to spontaneous mutagenesis.

Miller and Miller (1971) recognise adduct formation as a critical event in chemical carcinogenesis that is common between all genotoxins. The study of DNA adducts has accelerated in recent years with the discovery that adducts are caused not only by

environmental carcinogens but also from endogenous electrophiles from normal cellular metabolism. Adduction of DNA by endogenous electrophiles contributes to a spontaneous level of DNA damage and mutation responsible for background tumour incidence of 35-40% of a human population over a 75 year life span (Lutz, 1990). The most studied culprit of endogenous damage is reactive oxygen species (ROS) from mitochondrial metabolism, such as superoxide (O_2^-) and hydrogen peroxide (H_2O_2). Oxidative stress (when the level of ROS exceeds antioxidant capacities) has been shown to contribute to chemical carcinogenesis (Klaunig *et al*, 1998). Incidentally, exogenous agents such as dieldrin, an organochlorine pesticide, has been shown to cause a state of oxidative stress and subsequent liver cancer in rodent subjects. It can be considered as an indirect genotoxic carcinogen. ROS species (e.g. O_2^-) oxidise guanine bases forming adducts like, 8-hydroxydeoxyguanosine, a pro-clastogenic and pro-mutagenic adduct but useful oxidative stress biomarker in urine (Loft *et al*, 1999; Collins *et al*, 1996; Chiou *et al*, 2003). Humans accumulate 10^4 oxidative lesions per cell per day, 10 fold lower than rats (Cathcart *et al*, 1984;Ames, 1989).

Oxidative stress is not the only source of endogenous damage. Electrophiles are also produced from lipid peroxidation and endogenous oestrogens (De Bont 2004). Products from lipid peroxidation react with metals to form epoxides and aldehydes and form a variety of ethano and propano guanine adducts with varying mutagenic potential (Hecht *et al*, 2001). Redox cycling of oestrogens can cause oxidative DNA damage. Oestrogens themselves can cause DNA damage via a cytochrome-mediated activation into electrophilic quinone intermediates (Liehr, 2000;Cavalieri *et al*, 2000). Of interest here is the endogenous methylation of bases that can contribute to the naturally occurring adductome.

4.1.4.1. Endogenous methylation regulates gene expression and can be mutagenic.

Endogenous DNA methylation coupled with histone acetylation/phosphorylation play an important role in the epigenetic regulation of gene expression (Geiman and Robertson, 2002). Aberrant methylation causes inappropriate gene regulation causing genomic instability implicated in a number of human cancers (Jones and Baylin, 2002;Esteller and Herman, 2002). Methylation at CpG dinucleotides at gene promoters suppresses transcription and temporarily silences the gene. Methylation is

achieved by three DNA methyltransferases (DNMT); DNMT1, DNMT3a and DNMT3b. They have roles in epigenetic methylation, genetic imprinting and embryonic development (Chen and Li, 2004). Knowledge of how these are regulated in normal cells is lacking. DNMT's are not electrophilic but catalyse the transfer of methyl groups from a donor, S-adenosylmethionine (SAM) to cytosine in DNA forming 5-methylcytosine. 5-methylcytosine is not miscoding like O^6MeG but does cause spontaneous methylC→T transitions through deamination of 5-methylcytosine (Coulondre *et al*, 1978). To substantiate the mutability of 5-methylcytosine, Shen *et al* (1992) showed a higher rate of 5-methylcytosine deamination (5.8×10^{-13}/s) compared to un-methylated cytosine (2.6×10^{-13}/s) at physiologically relevant conditions. This has been shown in human germline (Rideout *et al*, 1990) and somatic cells (Cooper and Youssoufian, 1988). Cooper and Krawczak (1990) estimated that 32% of point mutations responsible for human genetic disease resulted from spontaneous deamination of 5-methylcytosine to thymine. SAM has been shown to methylate DNA at sites other than CpG islands non-enzymatically. This has received much attention due to the mutability of methyl adducts. The *in vitro* adduct spectra of SAM (Rydberg and Lindahl, 1982) showed that N7-MeG was the predominant adduct with lesser amounts of N3-Methyladenine (N3MeA) and O^6MeG (constituting >1% of N7MeG formed). This adduct spectra mimics that for exogenous MMS. Rydberg and Lindahl (1982) extrapolated the *in vitro* adduct to the *in vivo* condition and estimated that an intracellular SAM concentration of $4x10^{-5}$M would cause 4000 N7MeG, 600 N3MeA and 10-30 O^6MeG per cell per day. This suggests that the cells can tolerate a higher level of N7MeG than either N3MeA or O^6MeG. Posnick and Samson (1999) increased intracellular SAM concentration but saw no increase in spontaneous mutagenesis. The authors confirm, "that SAM is not a major contributor to the endogenous formation of O^6-methylguanine lesions in *E. coli*." Endogenous generation of O^6MeG, and also N7MeG, has been attributed to the *in vivo* generation of DNA reactive *N*-nitroso compounds (NOC). NOC's include; the nitrosamides (MNU and ENU) and the nitrosamines (DMN and DEN). Their adduct spectra show predominance of N7AlkylG and lesser amounts of O^6AlkylG at varying ratios (Beranek, 1990). NOC's are formed from nitrosylation of digestion products (amino acids such as glycine and proteins) of ingested red meat in the gastrointestinal tract (Tricker, 1997; Lewin *et al*, 2006; Kuhnle and Bingham, 2007; Winter *et al*, 2011). This being the hypothesized link between colon cancer and red meat consumption

(Hebels *et al*, 2009; Hebels *et al*, 2010; Hebels *et al,* 2011) although, other carcinogens in red meat also contribute such as heterocyclic amines (HCA) and polyaromatic hydrocarbons (PAH) (Chen *et al*, 1998).

4.1.4.2. Endogenous levels of O^6MeG, N7MeG and N3MeA.

The occurrence of O^6MeG, N7MeG and N3MeA in the natural adductome has been shown to contribute to spontaneous mutagenesis in yeast cells (Xiao and Samson, 1993). Levels of endogenously formed N3MeA is lacking and cannot be commented upon. Quantification of O^6MeG come from studies quantifying this adduct in human tissues of individuals with no known exposure to methylating agents. Such studies are labile to recall bias and suffer from a lack of sensitivity; employing antibody based techniques and enzyme activity inference to quantify levels of O^6MeG. **Table 4.2** shows a summary of reported spontaneous adduct levels.

Table 4.2. Levels of endogenous alkylation damage. It is considered that O^6MeG is naturally formed at lower levels than N7MeG. HPLC=high performance liquid chromatography, RIA=radio-immuno assay.

Method of quantitation	Quantity of N7MeG (per10^{-8} nucleotides)	Quantity of O^6MeG (per10^{-8} nucleotides)	Human tissue	Reference
32P post-labelling	25	-	Pulmonary alveolar cells	Petruzzelli *et al* (1996)
HPLC/32 P post-labelling	31-7900	-	Liver	Kang *et al* (1995)
32P/TLC/HPLC	29	-	White blood cells	Zhao *et al* (1997)
32P/AEC	34	-	White blood cells	Mustonen and Hemminki (1992)
32P/AEC	135	-	Lymphocytes	Mustonen and Hemminki (1992)
Prefractionation/32P post-labelling/Immunoprecipitation (PREPI)	-	11-67	Liver	Kang *et al* (1995)
PREPI	-	0.7-4.6	Peripheral blood	Kang *et al* (1995)
PREPI	-	0.1-1.6	Peripheral blood	Kang *et al* (1992)
PREPI	-	11-42	Liver	Kang *et al* (1993)
PREPI	-	6.78-4.6	Leukocytes	Kang *et al* (1993)
HPLC/RIA/immunoprecipitation	-	0.4-4.4	Maternal blood	Georgiadis *et al* (2000)
HPLC/RIA/immunoprecipitation	-	4.8	Chord blood	Georgiadis *et al* (2000)
ELISA	-	0.65	Maternal blood	Georgiadis *et al* (2010)
ELISA	-	0.38	Chord blood	Georgiadis *et al* (2010)

Spontaneous levels of N7MeG tend to be higher than O^6MeG (De Bont, 2004). This could reflect differences in;

1. Cellular tolerance to these adducts. It is known that N7MeG is relatively innocuous; Tudek, Boiteux and Laval (1992) showed naturally high levels after conversion to its imadazole ring-opened derivative; 2,6-diamino-4-

hydroxy-5N-methyl-formamidopyrimidine (Fapy-7-MeG) without severe mutagenesis. Whereas, O^6MeG is highly mutagenic (Kaina *et al*, 2007).

2. Formation of each adduct. It is known that the major endogenous methylating agent, SAM causes more N7MeG than O^6MeG.
3. Repair capacities, this influences the tissue specific half-lives ($t_{1/2}$) of the adducts (Jackson *et al*, 2000; Herron and Shank, 1981). Liver shows the most rapid half-life of O^6MeG (Kleihues and Bucheler, 1977) this is attributed to the higher level of its repair protein (O^6-methylguanine-DNA methyltransferase, MGMT) in liver samples (Souliotis *et al,* 1996). Beranek (1990) quote the *in vitro* half-life of O^6MeG as 2 days and N7MeG as 4.4-8 days. However, estimates of $t_{1/2}$ O^6MeG range from 1hr (Sklar and Strauss, 1981) to 14 days (Kleihues and Bucheler, 1977).
4. Ease of measurement (discussed later).

Due to the different methods of measurement, adduct levels are difficult to compare. However, Shields *et al* (1990) directly compared N7MeG to O^6MeG and found approximately 10-fold higher levels of N7MeG (140-720 N7MeG per 10^8 nucleotides) than O^6MeG (10-70 O^6MeG per 10^8 nucleotides). There are notable differences between levels in liver and lymphocytes. This could reflect target organ specificity of the endogenous NOC's. Additionally, Souliotis *et al* (1996) found that liver MGMT is most rapidly and significantly depleted, compared to lymphocytes, which accounts for the higher level of O^6MeG in these samples.

The ratio of N7MeG/O^6MeG are consistent with the adduct spectra of endogenous NOC's and SAM, hypothesized to contribute to spontaneous DNA methylation. It can be concluded that chemical damage to DNA is a natural occurrence, necessary for genetic variation, and may not contribute a substantial risk to hereditary mutation and cancer. However, endogenous damage can be mimicked and substantiated by exogenous electrophiles. Therefore the risk of genetic damage is much greater and exposure to exogenous genotoxins must be limited hence the need for genotoxicity testing.

4.1.5. Exogenous electrophiles.

Adducts, and adduct spectra, caused by exogenous electrophiles can mimic those formed from endogenously generated electrophiles. As previously discussed with

SAM and MMS. However, there is a distinction, endogenous damage is unavoidable but exposure to exogenous electrophiles can be limited to prevent further damage. Exogenous electrophiles are thought to have an additive effect on already existing endogenous adducts (Zito, 2001). At low levels, it seems that endogenous damage predominates. For example, Lu *et al* (2011) showed that 0.7ppm formaldehyde will produce 0.039+/-0.019 N^2-hydroxymethyl-dG/10^7G but endogenous adducts naturally exist at 3.62+/-1.33 N^2-hydroxymethyl-dG/10^7G. At this concentration, exposure risk seems negligible.

4.1.5.1. Exogenous adducts have a linear dose-response.

It is widely reported that, at low doses under first order kinetics, adduct formation from exogenous carcinogens accrues in a linear fashion proportional to dose (Zito, 2001). This has been shown for acrylamide and MMS (Swenberg *et al*, 2008). By distinguishing between endogenous and exogenous adducts by administering radiolabelled genotoxins, exogenous adducts accrue linearly from zero at increasing doses. However, if total adducts are analysed the level must have a nonzero background level of naturally occurring adducts, this is exemplified by Lu *et al* (2011). The authors quantified N^2-hydroxymethyl-dG resulting from formaldehyde exposure and distinguished adducts on the origin of formation by administering radio-labelled formaldehyde, which can be separated by mass from endogenously formed (non-radio-labelled) formaldehyde adducts. Despite an increase in exogenous adducts at increasing doses, if this is combined with the endogenous levels, the increase is hidden within the background level particularly following administration of 2 to 9.1ppm formaldehyde (**Figure 4.2**).

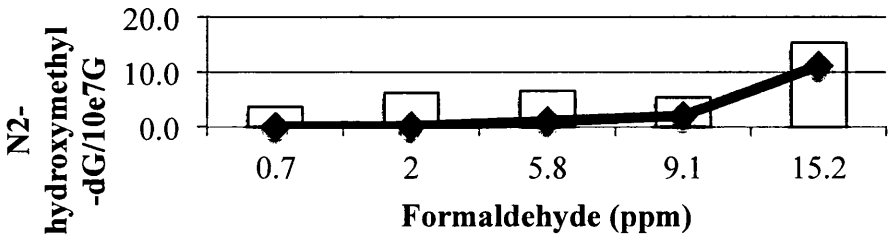

Figure 4.2. The levels of N^2-hydroxymethyl-dG adducts resulting from formaldehyde exposure (diamond). The increase from 2 to 9.1ppm is hidden when total (endogenous and exogenous) adducts were calculated (columns). Data taken from Lu *et al* (2011).

Swenberg *et al* (2008) report that under linear adduct relationships; the resulting mutation dose-response for these compounds observe thresholds. This is the case for MMS (**Figure 4.3**) and has also been shown for MNU (Pottenger *et al*, 2009).

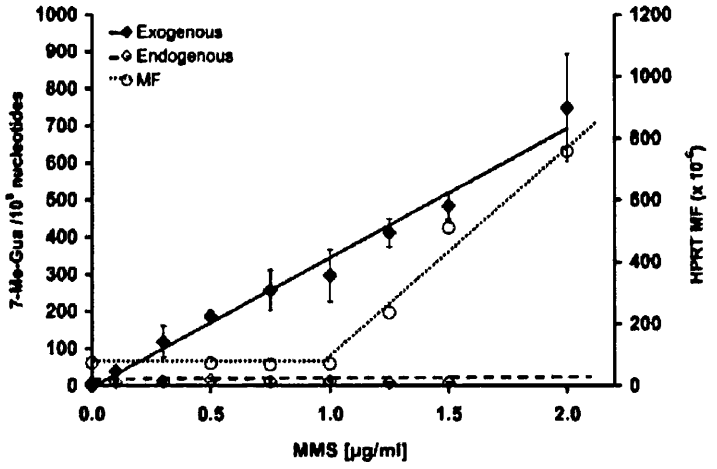

Figure 4.3. N7MeG adducts induced by MMS (solid diamonds) show a linear dose-response. Mutation induction by this agent is non-linear with a NOGEL at 1µg/ml (empty circles). At the NOGEL there are approximately 300 more adducts compared to 0µg/ml without an increase in mutant frequency. Taken from Swenberg *et al* (2008).

This holds true for different endpoints such as tumour formation (Poirier, *et al*, 2004). Dragan *et al* (1995) report that an anti-oestrogen drug, toremifen, does not induce hepatic neoplasms even though DNA adducts in liver tissue have been detected (Li *et al*, 1997). Otteneder and Lutz (1999) state that this is because "the limit of detection (LOD) of DNA adduct levels can be much lower than the limit of detection for a statistically significant increase in tumour incidence." Conversely, Groopman and Kensler (1999) highlight the correlated risk of hepatocellular carcinoma and presence of urinary aflatoxin B1 adducts and metabolites. It was recently concluded that adducts cannot be used to inform of cancer risk (HESI, 2010) and are not biomarkers of effect. It is considered that low doses of carcinogens can cause DNA damage but not all the damage causes mutation. For this reason adducts are considered biomarkers of exposure and not biomarkers of effect (Swenberg *et al*, 1987).

4.1.6. Adducts as biomarkers of exposure

The presence of adducts unequivocally demonstrates the presence of an electrophile. Adducts confer information about extent to which an individual or population is exposed to endogenously generated and exogenous carcinogens and are, therefore termed biomarkers of exposure. These are used to inform the Environmental Protection Agency (EPA) and other governing bodies as to the extent of environmental pollution. Detection of a carcinogen or its metabolites in bodily fluids quantifies the internal dose. Furthermore, detection of protein and DNA adducts in whole tissue give more relevant data on the biological effective dose which is more informative than administered dose (Ehrenberg and Osterman-Golkar, 1980). The ability to detect adducts depend on assay sensitivity and prior knowledge of route of exposure (Lehman-McKeeman, 2010). For example, Lu *et al* (2010) investigated N^2-$HOCH_2$-dG adducts as biomarkers of inhalation of formaldehyde. Exogenous adducts were only detected in nasal cavity and not liver and bone despite efforts to increase sensitivity. Protein adducts, as well as DNA adducts serve as "exposure monitors" (Farmer, 2004). Törnqvist *et al* (1988) investigated methyl adducts on amino acids in haemoglobin as potential biomarkers. The advantage of using haemoglobin as an exposure sensor is non-invasive sampling from patients. It is known that cyanate, a decomposition product of MNU (Melzer *et al*, 1983) is a carbamoylating agent and reacts with amine groups in guanine but also in proteins such as glutathione (GSH) (Trézl *et al*, 1987). Many other protein adducts have been useful as biomarkers (reviewed in Farmer, 1999). The time period following an acute exposure is essential when using adducts as biomarkers of exposure. Over time, a variety of adduct-dose relationships have been observed (Talaska *et al*, 1996; Herron and Shank, 1981). Following an acute dose of genotoxin, adduct levels initially rose but returned to a steady state level, reflecting a balance of endogenous formation and removal. Kleihues and Bucheler (1977) found that, in rat brain, an initial increase in O^6MeG following MNU injection took 180 days to plateau but only 28 days for N7MeG. A naturally higher level of N7MeG would explain this. A protracted curve for O^6MeG reduction was also observed by Medcalf and Lawley (1981). DNA adducts have received more attention due to their mutability but they are more difficult to measure than protein adducts and their location in the nucleotide sequence cannot be determined. Determining adduct location particularly in proto-oncogenes and tumour

suppressor genes or even coding regions of the genome, would increase their impact in cancer risk assessment. Despite this inability, with ever more increasing sensitivity in DNA adduct measurement, they are becoming an important biomarker but their risk to cancer is under contention and has been established for only a few carcinogens e.g. aflatoxin B1.

4.1.7. Biological effect of adducts is determined by cellular processing.

Once adducts have formed, their mutagenic potential is dependent on;

1. Adduct half life, which is determined by efficacy of cellular repair capacity
2. Adduct structure
3. The genomic location of adduct
4. Mis-coding potential
5. DNA replication (rate of cell division)

Different adducts have different mutagenic and carcinogenic potencies. For example, aflatoxin B1 is almost 40 times more carcinogenic than DMN adducts (Otteneder and Lutz, 1999) this can be explained by propensity for mutation and poor repair capabilities for aflatoxin B1 and other bulky adducts (Hang, 2010).

If an adduct is fixed as a mutation, there may not be a phenotypic change in the protein, if;

1. The adduct and resulting mutation occurs in non-coding DNA
2. The mutation is silent, coding for the same amino acid due to redundancy of the genetic code. In the HPRT assay, and other mutation assays, silent mutations will not be detected which would compromise the sensitivity of mutation detection assays.

Therefore, many possibilities exist whereby an adduct does not pose an adverse effect to DNA and may be irrelevant to mutagenesis. This may explain the presence of adducts but absence of mutations found in a number of studies that postulate a no observed mutagenic and carcinogenic effect level (Swenberg *et al*, 2008; Waddel, Fukishima and Williams, 2006) although the difference in limit of detection of each endpoint has a role (Jenkins *et al*, 2005).

4.1.7.1. DNA repair plays a crucial role in adduct removal, which prevents mutation.

DNA repair is the most heavily cited mechanism that prevents mutations by repair of adducts. A number of enzymes constitute a cell's inventory of DNA repair processes. This means a variety of structurally diverse adducts can be repaired, this represents "first line defence" from adduct induced mutation and cancer (O'Connor *et al*, 2000). The efficiency of repair is determined by the affinity an enzyme has for the adduct. For example, in a wildtype cell, methylating agents are less mutagenic than their ethylating equivalents, this is due to more effective repair capacities for removing methyl adducts (Beranek, 1990). The location of adducts within the genome affects the rate at which they are repaired given differential genome wide repair capacities (Madhani, Bohr and Hanawalt, 1986;Wasserman, Kohn and Bohr, 1990). Measuring pan-genomic repair efficiencies is currently being investigated (Teng *et al*, 2011). The repair of adducts is often without any permanent damage to DNA, excluding erroneous base excision repair (BER). Therefore, certain repair deficient cells are unable to repair specific adducts and are more vulnerable to mutations. However, some repair deficiencies actually confer resistance to genetic alterations (such as chromosomal aberrations, as previously discussed with mismatch repair (MMR) deficient cells conferring a methylation tolerant phenotype. Multiple studies comment on the increased mutagenicity of a variety of adducts in different repair deficient cell lines when compared to repair proficient cells following exposure to a variety of DNA damaging chemicals. For example, cisplatin induced mutations in xeroderma pigmentosa (XP, an NER deficient) cell line (Zhen *et al*, 1993), and mitomycin C (MMC) induced micronuclei in XP and fanconi anaemia (FA, cross-link repair deficient) cells (Speit *et al*, 2000). Of interest to the present study, O'Connor *et al* (2000) showed a higher level of O^6MeG in DNA of cells lacking MGMT, the error free repair protein capable of removing O^6MeG. 20hr following exposure, O^6MeG levels were measured at 10μmolO^6MeG/mole guanine in MGMT deficient cells compared to only 0.4μmolO^6MeG/mole guanine in MGMT proficient cells. With a higher level of unrepaired O^6MeG persisting in DNA through replication there is a higher likelihood of mutation, these being GC→AT changes after two replications of O^6MeG. These *in vitro* studies reflect intra-population polymorphisms in DNA repair

genes. With altered DNA repair capacities, altered susceptibility to mutation by the same adducts impacts in differential cancer risk (Terry *et al*, 2004) and also in applying a DNA repair mediated threshold dose-response to the human population (Jenkins *et al*, 2009).

4.1.8. Analytical methods for measuring DNA adducts.

Early adduct detection methods administered radioactive carcinogens to animal models. Upon sacrifice, the DNA is harvested from organs of interest. An increase in radioactivity of isolated DNA from treated animals compared to untreated controls gave support to the formation of DNA adducts (Phillips *et al*, 2000). This technique gave no chemical information about the adduct or conclusive proof of formation nor does it permit the bio-monitoring of humans or study of endogenous damage. Since then, technological advancements permit the highly accurate detection of specific chemical adducts on macromolecules. If an adduct is induced below the limit of detection it does not mean it is not there, therefore, the sensitivity of the method is critical and can change the shape of the dose-response relationship. The technique that offers the lowest limit of detection is favoured. Methods for adduct detection and quantification include:

^{32}P-postlabelling-The most sensitive technique requiring only 1-10μg DNA (Randerath *et al*, 1981) to achieve detection limits of 1 adduct/10^9 nucleotides (Farmer, 2004). It overcame the obstacle of using pre-labelled radioactive carcinogens, which prevented detection in humans. The technique radiolabels adducts *after* exposure to carcinogens. Isolated DNA is digested and the free nucleotides are labelled by [γ-P^{32}-ATP] at the free 5'-OH group (formerly a phosphodiester link of the DNA backbone). Labelled adducted bases are separated from unmodified bases by polarity using variations of chromatography to enhance sensitivity. The adducts are then resolved and quantified by autoradiography. The technique, however does not provide information about the structure of the adduct and its lack of specificity cannot resolve exogenous from endogenous (termed indigenous) adducts (Randareth *et al*, 1983;Gupta *et al*, 1999).

Antibody based methods-Include immunoassays and immunohistochemistry (Poirier, 1981; Strickland and Boyle, 1984) but recently Georgiadis *et al* (2011)

developed an enzyme linked immunosorbent assay (ELISA) type technique for detecting 1.5 adducts/10^9 nucleotides using 10μg of DNA. Mass spectrometry would require more than 100μg DNA for similar sensitivities (Dr Rajinder Singh, personal communication). The assay was used to correlate endogenous O^6MeG levels with NOC's in nitrite rich diets and was shown to have similar sensitivities as HPLC/RIA/immunoprecipitation (Georgiadis *et al*, 2000) but with higher throughput. However, this technique is not routinely used. Other attempts to quantify O^6MeG with antibodies was coupled with ^{32}P-postlabelling but only achieved a sensitivity of 1 O^6MeG/10^8 G (Cooper, Griffin and Povey, 1992).

Electrochemical-De Groot *et al* (1994) describe a technique for the analysis of O^6- and N7 ethyl and methyl guanine. The authors quote a LOD of 0.5 methyl adducts/10^6 nucleotides and 1 ethyl adduct/10^6 nucleotide. The discrepancy in LOD's between ethyl and methyl adducts is unclear.

Enzyme inactivation studies-Measuring the decrease in MGMT activity following repair of O^6MeG has been correlated to the presence of O^6MeG due to the stoichiomtery of the reaction. Authors refer to it as the competitive repair assay for O^6MeG (Souliotis *et al*, 1991; Georgiadis *et al*, 2000). Souliotis *et al* (1989) quote a LOD of 0.8μmol adduct/mol guanine. This equates to a LOD of 200 adducts/10^8nucleotides. The technique would require careful monitoring of MGMT transcription and translation levels to ensure a decrease in activity was not due to a decrease in expression.

Adduct induced polymerase blockage assay- Moore and Strauss (1979) developed the "stop assay." This technique allows the user to infer the location of adducts on plasmid DNA based on replication blockage. The "stop assay" has been used to identify bulky acetylaminofluorene (AAF) DNA adducts (Mah *et al*, 1991). However, these adducts only temporarily slow replication and are bypassed (Schorr *et al*, 2010) and so the "stop assay" may miss adducts. Jenkins, Burlinson and Parry (2000) report the successful detection of MNU, ENU and UV-C adducts. However, the assay lacks sensitivity.

Mass spectrometry-provides unequivocal evidence of the presence of adducts. Recent developments have improved the sensitivity of the technique to greater than ^{32}P-postlabelling without the need for radio –labelled substrates. The method has been used in this chapter and will be discussed further.

4.1.9. Mass spectrometry in DNA adduct analysis.

Mass spectrometry has been used in macromolecular adduct detection. Analysis of the unique molecular mass of an ion from an adduct using spectrometry coupled with prior chromatographic separation of the analyte, offers enhanced specificity and signal/noise ratio providing conclusive evidence of DNA binding by specific chemical groups. However it has limited sensitivity. Advances in mass spectral techniques have improved sensitivity. For example, Accelerator mass spectrometry (AMS) offers unrivalled sensitivities ($1/10^{11}$) but uses radioactive isotopes (Turteltaub *et al*, 1990). Many variations of chromatographic and mass spectral technologies exist for use in detection of different adducts (Farmer and Sweetman, 1995). Pieles *et al* (1993) used matrix assisted laser desorption-time of flight (MALDI-ToF) to analyse adducts within an oligonucleotide with the possibility of determining adduct location. Liquid chromatography tandem mass spectrometry (LC-MS/MS) with electrospray ionization (ESI), used in this chapter, surpasses gas chromatography (GC) MS that is restricted to the analyses of volatile and non-polar adducts. Swenberg *et al* (2010) quoted a 10- to 1000- fold increase in sensitivity achieved through LC MS-MS over traditional ^{32}P post-labeling techniques. However, Singh *et al* (2005) quote a LOD of 0.6 N7EtG adducts in 10^8 nucleotides which is approaching sensitivities of ^{32}P post-labeling.

4.1.9.1. Liquid chromatography electrospray ionization tandem mass spectrometry multiple reaction monitoring (LC-ESI-MS/MS-MRM).

Below is a brief account of the theory of LC-ESI-MS/MS-MRM used for the current detection of N7MeG (nucleo)base. LC-ESI-MS/MS has been used to detect macromolecular monomers (Banoub and Limbach, 2009). Alkyl adducts such as N7MeG and O^6MeG are released from DNA as adducted bases or nucleosides by thermal/acid-induced hydrolysis or enzymatic digestion, respectively. DNA digestion generates a high quantity of purine nucleosides that interferes with downstream analysis (Mallet, Lu and Mazzeo, 2004). Kato *et al* (2011) gave enzyme conditions for the removal of O^6MeGuanosine but these proved ineffective when repeated at Leicester University (Dr Rajinder Singh, personal communication). Additionally, Muller *et al* (1997) found that using acid caused genomic depurination that suppressed ionisation further in the method. Therefore, in the present study, thermal

hydrolysis is the preferred method allowing detection of N7MeG bases only and not O^6MeG nucleosides unfortunately. Following thermal depurination, the N7-methylated base is separated from unmodified DNA by filtration for purification. The filtrate (adducted base) is applied to the LC column for isolation (Singh *et al*, 2003). The adducted base (analyte) is retained in the column by the stationary phase while other molecules are eluted to waste. At the retention time (unique for each analyte), the analyte gains affinity for the liquid mobile phase (containing solvents and acids (such as formic acid, to enhance ionization) and is eluted into the electrospray for positive ionisation (protonation). A combination of nitrogen gas (nebulizing gas), heated nitrogen (drying gas) and high voltage is applied to the eluent at the source of the electrospray generating an aerosol spray of positive ions. The spray undergoes solvent evaporation (desolvation) producing a stream of gas phase ions into the mass spectrometer. The mass spectrometer has three quadrupoles designated Q1 (MS1), Q2 (collision cell) and Q3 (MS2). In Q1, the gaseous ions are filtered according to their mass to charge ratio (*m/z*) by an oscillating electric field within the quadrupole. *m/z* is defined as $[M+nH]^{n+}/n$, where M is the molecular mass of the analyte, *n* is the number of protons it can accept and H is the mass of the proton. Ions with the equivalent *m/z* of the major product ion of the analyte (precursor ion) will be detected and passed to Q2. In Q2, an inert gas at high collision energy fragments the precursor ion in a collision-induced dissociation (CID), forming the product ion, detected in Q3 as in Q1 (Sleno and Volmer, 2004). For N7MeG, the major precursor ion has an *m/z* $[(M+H)^+]$ of 166, following CID, the product ion has an *m/z* $[(B+H)^+]$ of 149 indicating the loss of exocyclic amine, stabilised by a proton; NH_3 (**Figure 4.4**) (Tuytten *et al*, 2006).

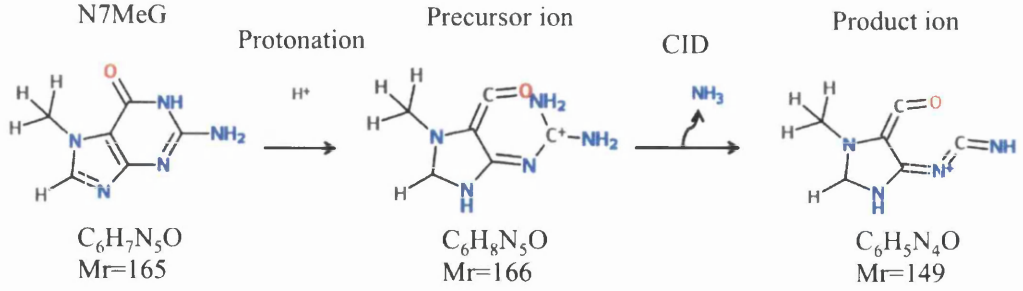

Figure 4.4. The structure of N7MeG base (precursor ion) and product ion following CID (collision-induced dissociation). With thanks to Dr Ed Dudley. Structures drawn using freeware at www.emolecules.com.

Identifying the specific product ion following CID in tandem mass spectrometry confirms the identity of the precursor ion and adds confidence to the data. There are three methods of detecting ions in Q1 and Q3 in tandem mass spectrometry;

1. Multiple/selective reaction monitoring (MRM/SRM)- Q1 and Q3 are set to the desired *m/z* and will only detect those ions.
2. Constant neutral loss (CNL) Q1 and Q3 scan a range of masses with a signal only being detected if Q3 detects a product ion of the desired *m/z*.
3. Single ion monitoring (SIM) either the product or precursor ion is detected.

With multiple reaction monitoring (MRM) the user specifies the *m/z* to detect in Q1 and Q3, being 166 and 149 for N7MeG, respectively. MRM offers the greatest sensitivity for use in LC-ESI-MS/MS (Ravanat *et al*, 1998; Singh and Farmer, 2006). The sample can be spiked with a base isotope that acts as an internal standard for quantification. An internal standard that is routinely used is [$^{15}N_5$]7MeG (Hu *et al*, 2011), which is distinguishable from the sample analyte. [$^{15}N_5$]7MeG is 5 mass units more than sample N7MeG, therefore, the precursor ion has a *m/z* of 171, following CID the subsequent product ion has a *m/z* of 153. MRM monitors this on a separate channel to the sample. Song (2011), when analysing chlorophenoxy herbicides, found interference when detecting analytes through MRM on two channels caused by the time in alternating between channels. To overcome this, the author ran samples and standards separately, which hinders quantitation.

4.1.10. Measuring N7MeG as a biomarker for MNU exposure.

Several questions are raised given the non-linear dose response for MNU induced point mutations in chapter 3. The threshold at low dose region may be due to the inability to detect an increase in mutant frequency as an artefactual high background frequency exists due to limited sensitivity in the HPRT assay. The following work aims to identify DNA adducts at increasing concentrations of MNU and produce an adduct dose-response as performed by Marsden *et al* (2009) for ethylene oxide (EO) adducts. Identifying exposure biomarkers at doses below the NOGEL would demonstrate MNU-DNA interactions, thereby, substantiating our hypothesis of adduct formation followed by DNA repair as a mechanism of low dose threshold for MNU. The following depicts the use of N7MeG as a biomarker for low dose MNU exposure

by LC-ESI-MS/MS-MRM analyses performed in Leicester University funded by a UKEMS transfer of knowledge bursary.

4.2. Materials and method.

4.2.1. Treatment of AHH-1 cells with MNU.

$1x10^7$ AHH-1 cells in 10ml cultures were treated with DMSO, 0.00075μg/ml and 0.025μg/ml MNU (details given in general materials and methods). This represented the negative control, below NOGEL and above LOGEL doses, respectively. After 1hr exposure, the cells were washed twice in PBS and pelleted for storage in -80°C for transport to Leicester University where the following analysis took place.

4.2.2. Isolation of genomic DNA from AHH-1 cells.

DNA was extracted using Blood and Cell culture DNA midi kit' (Qiagen, Sussex, UK). Cell pellets were resuspended in 2ml of PBS and vortexed. 1 volume (2ml) of ice-cold buffer C1 and 3 volumes (6ml) of ice-cold distilled, filtered water were added and the tube inverted until solution became translucent. This was incubated on ice for 10mins for sufficient cell lysis. The lysed cells were centrifuged at 3000rpm for 15min at 4°C and the supernatant discarded. The pelleted nuclei were digested using 5ml of Buffer G2 and vortexed until completely re-suspended. To this, 18.1μl (50U) of Bovine pancreatic ribonuclease (RNase) A (cat. R4642 Sigma-Aldrich, Poole, UK) and 5μl (5U) of RNase T_1 from *Aspergillus oryzae* (Cat. 10109193001 Roche, Sussex, UK) was added, briefly vortexed to mix and incubated at 37°C for 30min. The combination of two RNases sufficiently digests RNA into small alcohol soluble fragments that can be washed from the sample. Stock of RNase T_1 was provided at 100000U in 1ml (100U/μl) and diluted 1:100 to 1U/μl in phosphate buffered saline (PBS, Lonza, Slough, UK). After 30min incubation, 100μl of proteinase K (at 20mg/ml in water) was added and incubated at 37°C for a further 2hr to digest histones and other nuclear proteins. The genomic tip was equilibrated with 4ml buffer QGT and allowed to empty by gravity flow. The sample was applied and allowed to flow through by gravity. The column was washed twice with 7.5ml buffer QC. The

DNA was eluted using 5ml buffer QF and precipitated with 3.5ml ice-cold isopropanol with slow inversion until the DNA precipitate became visible. The sample was stored overnight at -20°C. The samples were centrifuged at 4000rpm for 30min at 4°C. The supernatant was discarded and the pelleted DNA washed with 500µl of absolute ethanol and centrifuged at 4000rpm for 15min. The supernatant was aspirated and the pellet air-dried to allow excess ethanol to evaporate. To dissolve the DNA pellet, 200µl of distilled, filtered water was added and gently vortexed. The concentration of DNA was determined by measuring the absorption at 260nm using a nanodrop 1000 spectrophotometer.

4.2.3. Preparation of the internal standard [$^{15}N_5$]N7MeG.

[$^{15}N_5$]7MeG base was synthesised as per Chao *et al* (2005). 2µg Dimethyl sulfate (DMS, Sigma-Aldrich, Poole, UK) and 1mg $^{15}N_5$-deoxyguanosine monophosphate (Sigma, Poole, UK) were dissolved in 20µl N,N-dimethylacetamide and left stirring for 6hr at room temperature. To remove impurities, 1mg celite was added to the mixture and centrifuged at 13000rpm for 30min. The supernatant was retained and pH increased to 8.0 by addition of ammonium hydroxide. The volume was increased to 100µl with acetone. The white precipitate of $^{15}N_5$-N7-methyldeoxyguanosine monophosphate was collected by centrifugation at 13000rpm for 1hr. The supernatant was discarded and washed with 100µl ice-cold absolute ethanol with repeat centrifugation. 100µl absolute ether was added and the sample was dried overnight in a savant DNA 110 concentrator speedvac at ambient temperature. Acid hydrolysis with 1M hydrochloric acid (HCl) and incubation at 80°C for 30min on a heating block (Stuart Scientific, Staffordshire, UK), depurinated the nucleoside, releasing the methylated base. Ammonium hydroxide was added drop-wise until [$^{15}N_5$]N7MeG base precipitated. The sample was air dried and reconstituted in 400µl 0.1M formic acid. The purity of the sample was analysed at 250nm by UV coupled chromatography using a Varian Prostar 210 HPLC system with Varian Prostar 310 UV detector (Varian CA, USA) connected to a phemomenex, synergi column (4µm, 250mmx4.6mm). A 40µl aliquot of the standard was injected onto the column using a Varian Prostar 410 autosampler. The column was eluted at 1ml/min with a gradient of

solvent A, 0.05M ammonium formate and solvent B absolute methanol. The gradient being; 98% A (2% B) 15min, 80% A 5 min then 98% A for 10min.

4.2.4. Preparation of the positive control.

With an easily detectable level of naturally occurring N7MeG, calf thymus DNA was used as the positive control. A length of un-sheared genomic DNA from calf thymus (Sigma-Aldrich, Poole, UK) was dissolved in distilled water. The concentration was determined via absorbance at 260nm using a nanodrop 1000 spectrophotometer. The positive control was subjected to the same procedure as experimental samples detailed below.

4.2.5. Preparation of DNA for LC-ESI/MS-MS-MRM analysis.

For each dose, four samples were pooled into two to increase the amount of DNA sufficient for mass spectrometry. Each sample, and positive control, were spiked with 26.668μl (1333.4 fmol) of [$^{15}N_5$]7MeG, (50fmol/μl) to be used as an internal standard in quantifying the amount of adduct in sample DNA. The samples were vortexed to mix and centrifuged for 1hr to dryness using a savant DNA 110 concentrator speedvac at ambient temperature. After drying, 100μl of HPLC-grade water (18.2MΩcm) was added and incubated for 1hr at 70°C in a heating block (Stuart Scientific, Staffordshire, UK) to release N7MeG from DNA. 80μl of ice-cold absolute ethanol was added to precipitate unwanted double stranded DNA. The adduct was filtered from unwanted DNA based on molecular weight by centrifuging at 14000rpm for 1hr through an Amicon Ultra 3,000 MWCO centrifugal filter (cat. UFC500396, Millipore, Watford, UK) pre-conditioned with 200μl HPLC grade water by centrifuging for 15min at 14000rpm. Following drying of the filtrate, 20μl of 0.1% formic acid was added to dissolve the base. 15μl of this was used for analysis. The 5μl loss of sample was taken into account when calculating the amount of DNA loaded on column (**equation 4.0**, overleaf).

4.2.6. Measuring N7MeG using LC-ESI/MS-MS-MRM.

A Waters Alliance 2695 separations module with a 100μl injections loop and automated column-switching device was coupled to a Micromass Quattro Ultima Pt. tandem quadrupole mass spectrometer. The electrospray source was at 110°C. Nitrogen gas (650L/h) was used as the desolvation gas (350°C) and the cone gas (25L/h). The capillary was set at 3.20kV while the cone was 42V, the RF1 lens at 15V and the photomultiplier at 950V. To tune the mass spectrometer, N7MeG standard solution (1μg/ml) in 0.1% formic acid/methanol solution (9:1 v/v) was continuously infused (10μl/min) by a Harvard model 22 syringe pump (Harvard Apparatus Ltd, Edenbridge, UK).

The LC system consisted of a trap column to purify the signal and an analytical column. The trap was composed of Phenomenex Synergi Fusion RP 80A (4μM, 2.0mm x 30mm) and a waste KrudKatcher (0.5μM) column whereas the analytical column consisted of a Phenomenex Synergi Fusion RP 80A column (4μM, 2.0mm x 250mm), KrudKatcher and guard column. The trap column was eluted with 0.1% formic acid/2% methanol (9:1 v/v) at 120μl/min. At this flow rate, the analyte remained in the trap column for 1.96+/-0.01min. To limit the volume of unwanted molecules entering the mass spectrometer and increase signal over noise, the trap column was diverted to waste until 1.4min, switched online into the analytical column until 3.2min then diverted back to waste. The analytical column was eluted at 120μl/min with 0.1% formic acid/5% methanol, which gave minimum background peak. The collision gas, argon, was set at 2.0×10^{-3} mbar and the collision energy at 12eV. The dwell time was set to 200ms and the resolution at two *m/z* units at peak base. The samples were analysed in positive electrospray ionisation in multiple/selected reaction monitoring (M/SRM) on two channels. One for the transitions of *m/z* 166 to 149 for N7MeG and a second channel monitored the transition *m/z* 171 to 153 for the internal standard [$^{15}N_5$]7MeG (Chao *et al*, 2005). MassLynx 4.0 software was used to obtain the area under the peak at 11.1+/-0.2min that corresponded to N7MeG or [$^{15}N_5$]7MeG of the resulting chromatograms. This was used to calculate the amount of adduct in DNA (**equation 4.0**).

4.2.7. Calculation of DNA adduct levels.

The following calculation was used to determine the moles of adduct:

Equation 4.0 $Q_{ADDUCT} = (A_{ADDUCT}/A_{STD}) \times Q_{STD}$

Where;

Q_{ADDUCT} = the amount (fmol) of adduct detected

A_{ADDUCT} = the peak area of the DNA adduct

A_{STD} = the peak area of the internal standard

Q_{STD} = the amount (fmol) of the internal standard loaded onto the column

4.2.8. Conversion of mole DNA adduct to adducts/10^8 nucleotides.

Using Q_{ADDUCT} from **equation 4.0**, the number of adducts/10^8 nucleotides was determined:

Equation 4.1

Number of adducts per 10^8 nucleotides= $(Q_{ADDUCT}/Q_{SAMPLE})/1 \times 10^{-8}$

Where;

Q_{ADDUCT} = the amount (mol) of adduct detected being amount in fmol x $1x10^{-15}$.

Q_{SAMPLE} = the amount (mole) sample DNA loaded onto LC column for analysis. This was derived assuming that 1μg of DNA=3240pmol (Tauteltaub *et al*, 1990).

Therefore; Q_{SAMPLE}= amount of DNA (μg) on column x $3.240x10^{-9}$

4.3. Results.

The results presented in this chapter quantify the levels of N7MeG in genomic DNA isolated from AHH-1 cells following treatment with 0.00075μg/ml MNU (below NOGEL) and 0.025μg/ml MNU (above LOGEL).

4.3.1. Purity of the internal standard [$^{15}N_5$]N7MeG.

The purity of the internal standard preparation was assessed by UV coupled HPLC, the resulting chromatogram (**Figure 4.5**). The methodology used to synthesise [$^{15}N_5$]N7MeG is taken from Chao *et al* (2005). The authors state a purity of 99% assessed by diode array detection.

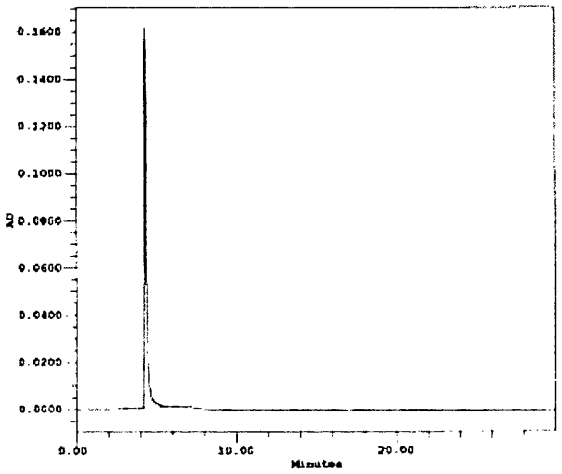

Figure 4.5. HPLC-UV chromatogram of the internal standard preparation. The peak represents [$^{15}N_5$]N7MeG showing absorbance at 250nm as a function of elution time using a solvent gradient at a flow rate of 1ml/min. Kindly provided by Jodie Sandhu with permission from Dr Rajinder Singh.

4.3.2. DNA extraction.

AHH-1 cells were treated for 1hr with DMSO, 0.00075μg/ml and 0.025μg/ml MNU to represent solvent control, below NOGEL and above LOGEL doses, respectively, and the DNA extracted. **Table 4.3** shows the purity and suitability of each DNA sample for mass spectrometric analysis.

Table 4.3. DNA yields from $1x10^7$cells using Blood and Cell culture DNA midi kit*. Each letter represents a different replicate for the specified treatment group. For each treatment, sample A and B were pooled into one and so was C and D. The amount of DNA on column is shown. This was the final amount of DNA used for analysis. Values were calculated after the samples were pooled and accounted for the unavoidable loss of sample. This occurred following filtration of adduct from unwanted DNA (15µl was retained in the filter) and on injection into the LC system (15µl of 20µl was used). These values were also used for equation 1.1. An absorbance ratio of 1.8-2.2 for 260/280 indicates no protein contamination and for 260/230 indicates no ethanol or solvent carryover.

Sample ID		DNA YEILD (ng/µl) @260nm	260/280 ratio	260/230 ratio	Amount of DNA (µg) on column
DMSO	A	152.6	1.91	2.20	53.42
	B	203.5	1.91	2.10	
	C	189.3	1.90	2.20	52.32
	D	159.5	1.90	2.20	
0.00075 (µg/ml)	A	163.7	1.91	2.20	53.03
	B	189.8	1.91	2.20	
	C	199.1	1.92	2.20	60.84
	D	206.5	1.92	2.20	
0.025 (µg/ml)	A	181.6	1.83	2.09	46.13
	B	125.9	1.90	2.12	
	C	171.5	1.89	2.20	49.31
	D	157.2	1.89	2.20	

4.3.3. LC-ESI-MS/MS-MRM chromatograms.

Ion chromatograms are shown in **Figure 4.6** for DNA extracted from AHH-1 cells following 1hr treatment with DMSO, 0.00075µg/ml and 0.025µg/ml MNU.

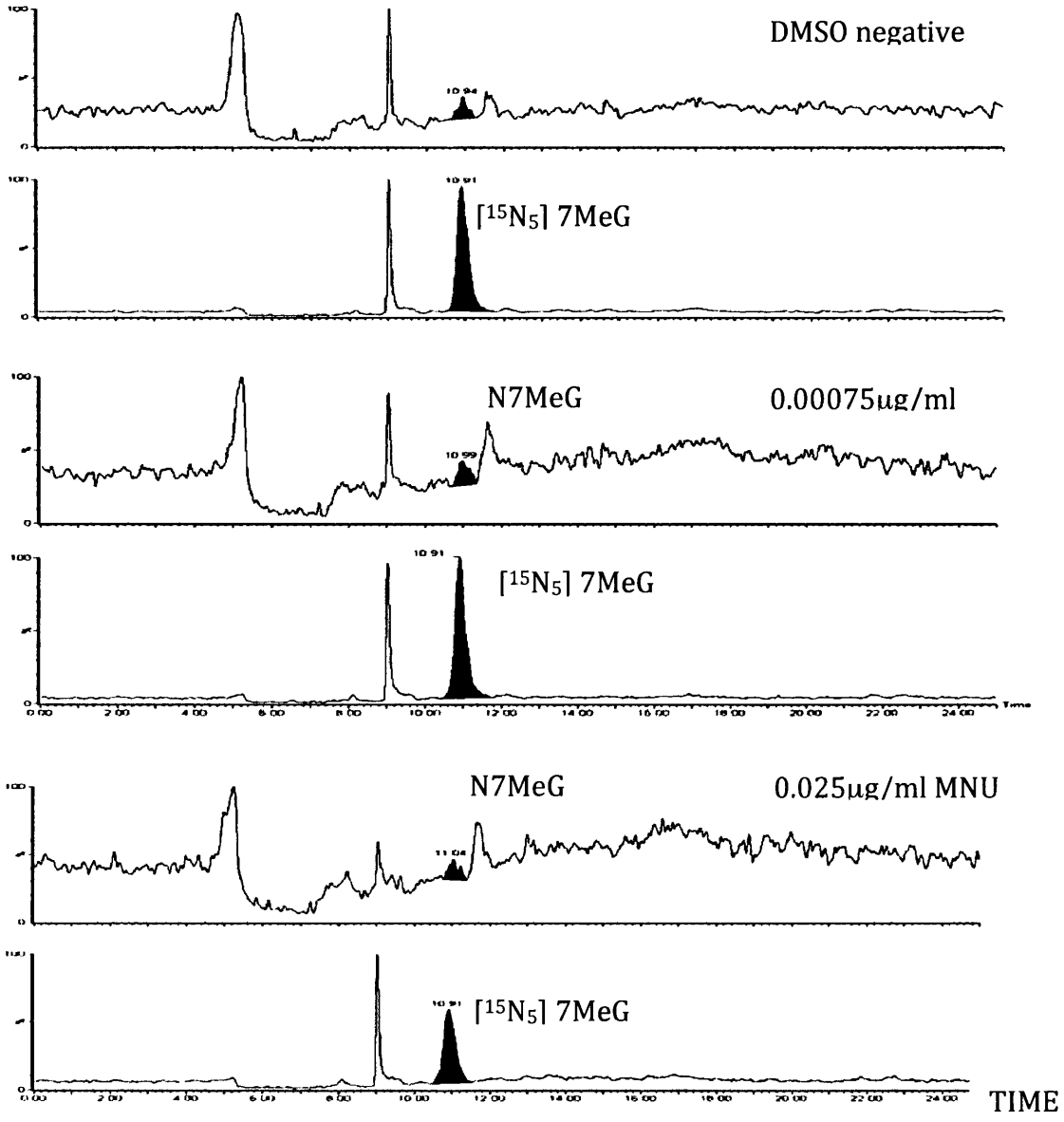

Figure 4.6. Typical LC-MS/MS chromatograms A.) 0.1% DMSO B.) 0.00075µg/ml MNU and C.) 0.025µg/ml MNU with respective internal standards. The numerical output for each DNA sample is shown in **Table 4.4**.

The area under the peaks (**Table 4.4**) was used to calculate the number of moles of adduct using **equation 4.0**. This was normalised against the amount of DNA loaded onto the column used for analysis (**equation 4.1**) to calculate number of adducts per 10^8 nucleotides (**Figure 4.7**).

Table 4.4. The area under the peaks and retention time for each sample is given. The peak area for N7MeG was normalised against the corresponding peak area of the internal standard (**equation 4.0**). The retention time for N7MeG is typically 0.1min later than for [$^{15}N_5$]7MeG. The mass spectrometer preferentially identifies higher mass ions first.

		***m/z* 166 to 149 (N7MeG)**		***m/z* 171 to 153 ([$^{15}N_5$]7MeG)**	
Sample ID		**Peak Area**	**Retention time (min)**	**Peak Area**	**Retention time (min)**
DMSO	A+B	3129	11.0	115536	10.9
	C+D	4965	10.9	140578	10.9
0.00075 (μg/ml)	A+B	5551	11.0	144684	10.9
	C+D	1922	11.1	71719	10.9
0.025 (μg/ml)	A+B	3140	11.0	66643	10.9
	C+D	2065	11.2	55702	10.9
Calf thymus DNA (+ve control)		132357	11.6	107827	11.6

4.3.4. N7MeG levels below and above the mutation NOGEL for MNU.

The level of N7MeG was quantified in DNA from cells exposed to DMSO, 0.00075μg/ml or 0.025μg/ml MNU and the dose-response obtained (**Figure 4.6**). The solvent control has similar adduct levels to low dose MNU being 18.2+/-3.7 (mean+/- standard deviation) N7MeG/10^8 nucleotides and 18.0+/-6.2 N7MeG/10^8 nucleotides respectively with an increase of 27.4+/- 5.9 N7MeG/10^8 nucleotides at 0.025μg/ml MNU.

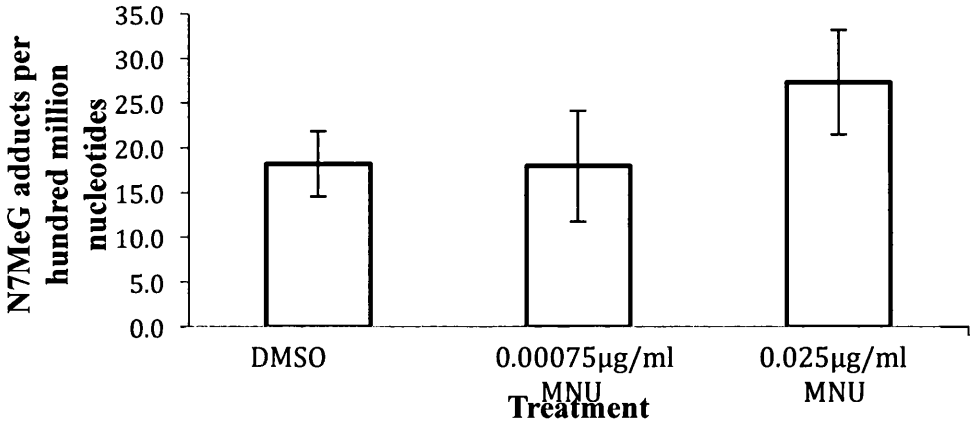

Figure 4.7. AHH-1 cells were treated with increasing concentrations of MNU for 1hr. DNA was extracted and N7MeG adducts quantified. N=2, error bars=s.d.

4.4. Discussion.

The aims of this chapter are to quantify N7MeG adducts as exposure biomarkers following MNU treatment through use of LC-MS/MS. O^6MeG would have been the preferred analyte since it is the hypothesised adduct behind the observed MNU-induced mutation dose-response in the HPRT assay. However, due to the difficulties in releasing the adducted guanine base/nuceloside/nucleotide from DNA, N7MeG was chosen as an appropriate biomarker (Swenberg *et al*, 2008). The adducted base of N7MeG is readily and selectively released from DNA by thermal hydrolysis meaning that other sites of methylation that are not heat labile, but require enzymatic or acid hydrolysis (Shuker and Bartsch, 1994), will not interfere with the analysis.

4.4.1. Assay methodology.

Since N7MeG constitutes 69% of the adduct spectra, it is the predominant adduct formed by MNU and all other methylating agents (Beranek, 1990). Due to this, it may be a more sensitive biomarker than lesser formed adducts (Pottenger *et al*, 2009). There is a well-established protocol in use at Leicester University for the quantitation of N7MeG using LC-MS/MS. The method described here, has been able to achieve sensitivities of 0.6 adducts/10^8 nucleotides with 100µg DNA, similar to ^{32}P-

postlabeling techniques (Singh *et al*, 2005). Assay sensitivity was compromised by poor DNA yields (**Table 4.5**) meaning only a maximum of 60μg of DNA was available for analysis but this proved to be sufficient. The method of DNA extraction is vitally important in downstream mass spectral analysis of adducts. For example, Claycamp (1992) concluded that DNA extraction by phenol-chloroform could overestimate 8-hydroxyguanine (oxidative damage adduct) by 2- to 20-fold. Qiagen's Blood and Cell culture DNA midi kit® was chosen for DNA extraction because the reagents do not react with DNA. The chromatograms (**Figure 4.6**) show miscellaneous peaks in all outputs for experimental samples. The output for calf thymus DNA showed an absence of miscellaneous peaks. The sample was prepared by Sigma using a different extraction method, therefore we hypothesise that the peaks are evidence of salts and trace impurities introduced throughout the DNA extraction method. This could be responsible for suppressing ionisation at the electrospray source, further compromising sensitivity. Sampling time post exposure is critical when determining adduct levels. An initial experiment quantified adduct levels at these doses after 24hr exposure, but there was no increase at 0.025μg/ml over background levels (**Figure 4.8**).

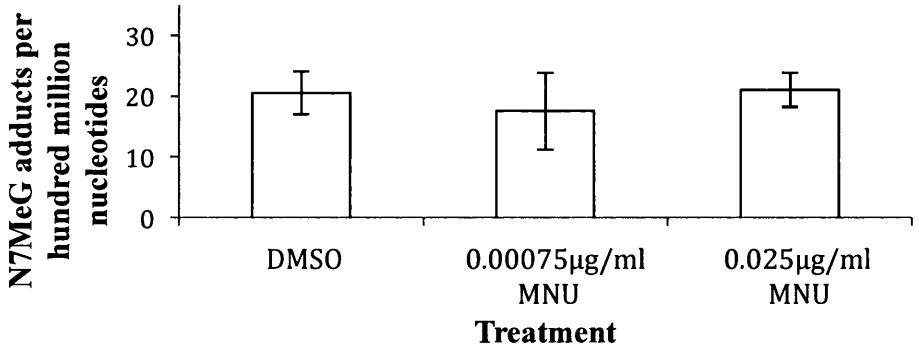

Figure 4.8. 50μg genomic DNA was assessed for the quantity of N7MeG adducts in AHH-1 cells treated with MNU for 24hr. This allowed time for repair, DNA replication and spontaneous depurination of chemically unstable N7MeG, which reduces the level of N7MeG. n=2.

The findings in **Figure 4.8** substantiate a study by Doniger *et al* (1985). The authors show a reduction in N7MeG over 24hr. Initial levels, following treatment with 100μM (10.308μg/ml), was reduced from 1550 adducts/10^8 nucleotides to 625 adducts/10^8 nucleotides, a reduction of 59%. A reduction in exogenous adduct levels

by 59% would not be detected in the current study and accounts for a lack of dose-response at 24hr. This is comparable to the findings of Warren, Crathorn and Shooter (1979) who found a half-life of 22hr for N7MeG in V79 cells treated with 1.2mM MNU (123.70μg/ml). The reduction could potentially involve spontaneous depurination. Additionally, the authors report a similar reduction in O^6MeG. Since O^6MeG is not spontaneously labile, the reduction could also be caused by dilution through DNA replication or removal by repair, which occurs more rapidly than spontaneous hydrolysis (Singer, 1985). Commonly, there is a reduction in adducts over time following a single, acute exposure until a balance of endogenous formation and removal is reached. The time to reach this differs drastically between different adducts, studies and tissues (Singer, 1985). A study by Shibata *et al* (1994) showed persistence of adducts 72hr post-MNU injection in rats. While, Medcalf and Lawley (1981) showed persistence of MNU adducts 180 days post-exposure. Conversely, a chronic exposure regime *in vivo* shows an accumulation of adducts as exposure continues over several weeks. Previously shown for BAP adducts (Talaska *et al*, 1996). In this study, N7MeG levels were determined after 1hr post-treatment with MNU. This gave sufficient time for DNA reaction and adduct formation and limited the time for removal by mechanisms previously discussed. Since DMSO is not DNA reactive and does not cause N7MeG adducts (Fischer *et al*, 2008), the levels in **Figure 4.7** and **Figure 4.8** reflect background levels of N7MeG adducts being 18.2+/-3.7adducts/10^8 nucleotides. This is comparable to *in vivo* background levels **Table 4.2**. For example, Petruzzelli *et al* (2006) quote a level of 25 N7MeG/10^8 nucleotides in DNA of blood cells using ^{32}P-post labelling.

4.4.2. Postulating a no observed genotoxic effect level for adducts.

The data presented in **Figure 4.7** gives the appearance of a no observed genotoxic effect level (NOGEL) of adduct formation. At 0.00075μg/ml MNU, there is a lack of increase in adducts over the spontaneous level in the solvent control. There are two explanations for the lack of increase at 0.00075μg/ml MNU:

1. Assay sensitivity, adducts are formed but are below the limit of detection of the mass spectrometric analysis
2. Biological mechanism to prevent DNA reaction and adduct formation.

4.4.2.1. Assay sensitivity.

This is the most likely conclusion from the available data. This possible lack of sensitivity could account for the similarity in adduct levels between the negative control and low dose MNU (0.00075μg/ml) giving the appearance of a potential NOGEL (**Figure 4.7**). For further confidence, more replicates and doses would be needed for full dose-response characterisation. Marsdon *et al* (2009) and Swenberg *et al* (2008) believe exogenous genotoxins produce adducts proportionally to dose, any no observed effect level can be explained by the assay's limit of detection rather than lack of DNA reactivity at the NOGEL. Swenberg *et al* (2008) distinguished endogenous from exogenous adducts by use of radio-labelled genotoxins. The linear response they found could only be applied to exogenous adducts which can be linear to the LOD. Without experimentally distinguishing between endogenous and exogenous adducts, a high level of endogenous damage may mask the appearance of MNU induced adducts (Professor James Swenberg, personal communication). However, one would expect that exogenous N7MeG adducts to be additive to endogenous N7MeG to give a linear response down to the endogenous (control level). The assay would need conclusive evidence that the endogenous level was true and not artefactually high due to poor assay sensitivity. Pottenger *et al* (2009) found a NOGEL of MNU induced N7MeG up to 6.9μM (0.7μg/ml MNU) but the endogenous level was much higher than the present study (1200 N7MeG adducts per 10^8 nucleotides) and may require higher concentration of MNU to cause an observable increase. At low doses, the limit of detection of the assay and also variability in the data plays critically in the appearance of a NOGEL.

4.4.2.2. Biological mechanism to prevent DNA reaction.

Another explanation is that MNU does not react with DNA at such low concentrations and a true NOGEL exists for adducts, However, This cannot be concluded in this study because more biological replicates and doses would be needed. To exemplify, 0.025μg/ml equates to 242.5301nM (mol/L, Mr of MNU is 103.08), where the number of moles is 2.425301×10^{-10} [moles=Molar concentration (M/L) x volume (L)] being, $2.425301 \times 10^{-10} \times 0.001$). Employing Avagadro's number of

$6.0221415x10^{23}$/mol, the number of molecules of MNU in 0.025μg/ml is $1.46055x10^{14}$. Assuming that 1 molecule is capable of forming one DNA adduct, predicted by a linear extrapolation, 0.025μg/ml is capable of $1.46055x10^{14}$ adducts. N7MeG constitutes 69% of the adduct spectra (Beranek, 1990), therefore, 0.025μg/ml theoretically produces $1.0078x10^{15}$ exogenous N7MeG adducts. The human genome contains $3164.7x10^{6}$ nucleotides (taken from http://www.ornl.gov/sci/techresources/Human_Genome/home.shtml). In the experiment reported here, $1x10^{7}$ AHH-1 cells were treated giving a total of $3.1647x10^{16}$ nucleotides. Assuming that all guanine nucleotides (approximately 40% of the human genome (Lander *et al*, 2001). Equates to $1.2659x10^{16}$ guanines therefore guanines are in excess) are substrates for DNA adduction, then there can be a total of $3.18450x10^{5}$ N7MeG adducts per 10^{8} nucleotides ($3.1647x10^{16}/1x10^{8}=31647x10^{4}$, therefore; $1.0078x10^{15}$N7MeG adducts/$31647x10^{4}=3.18450x10^{5}$ exogenous N7MeG adducts per nucleotide). Assuming that the *maximum* of amount of DNA extracted from $1x10^{7}$ AHH-1 cells, reported in **Table 4.5,** is the *total* amount of genomic DNA in $1x10^{7}$ AHH-1 cells i.e. $3.1647x10^{16}$ nucleotides then a comparison can be made between this theory and the data (**Figure 4.7**). Given that this study detected an average of 9.1 exogenous N7MeG adducts/10^{8} at 0.025μg/ml (quantity at solvent control subtracted from quantity detected at 0.025μg/ml), the theoretical ratio is far too high for the "one molecule=one adduct" interpretation of linear hypothesis. Although, the instability of N7MeG to spontaneous depurination is also a consideration and may lead to underestimation of the levels through loss of adduct during sample handling. When considering individual molecules, the linear hypothesis that states, one molecule of genotoxin forms one adduct, cannot hold true. It is, therefore, reasonable to hypothesise that adducts can display a NOGEL. A NOGEL has been found for 8-hydroxy-2'-deoxyguanosine adducts in murine liver DNA following exposure to increasing concentrations of 2-amino-3,8-dimethylimidazo[4,5-*f*]quinoxaline (MeIQx) (Fukushima *et al*, 2002). At such low doses, it is possible that carcinogens do not react with DNA. There are several explanations; membrane exclusion (Speit *et al*, 2000) or reaction with other macromolecules such as RNA (ubiquitously present in the cytoplasm) or components of cell culture media (proteins in supplements like horse serum) due to carbamoylation, which would not be detected in this assay. Woolley and Pinsky

(1981) show that MNU shows substantial propensity for methylation of sub-cellular organelles and modifications like methylation, carbamoylation and guanidination of nuclear proteins such as histone H2A, H3 and H1, respectively (Pinsky, Lee and Woolley, 1980; Jump *et al*, 1980). Since histones are ubiquitous throughout the genome they represent an abundant target for reaction with MNU and other alkylating agents, thereby preventing DNA adducts. However, this does not disprove linearity concerning the fraction of molecules that actually reach the DNA. This could only be proven with naked DNA in a chemically inert buffer. Suffice to say that at higher doses, with more MNU molecules there is a higher likelihood of reaction with DNA. The kinetics of spontaneous MNU decomposition are dependent upon buffer pH and temperature (Golding *et al*, 1997). Donovan *et al* (2010) state a $t_{1/2}$ of 0.34hr at pH8.4 but can be extended to 24hr at pH6 (Druckrey *et al*, 1967). The major decomposition, DNA reactive product of MNU is methyldiazonate. This has a half-life of 0.5-2min (Jensen, 1983), which was accelerated by bicarbonate, a constituent of buffering systems in cell growth media. It is plausible that rapid decomposition of MNU, and its subsequent mutagenic products, prevent reaction with DNA, which explains the elucidated NOGEL. In the *in vivo* situation, MNU can be metabolised into methanol and excreted as CO_2 and in urine (Swann, 1968). 15min following an intravenous injection of 100mg [^{14}C] MNU/kg body weight into the rat the levels were undetectable with radioactivity detected in excretory products. It could be possible that MNU is metabolised to prevent DNA reaction and adduct formation, further substantiating the NOGEL hypothesis despite recent efforts to suggest a linear response. The data presented here cannot substantiate a biological mechanism responsible for the observed NOGEL.

4.4.3. Adducts and HPRT mutant frequency.

The results of this chapter has been combined with the mutation indution dose-response obtained in chapter 3 (**Figure 4.9**).

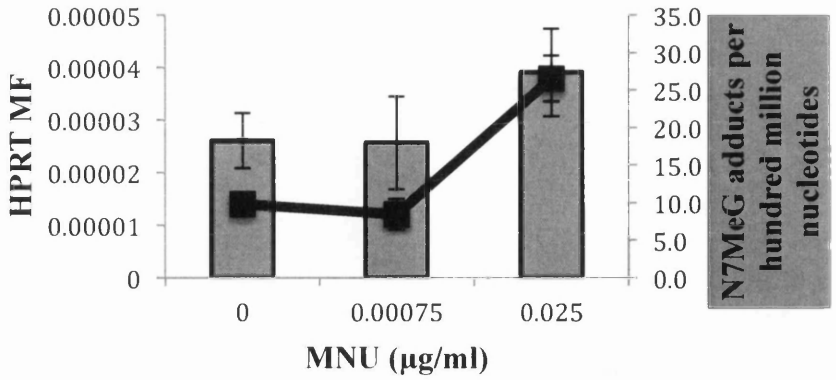

Figure 4.9. The adduct-dose relationship mimics that for mutation induction by MNU this suggests that the NOGEL is dependent upon adduct formation.

The observations of **Figure 4.9** suggest that adduct formation is the critical event in mutagenesis. The lack of adducts is responsible for the lack of increase in mutant frequencies observed below the NOGEL (0.0075g/ml). This has been previously observed by Pottenger *et al* (2009) when quantifying O^6MeG adducts at below NOGEL doses of MNU in mouse lymphoma cells. This is predominately due to a lack of mass spectrometric sensitivity since MNU specific N7MeG adducts were identified at the same doses. Incidentally, these doses were higher than those reported in the present study. The findings presented in this chapter would have implications in defining the mechanism behind the shape of the dose-response of MNU in wildtype AHH-1 cells. The mutational NOGEL could be explained by a lack of DNA reaction, which has been discussed, as opposed to adduct formation and repair. However, the dose tested here is 10-fold lower than the NOGEL. Adduct quantitation would need to be determined at more sub-NOGEL doses before this was concluded.

4.4.4. Concluding remarks.

The data obtained in this study, shows that 0.025µg/ml induces 9.1 exogenous N7MeG adducts/10^8 nucleotides over background levels. We can infer the number of O^6MeG adducts, which constitutes 8% of adducts according to the spectra of MNU. This is based on data from Beranek, (1990) obtained at high doses MNU exposure and so this may not hold true at low doses. If, 69% of adducts induced were N7MeG, being 9.1 adducts/10^8 nucleotides, 8% equates to 1.1adducts/10^8 nucleotides (to 1

d.p). We hypothesise that 1.1 O^6MeG adducts/10^8 nucleotides are sufficient to cause MGMT inactivation in AHH-1 cells and contribute to an increase in mutagenesis. It is likely that poor assay sensitivity prevented adduct detection at low doses of MNU. Therefore, this study does not provide conclusive proof of adduct induction at doses below the NOGEL (0.0075μg/ml MNU) found in chapter 3. In the following chapter, HPRT mutants resulting from MNU treatment were sequenced and the results contradict the findings presented here and show that MNU is capable of DNA reaction at doses below the NOGEL. An important question is raised; is DNA sequencing more sensitive at detecting changes than adduct quantitation?

Chapter 5.

Mutation Analysis.

Comparison Of Mutation Spectra At Increasing Concentrations Of MNU.

5.1. Introduction.

This chapter will discuss sequencing of HPRT mutants following MNU exposure. Sequencing is required for construction of mutation spectra and interpretation of changes in mutation induction. Therefore, changes in mutation induction from low, non-mutagenic doses to higher, mutagenic doses of MNU will be examined.

5.1.1. Establishing a mutation spectrum.

Mutation induction is observed as an increase in mutant frequency over background levels when quantified through the HPRT forward mutation assay. Like other assays at different loci (such as TK assay), the HPRT assay positively selects for mutants, facilitating downstream analysis of the mechanism of mutation induction. Mutations are important biomarkers of effect following mutagen exposure (Au, 2007). In chemical carcinogenesis, mutations are dependent upon adduct formation; adduct miscoding potential during DNA replication and cellular processing of the damaged base (**Figure 5.1**). This reflects cellular repair capacity and DNA replication rate (Swenberg *et al*, 2008). Downstream DNA sequence analysis of HPRT mutants allows construction of a mutation spectrum. Mutation spectra identify the frequency and location of mutations over a DNA sequence, in this example over the HPRT gene. Patterns of mutation induction are mutagen specific, as exemplified by analysis of mutations induced by ethyl nitrosourea (ENU) and Benzo-α-pyrene (B[α]P) (Kohler *et al*, 1991). However, mutation spectra at low doses of mutagen have not been previously analysed. The spectrum of mutations at the HPRT locus reflects the mechanism of action of mutation induction, in relation to the requisite steps in **Figure 5.1.**

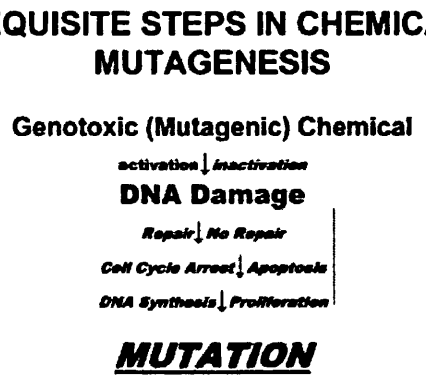

Figure 5.1. Mutations are biomarkers of effect;a combination of adduct formation and cellular processing. Image is taken from Swenberg *et al* (2008).

Mutation induction at the HPRT locus can act as a surrogate for mutation induction at other genomic sites relevant to cell growth control and cancer progression, such as *p53* (Aidoo, Morris and Casciano, 1997). HPRT mutation spectra also allows:

1. Comparison of mutation induction *in vitro* to the same locus *in vivo*
2. Comparison of mutation induction in repair deficient and proficient cells (Yang *et al*, 1994)
3. Comparison of mutation induction between different mutagens (Casciano *et al*, 1999)
4. Analysis of spontaneous mutation induction (Zhang *et al*, 1992)
5. Identification of mutagen specific hotspots

Methyl nitrosourea (MNU) produces an array of DNA adducts (Beranek, 1990). Examining the mutation spectra will identify the location and likely type of adduct responsible for specific mutations (Van Zeeland *et al*, 1989). The biological relevance of different adducts can also be ascertained. In this study, we are comparing mutation spectra at increasing concentrations of mutagen to elucidate the mechanisms of mutation induction, at doses below and above the NOGEL of MNU.

5.1.2. Point mutations caused by MNU induced adducts.

The three major DNA adducts resulting from treatment with MNU are O^6MeG (O^6-methylguanine), N7-methylguanine (N7MeG) and N3-methyladenine (N3MeG). These form 5.9-8.2%, 65-70% and 8-9% of the MNU specific adduct spectra, respectively (Beranek, 1990). Their conversion into point mutations has been

investigated. These adducts are also clastogenic lesions, responsible for sister chromatid exchanges (Quiros, Kaina and Roos, 2010) and chromosome aberrations (Zair *et al*, 2010). However, such chromosomal alterations will not be detected in the mutation spectra and will not be discussed.

5.1.2.1. O^6MeG is miscoding.

O^6MeG is a miscoding lesion and has a well-defined fixation mechanism in G:C→A:T transitions, unless O^6MeG is repaired by methylguanine methyltransferase (MGMT). As discussed in Chapter 1, unrepaired O^6MeG is mispaired with thymine, forming O^6MeG:T mispairs, following the first post-treatment DNA replication. The O^6MeG is then converted to adenine following a second S phase (**Figure 5.2**).

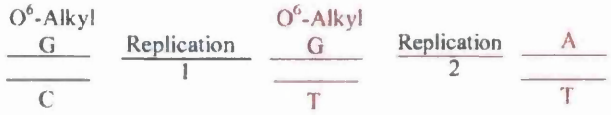

Figure 5.2. Fixation of O^6MeG into GC→AT transitions is a well-understood mechanism, requiring two rounds of replication. Image adapted from O'Neill (2000).

5.1.2.2. N7MeG and N3MeG are not miscoding.

Methylated purines (N7MeG and N3MeA) are not directly miscoding (Mhaskar *et al*, 1981). However, these adducts can be processed into point mutations following hydrolysis into non-coding apurinic (AP) sites (**Figure 5.3**).

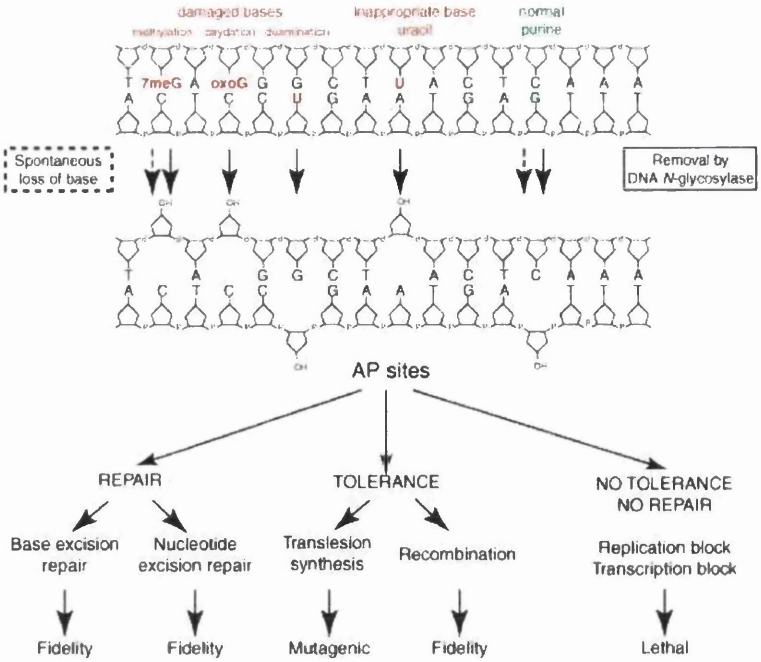

Figure 5.3. Enzymatic removal and unstable properties of methylpurines (as well as other mechanisms) lead to apurinic sites. These are substrates for repair to restore the original DNA sequence or can lead to point mutations and chromosome aberrations. Image taken from Boiteux and Guillet (2004).

Hydrolysis into an apurinic site can be caused:

- Spontaneously, due to the weakening of the glycosidic link following methylation
- Through enzymatic removal by DNA glycosylases.

The genome contains 10000 AP sites per mammalian cell per day (Lindahl and Nyberg, 1972), although only a small percent are lethal in double stranded DNA (Lafleur, Woldhuis and Loman, 1981). AP sites are substrates for repair that can restore the original guanine, or can contribute to mutagenesis should an incorrect base be inserted. N7MeG and N3MeA are substrates for repair, initiated by specific glycosylases of base excision repair (BER), an important protective mechanism from alkylpurine-induced carcinogenesis (Wirtz *et al*, 2010; Kondo *et al*, 2010). The glycosylases are N3-MeA DNA glycosylase/alkyladenine glycosylase (AAG) for removal of N3MeA (Engelward *et al*, 1996) and N-Methylpurine-DNA glycosylase (MPG) for the removal of N7MeG. These glycosylases cleave the glycosidic bond between the base and DNA backbone, thereby removing the base and leaving an AP site. Over-expression of these repair genes sensitises cells to methylpurine mutagenesis by creating more AP sites (Ibeanu *et al*, 1992). Replication can proceed

over an apurinic site at the expense of genome fidelity (Vos and Rommelaere, 1987; Schaaper, Kunkel and Loeb, 1983). Upon recognition of an AP site, the replicating polymerase (polymerase ε) is displaced and replaced through "polymerase switching" in the "replisome" to a polymerase (Lehman *et al*, 2007; Lovett, 2007) capable of translesion synthesis (TLS). These polymerases are polymerase λ, β and η (Villani *et al*, 2011), as identified in human cells. Polymerase β preferentially incorporates adenine opposite an AP site, although all dNMPs are substrates for incorporation opposite an AP site (Efrati *et al*, 1997). Whereas, polymerase λ incorporates guanine (Shtygasheva *et al*, 2008). Therefore, through translesion synthesis, N-methylpurines can give rise to a number of transversion and transition mutations. This pathway may account for the variety of mutations seen for S_N2 alkylators, e.g. MMS, which target N7MeG to a higher extent. The different patterns of mutations induced by alkylating agents (**Table 5.1**) can be attributed to the differences in adduct spectra. Due to the similarity in amount of O^6AlkG induced by ENU and MNU (7.8-9.5% and 5.9-8.2% of total alkylations, respectively) and the differences in GC→AT transitions (26% and 92% of total mutations, respectively), other adducts or mechanisms may cause GC→AT transitions. ENU causes more O^2Thymine (O^2T) and O^4Thymine (O^4T) than MNU, shown to cause AT→TA and AT→GC substitutions, respectively (Tosal, Comendador and Sierra, 1998).

Table 5.1. Mutation induction at the HPRT locus by three alkylators. The differences in proportions of substitutions likely reflect different mechanisms of action and adduct spectra. Taken from Jenkins *et al* (2005).

Mutation type	**ENU SN_1**	**%**	**MNU SN_1**	**%**	**MMS SN_2**	**%**
GC>AT	206	**26**	112	**92**	129	**69**
AT>GC	164	**21**	5	**4**	19	**10**
AT>TA	255	**33**	2	**2**	8	**4**
AT>CG	106	**14**	0	**0**	10	**5**
GC>TA	39	**5**	3	**2**	14	**7**
GC>CG	14	**2**	0	**0**	8	**4**
Totals	784	**100**	122	**100**	188	**100**
Transitions		**47**		**96**		**79**
Transversions		53		4		21

5.1.3. HPRT mutation spectra database.

HPRT has served as an important reporter gene for induced mutations following genotoxin exposure. As a result, there is a wealth of knowledge of mutation induction at the HPRT locus. Cariello (1994) compiled information from different hosts and different mutagens. Information is also available on the Mammalian Gene Mutation Database (MGMD). This facilitates the comparisons listed previously in section 5.1.1. There is an added impetus for mutation analysis of HPRT as missense mutations in HPRT cause Lesch-Nyhan syndrome (Puig *et al*, 2001). Therefore, DNA sequence analysis has received much attention. Tomita-Mitchell *et al* (2003) report significant concordance between mutational patterns found *in vitro* and *in vivo* at the HPRT locus, emphasising its suitability as an *in vitro* mutation detector.

5.1.4. Methods for mutation detection.

There are a variety of methods available for determining the type and location of mutations in DNA sequences (Reviewed by Nollau and Wagener, 1997). The following is a brief account of techniques used to identify genetic alterations.

Denaturing gradient gel electrophoresis (DGGE) coupled PCR. This technique is based on sequence specific denaturation of double stranded DNA (dsDNA) and subsequent mobility shifts on a low percentage denaturing acrylamide gel. A single base pair difference can be resolved using this method but its identity remains unknown. Cariello and Skopek (1993) have used this technique to identify the replicating fidelity of DNA polymerases and to purify mutant DNA from wildtype DNA, at heterozygous loci. A modification known as *constant* DGGE is able to determine the location of a mutation on an oligonucleotide (Hovig *et al*, 1991). This technique can accommodate as many samples as the size of the gel permits and can be useful for comparing multiple samples simultaneously. DGGE permits the analysis of mutations on strands less than 1kilobase (kb) with analysis taking up to 10hr. However, the "technique reveal(s) little about the nature or position of that mutation" (Cariello *et al*, 1988).

Single strand conformational polymorphism (SSCP). This assay is very similar to DGGE but is more robust (Hori *et al*, 2006). dsDNA is denatured *a priori* to single stranded DNA (ssDNA). The conformation of the secondary structures of ssDNA

formed upon self-annealing is sequence specific and will influence migration throughout a gel (Orita *et al*, 1989). This allows the user to identify ssDNA of different sequences. As with DGGE, the mutation type is not identified but only 200base pair (bp) fragment is optimal. DGGE and SSCP can only ascertain the proportion of samples that are mutated. Both techniques have been applied in analysis of mutations in exon 8 of the HPRT gene of rodent splenic lymphocytes following ENU treatment (Mittelstaedt and Heflich, 1994).

Restriction site mutagenesis (RSM) assay. RSM has been validated in our laboratory to identify ENU and MNU induced mutations in murine tissues (Jenkins, Takahashi and Parry *et al*, 1999; Suzen, Jenkins and Parry, 1998). The theory of this technique is shown in **Figure 5.4**.

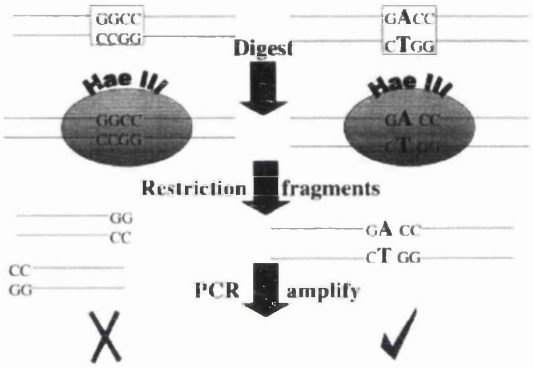

Figure 5.4. Theory of restriction site mutagenesis (RSM) assay. Image taken from Jenkins *et al*, (1999).

Mutations at a restriction site will prevent endonuclease cutting and the target will be amplified, giving a band on a DNA gel. The technique is similar to restriction fragment length polymorphism (RFLP), where PCR is performed before digestion. RSM will not detect mutagenic events outside of the restriction sites. In addition, further PCR and sequencing are required to determine the type of mutation.

Northern (DNA) and Southern (RNA) blotting. Labelled oligonucleotide probes will specifically bind to regions of interest, allowing the identification of nucleic acid sequences in a sample. Nucleic acid blotting can be used to detect deletions and insertions in genomic DNA, or exons in mRNA. This has been used in analysis of mutations at the TK locus following ethyl methanesulfonate (EMS) and mitomycin C (MMC) treatments (Davies, Phillips and Rumsby, 1993). Alternative RNA splicing causes a loss of exons throughout the HPRT mRNA (O'Neill *et al*, 1998), that would

be detected by Northern blotting. Single point mutations in the region of probe binding are unlikely to affect hybridisation and so will not be detected. Southern blotting has been used to detect 2-40kb deletions at the HPRT locus (Bradley *et al*, 1987). However, Southern-blot detectable genetic alterations account for only 10-20% of HPRT mutations (Recio *et al*, 1990).

Hybridisation to detect point mutations. With interests in disease genotyping, there is incentive to detect single base changes and point mutations within genes of interest. One approach hybridises sample ssDNA to wildtype ssDNA, forming a homoduplex or a heteroduplex if mutations are present in the sample DNA. The mismatches in the heteroduplex can be detected by a number of methods; a diminished electrocatalytic signal of methylene blue (Boon *et al*, 2000), a downward deflection of a cantilever in a cantilever-based optimal deflection assay (Hansen *et al*, 2001) and a change in frequency of a quartz resonator, upon mismatch repair (MMR) mediated recognition (Su *et al,* 2004). These techniques are designed to be highly specific but are expensive and laborious.

Differential amplification of mutant transcripts by real time PCR. Morlan, Baker and Sinicropi (2009) describe a technique that preferentially amplifies mutant transcripts. This would require prior knowledge of hotspots for appropriate primer design and is not appropriate for establishing mutation spectra over a large gene.

Direct sequencing of PCR-amplified targets. This technique has been used in this chapter as it provides unequivocal evidence of the location and type of mutation at a gene of interest, using computer software to compare to the wildtype.

5.1.5. DNA sequencing.

A variety of sequencing methodologies exist. These include mass spectrometry (Murray, 1996) and more recently, next-generation sequencing (NGS) (Metzker, 2010). NGS is offered commercially as a higher throughput method than traditional Sanger' chain termination-based methods and can achieve longer read lengths (Schuster, 2008), allowing the sequencing of entire cancer genomes (Aburatani, 2011). The most common methodologies for small-scale sequencing reactions are based on Sanger's method, but with automation for higher throughput and lower cost. The method replicates the sample DNA using deoxynucleotides spiked with equal volumes of each of the four dideoxynucleotides (ddATP, ddCTP, ddGTP and ddTTP),

each with a different fluorescent tag. These all lack a 3'-OH group and, as a consequence, block chain extension upon incorporation into the growing DNA strand. This results in a mixture of oligonucleotides of different sizes depending on where the chain terminator has been incorporated. They are separated based on fragment length, fluorescence emissions determined and order of bases starting from the shortest oligonucleotide.

5.1.6. Experimental approaches to sequence HPRT.

The HPRT gene occupies 47542 base pairs (bp) of the long arm of the X chromosome, designated Xq26. A significant portion of this region consists of intronic regions with the protein-coding region of 654bp over 9 interspersed exons (**Figure 5.5**), which are spliced together forming a mRNA of 1435bp.

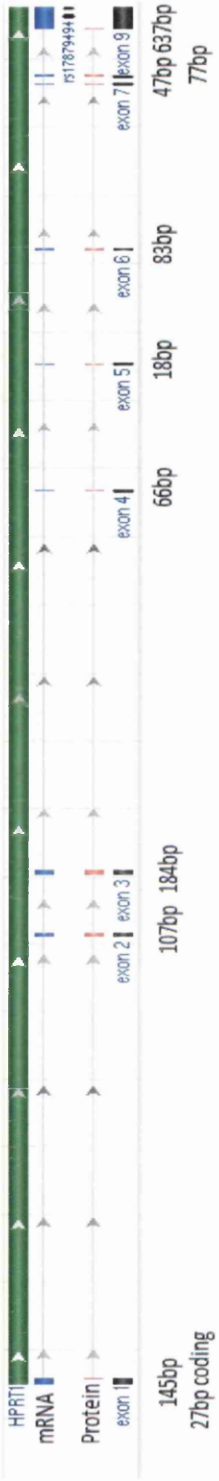

Figure 5.5. HPRT schematic showing intron/exon organisation. Adapted from http://www.ncbi.nlm.nih.gov/nuccore/NG_012329.1?from=1&to=51601&report =graph&content=5. Values taken from O'Neill *et al* (1998).

PCR amplification or cloning of HPRT into bacterial hosts, is needed to give sufficient yield for sequence analysis. As the length of template increases, the efficiency of cloning and PCR amplification diminishes. There have been several experimental approaches to overcome this problem. Edwards *et al* (1990) deconstructed the entire gene into a M13 library composed of overlapping contigs. Williams, Rainville and Nicklas (2002) devised a method, termed inverse PCR (iPCR), to sequence break sites, within the HPRT gene, of deletion or insertion mutants that gave an altered hybridisation pattern on a Southern blot. The advantage being that not all the gene needed to be sequenced. However, alterations such as point mutations, that are undetectable by Southern blot, would be excluded from further analysis. One approach used by Jenkins *et al* (2005) was to sequence one exon of interest, where known mutation hot spots exist. The authors sequenced exon 3 of HPRT following MMS exposure. However, mutations occurring at flanking exons will not be identified. Liu *et al* (2003) have avoided this. The authors used 18 primers in multiplex PCR to amplify each exon, with the advantage of easy detection of exon deletion on a DNA gel. However this technique is expensive and laborious. To overcome this, van Zeeland *et al* (1989) amplified cDNA (complementary DNA), synthesised from mRNA, via reverse transcription using reverse transcriptases from retroviruses (Simpson, Crosby and Skopek, 1988). HPRT has four reported homologous sequences present in human genomes; two on chromosome 11, one on chromosome 3 and another on chromosome 5 (Patel *et al*, 1984). Fuscoe *et al* (1983) demonstrated that these sequences are "unexpressed intronless pseudogenes". As pseudogenes are not represented in the transcriptome, these sequences are not amplified in mistake. cDNA will be shorter than the genomic region and has all 9 exons spliced together, containing the protein-coding region. cDNA is easier to clone and amplify (Jolly *et al*, 1983). Harbach *et al* (1995) was able to amplify 780bp including the protein coding region. In this chapter we report the successful development of PCR and sequencing methodology, with improved coverage (83%) of HPRT mRNA.

5.1.7. PCR and sequencing method optimisation.

Two methods of PCR were tested:

1. Nested PCR
2. Overlapping PCR primers

5.1.7.1. Nested PCR.

Following mRNA conversion into cDNA using Oligo(dT) primers, an initial strategy of PCR amplification used nested primers to copy cDNA in one contiguous sequence. This required the use of two primer sets, in two separate PCR reactions. The primers are shown in **Table 5.2**.

Table 5.2. Details of the nested PCR primers.

PCR reaction number	Primer name	Sequence	Primer binding site (bp in HPRT mRNA)	Length of product (bp)
1	Outer Forward	5'-CGGGGCCTGCTTCTCCTC-3'	3	1374
	Outer Reverse	5'-GGGAACTGCTGACAAAGATTCAC-3'	1376	
2	Inner Forward	5'-CCTCCGCCTCCTCCTCTG-3'	92	1146
	Inner Reverse	5'-CTTACTTTTCTAACACACGGTGG-3'	1238	

As can be seen in **Figure 5.6A**, the optimal annealing temperature that produces ample product with minimal miscellaneous bands, for PCR reaction number 1, is 61.5°C.

A).

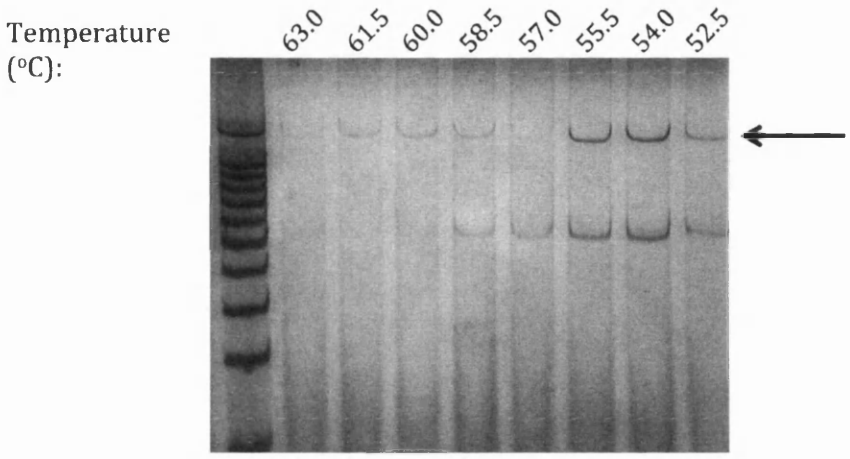

B).

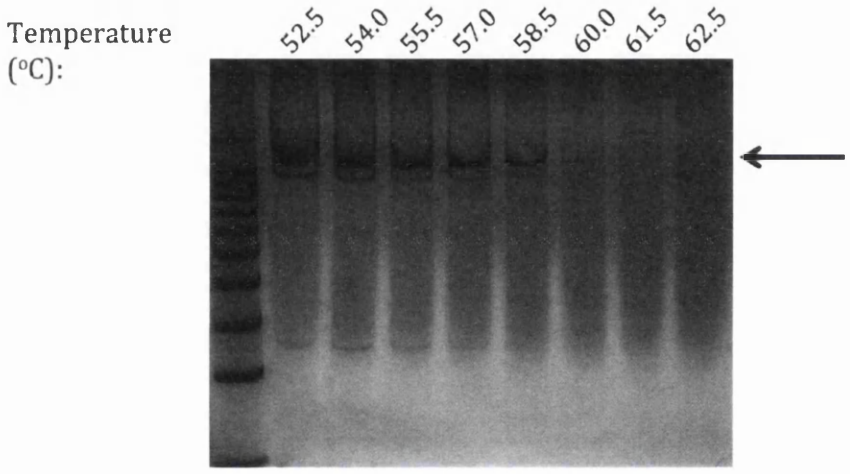

Figure 5.6. Temperature gradient for PCR reaction number 1 (A) and PCR reaction number 2 (B). Left most lane is 100bp-1500bp DNA ladder.

A 2µl aliquot of the product obtained at 61.5°C, in PCR reaction 1, was used in PCR reaction 2, using the nested primers. For reaction 2, 58.5°C was the optimal annealing temperature (**Figure 5.6B**). To improve yield, increasing volumes of PCR reaction number 1 product was used in PCR reaction 2 (**Figure 5.7**).

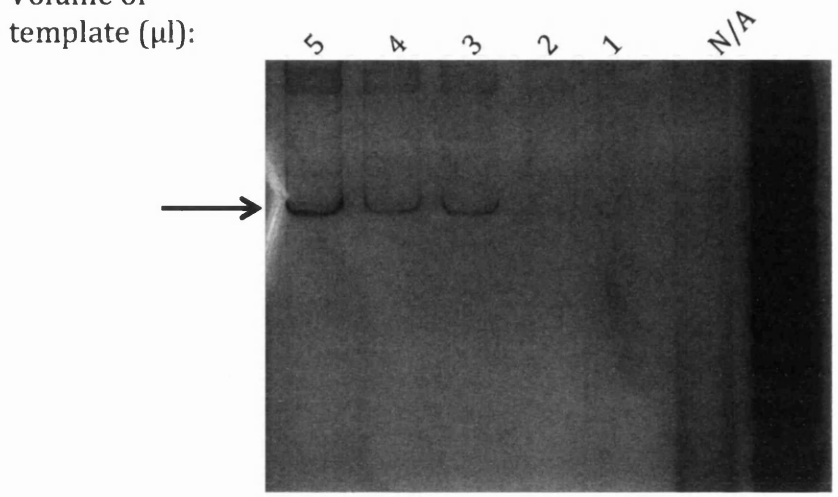

Figure 5.7. Concentration gradient. Optimal volume of product from PCR reaction 1 (template) for use in PCR reaction 2 is 5µl. Right most lane is 300-1500bp.

5µl was found to give the greatest yield. However, nested PCR was not reproducible. It is likely that the success of PCR was limited by the efficacy of cDNA conversion, which diminishes as the length of the target sequence increases. Therefore an alternative, more successful approach was to divide the amplicon into two shorter fragments by using overlapping primers (**Figure 5.8**).

5.1.7.2. Overlapping PCR primers.

Figure 5.8. Schematic of the technique of splitting HPRT mRNA into two overlapping oligos to shorten the length of amplicon and improve PCR success. Red primers are designated "D" and green are designated "K".

14 combinations of forward and reverse primers were designed using Beacon software (Premier Biosoft, Palo Alto, USA) and tested (at the optimal final concentration of 0.04µM in each 50µl reaction, **Figure 5.10**) and their annealing temperature experimentally determined. The two primer sets (one for each half of the gene) with identical annealing temperatures were further optimised; this meant that

both fragments of the gene could be amplified simultaneously, thereby saving time and running costs. These primer sets were designated D and K, targeting a fragment of 537bp and 714bp respectively.

5.1.8. Optimisation strategy.

The initial recipe for PCR reaction mixture was obtained from Dr Sarah Prior (personal communication). The annealing temperature, primer concentration, magnesium chloride concentration and number of cycles were manipulated to improve sensitivity, while maintaining specificity. The following is a stepwise account of how the technique was optimised;

1. An annealing temperature range from 51-58°C was performed (**Figure 5.9A**)
2. A 10-fold reduction in primer concentration over the same temperature range gave better specificity; further primer dilutions were unsuccessful (**Figure 5.9B**).
3. The optimal annealing temperature for D and K primers was 52.6°C (**Figure 5.10**).
4. Magnesium chloride dissociates into free positive magnesium ions to improve annealing of primer to target sequence, both of a negative charge. Therefore, 3-7µl (final concentration 0.5mM to 3.5mM) $MgCl_2$ was added per 50µl reaction (**Figure 5.11A** and **5.11B**). It was later found that 3µl of $MgCl_2$ for D primers gave inconsistent yields and so 4µl was used.
5. To further increase the yield, the number of cycles was increased to 40. However this gave miscellaneous bands of higher bp (**Figure 5.12**).
6. To overcome this the extension time was reduced to 10s (**Figure 5.13**).
7. Finally, both primer sets were added to one reaction mixture, as in multiplex PCR. However, primer dimers were evident which later interfered with sequencing (**Figure 5.14**).

A).

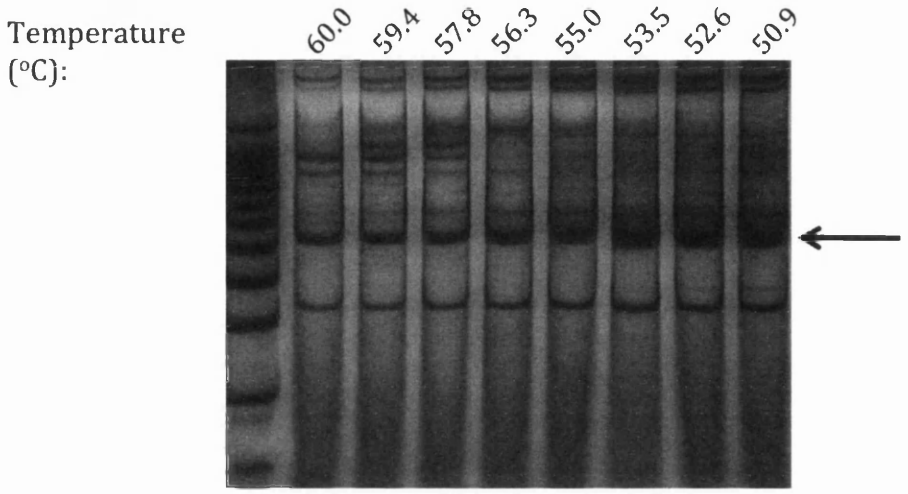

B).

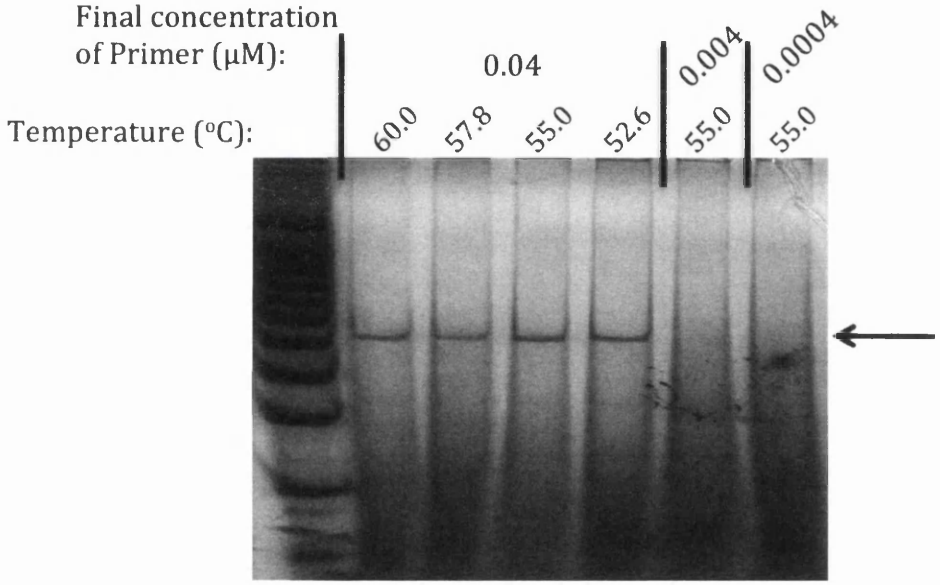

Figure 5.9. Optimal concentration of primers. (A) A temperature gradient with 2μM primers was too concentrated. (B) 1 in 10 dilution was sufficient. Leftmost lanes are 100bp-1500bp DNA ladder.

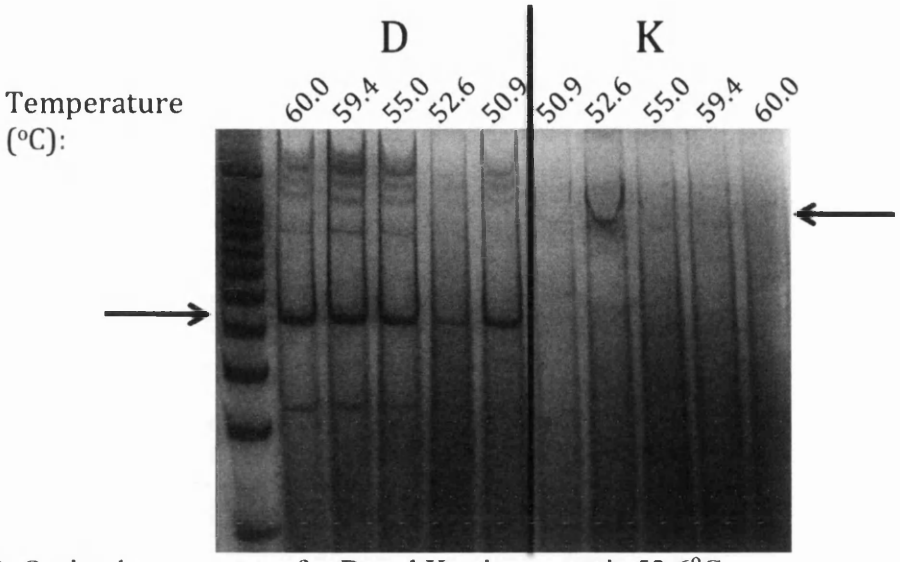

Figure 5.10. Optimal temperature for D and K primer sets is 52.6°C.

A).

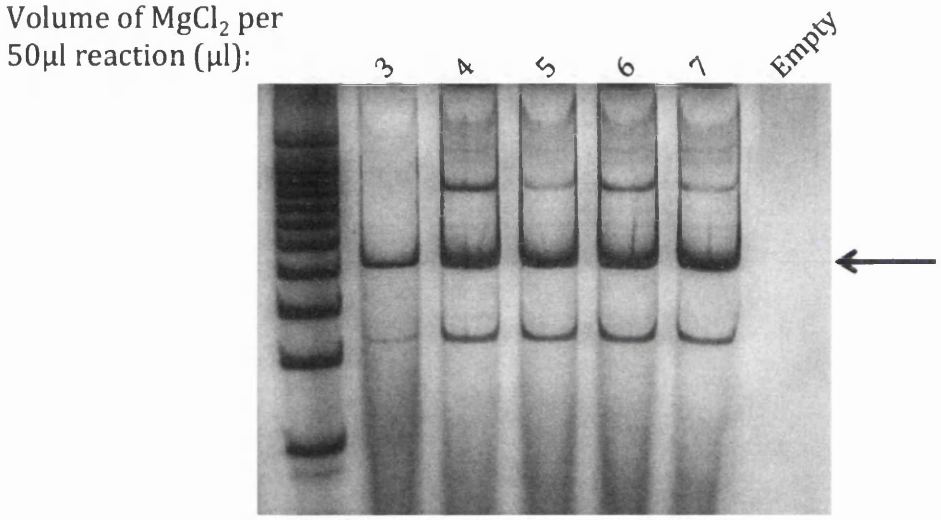

B).

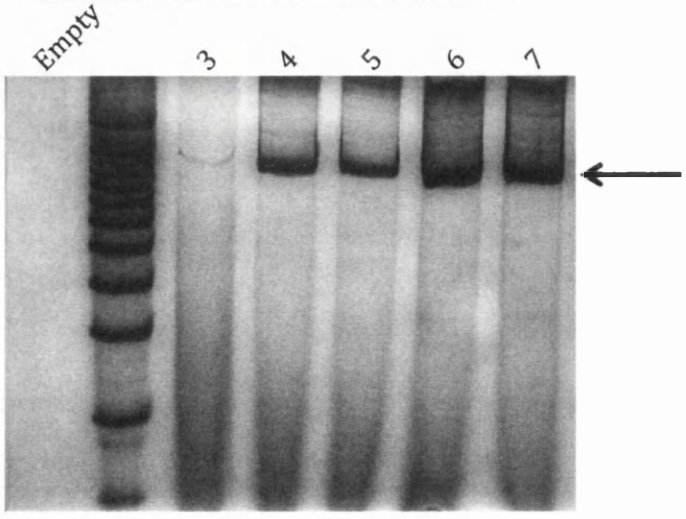

Figure 5.11. Magnesium chloride ($MgCl_2$) concentration gradients for D (A) and K (B) primer sets.

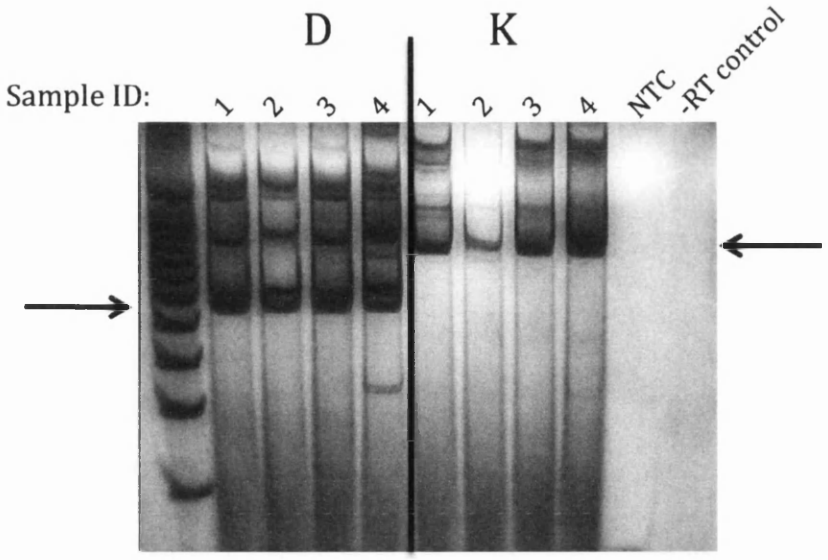

Figure 5.12. To increase yield, the number of cycles were increased to 40 and tested with RNA extracted from four HPRT mutant colonies. Once optimised, all RNA samples were tested for DNA contamination using RNA in PCR (-RT (without reverse transcription) control) and the PCR reagents were tested for contamination using water as a control (no template control, NTC).

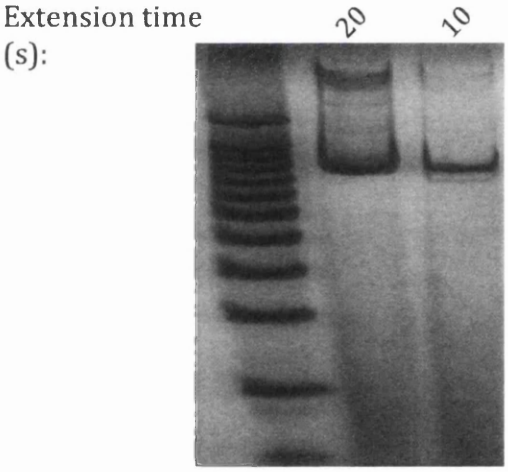

Figure 5.13. Halving the extension time to 10s reduced the appearance of high molecular weight bands.

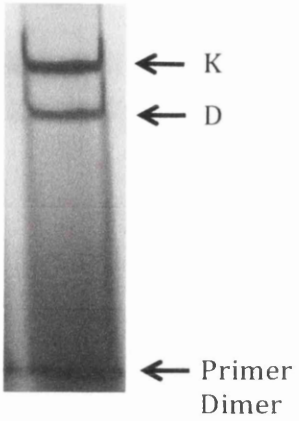

Figure 5.14. For convenience, both primer sets were added to one reaction tube to mimic multiplex PCR. However, primer dimers were evident and interfered with downstream sequencing, so D and K reactions were performed in separate tubes.

5.2. Materials and methods.

The finalised PCR and sequencing methodology is given in Chapter 2.

5.2.1. Principal component analysis.

To compare the inter-relationships between different spectra, multivariate principal component analysis (PCA) was performed using R software version 2.9.0 downloaded from http://www.r-project.org/index.html on 7/9/2009. Detailed instructions and coding is given in appendix 6.

5.2.2. Adam-Skopek test.

To reject the null hypothesis of no difference between spectra, the Adams-Skopek test was used in a pair-wise manner. Analysis was performed using HYPRG software downloaded from ftp://sunsite.unc.edu/pub/academic/biology/dna-mutations/hyperg on 13/2/2012 (Cariello *et al*, 1994).

5.3. Results.

This chapter constructs mutation spectra to comment on changes in mutation induction, over the hormetic dose-response observed in the previous chapter. The doses chosen for sequence analysis were 0, 0.00075μg/ml and 0.025μg/ml MNU (**Figure 5.15**). We hypothesise the involvement of O^6-methylguanine-DNA methyltransferase (MGMT) in preventing mutations, by repairing O^6MeG at 0.00075μg/ml MNU and doses up to the NOGEL (0.0075μg/ml MNU). Real time PCR analysis of MGMT transcripts and analysis of MGMT activity was performed to assess the response at this locus over the transition from "non-mutagen to mutagen".

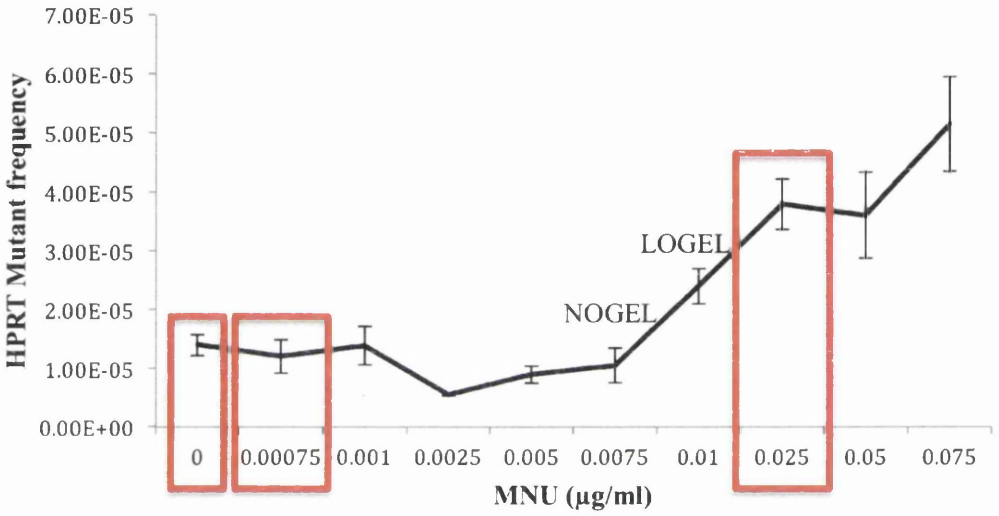

Figure 5.15. Data from Chapter 3 showing the doses (outlined in red) selected for sequence analysis at the *HPRT* locus.

5.3.1. Proportion of mutations identified.

Three treatments were chosen for further analysis of mutants. These were; DMSO which represents the solvent control (spontaneous mutagenesis), 0.00075μg/ml MNU and 0.025μg/ml MNU, representing below NOGEL and above LOGEL respectively. This allowed characterisation of differences in mutation induction over the dose-response observed in Chapter 3. For each treatment, 40 HPRT mutants were isolated and propagated at the end of the HPRT assay for sequence analysis. The proportions of all possible substitutions resulting from each treatment are shown in **Table 5.3**.

Table 5.3. Proportions of substitutions at the HPRT locus observed at increasing concentrations of MNU. The values in bold represent the most predominant substitution at each dose. n=22 for 0μg/ml, n=40 for 0.00075μg/ml, and n=36 for 0.025μg/ml (see text for details). Pairwise comparisons = $<1x10^{-60}$ for each treatment.

	Percentage of total mutations (%)		
Substitution type	0μg/ml MNU	0.00075μg/ml MNU	0.025μg/ml MNU
GC→AT	15.0	12.5	**45.9**
AT→CG	**29.0**	7.8	5.1
AT→GC	9.3	7.8	8.9
GC→TA	9.3	7.8	3.0
AT→TA	22.4	14.1	16.2
CG→GC	15.0	**50.0**	20.7
Total number of mutations found	112	64	**135**

18 mutants of the solvent control and 4 mutants following treatment with 0.025μg/ml were found to contain a contiguous sequence of changes found to occur elsewhere in the HPRT sequence. Whether this is a translocation or duplication cannot be resolved. These mutants were excluded from further analysis and only base substitutions (the main mutagenic mechanism of MNU) were considered. An interesting observation was the lack of this rearrangement in mutants resulting from treatment with 000075μg/ml. The proportions changed drastically over the dose range, suggesting the involvement of different mutational pathways at increasing concentrations of MNU. Pair-wise comparisons using a Chi^2 test on actual numbers and not percentages were performed. Each were highly significant. 0 vs 0.00075;$p=2.3x10^{-61}$, 0 vs 0.025;$p=4.7x10^{-65}$, 0.00075 vs 0.025;$p=1.0x10^{-154}$. In the solvent control, a total of 112 mutations were found in 40 mutants. The most prominent spontaneous substitutions were AT→TA transversions, constituting 38.1% of the spontaneous mutation spectra. Following treatment with 0.00075μg/ml, CG→GC transversions were the most abundant, constituting 32 of 64 (50%) substitutions observed. The spectrum changed upon treatment with 0.025μg/ml MNU, where GC→AT transitions were the predominant alterations, as expected from MNU exposure, forming 43.9% of

the mutation spectrum. The increase in GC→AT transitions most closely reflected the increase in mutant frequency observed in Chapter 3 (**Figure 5.16**). The change in proportion of GC→AT transitions was accompanied by a change in the number of mutants found to harbour a GC→AT transition, from 52.5% (21/40) mutants in the spontaneous spectrum, to 17.5% (7/40) mutants at 0.00075μg/ml, to 72.5% (29/40) mutants at 0.025μg/ml. Therefore, results were not biased by a mutant containing many GC→AT transitions.

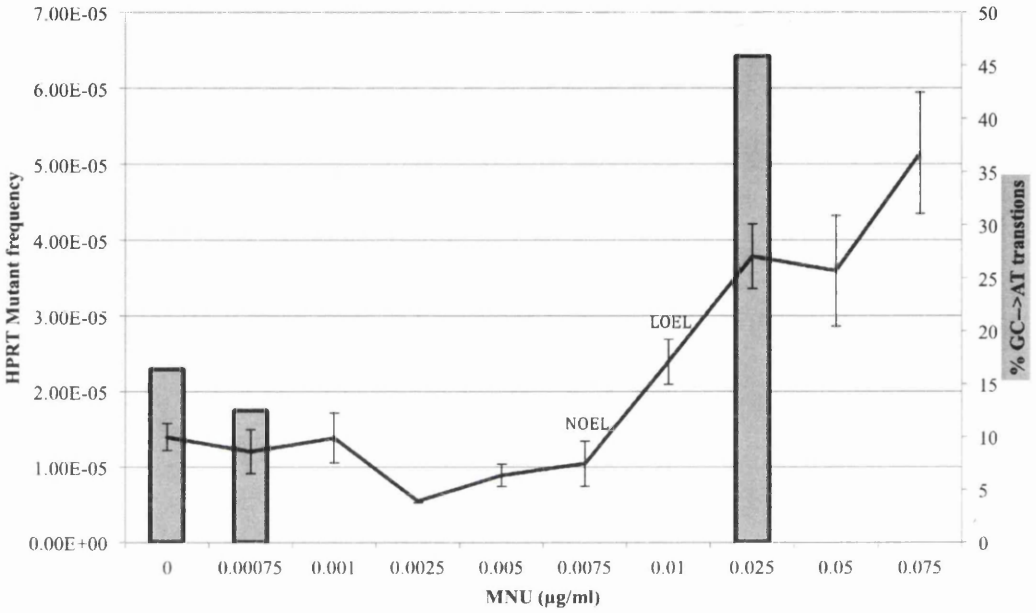

Figure 5.16. The proportion of GC→AT changes increases in concordance with the increase in HPRT mutant frequency observed in Chapter 3.

5.3.2. Mutation spectra

The spectrum of base substitutions along the HPRT mRNA sequence is shown for each treatment in **Figure 5.17**. As expected the vast majority of mutations occurred in the protein-coding region of the mRNA, from position 167bp to 824bp. The spectrum at 0.00075μg/ml MNU showed a different spectrum of mutations to the solvent control. A GC→TA transversion at 747 seems specific to MNU treatment, regardless of concentration. However, many of the GC→AT transitions are only present following treatment with 0.025μg/ml MNU. Each spectrum was significantly different (p=0.000), adjudged through pair-wise comparisons of each spectrum, using the Adams-Skopek test (Adams and Skopek, 1987) through HYPERG software

(Cariello *et al*, 1994). MNU specific hot spots were defined as mutations occurring at >5% of the total mutations for each spectrum. At 0.00075μg/ml one hotspot (shown in bold) occurred at 747; 5'T**G**A→T**C**A. This was also found at 0.025μg/ml with additional hotspots at 551; 5'A**G**A→A**A**A, 555; 5'T**G**T→T**A**T and 556; 5'G**T**C→G**A**C.

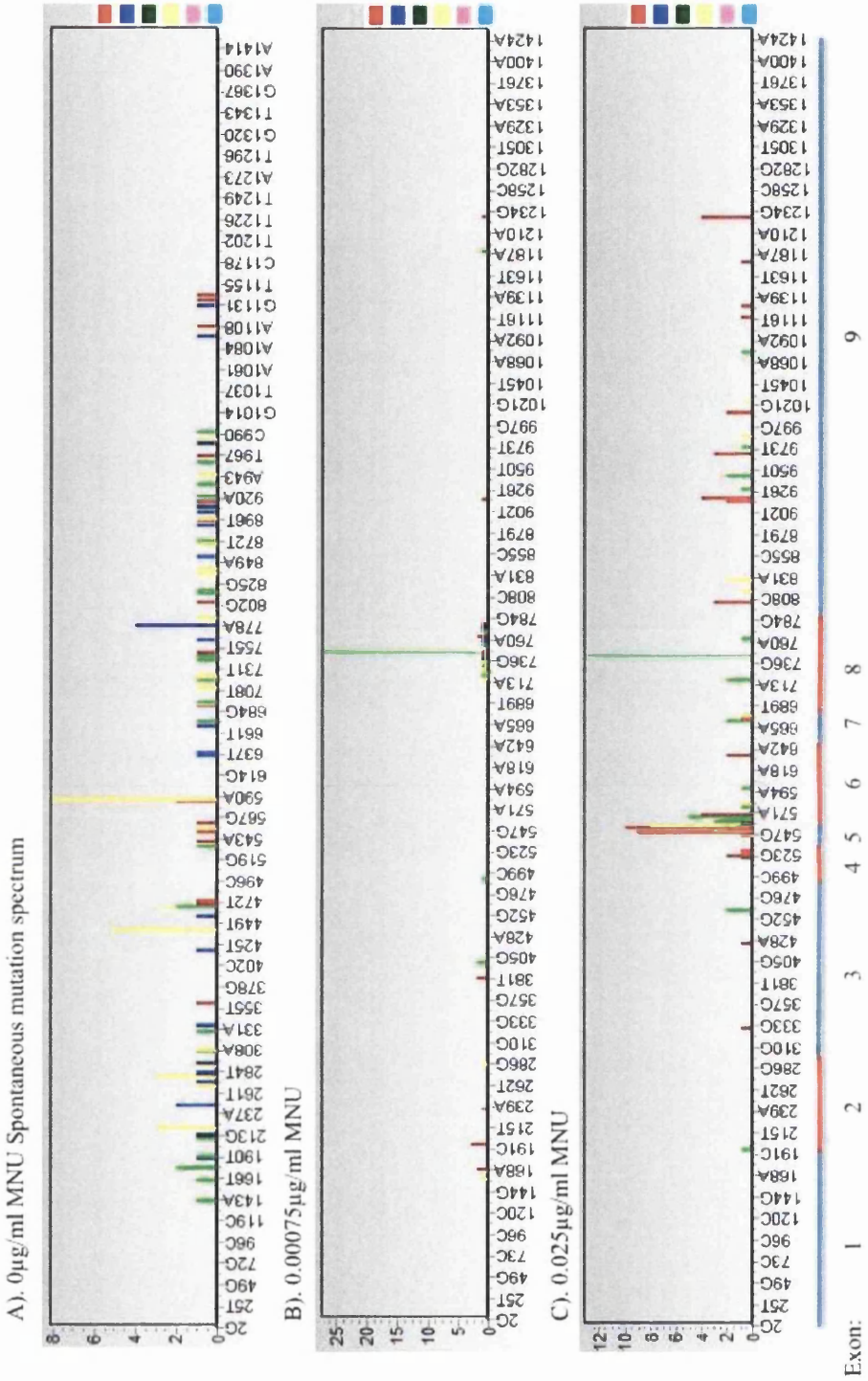

Figure 5.17. Summation of all mutations found along the non-transcribed strand of HPRT sequence, from 40 HPRT mutants for each treatment. For example, mutation at 747 in B). occurred in 27 mutants. Spectra were composed using iMARS software (Morgan and Lewis, 2006).

5.3.3. Principle component analysis (PCA) of mutation spectra

Principle component analysis (PCA) was conducted to reveal differences in mutable sites between spectra. The data was explained by two components, PCA 1 (correlation factor=0.9) and PCA2 (correlation factor=0.1). Therefore, 90% of the data is explained by PCA1 and PCA2 explains 10% of the data. The data is presented as a scatterplot in **Figure 5.18**, which allows the user to identify the differences between the spectra.

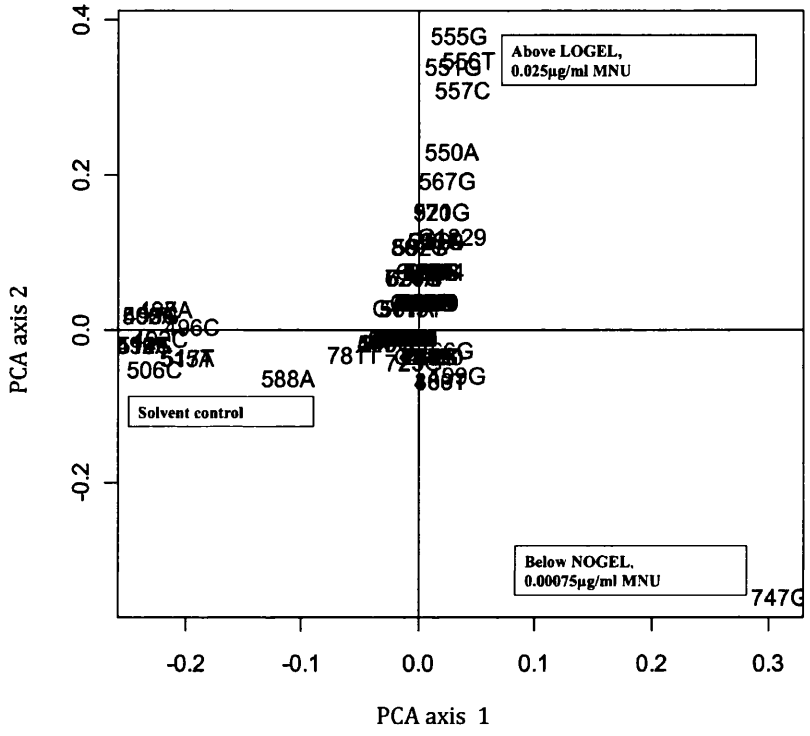

Figure 5.18. Scatterplot to visualise the differences in mutable sites between the spectra resulting from different doses of MNU.

Referring to **Figure 5.18**, PCA1 (x-axis) separates MNU treated from solvent control spectra. The second component (y-axis) separates the two MNU treatment groups suggesting different mutational mechanisms at increasing concentrations of MNU. Most notably, of the sites clustering at 0.025µg/ml, 67.7% were GC→AT transitions and equal proportions (11.1%) were TA→AT, GC→CG and AT→GC substitutions. These mutations were absent at 0.00075µg/ml MNU and the most prominent mutation occurred at 747, which was GC→TA transversion.

5.3.4. Measuring the effect of MNU treatment on MGMT.

5.3.4.1. MGMT activity in AHH-1 cells.

To test our hypothesis of O^6MeG induced MGMT activity saturation, the activity of MGMT was measured at increasing concentrations of MNU in AHH-1 cells. This was performed at the Institute of Toxicology, University of Mainz, by Professor Bernd Kaina and Karl-Heinz Tomaszowski, to whom I am incredibly grateful. Cells were treated for 1hr with MNU and left to recover for 90mins to allow for MGMT reaction. MGMT was undetected in AHH-1 cells but high quantities were detected in Caco-2 and Hela S3 cells, kindly provided by Mrs Margaret Clatworthy and Dr Sian-Eleri Owens respectively. These cells are known expressers of high level MGMT and were chosen as positive controls (Foote and Mitra, 1984) (**Table 5.4**). The limit of detection (LOD) of the assay is 1000 MGMT molecules/cell (Kaina *et al*, 1991). Given that 255 molecules/cell=0.16fmol/mg protein (Bobola *et al*, 2007), the LOD of 1000 molecules/cell equates to 0.63fmol/mg protein. It is possible that MGMT exists at a level below 0.63fmol/mg protein in AHH-1 cells and lack of assay sensitivity prevents detection.

Table 5.4. MGMT activity in AHH-1 cells was not detected (ND), but the positive controls were successful. It is possible that MGMT in AHH-1 cells is below the limit of detection or AHH-1 cells are MGMT deficient.

Dose MNU (µg/ml)	MGMT activity (fmol/mg protein)
0	ND
0.00075	ND
0.025	ND
HeLa S3 (positive control)	655.50
Caco-2 (positive control)	2,952.96

5.3.4.2. Expression analysis of MGMT in AHH-1 cells.

Real-time PCR quantified the fold changes in MGMT transcripts in response to increasing concentrations of MNU, at four time points over 24hr post-exposure (**Figure 5.19**).

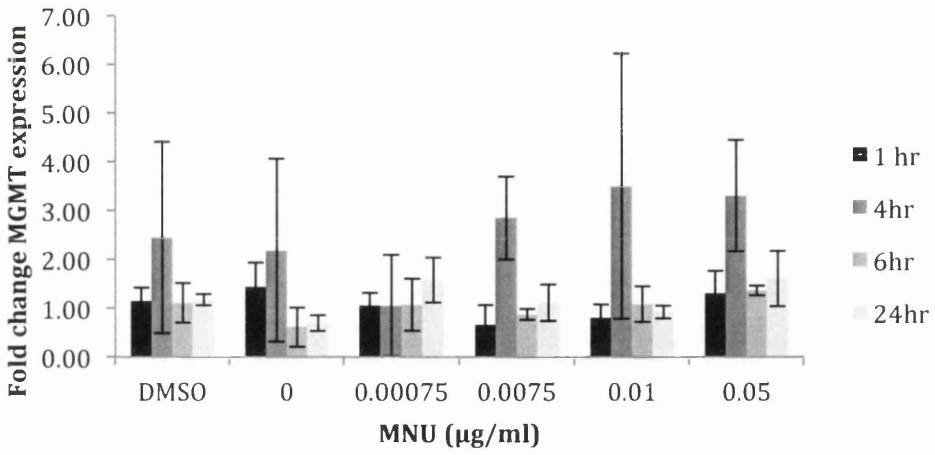

Figure 5.19. Real time PCR analysis of MGMT transcripts showed no statistically significant increase in expression in response to MNU exposure.

There seems to be a slight increase in expression 4hr following treatment with 0.01µg/ml. However, no treatment resulted in a statistically significant change (lowest α value being p=0.07 at 24hr treatment with 0.05µg/ml). Attempts to sequence the amplicon proved unsuccessful and so the product could not be verified.

5.3.4.3. MGMT promoter methylation analysis.

To assess MGMT promoter methylation status; methylation specific PCR (MS-PCR) was performed at the Institute of Toxicology, University of Mainz, by Professor Bernd Kaina and Karl-Heinz Tomaszowski, to whom I am incredibly grateful. **Figure 5.20** shows that, in AHH-1 cells, the MGMT promoter is methylated. This suggests that MGMT is not expressed, however, MGMT mRNA can be detected by real time analysis.

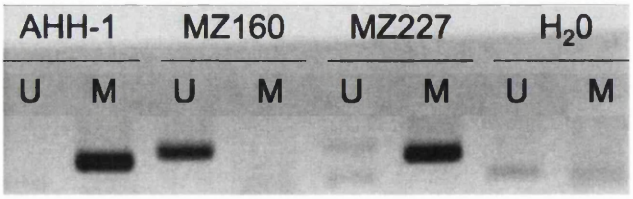

Figure 5.20. Methylation specific PCR (MS-PCR) suggests that MGMT promoter in AHH-1 is methylated. MZ160 is the unmethylated control and MZ227 is the methylated control.

5.4. Discussion.

The aim of the present chapter is to establish understanding of mutation induction by MNU, to determine a biological mechanism responsible for the observed dose-response in Chapter 3. The observed differences in treated mutation spectra can be explained by saturation of MGMT at 0.025μg/ml, due to increased concentration of O^6MeG at higher doses of MNU. To test this; MGMT activity, the response at the MGMT promoter and MGMT status of AHH-1 cells were investigated.

5.4.1. Mutagenesis at the HPRT locus.

Jinnah *et al* (2000) compiled Lesch-Nyhan disease (LND) causing point mutation along the HPRT gene (**Figure 5.21**). There is substantial spread in deleterious substitutions, which is replicated in **Figure 5.17**. Providing evidence that all exons of HPRT should be included in mutation analysis.

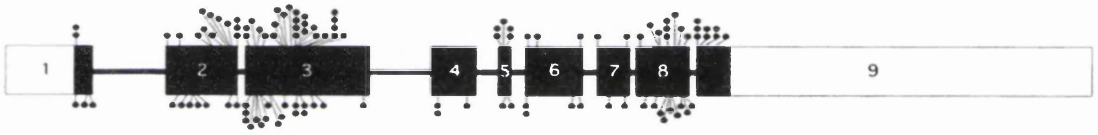

Figure 5.21. Base substitution along the protein-coding region of HPRT gene (black) shows substantial spread in the location of deleterious mutations. (Taken from Jinnah *et al*, 2000).

5.4.2. Spontaneous mutagenesis at the HPRT locus.

Mutagenesis in the absence of exogenous genotoxic treatment is referred to as spontaneous. DMSO, used here, is a solvent control in many mutation assays without causing mutagenesis (also observed in Chapter 3). Therefore, at the final concentration used here (0.01%) there is no evidence to suggest DMSO is mutagenic. Mannan *et al* (2010) showed that DMSO generated reactive oxygen species (ROS) only in rooted *Artemisia* annua shoots. ROS are capable of DNA reaction and mutagenesis. However, in animal cells, DMSO is a well-known scavenger of ROS (Yu and Quinn, 1994). Of course, without conclusive proof by comparing with the mutation spectra of untreated controls, we cannot be certain that DMSO treated

cultures reflect the spontaneous spectrum. However, given what is known of DMSO, this assumption may be valid. In the present study it is more value to compare to DMSO treated than untreated cultures in order to determine MNU specific effects. The importance of spontaneous mutagenesis is realised in ageing and carcinogenesis (Ames and Gold, 1991; Loeb, 1989). There are many well-known sources of endogenously generated genotoxins that can contribute to the spontaneously occurring mutation spectra. This is discussed in relation to alkylating agents in Chapter 4. At the HPRT locus, exon deletions are common due to mutations that abrogate appropriate splicing at intron-exon junctions during pre-mRNA maturation prior to translation (O'Neill *et al*, 1998). This did not occur in the present study but has been reported previously as a mechanism for spontaneous deletions in HPRT mRNA. Sources of spontaneous mutations include;

- DNA adduction by reactive oxygen species (ROS) from media components and intracellular metabolism (Wiseman and Halliwell, 1996). Each nucleotide is susceptible to oxidative damage, causing a variety of substitutions
- Replication over abasic sites from chemically unstable bases, hypothesised to cause a range of transversions and transitions as discussed
- Spontaneous deamination of 5-methylcytosine at CpG dinucleotides leading to GC→AT transitions
- Mistakes by the replicating polymerase in DNA synthesis (Tippin, Pham and Goodman, 2004)
- Transcription associated mutagenesis, which has been shown to cause GC→AT, TA→GC and AT→TA substitutions (Hudson, Bergthorsson and Ochman, 2003).

The mutational mechanisms above could account for the spontaneous substitutions observed at the HPRT locus. However, it is likely that another mechanism is involved, which would better explain the rearrangement seen in 18/40 mutants from positions 490 to 517 of the mRNA sequence (indicated with a line **Figure 5.17**) in , than would chemical alteration to individual bases. A colleague has also reported this in a separate experiment in untreated AHH-1 cells (Mrs Kulsoom Shah, personal communication). There is substantial variation in spontaneous mutagenesis between cell types. Lewis and Parry (2002) confirmed this at the SupF locus, which is also used as a mutation sensor. This variability is also evident at the HPRT locus (**Figure**

5.22). Different rates of spontaneous damage and genotypic variation in the repair capacities would account for the differences between cell lines. Additionally, variability is also observed between laboratories in the same cell lines. For example, de Jong *et al* (1988) report a high proportion (22/28, 79%) of spontaneous base substitutions to be GC→ AT transitions at the HPRT locus of Chinese hamster ovary (CHO) cell lines. Phear *et al* (1989) on the other hand, while working with the same cell line, found that these transitions accounted for only 40% of spontaneous base substitutions found at the HPRT locus. The observed variability reflects differences in cell handling, laboratory protocols and between batches of cells. This may explain the differences observed between AHH-1 and the derivative, MCL-5, which would be expected to have similar mutation spectra (**Figure 5.22**). Additionally, Corso and Parry (1999) found genetic differences between the two cell lines upon comparative genomic hybridisation (CGH) and fluorescent *in situ* hybridisation (FISH). AHH-1 cells were derived from RPMI 1788 cell line (Freedman *et al*, 1979), isolated from a healthy male donor and immortalised using Epstein-Barr virus (EBV) (Crespi *et al*, 1991). This method of transformation has been shown to increase genomic instability and DNA damage (Kamranvar *et al*, 2007), which would be implicated in spontaneous mutagenesis. Genetic drift within a population is a major source of population divergence in *in vitro* cell culture systems. As a result, over time and between laboratories, the genotypes and genomic stabilities of cells will change (Anderson *et al*, 1984) Hence the effort of the International Workshop on Genotoxicity Testing (IWGT) workshop to standardize cell culture (Pfuhler *et al*, 2011). It is therefore essential that spontaneous mutagenesis be considered in such studies, as featured in this chapter.

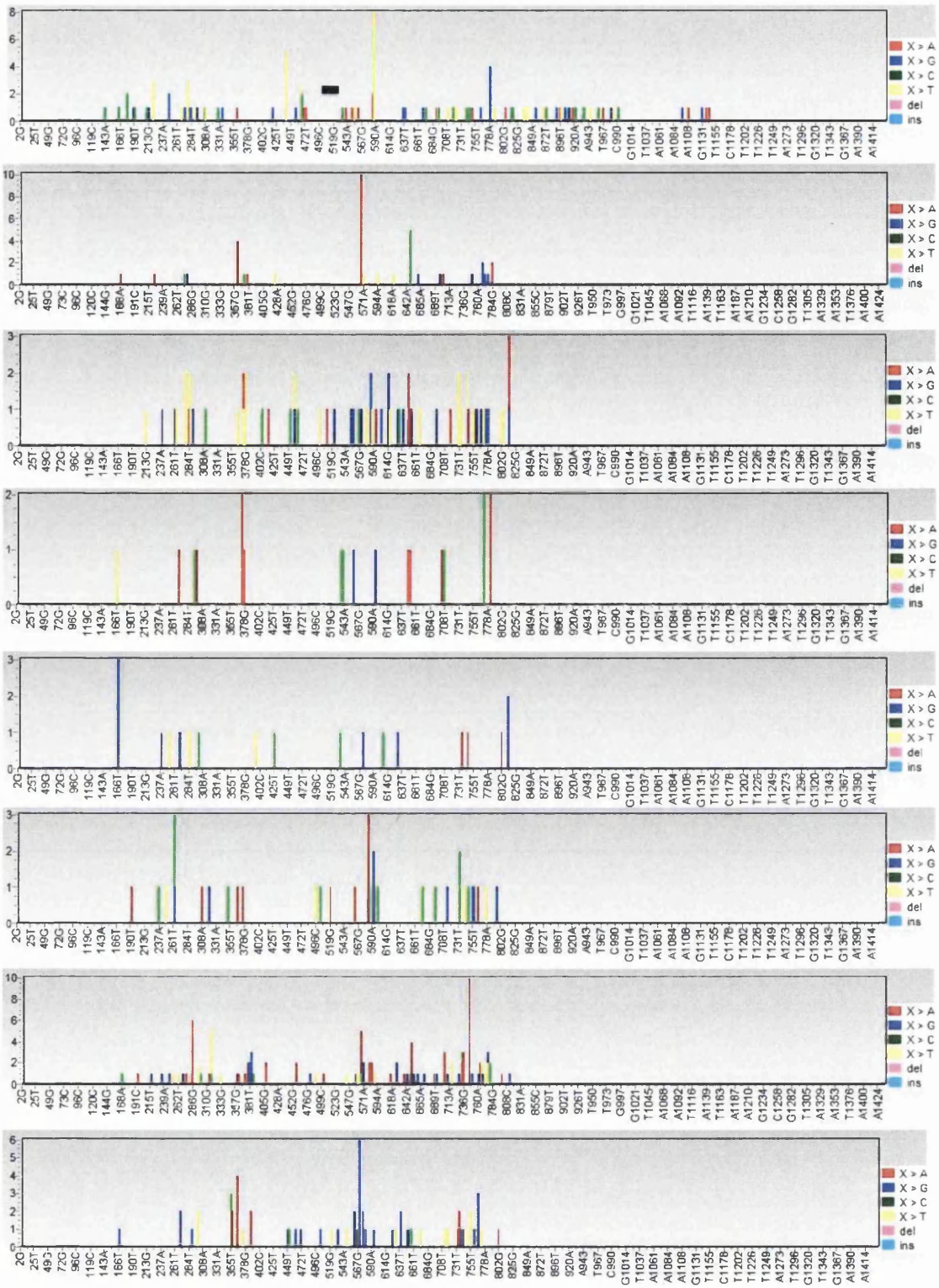

Figure 5.22. Comparison of spontaneous mutation spectra in different cells taken from Mammalian Gene Mutation Database (MGMD). Top to bottom: AHH-1 (own data), Chinese Hamster Ovary cell line (CHO), Human T lymphocyte, Cynomolgus Monkey T lymphocyte, Murine macrophage, Murine splenic T lymphocyte, TK6 and Chinese Hamster Lung cell lines (CHL). Axes are described in **Figure 5.17**.

5.4.3. Comparison of mutation spectra.

This study is the first to construct mutation spectra in order to analyse mutation induction at low doses of genotoxin. In addition, it is also the first study to comment upon the genotoxic transition around the NOGEL. Visual inspection of the mutation spectra in **Figure 5.17** shows drastic differences in mutation distribution. This is further emphasised through statistical analysis. The Adams-Skopek test is a robust statistical model widely used for pair-wise comparison of mutation spectra. PCA is a multivariate analysis first applied to mutation spectra by Benigni, Palombo and Dogliotti (1992) as a "reliable and sensitive tool" for analysing the inter-relationships between multiple spectra. PCA has been used in *exploratory* analysis to reveal unknown commonalities in mutation induction; between different treatments at the *supF* locus (Lewis and Parry, 2002) and between spectra from chemical treatments and spectra from tumours (Lewis *et al*, 2008). This study uses PCA as an *explanatory* tool to highlight differences in mutation induction at different doses of MNU.

The dissimilarity between solvent control and 0.00075μg/ml MNU highlights the cellular presence and effect of MNU. We could postulate that low dose of MNU upregulates cytoprotection, which would perturb spontaneous mutagenesis. However, the present study cannot confirm this and further investigation is needed. Further evidence is provided in **Table 5.5**.

Table 5.5. Analysis of the strand specificity of GC→AT transitions. The number of G→A transitions occurring on the non-transcribed strand (mRNA) are higher compared to C→T transitions following MNU treatment, which is indicative of the mechanism of action (MOA) of MNU.

MNU (μg/ml)	Number of G→A	Number of C→T	Proportion of GC→AT transitions that are G→A on non-transcribed strand (%)
0	9	9	50.0
0.00075	7	1	87.5
0.025	52	10	83.8

Referring to **Table 5.5**, there is a clear difference in the strand specificity of G→A transitions following MNU treatment. The sequence of mRNA, which has been used in the present study, is identical to the anti-sense/non-transcribed strand. Therefore,

the mutations identified in the mRNA, indicate mutagenesis in the non-transcribed strand of the double helix, but also take into account transcription-associated mutagenesis (TAM). The majority of spontaneously occurring GC→AT transitions observed were C→T transitions in the non-transcribed strand. This has been attributed to the strand-biased deamination of 5-methylcytosine into thymine (Beletski and Bhagwat, 1996). Although none of the observed C→T changes occurred at CpG islands, they are still targets for epigenetic methylation (Lister *et al*, 2009). In presence of MNU, the majority of GC→AT transitions were G→A changes in the non-transcribed strand. This is indicative of the MOA of MNU (Zhang and Jenssen, 1991) and is not the effect of transcription-coupled repair as this strand biased was independent of transcriptional status (Palombo *et al*, 1991). This potentially highlights the reactivity of MNU with DNA at doses below the NOGEL. The question whether MNU is still a hazard at this dose because of the change in mutagenic profile at a dose that does not increase MF over background levels still exists (Professor Bhaskar Gollapudi, personal communication). Although, this is the first study to show this for direct acting genotoxins, it has been reported for phenobarbitol, a non-genotoxic carcinogen. In a study by Shane *et al* (2000), changes in the mutation spectrum at a non-mutagenic, non-tumourigenic dose of phenobarbitol was attributed to oxidative stress through the induction of cytochrome P450 following exposure. Of interest, at 0.00075μg/ml MNU, is the absence of the suspected rearrangement observed in the negative control. This substantiates the hormesis argument developed in Chapter 3, whereby a small dose of MNU prevents endogenous damage from causing spontaneous mutations, through upregulation of DNA repair machinery. However, the present study cannot confirm this. Furthermore, at 0.00075μg/ml, the most predominant mutations were GC→TA transversions. This has been found in previous studies with MNU (Van Zeeland *et al*, 2008) and has been attributed to mutagenesis across apurinic sites, following hydrolytic release of N7MeG and insertion of adenine opposite the resulting gap (Loeb and Preston, 1986). The effect of a higher concentration of MNU was the increase in GC→AT transitions from 12.5% to 43.9% of the respective mutation spectra. The dose-dependency of GC→AT transitions was also evidenced in the PCA scatterplot (**Figure 5.18**), which accounted for the separation of the treated spectra. Incidentally, the vast majority of GC→AT mutations (76%) observed at 0.025μg/ml MNU occurred at guanines preceded by a purine (5'Pu-G-N), which is to be expected (Zhang and Jenssen, 1991). The GC→AT

hotspots identified in the present study were 551 and 555 in exon 5. A study by Tomita-Mitchell *et al* (2003) identified GC→AT hotspots in exon 3 by *N*-methyl-*N*'-nitro-*N*-nitrosoguanidine (MNNG), a similar alkylator to MNU. The increase in GC→AT transitions, we hypothesise, is due to the persistence of O^6MeG in the DNA following saturation of MGMT that possibly occurs at doses of MNU higher than the LOGEL of 0.01μg/ml MNU. To substantiate this, MGMT depletion by MNU has been observed in rodents (Kyrtopoulos, 1998). In light of this, we performed further analysis of MGMT.

5.4.4. Real time PCR methodology.

In this study, Taqman® probes were used to measure MGMT and housekeeper transcripts, as opposed to SYBR® green technology used in previous studies (Doak *et al*, 2008). Taqman® probes offer enhanced specificity over SYBR® green because of the use of an additional probe, in conjunction with forward and reverse primers. Therefore, there are three points of sequence recognition in mRNA detection. A comparison of both technologies is shown in **Table 5.6**

Table 5.6. Comparison of two fluorescence technologies for use in real time PCR.

Assay technology	Advantages	Disadvantages
Taqman® probes	Enhanced specificity	A different probe is needed for detection of different loci thereby increasing costs
	High level of fluorescence emission upon probe degradation during strand synthesis overcomes the inherent high background fluorescence	
	Use of different dyes on probes permits analysis of two or more genes in one sample well.	
	Many inventoried assays exist but custom probes can be made	
SYBR® green	Cost effective	Fluorescence upon binding to non-specific PCR products (primer dimers) thereby giving false positives
	Can be applied to the detection of all dsDNA	Melt curve required

The use of Taqman® probes permits the reverse transcription of mRNA into cDNA and subsequent real time detection in one-step in each reaction well, thereby simplifying setup time and labour. However, variability is introduced due to differing efficiencies of cDNA synthesis. It is, therefore, recommended that measurement of target gene and housekeeper transcripts are made from the same cDNA sample to minimise variation. This is termed two-step real time PCR. Analysis of the PCR reaction products on 6% polyacrylamide gel electrophoresis (PAGE) revealed that 1 step PCR gave miscellaneous bands (**Figure 5.23**).

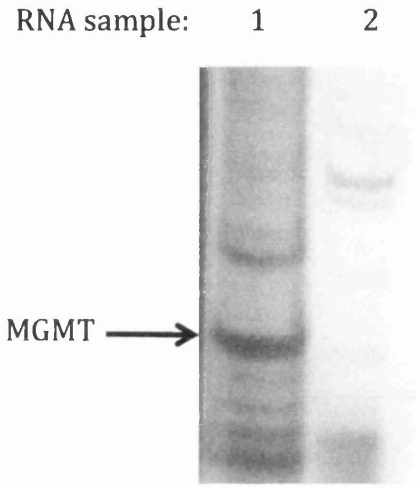

Figure 5.23. Amplification efficiencies of one-step PCR varied between samples.

The results presented in **Figure 5.19** suggest that MNU does not cause induction of MGMT expression. This is in agreement with popular opinion that states a lack of induction at the MGMT promoter in response to genotoxic insult (Professor Bernd Kaina, personal communication). Doak *et al* (2008) provided the first example of upregulation of MGMT in human cells in response to genotoxin; following 4hr treatment with 1μg/ml MMS. MNU is a more potent inducer of O^6MeG and reacts with DNA with faster kinetics than MMS. Therefore, it was expected that MNU would cause a more prominent MGMT induction at lower doses. The MGMT promoter contains multiple regulatory elements for transcriptional control including NF-κB (Lavon *et al*, 2007), activator protein-1 (AP-1), glucocorticoid response elements (GRE) and Sp-1 (Harris *et al*, 1991). Induction has also been shown in HeLa S3 cells in response to protein kinase C activators (Boldogh *et al*, 1998). Therefore, it would be reasonable to assume that MGMT promoter is inducible, particularly in

response to O^6-methylating agents, however substantial evidence is lacking (Kaina *et al*, 2007). Sequencing attempts were made to provide further confidence in the results, but these proved unsuccessful. It is possible that the PCR purification procedure was unsuccessful in removing the fluorescent dye and this interfered with downstream sequencing.

5.4.5. Method of expression quantitation.

The $2^{-\Delta\Delta Ct}$ method (Livak and Schmittgen, 2001) was chosen over the method developed by Pfaffl (2001). The methods are very similar but where the Pfaffl method calculates the actual efficiency of amplification, the Livak method assumes 100% efficiency, giving a 2-fold increase in target after each round of amplification. When using Taqman® probes this is a valid assumption to make, as all assays have 100% (+/-10%) amplification efficiencies. (The reader is referred to the following application note; http://www3.appliedbiosystems.com/cms/groups/mcb_marketing/documents/generaldocuments/cms_040377.pdf). Determining the actual amplification efficiencies required for the Pfaffl method requires construction of a standard curve over a 3-5 log sample dilution series for each replicate, thus requiring extra reagents and costs. Where the level of fluorescence exceeds the user defined threshold value, the sample is given a threshold cycle value (Ct). This indicates the number of cycles needed to exceed baseline fluorescence. The Ct is inversely proportional to target abundance. This study revealed that MGMT had a Ct of 34 in all samples, suggesting a low un-inducible level of constitutive expression. This also made construction of a dilution series, for use in the Pfaffl method, impossible (**Figure 5.24**).

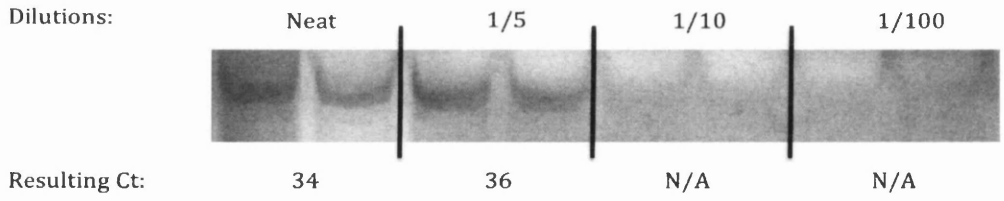

Figure 5.24. Low abundance of MGMT mRNA in AHH-1 cells means dilutions for a standard curve for use in the Pfaffl method are impossible.

To overcome this, the target gene could be induced to increase abundance, as has been shown by Doak *et al* (2008) following 4hr incubation with 1μg/ml methyl methanesulfonate (MMS). This was attempted but upregulation was not observed. Alternatively, the mRNA sequence can be cloned using a vector transfected into a microbial host and amplified to create a stock of concentrated amplicons, as performed for MPG by Zair *et al*, (2011). Other cell lines were tested to assess whether the Ct was an artefact of the assay. TK6 human lymphoblastoid cell lines had a Ct of 34 for MGMT, whereas, virus transformed human bronchial epithelial cells (Beas-2b) showed a Ct of 21. Therefore, it seems AHH-1 cells have a comparatively lower expression level. To substantiate this, MGMT protein levels were compared between cell types in our laboratory (**Figure 5.25**).

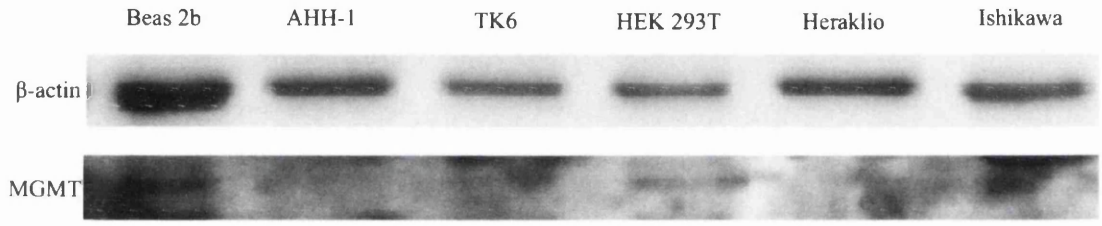

Figure 5.25. Western blot using 40μg protein from various cell types was analysed for MGMT protein. There was a no band for AHH-1 or TK6 cells demonstrating inter-cellular variation in MGMT levels.

Western blot analysis revealed obvious differences in MGMT protein levels between AHH-1 and TK6, Beas-2b (kindly provided by Mr Abdullah Al-Ali), HEK 293T (Human embryonic kidney cells, kindly provided by Dr Jo Forde), Heraklio and Ishikawa cells (Human endometrial adenocarcinomas, kindly provided by Miss Natalie De-Mello). AHH-1 cells showed the smallest amount of MGMT protein compared to other cell lines analysed. Inter-cellular differences in levels of MGMT between cell types is a well-known phenomenon (Fritz *et al*, 1991).

5.4.6. Promoter methylation analysis.

Promoter methylation at CpG islands is associated with gene silencing (Razin and Cedar, 1991). It was considered that MGMT promoter hypermethylation, and subsequent loss of MGMT expression, sensitises tumours to alkylating chemotherapy (Estellar *et al*, 2002) and MGMT promoter methylation status predicts patient

response to alkylating chemotherapy (Everhard *et al*, 2006). Therefore, MGMT promoter methylation status has received much attention. The results shown in **Figure 5.20** show that MGMT promoter is methylated. However, MGMT mRNA can be detected using real time PCR Taqman® probes, suggesting that the gene is expressed. There are several explanations:

- Methylation specific PCR (MS-PCR) used here lacks precision (Mikeska *et al*, 2007) and needs to be confirmed through bisulfite sequencing (Kitange *et al*, 2009).
- There are 97 CpG islands within the promoter region and each can differentially influence transcriptional activity of MGMT (Everhard *et al*, 2009). Shah *et al* (2011) suggest that promoter wide methylation analysis needs to be conducted for accurate determination of methylation status of the MGMT promoter.
- Sites downstream of the promoter are subjected to epigenetic modification that can influence expression status (Nakagawachi *et al*, 2003).
- The axiom of epigenetic transcriptional regulation does not hold true at the MGMT promoter. Treatment with 5-azacytidine causes global hypomethylation, which increases gene transcription of methylation-induced silenced genes. However, Pieper *et al* (1991) found that this reduced MGMT transcription.

Additionally, promoter hypermethylation is not correlated to a lack of protein in brain (Lavon *et al*, 2007). Similarly Della Puppa *et al* (2012) found that 41.5% of glioblastoma samples did not display the expected relationship between MGMT methylation and expression levels. The effects of MGMT promoter methylation are still poorly understood.

5.4.7. Concluding remarks: Mechanism for the observed dose-response.

The difference in spectra between 0.00075μg/ml MNU and the solvent control in **Figure 5.17** and evidence of MNU specific strand bias (**Table 5.5**) strongly suggest that MNU reacts with DNA below the NOGEL for point mutations. The difference between 0.00075μg/ml and 0.0025μg/ml MNU were GC→AT transitions, which are well-documented to be caused by O^6MeG following MNU exposure, and prevented by MGMT, which repairs O^6MeG. Attempts were made to measure the inactivation of

MGMT but these were unsuccessful. Real time PCR analysis of MGMT transcripts suggests MGMT is un-inducible and has a very low constitutive expression level in AHH-1 cells. At low levels of exposure to MNU, basal level MGMT is sufficient to repair O^6MeG, thus accounting for the NOGEL. However, MGMT is present in very small, finite amounts and can become limited following exposure to higher concentrations of MNU and other O^6-methylating agents. It is possible that saturation of MGMT occurs at the LOGEL, where mutation induction and GC→AT transitions are significantly increased over the control.

The data presented in this chapter strongly suggests that the biological effect of O^6MeG is observable once a threshold concentration of MNU, sufficient to cause MGMT inactivation, has been surpassed. The direct role of MGMT in the NOGEL will be discussed in the following chapter.

Chapter 6.

DNA Repair Analysis.

Biological Mechanism For Low Dose MNU Mutagenesis.

6.1. Introduction.

It is known that GC→AT transitions are the major mutation induced by MNU (Zhang and Jenssen, 1991). The data in previous chapters supports this and shows that the proportions of GC→AT transitions mimic the hormetic dose-response observed for overall mutation induction by MNU in the HPRT assay (**Figure 4.15**). MNU induces GC→AT transitions predominantly through O^6MeG adducts that mispair during replication. We hypothesise that a lack of GC→AT transitions observed at doses below the LOGEL is due to repair of O^6MeG by O^6-methylguanine-DNA methyltransferase (MGMT). We aim to test this by MGMT knockdown in AHH-1 cells because a MGMT deficient AHH-1 strain is not commercially available. If our hypothesis holds true, MGMT deficiency, will cause;

1. An increase in mutant frequency at and below the NOGEL for MNU (0.0075μg/ml).
2. An increase in GC→AT point mutations in MGMT deficient AHH-1 cells compared to MGMT proficient AHH-1 cells at and below the NOGEL for MNU.

6.1.1. Methods of MGMT knockdown.

Various MGMT deficient cell lines are commercially available. MT1, human T Lymphocyte cell line, has been used as an *in vitro* model for MGMT deficiency without adequate validation (Goldmacher, Cuzick and Thilly, 1986). It has been found that these cells are not deficient in MGMT but mismatch repair (MMR) processing (Dr Zoulikha Zair, personal communication). It is likely that they are deficient in MMR processing because the authors conclude MT1 cells are "highly resistant to killing but hypermutable by MNNG," this is the methylation tolerant phenotype indicative of MMR impairment. In order to compare with previous findings in AHH-1 cells, it was decided to knockdown MGMT in AHH-1 cells, thus minimising confounding effects by using two cell lines. Creating MGMT deficient cells has received much attention due to the implications in sensitising MGMT expressing tumours to alkylating chemotherapy. The most researched alkylating chemotherapeutic is temozolomide (TMZ) in the treatment of glioblastoma (Friedman, Kerby and Calvert, 2000). It has been shown that MGMT deficiency potentiates the cell killing and mutagenic effect of O^6MeG induced by TMZ (Hansen *et al*, 2006). Therefore, MGMT knockout strategies could be used as an adjuvant to improve patient response to chemotherapy. There are several methods that can create MGMT deficient cells; gene knockdown or pharmacological inhibition. Some studies propose a method of gene disruption that abrogates the protein coding function of the gene (Tsuzuki *et al*, 1996).

6.1.1.2. Gene knockdown.

The most widely used method of gene knockdown is RNA interference (RNAi), the sequence specific RNA induced post-transcriptional silencing of genes (**Figure 6.1**). Double stranded (ds)RNA oligonucleotides, homologous to the gene of interest (GOI), guide the degradation of homologous mRNA thereby suppressing protein translation and achieving gene specific knockdown. The advantage of this technique is that knockdown can be validated by reduced GOI mRNA through real time PCR and also a distinct lack of protein in western blot. There are two sources of the dsRNA oligonucleotides;

shRNA-short hairpin RNA. Cells are transfected with an expression vector which expresses desired dsRNA that forms a hairpin structure which act as substrate for DICER, an endoribonuclease (**Figure 6.1**). With continuous expression of double stranded RNA, knockdown is permanent. This is advantageous because it allows selection and propagation of successful transfectants creating a stable homogenous population. This was the method of MPG knockdown by Zair *et al* (2011).

siRNA-small interfering RNA. Cells are transfected with dsRNA 19-21 nucleotides in length. Since transfection is easier, this method is more achievable than shRNA. However, it is only temporary, lasting for up to 7 days. This method is recognised as crude knockdown, giving rise to a heterogenous population of varying knockdown successes. Successful transfectants can show up to 98% gene knockdown. However, transfection into lymphoid type cells, like AHH-1 is difficult.

Rosati *et al* (2008) describe down regulation of MGMT by Interferon β (IFN-β) to sensitise MGMT expressing cell lines to TMZ, used in clinical chemotherapy. The down regulation of MGMT by IFN-β has been attributed to up-regulation of p53 (Natsume *et al*, 2005; Natusme *et al*, 2008). Since IFN-β has pleiotropic effects on the cell, this method of knockdown is unfavourable.

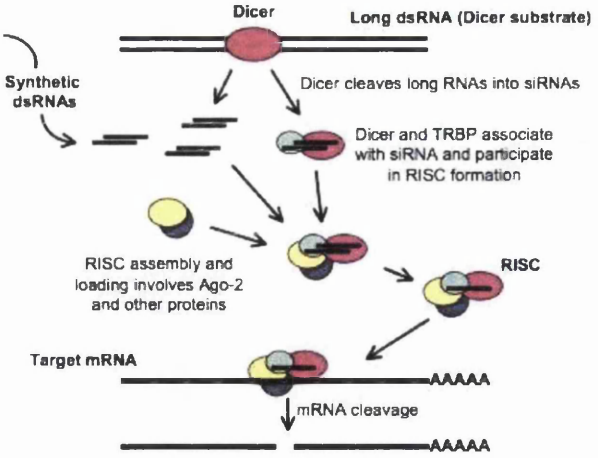

Figure 6.1. Schematic of siRNA mediated gene knockdown. siRNA molecules associate with proteins such as TRBP (transactivating response binding protein) forming RISC (RNA induced silencing complex) that degrades homologous mRNA sequences. Taken from Peek and Behlke (2007).

Incidentally, MGMT expression modulation by p53 has been reported (Grombacher, Eichorn and Kaina, 1998), but the mechanics are not well understood. It seems that when p53 levels are artificially high (following transfection of a wildtype p53 expression vector), MGMT is down regulated (Harris e*t al*, 1991; Grombacher, Eichorn and Kaina, 1998). However, a *decrease* in p53 levels by gene knockout has the same inhibitory effects (Blough, Zlatescu and Cairncross, 2007). It has been shown that wildtype p53 sequesters specificity protein 1 (SP1) transcription factors, preventing their binding to MGMT promoter and inhibiting transcription (Bocangel *et al*, 2009). AHH-1 are p53 heterozygotes, expressing a mutant p53 (Guest and Parry, 1999). Whether the same effect in AHH-1 cells is observed is unknown. A better understood method of MGMT knockdown uses pharmacological inhibitors to inactivate MGMT.

6.1.1.3. MGMT has a broad range of affinity for structures at the O^6 position of guanine.

MGMT (EC 2.1.1.63) is a protein of 21kDa composed of 207 amino acids encoded over 5 exons located at chromosome 10 (10q26.3). MGMT, also called **alkyl**guanine **alkyl**transferase (AGT), is able to remove a variety of alkyl structures covalently bound to oxygen at position 6 of guanine (O^6AlkylG); the result of reaction with highly nucleophilic

methylating agents (forming O^6MeG) or chemical synthesis (Moschel *et al*, 1992). Examples are shown in **Figure 6.2**.

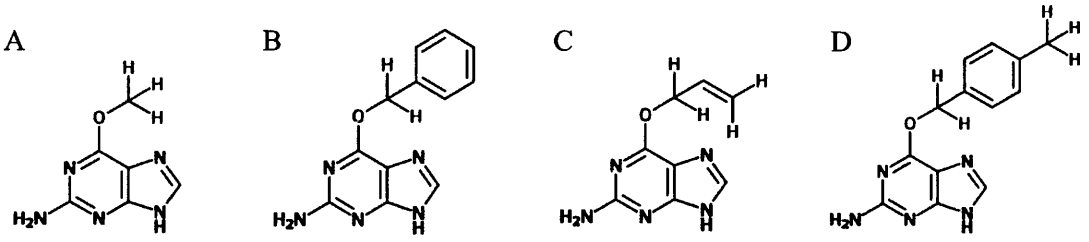

Figure 6.2. Examples of base substrates acted upon by MGMT. Each a guanine base with different adducts at O^6 **A.**) O^6-methylguanine (O^6MeG). **B.**) O^6-benzylguanine (O^6BG). **C.**) Allylguanine. **D.**) O^6-(*p*-methylbenzyl)guanine. From Moschel *et al* (1992). Structures drawn using freeware at www.emolecules.com.

Alkyl adducts fit into the active site of MGMT and are pseudosubstrates for repair where they inactivate MGMT by causing the suicidal inactivation (as with O^6MeG), hence their use as inhibitors of MGMT activity. MGMT acts on these substrates with differing affinities (Moschel *et al*, 1992), governed by steric effects within the active site (Daniels *et al*, 2000). Poor affinity correlates with poor MGMT inhibition (Pegg *et al*, 1993). Alkylation damage can be removed from mononucleotide guanine in the nucleotide pool and also when in dsDNA; this broad range activity enhances the efficacy of MGMT in protecting DNA from the carcinogenic effects of various endogenous and exogenous alkylating agents. It also gives the opportunity to manipulate MGMT activity by administering these agents.

Depleting the cells protection through MGMT inactivation potentiates the DNA damaging and cell killing effects of O^6alkylating agents (Dolan *et al*, 1990; Rabik *et al*, 2006; Fukuchi *et al*, 1997). Due to this, these pharmacological inhibitors have been extensively studied for their use in sensitising MGMT proficient tumours to O^6guanine alkylating chemotherapy (Gerson, 2002), particularly in the treatment of glioblastoma multiforme (GBM; Kato *et al*, 2010). They also have uses in studying the mechanism of mutation induction by alkylating agents (Kaina *et al*, 1991) and in assessing the role of MGMT in protecting against O^6alkylG induced carcinogenesis (Dolan *et al*, 1990). Many *in vitro* studies have evaluated the effectiveness of a variety of pseudosubstrates as pharmacological inhibitors of MGMT (Kaina, Margison and Christmann, 2010). They conclude that O^6-benzylguanine (O^6BG, **Figure 6.2B**) is a potent and simple pharmacological inhibitor of human MGMT (Dolan *et al*, 1985) and will be discussed further.

6.1.2. Effective inhibition of MGMT by O^6BG.

MGMT inactivation by O^6BG is ubiquitous in published literature. For example, a study by Pegg *et al* (1993) reports complete and selective decrease in human MGMT activity in the presence of O^6BG in cell free extracts (**Figure 6.3**).

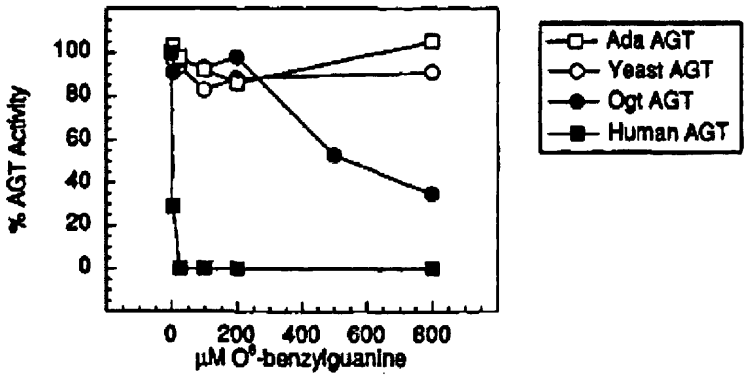

Figure 6.3. The inactivation of human AGT (MGMT) with low dose O^6BG. The difference in inter-species inactivation is explained through bioinformatics by Daniels *et al* (2000) which suggests that O^6BG is unable to bind at the active site of the respective species specific MGMT. Graph taken from Pegg *et al* (1993).

The efficacy of O^6BG as a pharmacological inhibitor is attributed to the following properties;

1. MGMT has higher affinity for O^6BG than it's natural substrate, O^6MeG as a free base (Zang *et al*, 2005). This is further emphasised by Moschel *et al* (1992), they concluded that the concentration of O^6BG used to achieve complete inhibition was far less than other alkylguanines used. Incidentally, MGMT has highest affinity for O^6MeG when in an oligonucleotide complex (Moschel *et al*, 1992).
2. Dolan *et al* (1990) compared the inactivating effects of O^6BG and O^6MeG in HT29 (human colorectal adenocarcinoma) cells. 10min incubation with 2.5µM O^6BG achieved 90% inactivation whereas 1hr with 0.2mM of O^6MeG was needed to achieve the same level.
3. O^6BG is a "low molecular weight substrate lacking polynucleotide structure" (Pegg *et al*, 1993) allowing passive diffusion into the cell (Reinhard *et al*, 2001).
4. It inhibits cytoplasmic and nuclear MGMT (Ueno, 2006).
5. It is not a substrate for DNA synthesis, it is not incorporated into DNA and does not cause mutations (Ueno, 2006).

6. O^6BG is more efficient at MGMT inhibition than other conjugated forms (Reinhard *et al*, 2001). The authors show that 0.62μM O^6BG causes 50% MGMT inhibition. The conjugates tested caused 50% MGMT inhibition at concentrations (IC_{50}) ranging from 0.009μM to 25μM. However, O^6BG was non-toxic at these doses compared to other conjugates.

6.1.3. How MGMT inactivation is achieved.

The reaction is a covalent transfer of adduct from O^6-position in guanine to MGMT and proceeds with the same stoichiometry where O^6MeG is the substrate. Cysteine at position 145 (Cys145) in the active site of MGMT is evolutionarily conserved through *E.coli*, rats and humans (Tano *et al*, 1990) and acts as the acceptor residue for the abstracted alkyl group (Xu-Welliver and Pegg, 2002), this being the benzyl group from O^6BG. This irreversibly forms *S*-benzylcysteine within the active site of MGMT with the stoichiometric release of guanine. Formation of *S*-benzylcysteine in the active site renders MGMT inactive (Pegg *et al*, 1993) (**Figure 6.4**).

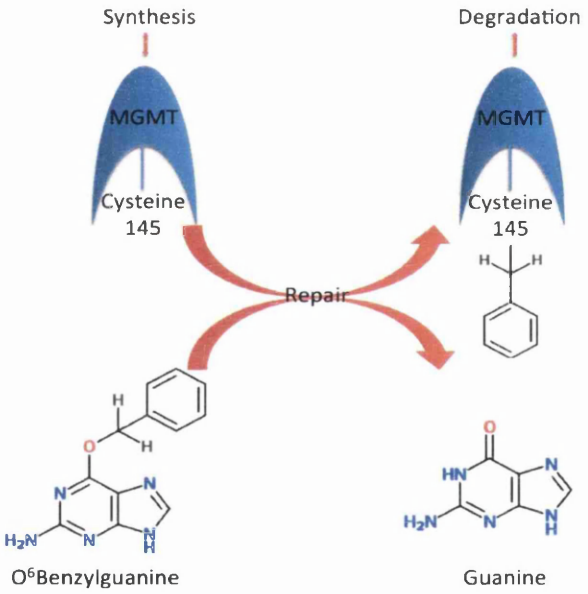

Figure 6.4. Reaction of O^6BG with MGMT. Direct transfer of alkyl group from O^6BG to cys145 restores guanine but inactivates the protein and targets it for degradation. Adapted from Kaina, Margisson and Christmann (2010).

Daniels *et al* (2000) and Rasimas *et al* (2003) suggest that a conformational change in the tertiary structure of MGMT is brought about by the disruption of complex hydrogen bonding

upon benzylation of Cys145. This causes protein instability (Crone *et al*, 1996) and renders the benzylated protein more labile to ubiquitination (Srivenugopal *et al*, 1996; Liu *et al*, 2002) followed by proteolysis by the 26S proteasome (Xu-Welliver and Pegg, 2002) leading to its degradation (Glickman and Ciechanover, 2002). The lack of induction of MGMT observed in AHH-1 cells (Chapter 5) and in human cells in response to genotoxic exposure (Fritz *et al*, 1991) suggests the existence of a basal and finite amount of MGMT within the cell, which is depleted once it has repaired the equivalent amount of O^6alkylated guanine. This means that MGMT molecules can become limited with increasing concentrations of O^6alkylated guanines (Pegg and Byers, 1992). The suicidal reaction mechanism, lack of induction in humans and sometimes-slow regeneration can deplete a cell's MGMT proficiency and is a viable target for inactivation by pharmacological inhibitors.

6.1.4. Measuring the inactivation of MGMT.

The concentration of O^6BG required for 50% MGMT inactivation (IC_{50}) is a measure of O^6BG efficacy. This can be measured through various experiments, these are:

1. Increased mutagenesis and cytotoxicity from exposure to alkylating agents following MGMT. However, this is not a direct measurement with confounding factors
2. Loss of MGMT protein through western blot analysis, although western blotting is not sufficiently sensitive to detect MGMT in AHH-1 cells
3. Lower rate of removal of O^6MeG from DNA using mass spectrometric analysis. However, O^6MeG is extremely hard to identify through mass spectrometry (Dr Rajinder Singh, personal communication). This has been further discussed in chapter 4
4. Loss of activity using activity assays involving radiolabelled substrates, this being the most direct measurement but it is costly and hazardous and is not sufficiently sensitive to detect MGMT in AHH-1 cells.

The quoted IC_{50} in the literature differs between studies. This may be due to the different measurements but also differences in sensitivity between cell lines used due to differential MGMT proficiences. We have previously discussed the lack of sensitivity of protein assays for MGMT detection in AHH-1 cells, these being western blot and activity detection (Chapter 5). Therefore, the most applicable method of validation of MGMT inactivation would be increased sensitivity to O^6MeG-induced toxicity following alkylating agent exposure.

6.1.5. Cellular influences on O^6BG efficacy.

A one-hour pre-treatment with O^6BG was shown to deplete MGMT for one cell cycle in Raji cells, a human male B lymphocyte cell line (Sklar *et al*, 1981). However, the efficiency and duration of O^6BG mediated inactivation differs between cell lines. It is noted that degradation rates of benzyl-inactivated MGMT differ between tumour and primary cells (Liu *et al*, 2001) (**Figure 6.5**) and also between cell lines (Ayi *et al*, 1994; Dolan *et al*, 1991).

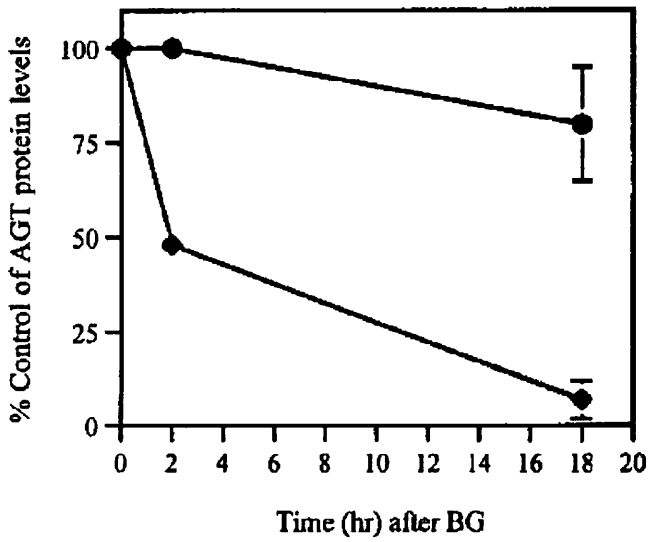

Figure 6.5. Time course showing more rapid degradation of MGMT post O^6BG treatment in tumour biopsies (diamonds) compared to peripheral blood mononucleocytes (PBMC's, circles). Taken from Liu *et al* (2001). Expressing the data as % control circumvents well-documented inter-tissue differences in MGMT levels (Gerson *et al*, 1986).

The differences highlighted in **Figure 6.5** reflect cellular differences in;

1. Ubiquitin dependent proteolysis (Gunn *et al*, 1977)
2. Initial MGMT levels (Dolan *et al*, 1991; Bobola *et al*, 1996; Heighway *et al*, 2003). Chen *et al* (1993) found that O^6BG had no effect on sensitivity in HeLa MR (MGMT deficient Human cervix cell line) but drastically increased toxicity of BCNU in HeLa S3 (MGMT proficient) cells.
3. Differential rates of basal level expression and therefore protein regeneration. Sklar *et al* (1981) found that it takes 49hr (one cell cycle) for Raji cells to regain full protection against O^6alkylating agents following complete removal by O^6BG.
4. Protein turnover which seems to be dependent on cell division (Gerson, 1988)

5. Polymorphisms within MGMT gene, which alters the affinity for protein O^6BG and also affecting degradation rates (Remington *et al*, 2008).

6.1.5.1. Polymorphism within MGMT can modify affinity for O^6BG.

Single-nucleotide polymorphisms (SNP's) within the coding region of the MGMT gene that change the amino acid sequence give variant forms of MGMT with altered functions and responses to O^6BG (Bacolod *et al*, 2004). In addition to polymorphisms, O^6BG resistant forms of MGMT can also arise through mutations in MGMT occurring in cell lines and through clonal expansion within tumours; noted by Bacolod *et al* (2004) as a reason for development of O^6BG resistant tumours. In D283 MED, D341 MED, and Daoy (human brain tumour cell lines) O^6BG resistant daughter cells evolve from MGMT proficient/O^6BG sensitive parental cells. Three mutations were identified (one in each cell line). Some of which have also been identified in other studies. Glycine→cysteine at position 156 of the primary sequence (Crone *et al*, 1994; Loktionova and Pegg, 1996; Xu-welliver and Pegg, 1996), tyrosine→phenylalanine at 114 and Lysine→threonine at 165 confer resistance to O^6BG. Other point mutations are shown in **Figure 6.6** and **Table 6.1.** Measuring resistance is the fold increase in the IC_{50} for mutant MGMT over the IC_{50} of the respective wildtype MGMT (typically <0.3μM). The higher the fold increase in IC_{50} the higher the resistance.

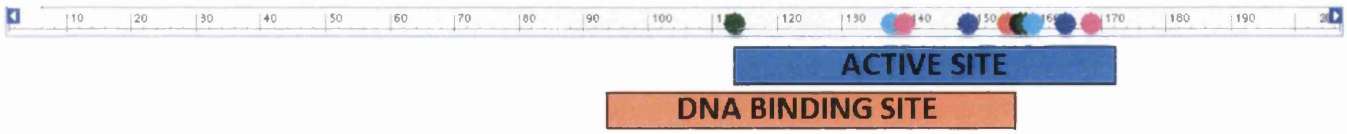

Figure 6.6. A schematic of the primary structure of MGMT. The coloured circles represent published mutations that de-sensitise cells to O^6BG. They all fall into the active site preventing O^6BG from binding and inactivating the enzyme (Daniels *et al*, 2000). The colours correspond to the mutations in **Table 6.1**. Mutations shown cause the most drastic difference.

Table 6.1. Fold change is given to negate differences in the IC50 for inhibition of wildtype MGMT in different cell types.

Mutation/ polymorphism	Fold increase in IC_{50} O^6BG over wildtype MGMT protein	Reference
Tyr114Phe	nd	Bacolod *et al* (2004)
Pro140Ala/Lys	20/12000	Crone *et al* (1993); Loktionova and Pegg (1996)
Pro140Ala with Pro138Lys	116	Crone *et al* (1994)
Pro140Ala with Gly156Ala	1200	Crone *et al* (1994)
Cys150Phe/Tyr/Glu/Leu	3-26	Xu-Welliver and Pegg (2000)
Gly156N	<40	Crone *et al* (1994); Loktionova and Pegg (1996); Xu-Welliver and Pegg (2000)
Tyr158His	7750	Xu-Welliver *et al* (1999)
Ser159Ile	110	Xu-Welliver and Pegg (2000)
Gly160Arg	20	Edara *et al* (1996); Imai (1995); Wu *et al* (1999)
Lys165Ser	600	Xu-Welliver and Pegg (2000)
Lys165Ala	100	Xu-Welliver and Pegg (2000)
Leu169Glu	860	Xu-Welliver and Pegg (2000)

The polymorphism, Gly160Arg, causes a 20-fold increase in the IC_{50} of O^6BG compared to wildtype (Edara *et al*, 1996) without hindering the repair of O^6MeG compared to controls (Wu *et al*, 1999). Individuals with this polymorphism had similar cancer incidence to matched controls (Kaur *et al*, 2000). Gly160Arg was found in 15% of the Japanese population (Imai *et al*, 1995) but Gerson *et al* (1999) suggest that it is at much lower frequency in the wider population. Imai *et al*, (1995) found Gly160Arg at much higher frequency (25%) in cancer patients. Since the majority of cell lines are derived from cancers, it is reasonable to assume that some cell types would be O^6BG resistant. O^6BG resistance in cancers cause problems in chemotherapy.

6.1.6. O^6BG in chemotherapy.

MGMT provides a pivotal role in protecting against mutagenesis and cytotoxicity caused by replication of O^6AlkylG. MGMT deficiency is an initiating event in carcinogenesis (Graham *et al*, 2010) and many human primary tumours (Gerson *et al*, 1986). However, in cancer treatment, patients with MGMT deficient tumours respond better to chemotherapy (Hegi *et al*, 2005; Esteller *et al*, 2000). Some human cancers over-express MGMT, making chemotherapy ineffective. Examples are;

1. Colon cancer (Zaidi *et al*, 1996)
2. Pancreatic carcinoma (Kokkinakis *et al*, 1997)
3. Melanoma (Lee *et al*, 1992)
4. Gliomas in the brain (Bobola *et al*, 2001)

Due to the protective effect that MGMT exerts, such malignancies are "4- to 10-fold more resistant" to alkylating chemotherapy (Liu and Gerson, 2006). Coincidentally, it is recognised that tumours with low levels of MMR proteins are more resistant to alkylating chemotherapy (Middlemas *et al*, 2000). This is understandable since MMR is responsible for O^6AlkylG toxicity. The importance of MGMT inhibitors, like O^6BG, in sensitising MGMT positive tumours to the cytotoxic effects of alkylating chemotherapy is realised. Since the *in vitro* mechanism of O^6BG mediated MGMT inactivation was elucidated by Pegg *et al* (1991). Several *in vivo* studies were then performed using murine models with human tumour xenografts. This circumvents the differences between human and murine MGMT (Liu *et al*, 1996). Gerson *et al* (1993) used a human colon cancer xenograft model and report 98% MGMT inhibition by O^6BG, reduced tumour growth rates at 3- to 4-fold lower BCNU concentration than without O^6BG. The usefulness of O^6BG is further substantiated by Wedge *et al* (1997) who report "a very significant increase in (melanoma) tumour growth delay" after 40mg/kg/day temozolomide with O^6BG over 5 days in a murine human melanoma xenograft model. These studies help to realise;

1. O^6BG alone is non-toxic at therapeutic doses.
2. It sensitises tumours to cell killing through MGMT depletion and not through additional toxicity (Wedge and Newland, 1996).
3. High level inactivation of MGMT could be achieved

4. A combination of alkylating agent with O^6BG had the desired toxic effect at lower concentrations than alkylating agent on its own (Gerson *et al*, 1993) potentially reducing unwanted toxicity in healthy tissues caused by excessive concentrations.

The studies led to clinical trials of O^6BG to potentiate cell killing by alkylating agents in the treatment of glioblastoma and in tumours of the central nervous system in children (Gerson 2002; Quinn *et al*, 2009). The consequence of using MGMT inhibitors is severe myelosuppression caused by increased toxicity in haematopoietic stem cells (Verbeek *et al*, 2008). Gene therapy represents one solution by introducing O^6BG resistant MGMT into haematopoietic stem cells as protection (Sorg *et al*, 2007). These complications have hindered the clinical use of O^6BG in chemotherapy. Since the advent of RNAi technology, new methods of MGMT inhibition in chemotherapy are being investigated (Kato *et al*, 2010).

6.1.7. O^6BG and low dose alkylating agent.

It is well documented that MGMT depletion enhances mutagenesis, toxicity and other genotoxic endpoints caused by O^6MeG (e.g. base substitutions and sister chromatid exchanges, SCE's) by a variety of S_N1, O^6-alkylating agents (Dolan *et al*, 1991; Kaina *et al*, 1991). However, this has only been ascertained for high doses of alkylating agent. The following chapter provides evidence to suggest low doses of MNU that are non-mutagenic, in MGMT proficient cells, become mutagenic following MGMT depletion. Thus, implicating MGMT in protection from low dose MNU mutagenesis. The following chapter details the use of siRNA and O^6BG as methods to create AHH-1 MGMT deficient cells to be used in the HPRT assay. A dose-response was obtained, in the HPRT assay, for direct comparison to the previous chapter in AHH-1 wildtype cells. For further evidence of the potential role of MGMT, the proportion of GC→AT transitions were calculated from HPRT mutant colonies treated with 0.0075μg/ml MNU (the NOGEL dose in AHH-1 wildtype cells for mutation induction) and compared between MGMT proficient and deficient AHH-1 cells.

6.2. Materials and method.

6.2.1. Preparation of O^6-benzylguanine stock.

O^6BG (Cas number 19916-73-5) was purchased from Sigma (Poole, UK) as a 50mg powder with ≥98% purity. Addition of 5ml 100% analytical grade methanol (Fisher Scientific, Loughborough, UK), gave a stock concentration of 10mg/ml. The stock was discarded after use.

6.2.2. O^6BG pre-treatment.

For all treatments with MNU, 1 flask of AHH-1 cells at sufficient volume was treated with 2.4µl of 10mg/ml O^6BG per 10ml media to obtain a final concentration of 10µM, for sufficient MGMT inhibition (Professor Bernd Kaina, personal communication). AHH-1 cells were exposed to O^6BG for 1hr at 37°C, 5% CO_2. At this time, the O^6BG treated cell stock was divided into 10ml cultures, one for each dose of MNU. This minimised pipetting errors of adding O^6BG to individual treatment flasks. Time 0 was taken after 1hr pre-treatment with O^6BG. At time 0, the appropriate solvents were added and immediately sampled.

6.2.3. HPRT assay.

Following 1hr pre-treatment with O^6BG, the procedure was performed as detailed in Chapter 2. However, 1800 wells per dose were sufficient for this mechanism of action analysis (Zair *et al*, 2011).

6.2.4. Cytotoxicity.

To assess the effect of O^6BG on MNU toxicity, RPD measurements were performed according Chapter 2. MNU without O^6BG (MNU-O^6BG) was compared to MNU+O^6BG at equal MNU doses, performed as discussed. Two dose ranges of MNU were performed. One being; 0.0075µg/ml, 0.01µg/ml and 0.05µg/ml (**Table 2.2**, Chapter 2) with relevant controls to assess toxicity of MNU in presence of O^6BG over the dose range in chapter 3. And the second dose range used toxic doses of MNU, which was prepared as follows. The stock of 0.1g/ml MNU (Chapter 2) was further diluted 1:100 to 1mg/ml in dimethyl sulfoxide (DMSO). This was used in **Table 6.2**.

Table 6.2. Dilutions of MNU used to cause cytotoxicity in AHH-1 cells.

Final Concentration MNU (μg/ml)	Volume of DMSO (μl)	Volume of MNU stock at 1mg/ml (μl)
0	500	0
2	100	400
4	200	300
6	300	200
8	400	100
10	500	0

6.2.5. Negative controls for O^6BG and MNU in the HPRT assay and cytotoxicity studies.

The negative controls were;

- **100μl DMSO** solvent control for MNU
- **Methanol + DMSO** 1hr pre-treatment with 2.4μl methanol (final concentration 0.024%) in 10ml cell culture (0.00024% methanol) followed by 100μl of DMSO, to assess the contribution of respective O^6BG and MNU solvents
- **Methanol** 1hr pre-treatment with 2.4μl methanol used as the solvent control of O^6BG
- **O^6BG-MNU** 1hr pre-treatment with 2.4μl (10μM) O^6BG only assessed the effects of just O^6BG
- **O^6BG + DMSO** 1hr pre-treatment with O^6BG followed by 100μl DMSO allowed comparison with the solvent control in Chapter 3.

6.2.6. Calculation of the RPD and RPE for the negative controls.

DMSO=population doubling (PD) or plating efficiency (PE) of DMSO treated cultures

PD of untreated cultures

Methanol and DMSO= PD or PE of Methanol + DMSO treated cultures

PD or PE of untreated cultures

Methanol= PD or PE of Methanol treated cultures

PD or PE of untreated cultures

O^6BG-MNU= PD or PE of O^6BG-MNU treated cultures

PD or PE of *methanol* treated cultures

O^6BG + DMSO= PD or PE of O^6BG + DMSO treated cultures

PD or PE of untreated cultures

6.2.7. Calculation of the RPD of treated control cultures

MNU-O^6BG= PD or PE of MNU-O^6BG treated cultures

PD or PE DMSO treated cultures

MNU+O^6BG= PD or PE of MNU+O^6BG treated cultures

PD or PE Methanol+DMSO treated cultures

6.2.8. Preparation of cells for MGMT activity analysis.

To validate inactivation of MGMT by O^6BG, AHH-1 cells were harvested at six time points over 48hr post-treatment and assayed for activity. For sufficient yields, $1x10^6$cells/ml were treated with 10μM O^6BG and divided into 10ml cultures for each time point and incubated at 37°C, 5% CO_2. Time of treatment was taken as time 0 and cells were harvested at 1,4,6,12,24 and 48hr post-treatment. Methanol was used for time-matched controls. Upon harvest, cells were washed twice in phosphate buffered saline (PBS, Lonzo, Slough, UK) and the pellet snap-frozen in liquid nitrogen for 30s. Samples were stored at -80°C awaiting shipment.

Assay for activity took place in University of Mainz, Germany with the help of Professor Bernd Kaina and Karl-Heinz Tomaszowski to whom I am incredibly grateful.

6.2.9. siRNA oligonucleotides

6.2.9.1. MGMT siRNA oligonucleotides.

The sequence of 3 MGMT siRNA oligonucleotides was obtained from Kato *et al* (2010). (**Table 6.3**).

Table 6.3. The sequences of the siRNA used in MGMT knockdown from Kato *et al*, (2010) including overhangs necessary for efficient transfection and silencing (Bellemin *et al*, 2007).

siRNA	Sense sequence	Antisense sequence
1	5'GAGCAGGGUCUGCACGAAdTdT3'	5'P-UUUCGUGCAGACCCUGCUCdTdT3'
2	5'CCAGACAGGUGUUAUGGAAdTdT3'	5'P-UUCCAUAACACCUGUCUGGdTdT3'
3	5'GGACUGGCCGUGAAGGAAUdTdT3'	5'P-AUUCCUUCACGGCCAGUCCdTdT3'

6.2.9.2. siRNA controls.

All control siRNA were purchased from Dharmacon (ThermoScientific, Loughborough, UK). GAPDH was targeted for knockdown as a positive control for optimisation using ON-TARGET plus GAPDH control siRNA number D-001830-01-05. The negative control was ON-TARGET plus non-targeting siRNA number D-001810-01-05.

6.2.9.3. Reconstitution of MGMT siRNA.

Upon delivery, tubes containing MGMT siRNA oligonucleotides were briefly centrifuged, and reconstituted to 40μM by addition of 1ml RNase free water per tube. The solution was pipetted up and down 4 times and vortexed on an orbital shaker for 30mins at room temperature. The tubes were centrifuged and the concentration determined by measuring absorbance at 260nm on a nanodrop 1000 spectrophotometer. Single use (10μl) aliquots were made and stored at -20°C.

6.2.9.4. Transfection optimisation.

Reverse transfection offered the most reliable method (Dr James Cronin, personal communication) and was performed in Nunc 24 well plates (Fisher Scientific, Loughborough,

UK) according to instructions provided with the transfection reagent, Lipofectamine™ RNAiMAX (Invitrogen, Paisley, UK). For GAPDH, a range of 0.6pmol to 30pmol ON-TARGETplus siRNA was used per well with 0.5µl to 5µl Lipofectamine™ RNAiMAX. For maximum effect on MGMT knockdown (Kato *et al*, 2010), all 3 MGMT targeting siRNAs were used in combination. The amount of siRNA added per well ranged from 1.8pmol (0.6pmol per siRNA) to 150pmol (50pmol per siRNA) and the volume of Lipofectamine™ RNAiMAX ranged from 0.5µl to 5µl per well of a 24 well plate. The same amount of each siRNA was diluted in 100µl Opti-MEM® I medium without serum (Invitrogen, Paisley, UK) in one well of the culture plate. Lipofectamine™ RNAiMAX was added to the well, mixed and incubated at room temperature for 20min to allow siRNA to be enveloped in liposomes. AHH-1 cells were diluted to $1x10^5$cells/ml and 500µl added to each well ($5x10^4$cells/well). The plate was incubated at 37°C, 5% CO2 for 24hr for RNA extraction to assess knockdown by real time PCR.

6.2.9.5. Real time analysis of siRNA treated cells.

Real time analysis was performed as detailed in Chapter 2. Each siRNA treatment was performed in triplicate and real time PCR performed in triplicate on three separate occasions. However, to save on cost of real time PCR master mix reagents, each sample was only assayed once per plate. GAPDH specific probes (Applied Biosystems, Warrington, UK assay ID; Hs99999905_m1) were used to assess knockdown following treatment with GAPDH specific siRNA, which was used as the positive control for transfection optimisation.

6.3. Results.

The results of this chapter report on the two methods used to create an AHH-1 MGMT deficient phenotype, through knockdown of MGMT using siRNA and the use of O^6BG to inactivate MGMT, with subsequent validations. The HPRT assay was repeated using MGMT knockdown cells. In comparison to wildtype AHH-1 cells, (Chapter 3) a change in dose-response and mutation spectra was observed which implicates MGMT in low dose alkylation exposure.

6.3.1. siRNA and O^6BG in creating a MGMT deficient phenotype.

6.3.1.2. siRNA trial.

siRNA experiments were set up as detailed but with limited success. To validate gene knockdown, RNA was extracted 24hr following treatment with gene specific siRNA. GAPDH (positive control) or MGMT mRNA was measured by real time PCR using TBP as the reference housekeeping gene for MGMT and GAPDH quantitation. TBP was shown to be constitutively expressed in AHH-1 (supplementary figure Zair *et al*, 2011) and is an appropriate housekeeper. The fold change in GAPDH (Figure 6.7 and Figure 6.8) and MGMT (Figure 6.9) mRNA levels, between treated and control, is recorded as a function of increasing concentrations of transfection reagents.

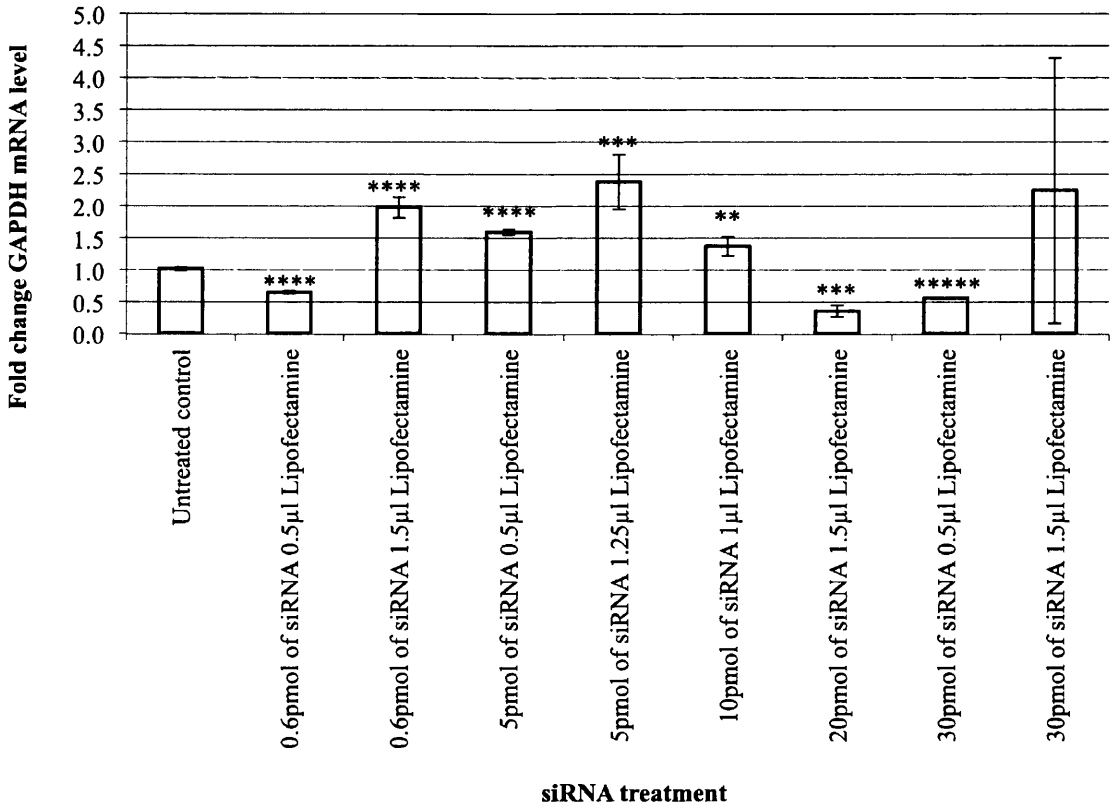

Figure 6.7. The first attempt at GAPDH knockdown using siRNA. 20pmol siRNA with 1.5µl Lipofectamine™ RNAiMAX showed greatest fold decrease. n=3. Error bars represent standard deviation (SD), **p=<0.01*** p=<0.001, ****p=<0.0001, *****p=<0.00001.

From **Figure 6.7**, treatment using 20pmol of ON-TARGETplus GAPDH siRNA with 1.5µl Lipofectamine™ RNAiMAX significantly decreases the fold change to an average of 0.36 (p=0.0007), giving an average of 64% (1-0.36=0.64; 0.64x100=64%) GAPDH knockdown compared to the untreated control. Using higher amounts of reagents (**Figure 6.8**) a maximum average knockdown of 80% was achieved using 20pmol of siRNA with 5µl Lipofectamine™ RNAiMAX (p=0.0005). Although, neither **Figure 6.7** nor **Figure 6.8** shows a dose-response (an increase in efficacy) as would be expected with increasing concentration of siRNA reagents until toxicity is reached.

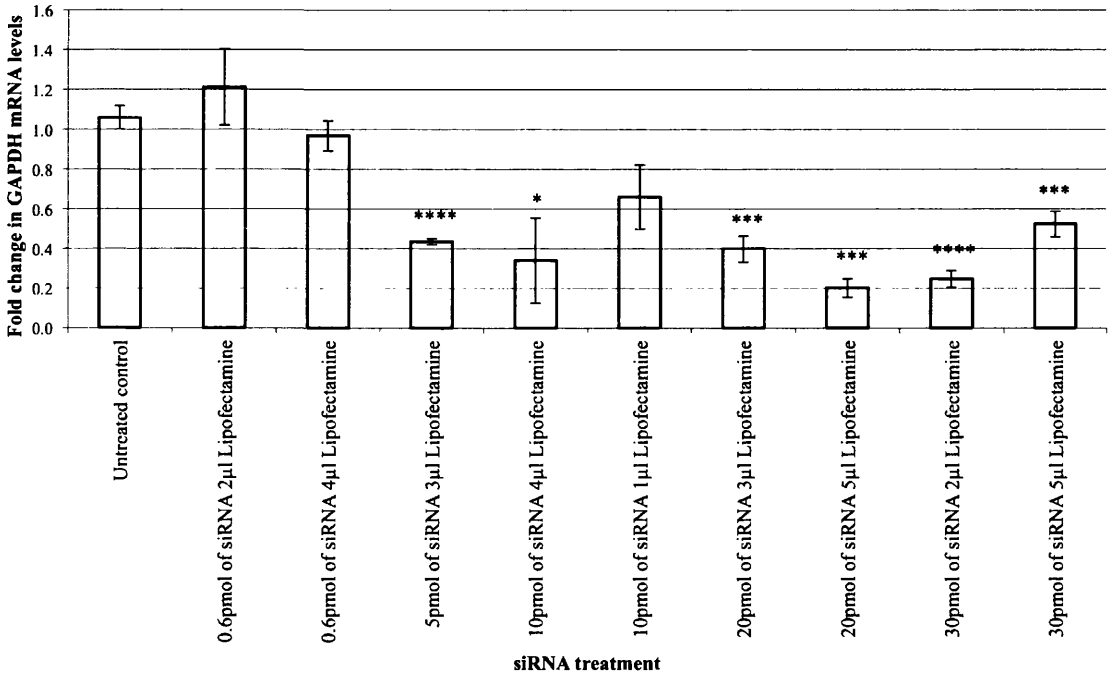

Figure 6.8. Fold change in GAPDH at higher concentrations of siRNA reagents. n=3. Error bars are SD *p=<0.05, ***p=<0.001, ****p=<0.0001.

The treatment conditions used in **Figure 6.8** were repeated using a combination of all three MGMT targeting siRNA's. Four of ten treatments analysed gave threshold cycle values for MGMT at the end of real time PCR. Of these four samples, not one treatment method was found to reduce MGMT expression (**Figure 6.9**).

The following treatments gave no Ct values in one or more replicates for MGMT;

1. 10pmol each siRNA 4µl Lipofectamine
2. 20pmol each siRNA 1.5µl Lipofectamine

3. 20pmol each siRNA 5µl Lipofectamine
4. 30pmol each siRNA 2µl Lipofectamine
5. 30pmol each siRNA 5µl Lipofectamine
6. 50pmol each siRNA 4µl Lipofectamine

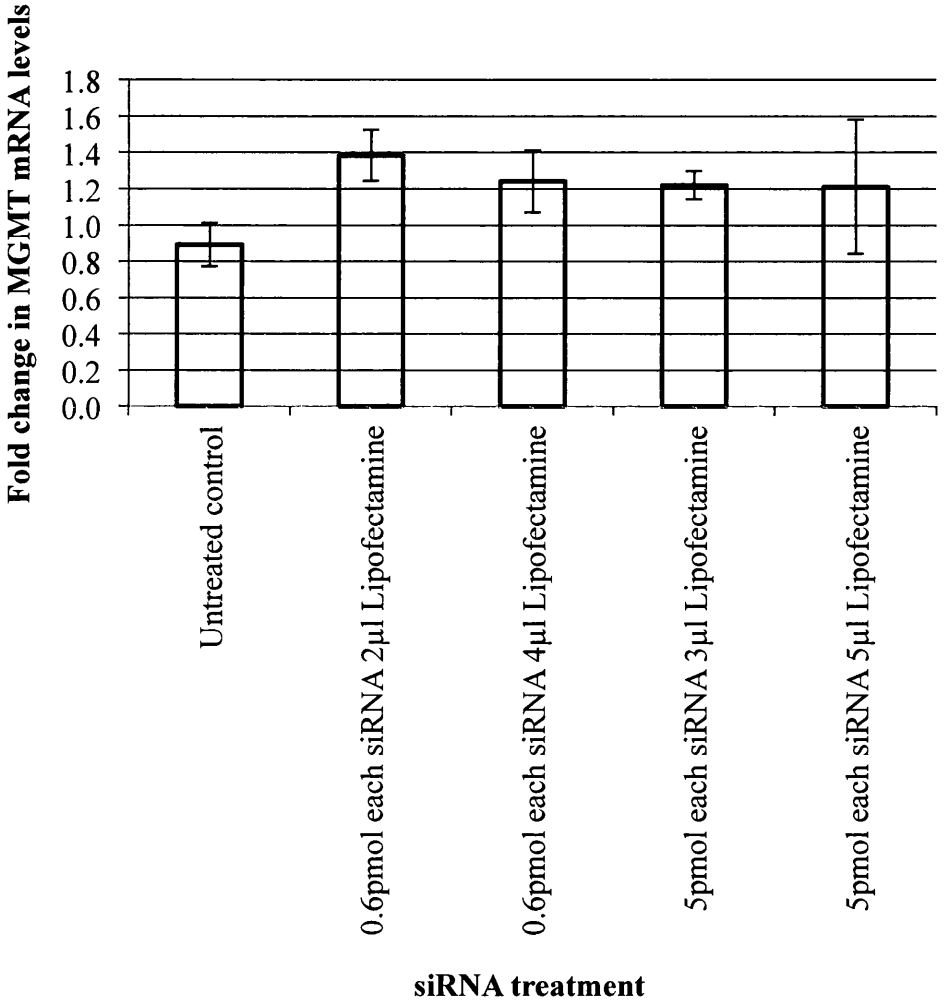

Figure 6.9. There was no decrease in MGMT mRNA level following siRNA transfection. n=3, error bars are SD.

Six treatments did not yield Ct (threshold cycle) values, suggesting 100% knockdown since the mRNA could not be detected. This was not reproducible with at least one replicate per treatment showing no change in fold change compared to control.

6.3.2. O^6BG.

6.3.2.1. Assessing the cellular presence of O^6BG through increased toxicity by MNU.

An alternative method of MGMT knockdown using O^6BG as a pharmacological inhibitor was investigated. To provide evidence of the cellular presence of O^6BG, we compared the toxicity of high dose MNU with and without O^6BG pre-treatment. Relative population doubling (RPD) was used as a measure of toxicity. RPD compares the number of cells at 24hr and 48hr post-MNU treatment to the number of cells before treatment. In **Table 6.4**, the TD_{50} (dose of MNU that causes 50% reduction in RPD. i.e. 50% toxicity) is shown for each time point and treatment.

Table 6.4. Pre-treatment with O^6BG reduces the dose of MNU needed to achieve 50% cytotoxicity at both time points. n=2.

Time Point (hr post MNU treatment)	Treatment group	Average TD_{50} (μg/ml)
24	MNU-O^6BG	3
24	MNU+O^6BG	2
48	MNU-O^6BG	2
48	MNU+O^6BG	1

Referring to **Table 6.4,** at comparative time points, treatment with O^6BG reduces the TD_{50} suggesting that MNU toxicity is potentiated by O^6BG. For example, at 24hr the TD_{50} was reduced from 3μg/ml MNU to 2μg/ml MNU following 1hr pre-treatment with 10μM O^6BG, used to inactivate MGMT. O^6BG further potentiated MNU toxicity when cell counts were measured at 48hr post MNU treatment, reducing its TD_{50} from 2μg/ml to 1μg/ml. For both treatment groups, MNU was more toxic 48hr post treatment than when toxicity is assessed 24hr post exposure. For MNU-O^6BG, the TD_{50} of MNU was reduced from 3μg/ml to 2μg/ml, with a similar reduction over 48hr in the presence of O^6BG.

6.3.2.2. Does O^6BG render low dose MNU toxic?

MNU was assayed for cytotoxicity following pre-treatment with O^6BG and compared to toxicity of MNU alone over the dose range used in the HPRT assay (0.00075g/ml to 0.075g/ml). The results are shown in **Figure 6.10**.

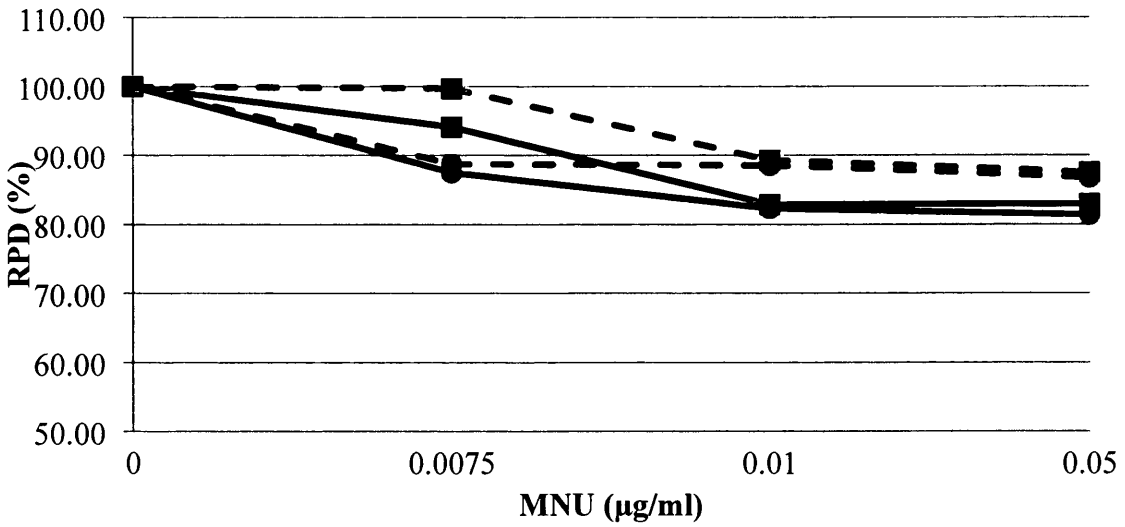

Figure 6.10. Toxicity curves for the dose of MNU used in the HPRT assay in absence and presence of O^6BG showing that O^6BG. Key; MNU-O^6BG (Dashed line), MNU+O^6BG (solid line), 24hr (squares) 48hr (circles). n=3.

Weak toxicity was observed over the MNU dose-range over 48hr. At 24hr, the top dose of 0.5µg/ml used here, gave maximum toxicity, an average of 13.2% (86.8% RPD) of 2 replicates. This was only slightly enhanced following O^6BG pre-treatment to an average of 18.6% toxicity (81.4% RPD). Toxicity at 48hr was higher at all doses than at 24hr post-treatment. The toxicity of the solvent controls was also assessed over 48hr (**Table 6.5**).

Table 6.5. The contribution of the respective solvent controls to the observed toxicity of MNU and O^6BG. It can be seen that the solvent treatments did not cause a substantial reduction in RPD. n=2.

	Average RPD (%)	
Control treatment	**24hr**	**48hr**
DMSO	97.7	98.7
Methanol and DMSO	95.7	98.2
O^6BG-MNU	100.0	102.1
Methanol	96.8	98.4
O^6BG+DMSO	102.4	96.0

It is evident that the solvent controls did not cause a drastic reduction in RPD highlighting their suitability in the assay.

6.3.3. The effect of MGMT inactivation on the shape of the dose-response.

The HPRT assay was performed as detailed in Chapter 2 following 1hr pre-treatment with 10μM O^6BG to inactivate MGMT prior to addition of MNU. The cells ability to form a colony in 96 well plates, under non-selective conditions (without 6-thioguanine) was assessed using plating efficiency (PE) shown in **Figure 6.11**. At the higher doses there was a general decrease in cell viability particularly at 0.01μg/ml MNU, where the lowest was 77.3 +/- 13.7% at 0.025μg/ml MNU which was comparable to Doak *et al* (2007). All values were normalised to the PE of cultures treated with 1hr methanol, and then 100μl DMSO, which represented the solvent control. The PE of all control treatments is shown in **Table 6.6**. All were normalised against the untreated PE with the exception of O^6BG that was divided by the PE of methanol, the solvent control for O^6BG.

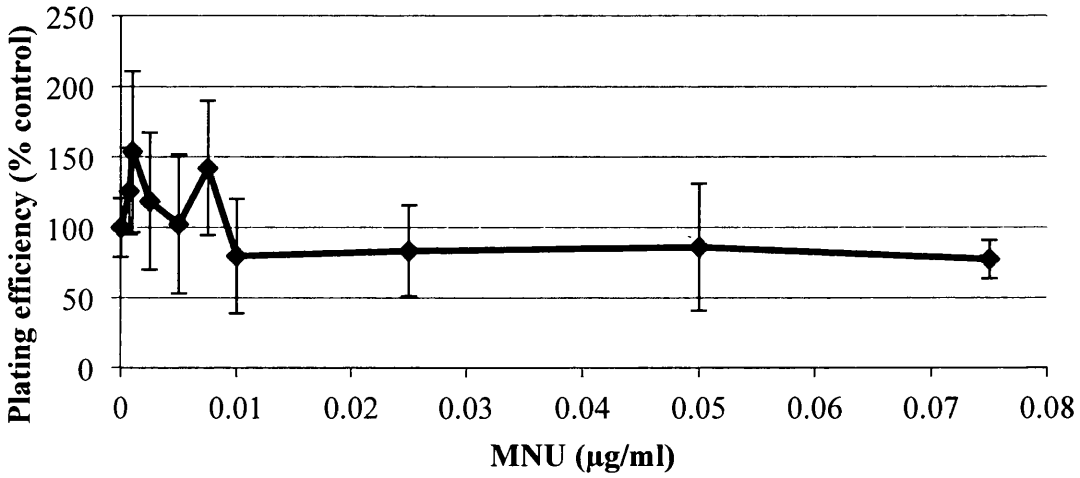

Figure 6.11. Plating efficiency as a measure of AHH-1 cell viability following MGMT inactivation with O^6BG at increasing concentrations of MNUover the HPRT assay. The solvent control represents DMSO+methanol compared to untreated controls. n=3 error bars represent standard deviation.

A number of solvent treatments were used to ensure the experiment was appropriately controlled and to assess the contribution of each treatment on mutant frequency (MF) at the *HPRT* locus (**Table 6.6**).

Table 6.6. The effects of solvent controls and O^6BG on mutant frequency and plating efficiency compared to untreated cultures as calculated using equations in materials and method. n=3.

Treatment type	Average mutant frequency ($x10^{-5}$)	Standard deviation ($x10^{-5}$)	Relative plating efficiency (%)	Standard deviation
Untreated (chapter 3)	1.41	0.31	100	-
O^6BG	1.00	0.78	155.36	47.19
Methanol + DMSO	1.49	0.59	87.46	20.99
DMSO +O^6BG	1.33	1.52	83.18	22.75
Methanol	1.86	0.36	80.74	25.82

The MFs and PE of each solvent were not significantly different compared to the untreated control using a one-way ANOVA (lowest p=0.475 and lowest p=0.343, respectively). Therefore, a valid comparison can be made between AHH-1 cutures pre-treated with O^6BG and those without in chapter 3. The mutant frequencies, over the same dose range in chapter 3 (0.00075μg/ml to 0.075μg/ml MNU) of O^6BG treated cultures are shown in **Figure 6.12**.

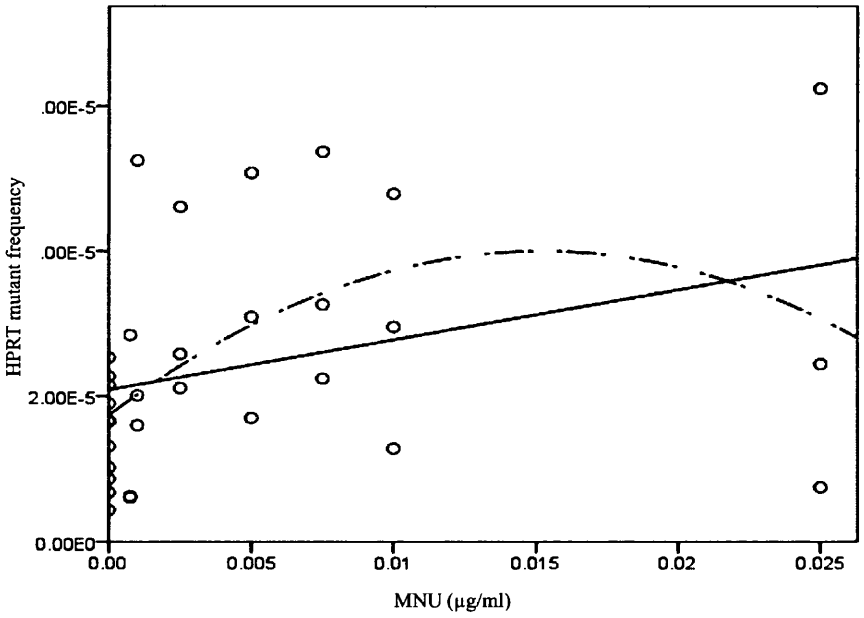

Figure 6.12. Linear increase (p=0.15) in HPRT mutant frequencies following 24hr exposure to MNU in AHH-1 cells pre-treated with O^6BG. The solvent control (at 0.00) represents the MF of cells treated with Methanol and DMSO. n=3.

The dose-response shows high variability between MNU doses. However, curve estimations reveal that the dose response was linear (p=0.15) which is in contrast to the results of Chapter 3 in wildtype AHH-1 cells. Statistical analysis using a two-tailed t-test, revealed the lowest observed genotoxic effect level to be 0.001μg/ml MNU (p=0.04).

6.3.4. Comparisons of dose-response with MGMT active AHH-1 cells in Chapter 3.

O^6BG is known to specifically inhibit MGMT activity and so cells treated with O^6BG are assumed to represent MGMT inactive cells. A comparison of mutation induction by MNU is made between MGMT inactive AHH-1 cells and MGMT active AHH-1 cells. There was a marked increase in mutagenicity by MNU in O^6BG treated cells, particularly at sub-NOGEL doses. For example, the previously observed NOGEL dose of MNU (0.0075μg/ml) gave $1.03x10^{-5}$+/-$3.21x10^{-5}$ HPRT mutants, whereas cultures pre-treated with O^6BG gave a 3-fold increase in MF to $3.62\ x10^{-5}$ +/-$1.60\ x10^{-5}$. This suggests that O^6BG sensitises AHH-1 cells to MNU mutagenesis. In addition, there is a 10-fold reduction in the LOGEL from 0.01μg/ml MNU ($p=0.015$) in wildtype AHH-1 cells to 0.001μg/ml ($p=0.04$) in O^6BG treated cells as adjudged by a two tailed t-test between control and treatment mean MF's. Comparison of the dose-response at sub-NOGEL doses in presence and absence of O^6BG is shown in **Figure 6.13**.

A).

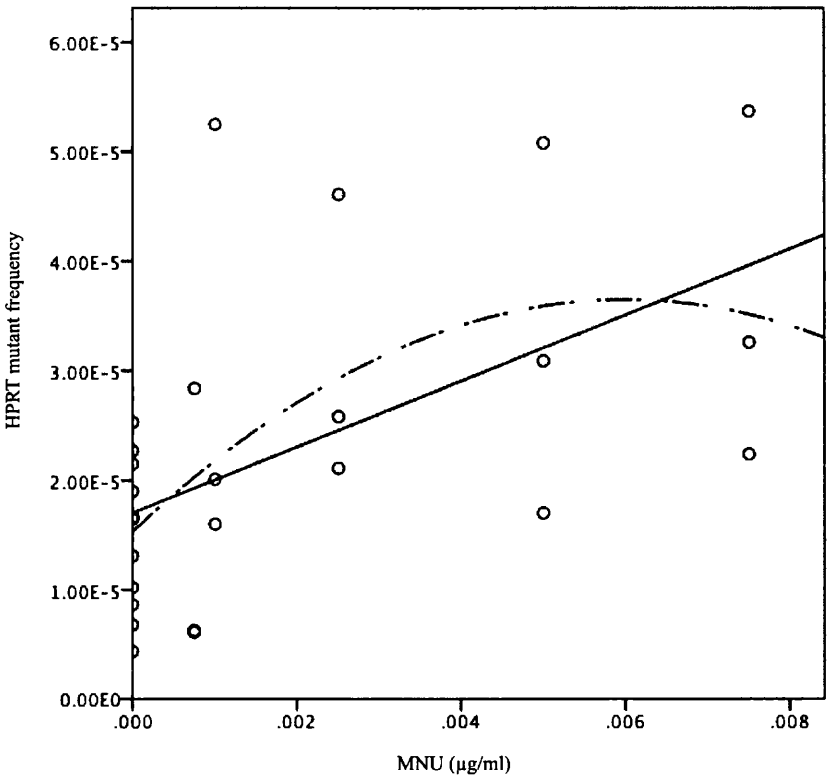

B).

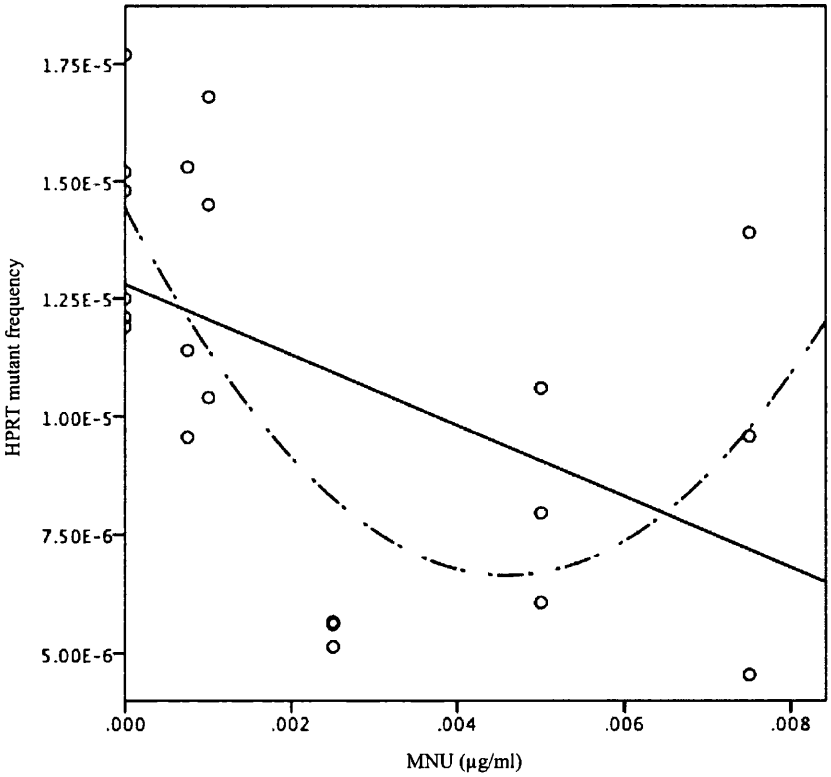

Figure 6.13. HPRT data comparing the dose-response at sub-NOGEL MNU doses (<0.0075µg/ml) in presence (A) and absence (B) of O^6BG.

Pre-treatment with O^6BG to inactivate MGMT has drastically changed the shape of the dose-response up to 0.0075μg/ml MNU, which was the statistical NOGEL found in Chapter 3. Previously, a quadratic model was the better fit of **Figure 6.14B** (p=0.01). However, the linear model better explained the data following inactivation of MGMT in **Figure 6.14A** (p=0.4). The change in MNU dose-response is further evident in **Table 6.7**.

Table 6.7. Numerical values for the slopes of **Figure 6.13**.

Treatment	Gradient of the slope	95% confidence limits
-O^6BG	-0.000749	-0.001327 to -0.000748
+O^6BG	0.003012	0.004801 to 0.001223

For both treatments, the confidence limits of the gradient do not pass 0, which is the gradient expected if the dose-response observed a true NOGEL, where the slope would run parallel to the x-axis, therefore, there was definite deviation from the control value (Gocke and Wall, 2009). However, where the gradient was negative in absence of O^6BG, it was positive in the presence of O^6BG. This highlights the change from a reduction in MF (-O^6BG) to an increase in MF (+O^6BG).

6.3.5. Comparison of benchmark dose (BMD).

The benchmark dose (BMD) is a more sophisticated model than NOGEL and has been used in risk assessment (EFSA, 2009) and is used in an analogous way. Gollapudi *et al* (2012) and Filipsson *et al* (2003) suggest that BMD should be the first choice in dose-response modelling of all continuous data where a significant response is seen compared to the control. The authors of the ILSI-HESI quantitative subgroup, further emphasise the use of $BMDL_{10}$ (lower limit of the BMD) as a point of departure (PoD) over NOGEL and threshold dose (Td). There is current debate as to which parameter should be used to define the PoD. Here, using PROAST software, the BMD was determined for both dose-responses (+O^6BG and –O^6BG) and are shown in **Table 6.8**.

Table 6.8. The benchmark dose (BMD) that marks the critical event in a dose-response, analogous to the NOGEL/LOGEL approach. 90% confidence limits are given either side of the BMD. The BMD is lower following O^6BG pre-treatment.

		90% confidence limits	
Treatment	**BMD**	**Lower (BMDL)**	**Upper (BMDU)**
-O^6BG	0.00956	0.00667	0.00981
+O^6BG	0.00020	0.00006	0.00112

The data in **Table 6.8** importantly shows that AHH-1 cells without prior MGMT inactivation (-O^6BG) can tolerate 50-fold higher concentration of MNU before a significant response is seen compared to cells with MGMT activation (+O^6BG). The BMD and the lower confidence limit (BMDL) of MNU in MGMT inactivated cells are extremely low (0.0002μg/ml and 0.00006μg/ml MNU, respectively) and are below the level of doses tested, therefore we could not state that a point of departure (PoD) exists for this data set, further highlighting the increased potency of MNU in MGMT inactivated cells.

6.3.6. Fold difference in MF.

The fold change in MF between AHH-1 cells differing in MGMT proficiency was calculated by dividing the MF in presence of O^6BG (MGMT inactive) by the MF in absence of O^6BG (MGMT active) at each dose (**Figure 6.14**).

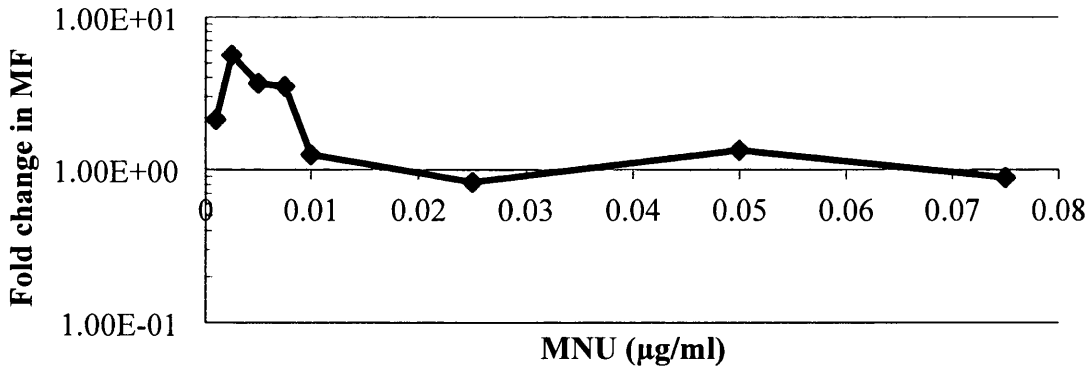

Figure 6.14. The fold difference in MF between +O^6BG and -O^6BG is greatest at doses below the statistical LOGEL of 0.01μg/ml. Plotted on Log-Linear axis.

A maximum 5-fold increase in MF in MGMT inactivated cells was observed at doses below the LOGEL (0.01μg/ml MNU, identified in Chapter 3). There was very little difference in MF fold change at the LOGEL and higher doses of MNU. This suggests that the effects of MGMT loss are more noticeable at doses below the LOGEL. This is further emphasised by

statistics (**Table 6.9**), which compares the MF at each concentration of MNU. Since the MF of solvent controls did not differ significantly to the untreated control, the MF in presence and absence of O^6BG was compared at each dose using a two-tailed t-test. Significance was only seen at doses below the LOGEL.

Table 6.9. A two-tailed t-test compared each dose for significance to see the effect of O^6BG on MF. Significance (show in bold) was only achieved at doses below the NOGEL. p=<0.05 except 0.005μg/ml where p=<0.01.

	HPRT Mutant Frequencies (MF)			
MNU (μg/ml)	**Replicate 1**	**Replicate 2**	**Replicate 3**	**p-value**
0.00075-O^6BG	9.56E-06	1.14E-05	1.53E-05	
0.00075+O^6BG	2.84E-05	6.27E-06	6.11E-06	0.852
0.001-O^6BG	1.04E-05	1.68E-05	1.45E-05	
0.001+O^6BG	5.25E-05	2.01E-05	1.60E-05	0.251
0.0025-O^6BG	**5.66E-06**	**5.61E-06**	**5.14E-06**	
0.0025+O^6BG	**4.61E-05**	**2.58E-05**	**2.11E-05**	**0.029**
0.005-O^6BG	**1.06E-05**	**7.96E-06**	**6.07E-06**	
0.005+O^6BG	**5.08E-05**	**1.70E-05**	**3.09E-05**	**0.067**
0.0075-O^6BG	**4.55E-06**	**1.39E-05**	**9.58E-06**	
0.0075+O^6BG	**5.37E-05**	**3.26E-05**	**2.24E-05**	**0.049**
0.01-O^6BG	2.51E-05	2.63E-05	2.03E-05	
0.01+O^6BG	2.95E-05	1.28E-05	4.79E-05	0.583
0.025-O^6BG	4.29E-05	3.63E-05	3.47E-05	
0.025+O^6BG	2.44E-05	7.49E-06	6.24E-05	0.713
0.05-O^6BG	3.02E-05	3.14E-05	3.22E-05	
0.05+O^6BG	4.81E-05	6.79E-05	2.89E-05	0.205
0.075-O^6BG	6.51E-05	5.30E-05	4.66E-05	
0.075+O^6BG	6.90E-05	2.79E-05	3.99E-05	0.524

6.3.7. Fraction of lesions unrepaired by MGMT.

Gocke, Tang and Singer (in press) divided the MF in MGMT active cells (-O^6BG) by the MF in MGMT inactive cells (+O^6BG) to infer the fraction of unrepaired lesions by MGMT. This mathematical model assumes that the only difference between these two conditions is the

efficiency of repair of DNA adducts. This has been applied to the data presented here (**Figure 6.15**).

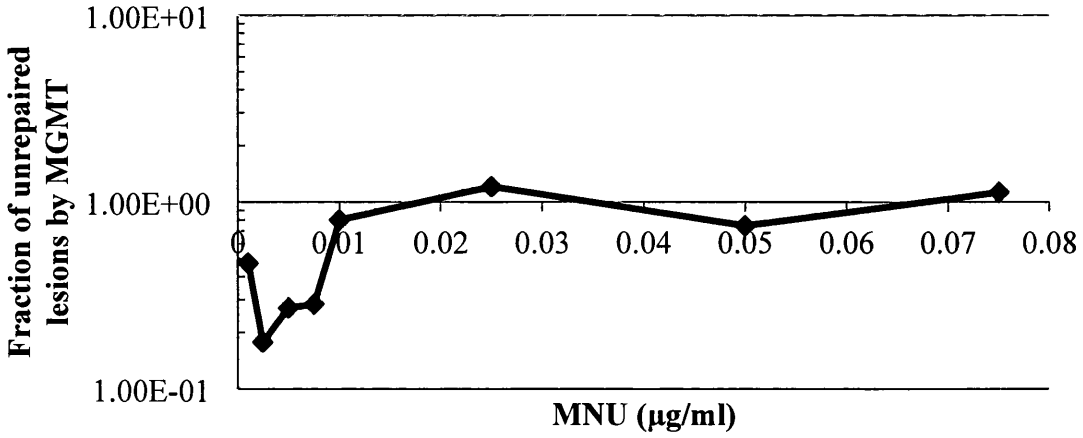

Figure 6.15. Fewer adducts are unrepaired at doses below the LOGEL of 0.01µg/ml. Values approaching 1 at higher doses suggest that all adducts are unrepaired. Plotted on Log-Linear axis.

As shown in **Figure 6.15**, at doses below the LOGEL (0.01µg/ml MNU) there was a lower fraction of unrepaired adducts for example, at 0.001µg/ml MNU (10-fold lower than the LOGEL found in Chapter 3) four in every ten adducts were unrepaired ($4x10^{-1}$). At, 0.0025µg/ml (which caused a significant reduction in MF in chapter 3) one in every ten ($1x10^{-1}$) adducts were unrepaired suggesting a higher efficiency of DNA repair. Ratios at doses above the LOGEL (<0.01µg/ml MNU) were close to 1. There was no difference in repair efficiency between AHH-1 cells in absence and in presence of O^6BG at higher doses of MNU.

6.3.8. Real time analysis of MGMT transcripts over MNU dose range with O^6BG.

To assess the response at the MGMT promoter to O^6BG and MNU treatment, MGMT expression analysis was conducted over 24hr at increasing concentrations of MNU following 1hr pre-treatment with O^6BG (**Figure 6.16**).

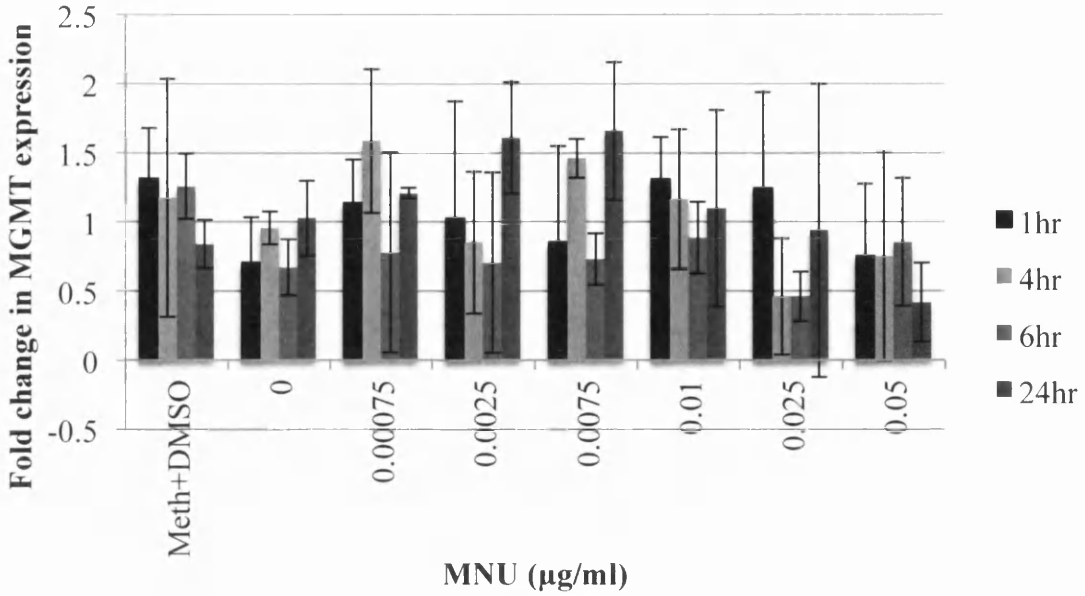

Figure 6.16. MGMT mRNA was analysed at different time points following treatment with MNU in MGMT inactivated cells.

Due to the high variability of data, gene expression was found not to differ significantly from the solvent control (lowest p=0.07, a decrease in expression at 0.05µg/ml following 24hr exposure). There seemed to be a dose response at 24hr where expression increases to a peak at 0.0075µg/ml (previously found to be the NOGEL in wild type AHH-1 cells) and then declines at higher doses.

6.3.9. Mutation spectra at the HPRT locus following MGMT inactivation.

MGMT has a well-established role in preventing GC→AT transitions by removing O^6MeG, formed in comparatively high quantities by MNU and other S_N1 alkylating agents. To further emphasise the role of MGMT in the dose-response for MNU mutation induction, we sequenced HPRT mutants treated with 0.0075µg/ml MNU and compared proportions of GC→AT transitions in cultures pre-treated with O^6BG to inactivate MGMT (**Table 6.10**).

Table 6.10. A comparison of the mutation spectra at the HPRT locus in AHH-1 cells following treatment with 0.0075μg/ml MNU (NOGEL, chapter 3), with and without pre-treatment with O^6BG and the spontaneous mutation spectra following pre-treatment of O^6BG which has been shown to inactivate MGMT.

	Percentage of total mutations			
Substitution type	**0μg/ml MNU n=22**	**0+O^6BG n=8**	**NOGEL -O^6BG n=6**	**NOGEL +O^6BG n=7**
GC→AT	15.0	1.0	28.6	**45.8**
AT→CG	**29.0**	28.3	0.0	25
AT→GC	9.3	24.2	24.5	14.5
GC→TA	9.3	4.0	6.1	0.0
AT→TA	22.4	14.1	**40.8**	4.2
CG→GC	15.0	**26.3**	0.0	10.4
Single nucleotide deletion	0.0	2.0	0.0	0.0
Total number of substitutions	112	198	49	48

A total of 12 mutants were sequenced following MGMT inactivation and 0.0075μg/ml MNU (NOGEL +O^6BG). Of these, 5 were found to contain the rearrangement to the HPRT gene as found in chapter 3. Likewise, these were removed from analysis and only base substitutions are shown. An interesting finding was that O^6BG drastically changed the spontaneous mutation spectra where only 1% of mutations were GC→AT transitions compared to 15.0% found in the spectrum of the negative control in chapter 3 (0μg/ml MNU-O^6BG). The most predominant change, AT→CG transversions, constituted 29.0% of this mutation spectra. A deletion of a single adenine at 303 occurred in 2/8 mutants. These changes did not occur in the treated samples as can be seen in their respective spectra in **Figure 6.17**. The important finding in MNU treated cells was the increase in GC→AT transitions in samples pre-treated with O^6BG from 28.6% to 45.8% at the same doses of MNU (0.0075μg/ml). This increase is not biased by a heavily mutated colony at 0.0075μg/ml MNU +O^6BG, since the number of mutants harbouring GC→AT transitions also increased from 3/6 (50%) to 5/7 (71%) following MGMT inactivation by O^6BG.

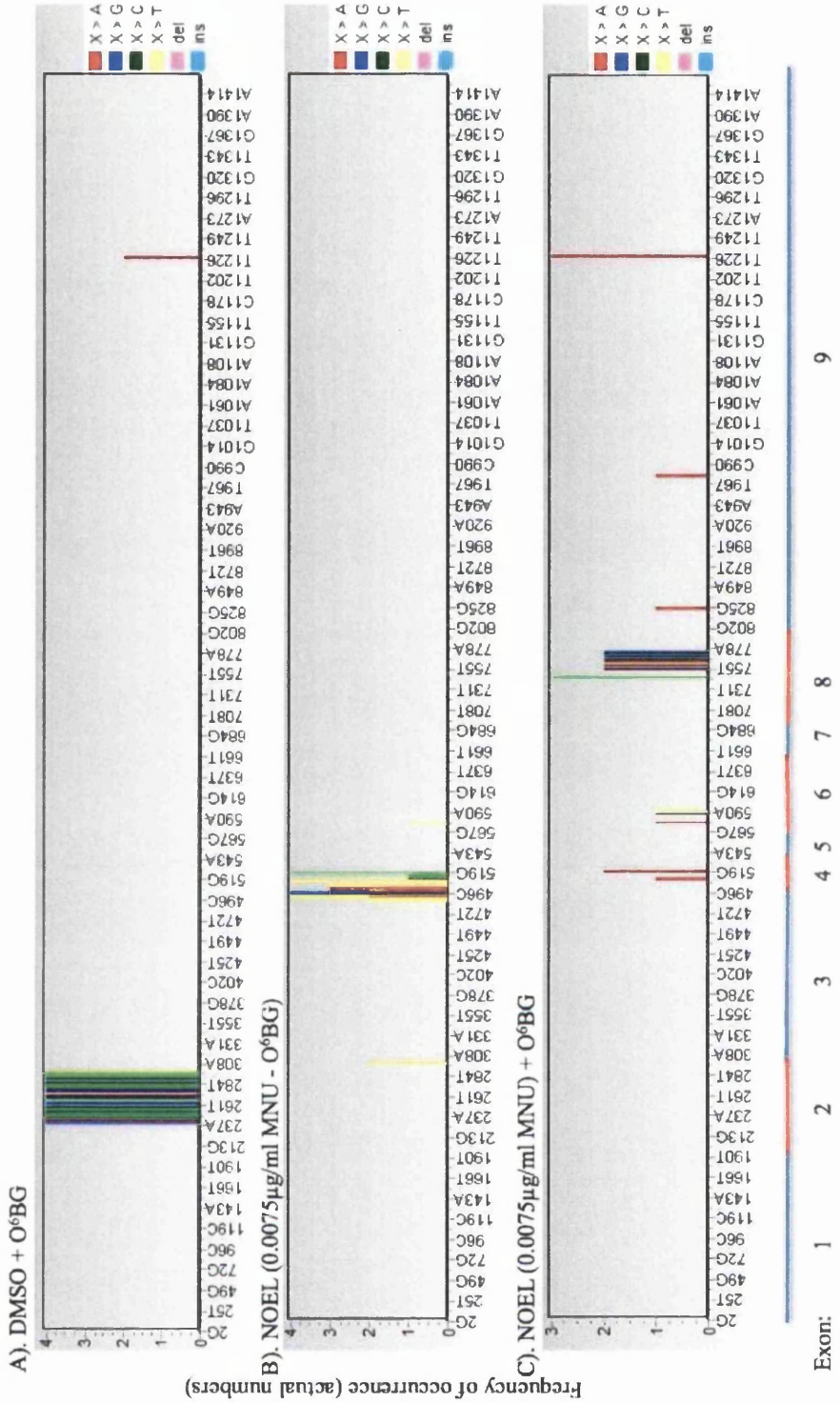

Figure 6.17. Control mutation spectra (A) and mutations induced by 0.0075µg/ml MNU without O^6BG treatment (B) and with O^6BG pre-treatment, a potent inducer of MGMT inactivation (C).

6.4. Discussion.

6.4.1. siRNA as a method for MGMT knockdown.

RNAi is a widely used technique for reducing gene function, and can be used in all aspects of research. siRNA is a crude method of RNAi whereby, addition of sequence specific dsRNA oligonucleotides to culture medium is sufficient for knockdown. However, this requires robust optimisation and validation (Cheng, Magdaleno and Vlassov, 2011). Many studies use real time PCR and western blot to confirm knockdown on mRNA and subsequent protein levels, respectively. Knockdown by siRNA is only temporary and so a gene of interest deficient cell species cannot be stably passaged which introduces variation between experiments. We describe a method of chemical transfection using Lipofectamine™RNAiMAX transfection reagent to deliver siRNA oligonucleotides into cells. This method is routinely used by colleagues in our laboratory and was found to be the most convenient method of siRNA delivery compared to electroporation, which has been used by Zair *et al* (2011) for delivery of shRNA expression vectors into cells. Chemical transfection achieved a maximum knockdown of 80% in GAPDH mRNA levels using 20pmol GAPDH ON-TARGETplus with 5µl Lipofectamine RNAiMAX. This level of knockdown is lower than manufacturers' expectations. However, 3µl of Lipofectamine and above caused increasing cytotoxicity after 24hr when examined under the microscope and the cells were not viable after 3days. This may be due to off target effects by siRNA oligonucleotides (Fedorov *et al*, 2006) or lipofectamine-induced toxicity (Zhong *et al*, 2008). A more comprehensive cytotoxicty study was not undertaken due to limited reagents. This reduction in fold change importantly demonstrated the success of siRNA delivery into the cells and so the experiment was repeated with MGMT specific siRNA oligonucleotidess (**Figure 6.9**). Real time PCR analysis of cultures treated for 24hr with concentrations exceeding 10pmol of each siRNA and 4µl Lipofectamine revealed that MGMT mRNA was not detectable. This suggests 100% knockdown, which was not reproducible across the replicates. Upon closer inspection of the raw real time data, amplified MGMT cDNA had a threshold cycle (Ct) value of approximately 34 cycles and TBP has a Ct value of approximately 19 cycles in AHH-1 cells. At the same concentration of RNA starting material, where a lack of Ct value for MGMT was observed, it was accompanied by an increase in TBP Ct, up to Ct 24. For genes with very low expression (a high Ct value) like MGMT, siRNA knockdown validation using real time PCR and western blotting is difficult, because of this, and the induced toxicity, another method of MGMT knockdown was sought.

6.4.2. O^6BG as a method of MGMT inhibition.

The use of O^6BG in MGMT inactivation is the more widely researched *in vitro* method to produce MGMT deficiency than gene disruption (Tsuzuki *et al*, 1996) or siRNA (Kato *et al*, 2010).

6.4.2.1. Assessing the toxicity of MNU with O^6BG.

Referring to the toxicity curves (**Figure 6.10**), relative population doubling (RPD) was used based on recommendations in OECD test guidelines 487 for the micronucleus assay (OECD, 2010). It is a measure of cell proliferation, calculated from cell counts obtained before and after treatment. RPD has an inverse relationship with toxicity. For example, 80% RPD indicates (100-80=) 20% toxicity. A study by our group suggests that RPD offers the most reliable estimation of acute toxicity (Johnson *et al*, 2010). A more accurate assessment can be made through apoptosis assays. For example, the caspase assays that detect the activity of caspases, a class of proteases that elicit the apoptotic response. However, this would involve cost.

6.4.2.2. Ensuring the experiment was appropriately controlled.

The solvents used for dilution of MNU and O^6BG are DMSO and methanol, respectively, in accordance with manufacturers instructions. DMSO is acknowledged as causing low toxicity and is used as a solvent for water-insoluble chemicals (Brown, Robinson and Stevenson, 1963). Methanol is a strong solvent but many studies report high level-toxicity caused by 100% methanol in humans and non-human models. The reader is referred to http://ntp.niehs.nih.gov/index.cfm?objectid=E8820866-BDB5-82F8-F588ACF109C14CE2 for a comprehensive list of methanol toxicity studies. It was necessary to determine solvent specific effects on RPD (shown in **Table 6.5**) to ascertain their contribution in the observed toxicity of the test substance. For MNU-O^6BG, DMSO was used as the solvent control causing very minor toxicity giving 97.7% and 98.7% RPD at 24hr and 48hr post-treatment. The solvent control for MNU+O^6BG treatments required 1hr pre-treatment with methanol (final concentration of 0.00024%) followed by 100µl addition of DMSO (final concentration of 0.001%). This mimicked the treatment protocol for the test substances and was the appropriate strategy. The PD was compared to that of untreated controls to determine the effects of both solvents on RPD. This being, 95.7% at 24hr and 98.2% at 48hr post treatment, which suggested that the solvent controls caused insubstantial toxicity and had no substantial

bearing on the results. Elucidation of the toxic potential of O^6BG had important implications that are discussed later. The RPD was calculated by dividing the PD of O^6BG treated cultures, with the PD of cultures treated with methanol, it's solvent control. This gave RPD values of 100% at 25hr and 102.1% at 49hr (given the additional 1hr during pre-treatment) compared to control suggesting that O^6BG is not toxic. Incidentally, methanol was used as the solvent control, which was not significantly toxic, compared to untreated controls.

6.4.2.3. Assessing the cellular presence of O^6BG through increased MNU toxicity.

The toxicity of MNU is attributed to O^6MeG because it is formed in higher levels than other toxic adducts such as N7MeG and N3MeA reviewed by Shiravstav *et al* (2010). Cells deficient in MGMT would therefore show increased toxicity to MNU due to ineffective repair of O^6MeG. This has been inferred by a decrease in the TD_{50} (**Table 6.4**). TD_{50} is defined as the dose that causes 50% toxicity observed as a 50% reduction in cell viability (50% RPD). TD_{50} is a standard measure used to compare cell sensitivities, toxic potencies of chemicals and concordance of methodologies (Johnson *et al*, 2010). TD_{50} is documented in various databases throughout genetic toxicology, e.g. the national toxicology programme (NTP) found at http://ntp.niehs.nih.gov/. The decrease in TD_{50} of MNU following pre-treatment with O^6BG suggests increased sensitive to the toxic effects of MNU. This is in concordance with other studies. For example, Wagner *et al* (2007) report the concentration of TMZ required for 50% growth inhibition of neuroblastoma tumours (IC_{50}) alone is 41μM, which is reduced to 3.4μM when used with O^6BG. Furthermore, **Table 6.5** shows that O^6BG was, by itself, non-toxic. Many reports support this (Batts *et al*, 2007; Berg *et al*, 1998). Therefore, the additional toxicity of MNU+O^6BG is not due to additive toxicity but O^6BG potentiation of MNU toxicity. The well-documented explanation is the inactivation of MGMT by O^6BG rendering the protein unable to repair O^6MeG, from alkylating agent exposure that can cause cell death. Determining the causative adduct is difficult since multiple adducts are formed. Increased sensitivity to MNU toxicity as a result of MGMT deficiency has been reported in mice (Glassner *et al*, 1999). The authors report a dramatic decrease in TD_{50} from 107mg/kg to 9mg/kg. Such a significant difference is not represented in this study. Wildtype AHH-1 have only a low natural level of MGMT and so removing what little protection they have only produces a modest difference. Konduri *et al* (2009) suggest that O^6BG by itself causes repression of MGMT expression. The authors used 207μM O^6BG for 48hr exposure, far more than featured in this study. In a *luc* reporter gene construct, under the control of MGMT promoter, the authors report a significant reduction in

luciferase activity upon treatment with O^6BG. However the authors fail to produce real time data confirming this.

6.4.3. O^6MeG toxicity.

O^6MeG requires MMR processing and two rounds of replication to exert toxic effects (Kaina *et al*, 1997; Roos and Kaina, 2008; Shrivastav, Li and Essigmann, 2010), hypothesised to be via apoptosis. There are two mechanisms for apoptosis induction:

- Futile MMR processing of O^6MeG:Thymine mispairs, from the first post treatment S phase, leading to pro-apoptotic secondary lesions such as double strand breaks in the second post-treatment S phase (Roos *et al*, 2009).
- Direct apoptotic signalling by MMR proteins upon recognition of mispairs.

Presumably, the second possibility would not require two S phases to convert O^6MeG into a cell-killing event and may explain the observed increase in toxicity at 24hr in presence of O^6BG. Given the cell cycle time of AHH-1 as 22-24hr (Crespi *et al*, 1991), one would expect AHH-1 to be in the second cell cycle by 48hr, the last time point in this experiment. In both treatment groups, the TD_{50} is comparatively lower at 48hr than at 24hr suggesting that MNU is more toxic in the second cell cycle. This is consistent with the toxic mechanism of action of O^6MeG (Kaina *et al*, 2007). However, MNU is toxic in the first cell cycle given the TD_{50} of 3μg/ml at 24hr, this is reduced to 2μg/ml following O^6BG pre-treatment. Assuming that, this decrease is the effect of increased persistence of O^6MeG, the result of MGMT inactivation by O^6BG. The contribution of O^6MeG to the toxicity observed in first cell cycle cannot be ignored. The data presented importantly demonstrates the cellular presence of O^6BG in AHH-1 cells following addition to culture media by the increased toxicity of MNU.

6.4.4. Effect of MGMT inactivation on HPRT mutant frequencies.

The HPRT assay was repeated in AHH-1 cells following pharmacological inactivation of MGMT by O^6BG. This allows direct comparison with HPRT data in Chapter 3 to test the hypothesised involvement of MGMT in protection from low dose MNU.

6.4.4.1. Comparing background mutant frequency +/-O^6BG.

MGMT inactivation can only be inferred from the experiments and without conclusive evidence of decreased activity, it is assumed that AHH-1 cells treated with O^6BG are MGMT deficient. Wildtype AHH-1 cells have a spontaneous mutant frequency (MF) of $1.4x10^{-5}$+/-

$1.78x10^{-6}$ HPRT mutants in a population as discussed in Chapter 3. MGMT deficient cells have a comparative spontaneous MF of $1.3x10^{-5}$+/-$1.05x10^{-5}$. This suggests that MGMT does not play a major role in protecting cells from background mutagenesis. This is logical since it is known that O^6BG is not mutagenic (Ueno, 2006) and O^6MeG does not form a large proportion of endogenously formed damage and so MGMT may not be "needed" in unexposed individuals but is essential in protecting against exposure to exogenous alkylating agents (Nakatsuru *et al*, 1993). However, in microbial hosts, deficiency at both MGMT loci (*ada* and *ogt*) renders the cell sensitive to increased spontaneous mutagenesis, which is correlated to a 10-fold increase in GC→AT transitions (Mackay, Han and Samson, 1994). However, in mammalian hosts, spontaneous MF at a *lacI* reporter gene was 1.5-fold lower in liver of MGMT deficient mice compared to wildtype mice (Sandercock *et al,* 2004). However, this could be the result of *lacI* integration at a locus of improved repair capacities or reduced endogenous damage. Similarly, MGMT deficiency did not have any effect on spontaneous tumour rates (Bugni, Meira and Samson, 2009). This suggests that MGMT loss is not a causal event in spontaneous carcinogenesis of unexposed individuals. Contrary, Rydberg and Lindahl (1982) showed that *S*-adenosyl methione (SAM) is a weak endogenous DNA methylator that may cause 10-30 sporadic O^6MeG molecules per cell, although this was not experimentally determined. One would expect this to contribute to the spontaneous mutation spectra in absence of MGMT. Incidentally, MGMT loss is thought to be a critical early carcinogenic event, causing "field cancerisation" of tissue in sporadic colon cancer (Shen *et al* 2005; Graham and Leedham, 2010), where alkylating agents from digestion products are in high concentration. Without an increase in spontaneous mutagenesis in MGMT deficient cells, there may be a compensatory mechanism potentially involving MMR but this has not been substantiated. Interestingly, Glassner *et al* (1999) found residual transferase activity in MGMT knockout mice. This could be the limit of detection of the activity assay, although, there may exist MGMT paralogues or an alternative repair mechanism. Given the lack of MGMT activity in AHH-1 cells (Chapter 5), this isn't the case in AHH-1 cells. Also, It can be assumed that O^6BG would inactivate all potential MGMT paralogues if they share same activity kinetics. Therefore, MGMT paralogues would not affect results observed in this study. It has been shown that MGMT deficiency may not be important in spontaneous mutagenesis but has important implications in chemical exposure (Nakatsuru *et al*, 1993). The data presented in this chapter supports this notion.

6.4.4.2. O^6BG sensitises AHH-1 cells to (below LOGEL doses) MNU mutagenesis.

The evidence provided in Chapter 5 postulates that MNU mutation induction is attributed to O^6MeG, the main mutagenic lesion formed by MNU. We hypothesise that this adduct is formed at all doses of MNU but is repaired by MGMT at doses below the NOGEL of 0.0075μg/ml MNU. At higher doses, MNU produces more O^6MeG that saturates MGMT and mutation induction accrues linearly because the protection is lost. We tested this hypothesis by creating MGMT deficient AHH-1 cells (+O^6BG) and comparing mutant frequencies to MGMT proficient AHH-1 cells (-O^6BG) over increasing concentrations of MNU over the hormetic dose range. The role of MGMT in low dose protection is evidenced by the drastic change in the shape of the dose response (**Figure 6.13**) due to an increase in sensitivity to low dose MNU when MGMT is inactivated. This is emphasised by the 10-fold decrease in the LOGEL from 0.01μg/ml in MGMT proficient AHH-1 cells to 0.001μg/ml in MGMT deficient cells. There is considerable variation in the data of **Figure 6.13A**, this may reflect differences in independent observations made between **Figure 6.13A** and **Figure 6.13B**, where increasing the number of wells scored from 600 to 10033 may reduce the error bars. Alternatively, this may be a true representation of the heterogeneity in MGMT activity between the AHH-1 populations following administration of O^6BG.

Evidence is provided to support our hypothesis of MGMT saturation at doses above the NOGEL. Such as:

1. The fold increase in sensitivity in MGMT deficient cells is greatest at doses below the NOGEL (0.0075μg/ml). O^6BG had no effect at doses above the LOGEL (0.01μg/ml) since MGMT has been potentially saturated by increased dose of MNU (**Figure 6.14**; **Table 6.9**).
2. The fraction of unrepaired lesions (**Figure 6.15**) shows that MGMT repairs more adducts at doses below the LOGEL than above. This is based on the logical assumption that cells treated with O^6BG are MGMT deficient and the only consequence is defective lesion repair. O^6MeG levels would need to be determined for substantiation of this statement.

Referring to **Table 6.9**, at 0.01μg/ml MNU and above, the MF seems to plateau giving the appearance of a supra-linear dose response. Real time expression analysis of MGMT transcripts was undertaken to investigate whether induction at the MGMT promoter was responsible for this (**Figure 6.16**). A student's paired t-test of deltaCT values (Doak *et al*,

2008) revealed that there was no statistically significant increase in fold change of MGMT mRNA (lowest p=0.07). A likely explanation of the observed supra-linearity is the increased toxicity observed as a decrease in plating efficiency (PE) (**Figure 6.11**) observed at 0.01μg/ml and above, this would remove the cells carrying the most genetic damage thereby reducing the number of mutant colonies. The lack of increase at 0.00075μg/ml MNU in O^6BG treated cells suggests that 10μM O^6BG is not sufficient to inactivate all MGMT and a residual amount remain to remove O^6MeG induced at this dose and it's the combination of higher dose of MNU and 10μM O^6BG that are required for complete inactivation. Increasing concentrations of O^6BG with 0.00075μg/ml MNU would have supported this but this was not undertaken due to the time consuming and labour intensive nature of the HPRT assay. This finding correlates to the lack of increase in N7MeG adducts at this dose compared to the solvent control, as concluded in Chapter 5. But it cannot be concluded that MNU does not react with the DNA because the mutation spectra at this dose is significantly different to the solvent control.

6.4.5. Real time MGMT analysis.

Doak *et al* (2008) found an increase in MGMT expression that peaks at the NOGEL dose of MMS (1μg/ml) 4hr after exposure. The pattern is similar here although there was no significant increase in expression. MGMT expression is highest at 24hr post-exposure with the NOGEL dose of MNU (0.0075μg/ml). MNU reacts with DNA and produces more O^6MeG via a S_N1 reaction mechanism, which has faster kinetics than S_N2 reaction mechanics of MMS. Therefore, one would expect more emphatic and rapid MGMT induction following MNU exposure. The discrepancy in time for MGMT induction is not known.

6.4.6. Spontaneous mutant spectra +/-O^6BG.

MGMT loss is associated with increased GC→AT transitions (Esteller *et al*, 2001). This is most notable upon exposure to O^6-methylating agents (Nakatsukri *et al*, 1993; Sandercock *et al*, 2008). The effects of MGMT deficiency on spontaneous mutation spectra are less well defined. An increase in spontaneous GC→AT transitions is generally observed, however the extent is possibly dependant on;

- Original MGMT levels
- Intracellular *S*-adenosylmethionine (SAM) concentration.

The study by Sandercock *et al* (2004) found a modest increase in GC→AT transitions from 49% to 56% in the liver of MGMT deficient mice. Whereas, Aquilina *et al* (1992) found a greater increase from 8.3% to 25% in MGMT deficient Chinese hamster ovary (CHO) cells. These studies were not carried out at the HPRT locus. In this study, analysis of 40 spontaneously occurring mutants in a wildtype AHH-1 population, found that GC→AT transitions constitute 28% of the mutation spectra. There is a dramatic decrease in GC→AT transitions to 1% of the spontaneous mutation spectra in MGMT deficient AHH-1 cells (**Table 6.10**). However, only eight mutants were analysed and so this may not be a true reflection. It is hypothesised that the majority of spontaneous GC→AT transitions occur through deamination of 5-methylcytosine into thymine and not through O^6MeG. Therefore, MGMT loss would not dramatically change the proportion of these spontaneous transitions. Interestingly however, the only spontaneous GC→AT transitions to occur in MGMT deficient cells, found at position 1229. This mutation was also found in the spectra treated with 0.0075μg/ml+O^6BG and also in 0.025μg/ml in Chapter 3. This evidence suggests that this mutation is only found in samples where MGMT has been inactivated. Aquilina *et al* (1992) found concordance of spectra between MGMT proficient and deficient CHO cells with the differences being the increase in GC→AT transitions and decrease in GC→TA transversions. This is in contrast to the results found in this study. We found that the spontaneous mutation spectra of MGMT deficient AHH-1 cells are drastically different to that of MGMT proficient AHH-1 cells in Chapter 3. The array of mutations at 241 to 300 all occurred in unison in 50% of the mutants analysed. Individual damage to each base is unlikely to account for this change of 49 base substitutions and more likely that they share a common mutagenic pathway and the loss of MGMT in AHH-1 cells causes dysregulation of DNA maintenance. Further mutants would need to be screened before firm conclusions can be made.

6.4.7. The effects of MGMT inactivation on MNU induced mutations.

Comparing the mutation spectra from MNU treated mutants (**Figure 6.17**) revealed that some mutations are only present following O^6BG induced MGMT inactivation. Of these, the majority are GC→AT changes caused by O^6MeG from MNU that are not repaired once MGMT has been inactivated. When reviewing the mutation spectra, caution is urged due to the differences in the number of mutants sequenced for each treatment, which may bias the spectra. The drastic increase in proportions of GC→AT transitions was accompanied by an increase in number of mutant harbouring these transitions from 50% to 71% following

MGMT inactivation. This shows that the increase was not due to a heavily mutated colony that would misrepresent the data. The observed increase in MGMT deficient cells, at the same concentration of MNU (0.0075μg/ml), supports our hypothesis of the involvement of MGMT in low dose protection. The use of 0.0075μg/ml was appropriate here since we are examining the effects of MGMT deficiency. However, this dose is not recommended for use to examine the effects of different concentration of MNU because 0.0075μg/ml was the highest dose tolerated, since this "tolerance" is an average response of the population it may be possible that individual cells may have different responses to this dose. Multivariate analysis was not performed on these data to due lack of statistical power (requiring n=40 mutants per spectra as used in Chapter 3). However, the numbers were sufficient for visual comparison of spectra. An interesting comparison was made between the spectra of 0.0075μg/ml MNU+O^6BG and 0.025μg/ml MNU (analysed in Chapter 3), both of which we hypothesise to have inactivated MGMT (**Figure 6.18**).

A).

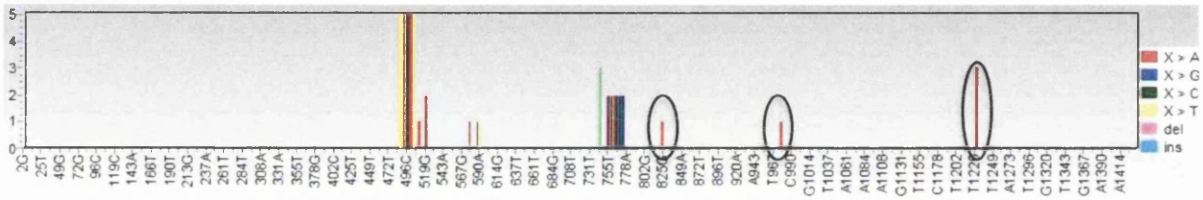

B).

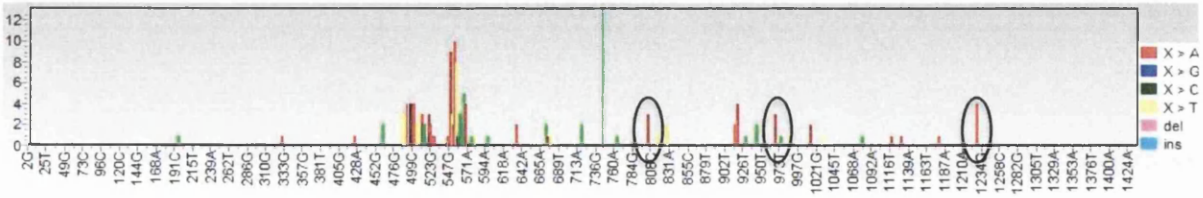

Figure 6.18. Mutation spectra for 0.0075μg/ml MNU+O^6BG (A) and 0.025μg/ml MNU (B). Similarities unique to these spectra are circled. They also share the rearrangement at 490bp. Axis given in **Figure 6.17**.

There are striking similarities between the two spectra that are absent in all other spectra. Most notable are GC→AT transitions (circled in **Figure 6.17**). These mutations are not found in any other spectra; therefore, it is reasonable to state that 0.0075μg/ml MNU in combination with MGMT inactivation resembles mutation induction seen at a higher dose of MNU, which is sufficient to cause MGMT inactivation.

6.4.8. Conclusion: Evidence for the role of MGMT.

The cellular presence of O^6BG was confirmed through toxicity studies that showed an increase in MNU induced toxicity at high doses (**Table 6.6**). Since it is well established that O^6BG has no other mechanism of action than to inhibit MGMT, we can confidently assume that the increased toxicity is due to MGMT inactivation and as a result, increased persistence of O^6MeG in DNA following MNU treatment. Therefore O^6BG treated cultures are deficient in MGMT. This causes the increased sensitivity to low dose MNU evident in **Figure 6.13**. The J-shaped curve becomes more linear with a 10-fold lower LOGEL and 50-fold lower BMD. Further evidence of the role of MGMT is also provided by the increase in proportions of and number of mutants with GC→AT transitions seen in MGMT deficient cells treated with 0.0075μg/ml MNU. We noted an increase from 28.3% to 48.1% in MGMT proficient and deficient cells, respectively. In conclusion, the experimental evidence provided in this chapter implicates MGMT in the NOGEL for MNU mutation induction that is summarised in **Figure 6.19**.

A). B).

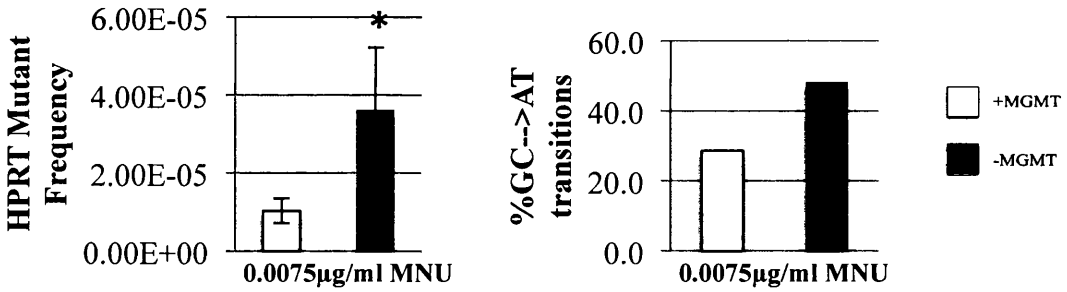

Figure 6.19. Inactivation of MGMT by O^6BG causes increases in MF (A) and GC→AT transitions (B). Error bars in A) represent standard deviation, * p=<0.05.

Following the inactivation of MGMT the 0.0075μg/ml MNU causes 3.5-fold increase in MF (**Figure 6.19A**). This is accompanied by a 68.5% increase in GC→AT transitions (**Figure 6.19B**) and a 66% increase in the number of mutants harbouring a GC→AT transition. The data presented in this chapter strongly defines the role of MGMT in creating the NOGEL for MNU induced point mutations.

Chapter 7.

General Discussion.

7.1. General Discussion.

The purpose of the project was to clarify the *in vitro* biological mechanism of point mutation induction at low doses of methyl nitrosourea (MNU). This has important implications because:

1. MNU is the most mutagenic of the four model alkylators (MNU, ethylnitrosourea (ENU), ethyl methanesulfonate (EMS) and methyl methylsulfonate (MMS). Therefore, describing low dose effects sets precedence for lesser mutagenic alkylating agents.
2. There is real impetus for defining the mechanism of mutation induction given the biological relevance of point mutations in carcinogenesis.

In addition, this study provides evidence for the applicability of *in vitro* tests for use in mechanism of action studies and dose-response modelling to provide more quantitative information than the dichotomy of genotoxic/non-genotoxic (Gollapudi *et al*, 2012). This is particularly pertinent with the 7th amendment to the EU cosmetics directive that puts emphasis on *in vitro* toxicology as a replacement for animal models in cosmetic testing (Tweats *et al*, 2007). An addendum written by Pottenger *et al* (2011) discuses 6 key events (KE) in MOA analysis and relevant endpoints for each. These including:

KE1: Internal Dose (Portine adducts) not relevant to *in vitro* studies.

KE2: Dose to critical target (DNA adducts)

KE3: Altered homeostasis (gene expression)

KE4: Genotoxic stress (increase in unrepaired adducts)

KE5: Cell replication (Mitotic index)

KE6: Mutation (Genotypic change).

With these in mind, this study is a comprehensive study into the MOA of mutation induction by MNU.

7.2. Findings of this thesis.

The following is an account of the main findings of this thesis and their implications in dose-response modelling. The conclusions from each of the results chapters are:

- MNU has a No-Observed Genotoxic Effect Level (NOGEL) for point mutation (Chapter 3) and an apparent J-shaped dose-response.
- MNU reaches and damages DNA without an increase in HPRT mutant frequency at doses <NOGEL (Chapter 4 and 5)
- GC→AT transitions caused by O^6MeG are the major mutagenic event responsible for the increase in MF at doses >NOGEL (Chapter 5)
- MGMT is responsible for repair of O^6MeG until it is saturated by increased concentrations of MNU, thereby creating the NOGEL (Chapter 6)

These will be discussed in turn.

7.2.1. NOGEL for MNU induced point mutations (Chapter 3).

A NOGEL for mutations has previously been found for two alkyl sulfonates; EMS and MMS but not for the alkyl nitrosoureas; ENU and MNU at the doses tested (Doak *et al*, 2007). MNU is known to be 20 times more mutagenic than MMS, which has been attributed to O^6-methylguanine (O^6MeG), which is the major mutagenic lesion (Doak *et al*, 2007). It was therefore hypothesised that a NOGEL for MNU would exist but at lower doses. A NOGEL has since been found for MNU using the TK assay in L1587Y mouse lymphoma cells (Pottenger *et al*, 2009) and the *in vivo* Pig-a assay (Lynch *et al*, 2011). Chapter 3 of this thesis reports a NOGEL for MNU in the same test system as Doak *et al*, (2007), this being; AHH-1 cells using the HPRT assay to quantify Mutant Frequency (MF) within a population (**Figure 3.9**). The NOGEL occurred at 0.0075μg/ml MNU, 117-fold lower than MMS. At such low doses, the adduct spectra of MNU and MMS may be different to that found in Beranek (1990) and such a drastic fold difference in NOEL may be expected.

7.2.2. Hormesis of low dose MNU on mutation induction (chapter 3).

Using curve estimations, the shape of the dose-response in chapter 3 (**Figure 3.9**) was J-shaped. There was a statistically significant and reproducible decrease in MF at 0.0025μg/ml compared to the control, potentially owing to the induction of DNA repair. This is indicative of hormesis, whereby MNU had a beneficial effect in reducing the frequency of HPRT mutants in a wildtype AHH-1 population. Such a

finding was not expected but it importantly demonstrates that current statistical analysis of Gocke and Wall (2009) and Johnson *et al* (2009), designed to identify a NOGEL, can detect a variety of dose-responses. Hormesis as a concept of low dose effects is a controversial area of genotoxicology, particularly for MNU, which is a very potent genotoxic carcinogen. Proponents state that hormesis better predicts low dose exposures to carcinogens (Calabrese and Baldwin, 2001). While on the other hand some argue that there is a lack of supportive evidence of hormesis (Calabrese and Baldwin, 2000). Gocke and Wall (2009) identified hormesis through statistical analysis of mutation induction by EMS at the *lacZ* locus *in vivo*. The same analysis has been used in this thesis (**Figure 3.11**). Additionally, a colleague has also reported the reduction in micronuclei frequency in the mononuclear micronucleus assay after acute exposure to MNU in TK6 human lymphoblast cells (Kate Chapman, personal communication). Whether the same effect at low dose MNU is observed *in vivo* has not been established. Currently, hormesis is not an accepted dose-response model used for risk characterisation of genotoxins, primarily due to lack of applicability across populations and genotoxins and firm mechanistic understanding. However, the model is gaining credence and this study may aid in the recognition of hormesis as a legitimate model for low dose exposure to MNU and similar alkylating agents. This would require substantial evidence across a broad range of studies.

7.2.3. MNU interacts with DNA at doses below the NOGEL (Chapter 4 and Chapter 5).

It was important to test for MNU induced DNA damage (adducts) at doses below the mutagenic NOGEL. This implicates DNA repair in the removal of the damage to account for the lack of increase in MF in chapter 3. Adducts are well known to have a linear dose-response, in situations where mutations have a non-linear dose-response (Swenberg *et al*, 2008). Adduct detection by mass spectrometry provides unequivocal evidence of DNA damage, which is used as a biomarker of exposure (Swenberg *et al*, 2008). Levels of N7-methylguanine (N7MeG), a relatively innocuous adduct formed in large quantities naturally and by MNU, was quantified in AHH-1 cells following exposure to MNU at doses below (0.00075μg/ml) and above (0.025μg/ml) the NOGEL (**Figure 4.6**). A lack of sensitivity and biological replicates overestimated the

levels of N7MeG in absence of MNU treatment, gave the impression of a NOGEL for adduct formation. However, given the statistically significant difference in mutation spectra between solvent control (DMSO treated) and following MNU treated (0.00075μg/ml) (**Figure 5.17**) suggests that MNU had an effect on the DNA sequence at doses below the NOGEL.

7.2.4. MNU induced O^6MeG causes GC→AT transitions that are increased above the NOGEL (Chapter 5).

Referring to chapter 5, mutation spectra analysis of HPRT mutants resulting from spontaneous (inferred through the solvent control), 0.0075μg/ml and 0.025μg/ml MNU treatments reveal significant differences in mutation induction. There was an increase in proportions of GC→AT transitions from 12.5% to 43.9% as the NOGEL was surpassed (**Table 5.3**). The dose-dependency of GC→AT changes was further emphasised using multivariate principle component analysis (PCA). 67% of the differences between treated spectra were GC→AT changes (**Figure 5.18**). GC→AT transitions are caused by replication over O^6MeG, formed following MNU exposure. O^6MeG is stoichiometrically repaired by MGMT. At low doses of MNU, there are sufficient MGMT molecules per cell for successful repair, creating the NOGEL for mutation induction at 0.0075μg/ml MNU. At increasing concentrations of MNU, demand for repair exceeds the number of MGMT molecules per cell, O^6MeG remains in the DNA and causes GC→AT transitions. The data obtained in chapters 4 and 5 shows that 0.025μg/ml induces 9.1 exogenous N7MeG adducts/10^8 nucleotides over background levels. We can infer the number of O^6MeG adducts, which constitutes 8% of adducts according to the spectra of MNU. This is based on data from Beranek, (1990) obtained at high doses MNU exposure and so this assumed to hold true at low doses. If, 69% of adducts induced were N7MeG (9.1 adducts/10^8 nucleotides), 8% equates to 1.1adducts/10^8 nucleotides (to 1 d.p). We hypothesise that 1.1 O^6MeG adducts/10^8 nucleotides are sufficient to cause MGMT inactivation in AHH-1 cells and contribute to a 15.8% increase in GC→AT mutations observed at 0.025μg/ml over the background level.

7.2.5. MGMT protects DNA from GC→AT changes below the NOGEL (Chapter 6).

Evidence is provided in chapter 6 that implicates MGMT in the protection of DNA at doses below the NOGEL. In the absence of MGMT, following inactivation with O^6BG, MNU is more mutagenic.

This is observed as:

1. A 10-fold decrease in the Lowest Observed Genotoxic Effect Level (LOGEL) (0.01μg/ml compared to 0.001μg/ml without priori inactivation) and a reduction in benchmark dose (BMD) (**Table 6.8**).
2. A 3-fold increase in MF at 0.0075μg/ml MNU in MGMT inactivated cells (**Figure 6.19A**)
3. An increase in GC→AT transitions 28.6% to 48.1% at 0.0075μg/ml MNU (**Table 6.10**)
4. An increase in the number of mutants with GC→AT transitions at 0.0075μg/ml from 50% (3/6) to 83% (10/12) (**Figure 6.19B**).

O^6BG did not potentiate mutagenicity of doses higher than the NOGEL (0.0075μg/ml). This can be explained by inactivation of MGMT by increasing concentrations of O^6MeG at higher doses of MNU, which is a well-documented phenomenon (Daniels *et al*, 2000) thus rendering O^6BG ineffective once MGMT has been inactivated by high dose MNU. We have found that MGMT is present at comparatively low levels in AHH-1 cells and its level does not increase in response to MNU treatment (**Figure 5.26** and **Figure 5.19**). This is in agreement with the majority of published data (Fritz *et al*, 1991). Therefore, AHH-1 cells have a basal number of MGMT molecules that decrease upon repair of O^6MeG. Replenishment is dependant upon a low level of constitutive expression and has been shown to require one cell cycle in Raji cells (Sklar *et al*, 1981). As a result, the levels of MGMT can become limited at higher concentrations of O^6MeG at higher doses of MNU. Thus accounting for the increase in MF and increase in GC→AT transitions observed. These main conclusions are summarised in **Figure 7.1**. We can reason that the level of MGMT in AHH-1 cells, although low, is sufficient to protect against a 10-fold increase in MNU concentration (from 0.00075μg/ml to the NOGEL of 0.0075μg/ml). It must be said that other DNA repair proteins could contribute to cellular tolerance to

O^6MeG particularly MMR proteins, which have an emerging role in O^6MeG repair (Kaina, 2007).

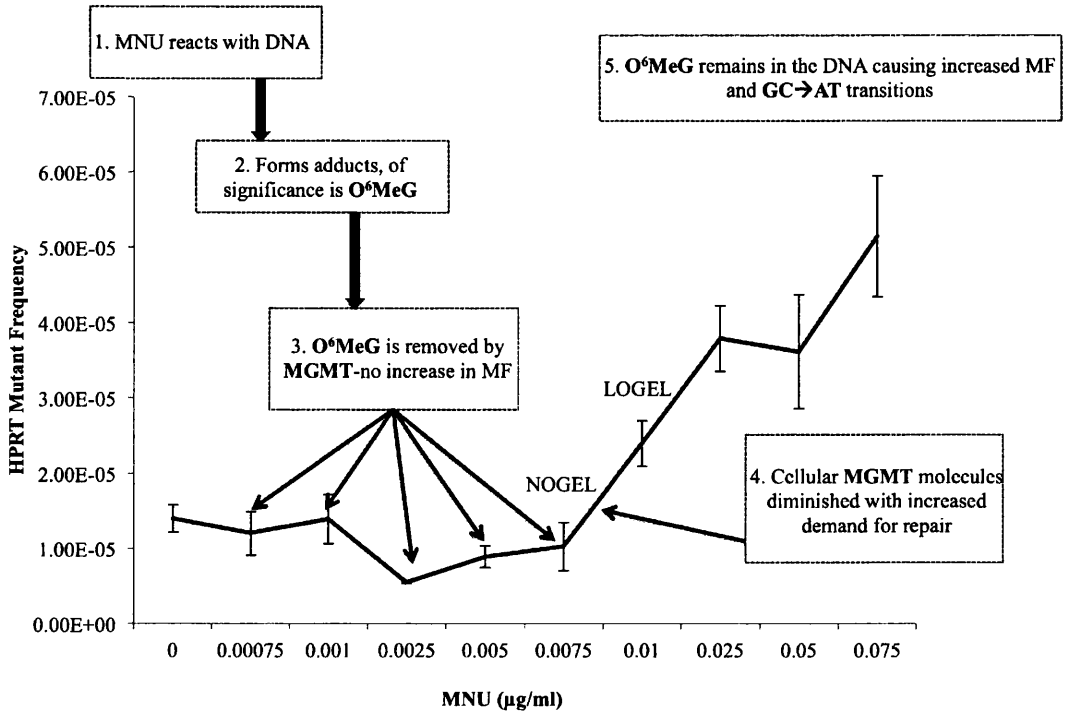

Figure 7.1. Representation of the conclusions of this thesis.

7.3. Linear dose-response model challenged; implications in hazard identification.

Dose-response modelling is an integral part of hazard identification and characterisation and plays critically in determining safe exposure margins (NRC, 1983). Establishing a safe-level of exposure requires extrapolations from high dose, necessary to elicit a statistically significant increase in genotoxicity over the control, to low doses that are relevant for human exposure levels. Various mathematical models exist for extrapolation to low dose. The method employed depends upon the mode of carcinogenic action and potency of chemical. There is an accepted distinction between non-genotoxic carcinogens (e.g. hormones) (and indirect genotoxins (e.g. aneugens)) and genotoxic carcinogens (Bolt *et al*, 2004). Due to the redundancy in the number of targets, non-genotoxins and indirect genotoxins have been shown to have threshold dose-responses, where extrapolations are based upon NOGELs. Genotoxic carcinogens (e.g. MNU), however, are thought to abide by the single hit, single target

hypothesis, where every dose has potential to cause an adverse effect. This is governed by the linear (no threshold) model. As such, safe exposure margins for, genotoxic impurities, are determined using the As Low As Reasonably Practicable (ALARP) principle (**Figure 7.2**).

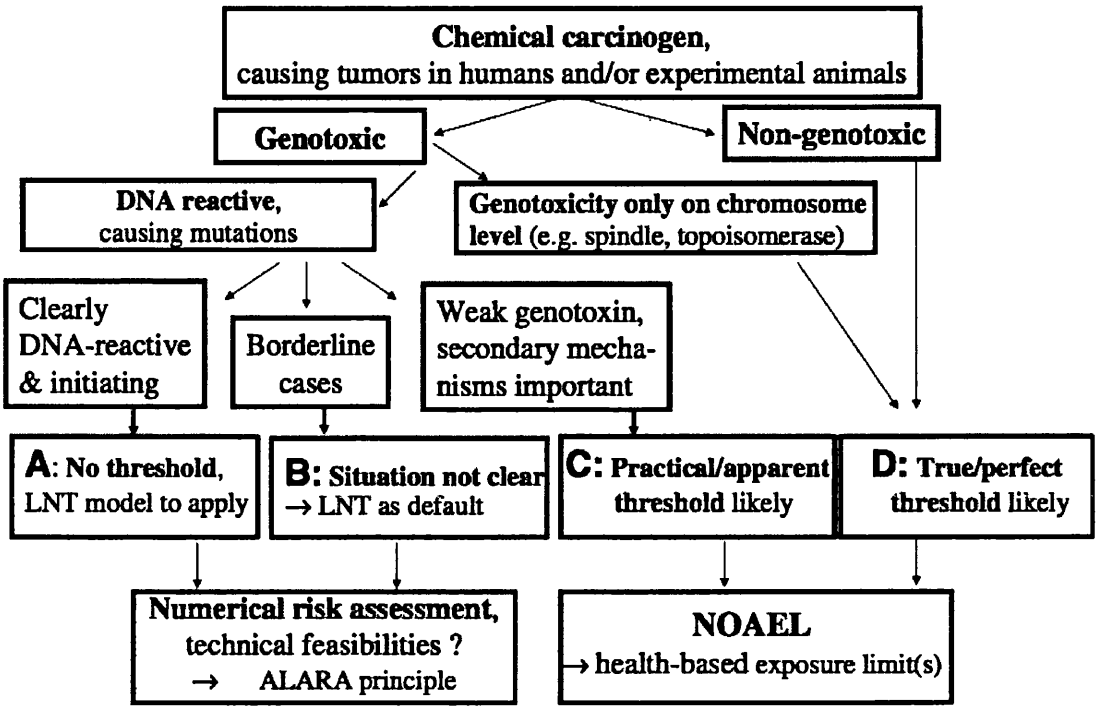

Figure 7.2. Current thinking in genotoxicology distinguishes carcinogens based on their MOA (non-genotoxic/genotoxic potential) as to the mathematical model for extrapolations to low dose. LNT=linear no threshold, ALARA=As Low As Reasonably Achievable, NOAEL=no observed adverse (genotoxic) effect level.

Evidence from Koana *et al* (2004) found a threshold for X-ray induced point mutation. Radiation was used as the model genotoxin, which defined the linear model. Together with work published from our laboratory (Doak *et al*, 2007), there has been a paradigm shift in the accepted dose-response relationship for genotoxins (particularly with increasing evidence using the four alkylators, as previously discussed). Thus having substantial implications in setting safe exposure levels for genotoxins with proven thresholds (Jenkins *et al*, 2005) (evident in **Figure 7.2**). Currently, this is assessed on a case-by-case basis, however, with the work presented in this thesis, it is plausible that hazards are assessed based on the adducts induced (Jenkins *et al*, 2005) and mechanism of action. Dose-response modelling has implications in assessment of genotoxic impurities (**Figure 7.3**). Genotoxic impurities

exist throughout drug research and development e.g. EMS in Viracept® (Muller and Singer, 2009), food manufacturing e.g. N-nitroso compounds (MNU) in heat processed foods (Tricker and Preussmann, 1991) and in the environment from agricultural and industrial sources.

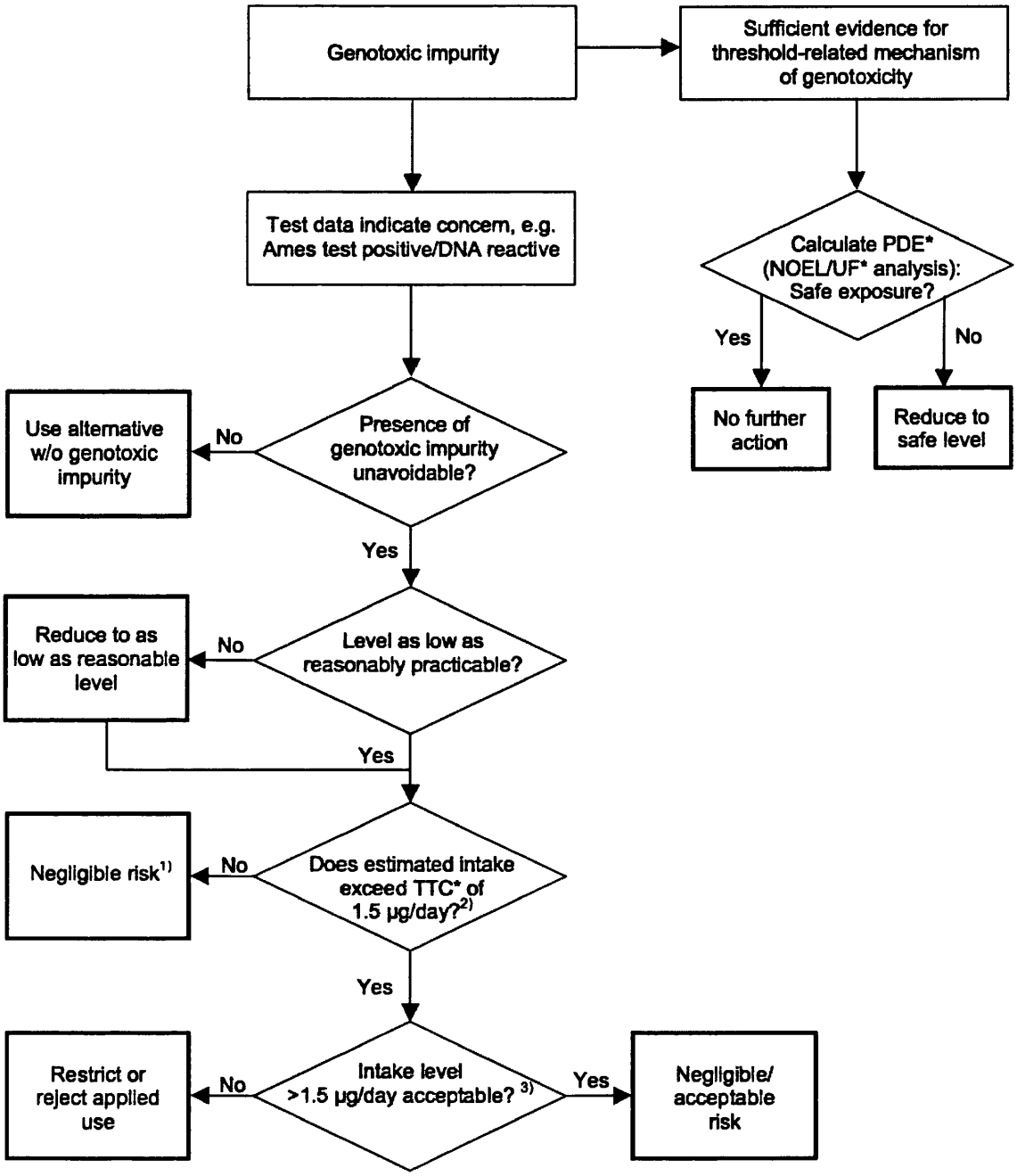

Figure 7.3. Schematic of a decision tree to evaluate the most appropriate method to deal with low levels of genotoxic impurity once ALARP has been applied. Abbreviations: PDE=Permitted Daily Exposure, UF=Uncertainty Factors, TTC=Threshold of Toxicological Concern. Taken from EMEA (2006).

As can be seen from **Figure 7.3**, impurities with established NOGELs are permitted at given concentrations. However, contaminants with insufficient evidence of a NOGEL are assumed to have a linear dose-response and may prevent the product from entering the market. While this is logical if it was perceived to cause harm, if the assumption of linearity was disproved, this may be unnecessary.

7.4. Concluding remarks.

To overcome the default linear assumption for genotoxins, there must be "convincing evidence to support a proposed thresholded mechanism of action" (Henderson, 2000). The data presented provide strong *in vitro* mechanistic evidence in support of a non-linear dose-response for mutation induction by MNU, which is dependent upon repair of DNA adducts. While sufficient evidence is not provided to challenge the hypothesis of "one molecule causes one adduct" we do challenge the latter part of the theory that states "one adduct causes one mutation." The evidence provided in this thesis will contribute to weight of evidence (WOE) (Kirkland, 2005) to help determine low dose effects of MNU. This has been performed with EMS using data generated from our research group (Doak *et al*, 2007:Zair *et al*, 2011) that has been used in conjunction with *in vivo* work (Muller and Singer, 2009:Muller *et al*, 2009) to draw firm conclusions on low dose EMS genotoxicity.

This thesis has clarified a robust mechanism of action for MNU induced point mutations that can support a non-linear dose-response.

7.5. Future Work.

For further understanding of mutation induction by MNU, the mechanism responsible for the reduction in MF at 0.0025μg/ml MNU needs to be elucidated. We hypothesise the upregulation of DNA repair enzymes involved in repair of endogenous damage. In addition, there is a lack of understanding of MGMT protein turnover and regulation. This has important implications in chemotherapy. The difficulty in administering alkylating agents and observing mutagenic effects is that a number of adducts are

induced. The relative MOA of each adduct and relative repair mechanims e.g. N7MeG and MPG. The findings of this thesis would be strengthened if:

1. The same conclusions were found by studies using prolific expressers of MGMT where validation of knockdown would be easily achievable.
2. Transfection of a MGMT expression vector (e.g. TET-on inducible system) into AHH-1 cells proffered increased tolerance to MNU and shifted the NOGEL to the right on the x-axis.

List of appendices

3050 Spruce Street, Saint Louis, MO 63103, USA
Website: www.sigmaaldrich.com
Email USA: techserv@sial.com
Outside USA: eurtechserv@sial.com

Product Specification

uct Name:
troso-N-methylurea - ISOPAC®

uct Number:	**N1517**
S Number:	684-93-5
	MFCD00014794
ula:	C2H5N3O2
ula Weight:	103.08 g/mol
age Temperature:	2 - 8 °C

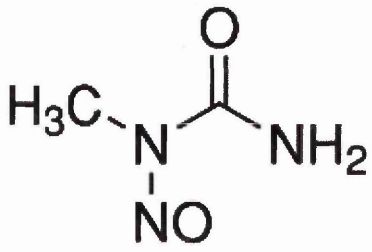

ST	Specification
arance (Color)	Off-White to Light Yellow
arance (Form)	Pass
Vet Solid or Suspension	
on NMR spectra	Conforms to Structure
on NMR	≥ 13 %
Solvent content: % Water and acetic acid combined	

ification: PRD.0.ZQ5.10000018171

Appendix 2:Raw HPRT data (Chapter 3).

Replicate A	6-TG (selective conditions)		-6-TG (non-selective conditions)					
Dose MNU (µg/ml)	Number of wells without colonies	Total number of wells scored	Number of wells without colonies	Total number of wells scored	Dilution Factor	Mutant Frequency (MF)	Average of replicates	Standard deviation
0	3009	3360	22	1824	0.0005	1.25E-05	1.40E-05	3.22E-06
DMSO	3052	3360	34	1920	0.0005	1.19E-05	1.40E-05	1.82E-06
0.00075	2946	3360	2	1920	0.0005	9.57E-06	1.21E-05	2.90E-06
0.001	2943	3360	3	1920	0.0005	1.03E-05	1.39E-05	3.33E-06
0.0025	3152	3360	7	1920	0.0005	5.69E-06	5.53E-06	2.20E-07
0.005	3038	3360	17	1920	0.0005	1.07E-05	8.93E-06	1.50E-06
0.0075	3000	3360	2	1920	0.0005	8.25E-06	1.05E-05	2.99E-06
0.01	2570	3360	9	1920	0.0005	2.50E-05	2.40E-05	2.98E-06
0.025	2243	3360	17	1920	0.0005	4.27E-05	3.79E-05	4.28E-06
0.05	2013	3360	6	1920	0.0005	4.44E-05	3.60E-05	7.30E-06
0.075	2522	3360	181	1920	0.0005	6.07E-05	5.15E-05	8.00E-06

Replicate B	6-TG (selective conditions)		-6-TG (non-selective conditions)			
Dose MNU (µg/ml)	Number of wells without colonies	Total number of wells scored	Number of wells without colonies	Total number of wells scored	Dilution Factor	Mutant Frequency (MF)
0	2999	3360	16	1920	0.0005	1.19E-05
DMSO	2890	3360	12	1920	0.0005	1.48E-05
0.00075	2987	3360	11	1920	0.0005	1.14E-05
0.001	2782	3360	7	1916	0.0005	1.68E-05
0.0025	3174	3360	12	1920	0.0005	5.61E-06
0.005	3116	3360	17	1920	0.0005	7.97E-06
0.0075	3004	3360	34	1916	0.0005	1.39E-05
0.01	2612	3360	16	1919	0.0005	2.63E-05
0.025	2603	3360	57	1920	0.0005	3.63E-05
0.05	2788	3360	98	1920	0.0005	3.14E-05
0.075	2571	3360	112	1920	0.0005	4.71E-05

Replicate C	6-TG (selective conditions)		-6-TG (non-selective conditions)			
Dose MNU (µg/ml)	Number of wells without colonies	Total number of wells scored	Number of wells without colonies	Total number of wells scored	Dilution Factor	Mutant Frequency (MF)
0	2995	3360	75	1920	0.0005	1.77E-05
DMSO	2936	3360	23	1920	0.0005	1.52E-05
0.00075	2885	3360	13	1920	0.0005	1.53E-05
0.001	2943	3360	20	1920	0.0005	1.45E-05
0.0025	3220	3360	34	1920	0.0005	5.28E-06
0.005	3132	3360	26	1920	0.0005	8.17E-06
0.0075	3033	3360	8	1920	0.0005	9.34E-06
0.01	2800	3360	23	1920	0.0005	2.06E-05
0.025	2722	3360	92	1920	0.0005	3.47E-05
0.05	2836	3360	138	1920	0.0005	3.22E-05
0.075	2550	3360	100	1920	0.0005	4.67E-05

Appendix 3:Raw HPRT plating efficiency data (Chapter 3).

	Rep A		Rep B		Rep C				
Dose MNU (µg/ml)	PE	RPE (%)	PE	RPE (%)	PE	RPE (%)	Average cell viability	Standard deviation	TTEST
0	441.77	109.52	478.75	94.33	324.26	73.29	92.38	18.20	0.438
Solvent control	403.37	100.00	507.52	100.00	442.46	100.00	101.96	11.89	-
0.00075	686.69	170.24	516.22	101.71	499.51	112.89	128.28	36.76	0.742
0.001	646.15	160.19	561.21	110.58	456.43	103.16	124.64	31.01	0.387
0.0025	561.42	139.18	507.52	100.00	403.37	91.17	110.12	25.56	0.013
0.005	472.69	117.18	472.69	93.14	430.20	97.23	102.52	12.87	0.073
0.0075	686.69	170.24	403.16	79.44	548.06	123.87	124.51	45.40	0.343
0.01	536.29	132.95	478.70	94.32	442.46	100.00	109.09	20.86	0.025
0.025	472.69	117.18	351.70	69.30	303.83	68.67	85.05	27.83	0.045
0.05	576.83	143.00	297.51	58.62	263.28	59.50	87.04	48.46	0.202
0.075	236.16	58.55	284.16	55.99	295.49	66.78	60.44	5.64	0.001

Appendix 4:Instructions for dose-response modeling (Chapter 3 and Chapter 6).

The following are detailed instructions detailing the statistical analyisis for does-response modelling perfomed on data from the HPRT assay.

Step 1. Test for differences in controls using one way ANOVA in SPSS.

1. Arrange data so that control treatments are in VAR00001 and MF in VAR00002

	VAR00001	VAR00002
Untreated	.00	.00
	.00	.00
	.00	.00
Solvent control	1.00	.00
	1.00	.00
	1.00	.00

2. Click Analyze,
3. Compare means,
4. One-Way ANOVA
5. VAR00001 in dependent list and VAR00002 in factor
6. Click OK
7. Output table opens in new window

ANOVA

VAR00002

	Sum of Squares	df	Mean Square	F	Sig.
Between Groups	.000	1	.000	.004	.952
Within Groups	.000	4	.000		
Total	.000	5			

8. Sig. value >0.05 means control MF's are not statistically significant.
9. All the control treatments can be labeled as 0 and can be used in further analysis.

Step 2. Quadratic vs Linear fit over the entire dose-response.

1. Paste all doses in VAR00001and corresponding MF's in VAR00002
2. Click Analyze
3. Regression
4. Curve estimation
5. VAR00001 in variable and VAR00002 in dependent
6. Tick Linear, Quadratic and display ANOVA table
7. OK
8. Compare R values in Linear and Quadratic model summary, The model with greatest R value gives rough estimation that it is a better fit than the other.

Linear

Model Summary

R	R Square	Adjusted R Square	Std. Error of the Estimate
.882	.779	.772	.000

The independent variable is VAR00001.

Quadratic

Model Summary

R	R Square	Adjusted R Square	Std. Error of the Estimate
.884	.781	.766	.000

The independent variable is VAR00001.

9. For further confidence, Copy and paste into excel; ANOVA table for Linear and ANOVA table for Quadratic
10. Paste required values into table as shown by colours;

ANOVA

	Sum of Squares	df	Mean Square	F	Sig.
Regression	.000	1	.000	109.059	.000
Residual	.000	31	.000		
Total	.000	32			

The independent variable is VAR00001.

ANOVA

	Sum of Squares	df	Mean Square	F	Sig.
Regression	.000	2	.000	53.489	.000
Residual	.000	30	.000		
Total	.000	32			

The independent variable is VAR00001.

A	B	C	D	E	F	G
		Sum of Squares	df	Mean Square	F	Sig.
Quadratic	Regression	.000	2	.000	53.489	.000
Linear	Regression	.000	1	.000	109.059	.000
R2 change		0.000000000016944398	1	1.69444E-11	0.31790188	**0.0177062233**
	Residual	.000	30	.000		

Where;

C4=C2 minus C3

D4=D2 minus D3

E4=C4 divided by D4

F4=E4 divided by E5

G4=Fdist(F4,D4,D5)

If G4=<0.05 then null hypothesis of linearity is rejected and Quadratic is the best fit.

Step 3. If Quadratic, identify NOEL/LOEL by Dunnet's in SPSS.

1. Set up data as for step 2 in SPSS
2. Click transform
3. Click compute variable
4. Type "Log" into Target variable
5. "Function group": click Arithmetic
6. "Functions and Special variables": double click Lg10
7. Move VAR0002 to replace "?" in LG10(?) giving LG10(VAR00002) in "Numeric expression.
8. Log appears in column next to VAR00002
9. Repeat but type Log05 into target variable and type "+05" this appears in column next to log
10. Click analyze
11. Compare means
12. One-way Anova
13. VAR00001 in Factor, VAR00002, Log and Log05 in Depedent list
14. Click Post Hoc…
15. Tick Dunnett
16. Control category:first
17. Test click >control
18. Continue
19. OK
20. Output table opens in new window
21. Identify LOEL as lowest dose with Sig. <0.05 and NOEL as the dose below that. Ensure they are the same for VAR00002, Lohg and Log05 (test of normality) if they do not correspond the data is not normally distributed and the assumed Poisson distribution is incorrect.

Step 4. Test linear vs quadratic best of fit below NOEL.

1. Repeat step 2 but only include NOEL and below doses for testing.

Calculating the gradients 95% confidence limits.

1. In coefficients table, under quadratic from SPSS output;

A B C D E F

Coefficients

		Unstandardized Coefficients		Standardized Coefficients		
		B	Std. Error	Beta	t	Sig.
1	VAR00001	-.001	.000	-.503	-2.535	.020
2	(Constant)	.000	.000		12.153	.000

2. Gradient of the slope is given in 1B.
3. 95% confidence limits = 1C x 1.96
4. lower limit = 1B-95% Cl
5. Upper limit = 1B+95% Cl.

Appendix 5:Raw N7MeG adduct levels.

Dose MNU (µg/ml)	Amount DNA yield used (µg)	Amount adduct detected (fmol)	Number of adducts/10^8 nucleotides	Amount DNA yield used (µg)	Amount adduct detected (fmol)	Number of adducts/10^8 nucleotides
DMSO	53.42	27.08	15.65	52.32	35.32	20.83
0.00075	53.03	38.37	22.33	60.84	26.80	13.60
0.025	46.13	47.12	31.52	49.31	37.07	23.20

Appendix 6:Raw sequence data (Chapter 5).

Due to the large number of pages required, the raw mutation spectra, data and instructions for analysis, are available at www.dropbox.com.
Using the login details:
Email:hprtseq@hotmail.co.uk,
Password:HPRTSeq.

Appendix 7: Coding for Principle component analysis (Chapter 5).

1. Save data as "name".txt file in the following format;

Nucleotide sequence	Sum of substitutions at each nucleotide spectrum 1 (0μg/ml)	Sum of substitutions at each nucleotide spectrum 2(0.00075μg/ml)	Sum of substitutions at each nucleotide spectrum 3 (0.025μg/ml)

2. In R,File→change directory→choose file where data is saved.
3. Type:

```
dat<-read.table('data.txt', header=T, row.names=1)
pca<-prcomp(t(dat))
summary(pca)
```

This brings up the following output and allows user to identify the number of components and their importance in explaining the data:

Importance of components:

		PC1	PC2	PC3
Standard deviation	40.8948	13.9386	1.325e-13	
Proportion of Variance	0.8959	0.1041	0.000e+00	
Cumulative Proportion	0.8959	1.0000	1.000e+00	

For construction of Scatter plots:

4. Type:

```
plot(pca$rotation[,1], pca$rotation[,2],col='white')
text(pca$rotation[,1], pca$rotation[,2], row.names(dat), cex=0.7)
```

Appendix 8:Raw real time data (Chapter 5).

1 hour post MNU treatment.

Rep A							
Dose (µg/ml)	**Mean MGMT Ct**	**Mean TBP Ct**	**ΔCt**	**ΔΔCt**	**Fold change**	**Average**	**Standard deviation**
DMSO	33.37	22.07	11.30	0.00	1.00	1.14	0.28
0.00000	33.57	21.89	11.68	-0.37	1.30	1.44	0.49
0.00075	33.84	22.77	11.07	-0.24	1.18	1.05	0.27
0.00750	33.99	22.64	11.35	0.05	0.97	0.66	0.42
0.01000	33.94	22.15	11.80	0.49	0.71	0.81	0.26
0.05000	33.84	22.23	11.61	0.31	0.81	1.31	0.46

Rep B					
Dose (µg/ml)	**Mean MGMT Ct**	**Mean TBP Ct**	**ΔCt**	**ΔΔCt**	**Fold change**
DMSO	34.11	22.26	11.85	-0.55	1.46
0	34.33	21.49	12.85	-0.99	1.99
0.00075	34.02	21.74	12.29	0.43	0.74
0.0075	36.09	21.79	14.30	2.45	0.18
0.01	34.44	21.87	12.57	0.72	0.61
0.05	32.97	21.89	11.08	-0.77	1.71

Rep C					
Dose (µg/ml)	**Mean MGMT Ct**	**Mean TBP Ct**	**ΔCt**	**ΔΔCt**	**Fold change**
DMSO	33.49	22.24	11.24	0.06	0.96
0	33.31	22.02	11.29	-0.05	1.03
0.00075	33.29	22.35	10.94	-0.30	1.23
0.0075	33.75	22.22	11.53	0.28	0.82
0.01	33.21	22.11	11.09	-0.15	1.11
0.05	32.95	22.21	10.74	-0.50	1.42

4hr post MNU treatment.

Rep A							
Dose (µg/ml)	**Mean MGMT Ct**	**Mean TBP Ct**	**ΔCt**	**ΔΔCt**	**Fold change**	**Average**	**Standard deviation**
DMSO	36.34	19.09	17.25	2.12	0.23	2.45	1.96
0	34.67	19.54	15.13	-2.12	4.35	2.19	1.87
0.00075	37.91	19.64	18.27	1.02	0.49	1.05	1.04
0.0075	34.69	19.30	15.39	-1.86	3.64	2.85	0.85
0.01	33.86	19.30	14.57	-2.69	6.44	3.50	2.72
0.05	33.18	18.13	15.06	-2.20	4.58	3.31	1.14

Rep B					
Dose (µg/ml)	**Mean MGMT Ct**	**Mean TBP Ct**	**ΔCt**	**ΔΔCt**	**Fold change**
DMSO	35.25	19.67	15.58	-1.67	3.19
0	34.67	19.15	15.52	-0.06	1.04
0.00075	35.86	19.01	16.86	1.28	0.41
0.0075	33.51	18.89	14.62	-0.96	1.95
0.01	32.96	18.96	14.00	-1.58	3.00
0.05	33.46	19.12	14.33	-1.25	2.37

Rep C					
Dose (µg/ml)	Mean MGMT Ct	Mean TBP Ct	ΔCt	ΔΔCt	Fold change
DMSO	34.42	19.14	15.28	-1.97	3.93
0	34.18	19.14	15.04	-0.24	1.18
0.00075	33.25	19.14	14.11	-1.17	2.25
0.0075	32.85	19.14	13.71	-1.57	2.97
0.01	34.32	19.14	15.18	-0.10	1.07
0.05	32.85	19.14	13.71	-1.57	2.97

6 hour post MNU treatment.

Rep A							
Dose (µg/ml)	Mean MGMT Ct	Mean TBP Ct	ΔCt	ΔΔCt	Fold change	Average	Standard deviation
DMSO	33.37	20.90	12.47	0.00	1.00	1.11	0.40
0	36.17	21.03	15.14	2.67	0.16	0.62	0.40
0.00075	34.50	21.76	12.74	0.28	0.83	1.07	0.53
0.0075	34.12	21.50	12.62	0.16	0.90	0.87	0.11
0.01	34.19	21.13	13.06	0.59	0.66	1.09	0.37
0.05	33.52	21.45	12.08	-0.39	1.31	1.36	0.10

Rep B					
Dose (µg/ml)	Mean MGMT Ct	Mean TBP Ct	ΔCt	ΔΔCt	Fold change
DMSO	34.42	21.57	12.85	0.38	0.77
0	34.67	21.52	13.15	0.30	0.81
0.00075	33.05	20.95	12.10	-0.75	1.68
0.0075	34.31	21.06	13.25	0.40	0.76
0.01	33.61	21.08	12.53	-0.32	1.24
0.05	33.76	21.47	12.29	-0.56	1.48

Rep C					
Dose (µg/ml)	Mean MGMT Ct	Mean TBP Ct	ΔCt	ΔΔCt	Fold change
DMSO	33.76	21.93	11.83	-0.63	1.55
0	33.83	21.82	12.02	0.19	0.88
0.00075	34.14	21.79	12.35	0.51	0.70
0.0075	34.05	22.17	11.87	0.04	0.97
0.01	33.62	22.22	11.40	-0.43	1.35
0.05	33.33	21.88	11.45	-0.38	1.30

24hour post MNU treatment

Rep A							
Dose (µg/ml)	Mean MGMT Ct	Mean TBP Ct	ΔCt	ΔΔCt	Fold change	Average	Standard deviation
DMSO	34.52	21.65	12.88	-0.22	1.17	1.18	0.12
0	34.06	20.96	13.10	0.22	0.86	0.69	0.16
0.00075	35.07	22.28	12.79	-0.08	1.06	1.58	0.46
0.0075	34.03	21.77	12.26	-0.61	1.53	1.11	0.37
0.01	34.08	21.21	12.87	-0.01	1.01	0.92	0.13
0.05	33.53	21.65	11.88	-0.99	1.99	1.61	0.57

Rep B

Dose (µg/ml)	Mean MGMT Ct	Mean TBP Ct	ΔCt	ΔΔCt	Fold change
DMSO	34.60	21.82	12.78	-0.09	1.07
0	34.80	21.11	13.68	0.90	0.54
0.00075	33.74	21.76	11.99	-0.79	1.73
0.0075	34.21	21.42	12.79	0.01	1.00
0.01	34.38	21.58	12.81	0.02	0.98
0.05	33.53	21.65	11.88	-0.90	1.87

Rep C

Dose (µg/ml)	Mean MGMT Ct	Mean TBP Ct	ΔCt	ΔΔCt	Fold change
DMSO	33.72	21.22	12.50	-0.38	1.30
0	34.24	21.20	13.04	0.54	0.69
0.00075	33.52	21.97	11.55	-0.95	1.94
0.0075	34.31	21.51	12.80	0.30	0.81
0.01	34.08	21.21	12.87	0.37	0.77
0.05	34.00	21.43	12.56	0.06	0.96

Appendix 9: Real time PCR statistics (Chapter 5).

Statistics on Delta Ct values.

Calculated using the formula;

=TTEST(DMSOrepA:C,TREATMENTrepA:C,2,2)

1 hr	ΔCt Rep A	ΔCt Rep B	ΔCt Rep C	TTEST
DMSO	11.30	11.24	11.85	
0	11.68	11.29	12.85	0.40
0.00075	11.07	10.94	12.29	0.94
0.0075	11.35	11.53	14.30	0.40
0.01	11.80	11.09	12.57	0.49
0.05	11.61	10.74	11.08	0.37
4hr	**ΔCt Rep A**	**ΔCt Rep B**	**ΔCt Rep C**	**TTEST**
DMSO	17.25	15.58	15.28	
0	15.13	15.52	15.04	0.27
0.00075	18.27	16.86	14.11	0.80
0.0075	15.39	14.62	13.71	0.13
0.01	16.57	14.00	15.18	0.46
0.05	15.06	14.33	13.71	0.08
6hr	**ΔCt Rep A**	**ΔCt Rep B**	**ΔCt Rep C**	**TTEST**
DMSO	12.47	12.85	11.83	
0	15.14	13.15	12.02	0.33
0.00075	12.74	12.10	12.35	0.97
0.0075	12.62	13.25	11.87	0.71
0.01	13.06	12.53	11.40	0.93
0.05	12.08	12.29	11.45	0.32
24hr	**ΔCt Rep A**	**ΔCt Rep B**	**ΔCt Rep C**	**TTEST**
DMSO	12.88	12.78	12.50	
0	13.10	13.68	13.04	0.08
0.00075	12.79	11.99	11.55	0.19
0.0075	12.26	12.79	12.80	0.65
0.01	12.87	12.81	12.87	0.33
0.05	11.88	11.88	12.56	0.07

Appendix 10:Raw data for real time validation of siRNA.

Rep A							
Treatment	**Ct GAPDH**	**Ct TBP**	**ΔCt**	**ΔΔCt**	**Fold change**	**Average fold change**	**Standard deviation**
Untreated control	21.62	21.12	0.50	0.00	1.00	1.02	0.03
0.6pmol of siRNA 0.5µl Lipofectamine	22.15	21.00	1.15	0.65	0.64	0.65	0.02
0.6pmol of siRNA 1.5µl Lipofectamine	20.53	20.99	-0.46	-0.96	1.94	1.98	0.16
5pmol of siRNA 0.5µl Lipofectamine	18.99	19.15	-0.16	-0.66	1.58	1.60	0.04
5pmol of siRNA 1.25µl Lipofectamine	20.86	21.38	-0.52	-1.02	2.02	2.38	0.43
10pmol of siRNA 1µl Lipofectamine	20.42	20.55	-0.13	-0.63	1.55	1.38	0.15
20pmol of siRNA 1.5µl Lipofectamine	21.93	20.34	1.59	1.09	0.47	0.36	0.09
30pmol of siRNA 0.5µl Lipofectamine	22.24	20.95	1.29	0.79	0.58	0.56	0.02
30pmol of siRNA 1.5µl Lipofectamine	19.94	21.64	-1.70	-2.20	4.61	2.24	2.07

Rep B					
Treatment	**Ct GAPDH**	**Ct TBP**	**ΔCt**	**ΔΔCt**	**Fold change**
Untreated control	21.62	21.20	0.42	-0.08	1.05
0.6pmol of siRNA 0.5µl Lipofectamine	22.06	20.99	1.07	0.65	0.64
0.6pmol of siRNA 1.5µl Lipofectamine	20.52	20.98	-0.46	-0.88	1.85
5pmol of siRNA 0.5µl Lipofectamine	19.86	20.09	-0.23	-0.65	1.57
5pmol of siRNA 1.25µl Lipofectamine	20.78	21.87	-1.09	-1.52	2.86
10pmol of siRNA 1µl Lipofectamine	20.61	20.54	0.07	-0.36	1.28
20pmol of siRNA 1.5µl Lipofectamine	22.10	19.99	2.11	1.69	0.31
30pmol of siRNA 0.5µl Lipofectamine	22.31	21.01	1.30	0.88	0.54
30pmol of siRNA 1.5µl Lipofectamine	20.89	20.00	0.89	0.46	0.73
Rep C					
Treatment	**Ct GAPDH**	**Ct TBP**	**ΔCt**	**ΔΔCt**	**Fold change**
Untreated control	21.66	21.16	0.50	-0.01	1.00
0.6pmol of siRNA 0.5µl Lipofectamine	22.06	21.01	1.05	0.56	0.68
0.6pmol of siRNA 1.5µl Lipofectamine	20.49	21.11	-0.62	-1.11	2.16
5pmol of siRNA 0.5µl Lipofectamine	18.77	19.00	-0.23	-0.72	1.65
5pmol of siRNA 1.25µl Lipofectamine	20.99	21.68	-0.69	-1.18	2.27
10pmol of siRNA 1µl Lipofectamine	20.73	20.61	0.12	-0.38	1.30
20pmol of siRNA 1.5µl Lipofectamine	22.22	20.01	2.21	1.72	0.30
30pmol of siRNA 0.5µl Lipofectamine	22.28	20.98	1.30	0.81	0.57
30pmol of siRNA 1.5µl Lipofectamine	19.04	19.03	0.01	-0.49	1.40

Rep A							
Treatment	**Ct GAPDH**	**Ct TBP**	**ΔCt**	**ΔΔCt**	**Fold change**	**Average fold change**	**Standard deviation**
Untreated control	16.84	19.82	-2.97	0.00	1.00	1.06	0.06
0.6pmol of siRNA 2µl Lipofectamine	16.90	20.36	-3.46	-0.49	1.40	1.21	0.19
0.6pmol of siRNA 4µl Lipofectamine	16.87	19.73	-2.86	0.11	0.93	0.97	0.08
5pmol of siRNA 3µl Lipofectamine	17.34	19.15	-1.81	1.16	0.45	0.44	0.02
10pmol of siRNA 4µl Lipofectamine	17.62	18.33	-0.71	2.26	0.21	0.34	0.22
10pmol of siRNA 1µl Lipofectamine	17.99	20.10	-2.11	0.86	0.55	0.66	0.16
20pmol of siRNA 3µl Lipofectamine	17.87	19.75	-1.87	1.10	0.47	0.40	0.07
20pmol of siRNA 5µl Lipofectamine	18.64	19.15	-0.50	2.47	0.18	0.20	0.05
30pmol of siRNA 2µl Lipofectamine	17.24	18.46	-1.22	1.76	0.30	0.25	0.04
30pmol of siRNA 5µl Lipofectamine	16.90	19.10	-2.20	0.78	0.58	0.52	0.07

Rep B					
Treatment	**Ct GAPDH**	**Ct TBP**	**ΔCt**	**ΔΔCt**	**Fold change**
Untreated control	16.89	19.95	-3.06	-0.08	1.06
0.6pmol of siRNA 2µl Lipofectamine	16.89	19.97	-3.08	-0.02	1.02
0.6pmol of siRNA 4µl Lipofectamine	16.81	19.95	-3.14	-0.08	1.06
5pmol of siRNA 3µl Lipofectamine	17.19	18.99	-1.80	1.26	0.42
10pmol of siRNA 4µl Lipofectamine	17.56	18.46	-0.91	2.15	0.23
10pmol of siRNA 1µl Lipofectamine	17.72	20.00	-2.28	0.78	0.58
20pmol of siRNA 3µl Lipofectamine	18.08	19.82	-1.74	1.32	0.40
20pmol of siRNA 5µl Lipofectamine	18.67	19.19	-0.51	2.54	0.17
30pmol of siRNA 2µl Lipofectamine	17.38	18.24	-0.86	2.20	0.22
30pmol of siRNA 5µl Lipofectamine	16.94	19.09	-2.15	0.91	0.53

Rep C					
Treatment	**Ct GAPDH**	**Ct TBP**	**ΔCt**	**ΔΔCt**	**Fold change**
Untreated control	16.98	20.11	-3.13	-0.16	1.12
0.6pmol of siRNA 2µl Lipofectamine	16.91	20.34	-3.42	-0.29	1.22
0.6pmol of siRNA 4µl Lipofectamine	16.76	19.78	-3.02	0.12	0.92
5pmol of siRNA 3µl Lipofectamine	17.21	19.17	-1.96	1.17	0.44
10pmol of siRNA 4µl Lipofectamine	17.73	20.10	-2.37	0.76	0.59
10pmol of siRNA 1µl Lipofectamine	17.78	20.68	-2.90	0.24	0.85
20pmol of siRNA 3µl Lipofectamine	18.11	19.65	-1.54	1.59	0.33
20pmol of siRNA 5µl Lipofectamine	18.84	20.00	-1.16	1.97	0.26
30pmol of siRNA 2µl Lipofectamine	17.31	18.33	-1.02	2.11	0.23
30pmol of siRNA 5µl Lipofectamine	17.10	19.10	-2.00	1.14	0.45

Rep A

Treatment	Ct GAPDH	Ct TBP	ΔCt	ΔΔCt	Fold change	Average fold change	Standard deviation
Untreated control	33.64	19.29	14.35	0.00	1.00	0.89	0.12
0.6pmol each siRNA 2µl Lipofectamine	33.13	19.11	14.02	-0.33	1.26	1.38	0.14
0.6pmol each siRNA 4µl Lipofectamine	33.86	19.62	14.24	-0.12	1.08	1.24	0.17
5pmol each siRNA 3µl Lipofectamine	33.68	19.61	14.08	-0.28	1.21	1.22	0.08
5pmol each siRNA 5µl Lipofectamine	33.85	20.19	13.67	-0.69	1.61	1.21	0.37
10pmol each siRNA 4µl Lipofectamine	N/A	22.17	-	-	-	-	-
20pmol each siRNA 1.5µl Lipofectamine	N/A	23.62	-	-	-	-	-
20pmol each siRNA 3µl Lipofectamine	N/A	24.40	-	-	-	-	-
30pmol each siRNA 2µl Lipofectamine	34.01	20.38	13.63	-0.04	1.03	-	-
30pmol each siRNA 5µl Lipofectamine	33.86	19.18	14.68	-	-	-	-
50pmol each siRNA 4µl Lipofectamine	N/A	23.70	-	-	-	-	-

Rep B

Treatment	Ct GAPDH	Ct TBP	ΔCt	ΔΔCt	Fold change
Untreated control	**33.94**	**19.19**	**14.74**	**0.39**	**0.76**
0.6pmol each siRNA 2µl Lipofectamine	33.19	19.07	14.12	-0.62	1.54
0.6pmol each siRNA 4µl Lipofectamine	34.07	19.61	14.45	-0.29	1.22
5pmol each siRNA 3µl Lipofectamine	34.22	19.67	14.54	-0.20	1.15
5pmol each siRNA 5µl Lipofectamine	34.73	19.81	14.92	0.18	0.88
10pmol each siRNA 4µl Lipofectamine	34.79	20.70	14.09	-0.65	1.57
20pmol each siRNA 1.5µl Lipofectamine	N/A	23.43	-	-	-
20pmol each siRNA 3µl Lipofectamine	N/A	23.34	-	-	-
30pmol each siRNA 2µl Lipofectamine	N/A	24.53	-	-	-
30pmol each siRNA 5µl Lipofectamine	N/A	25.19	-	-	-
50pmol each siRNA 4µl Lipofectamine	34.81	19.76	15.05	-	-

Rep C

Treatment	Ct GAPDH	Ct TBP	ΔCt	ΔΔCt	Fold change
Untreated control	**34.26**	**19.39**	**14.87**	**0.13**	**0.91**
0.6pmol each siRNA 2µl Lipofectamine	33.51	19.09	14.43	-0.44	1.36
0.6pmol each siRNA 4µl Lipofectamine	34.14	19.78	14.36	-0.51	1.42
5pmol each siRNA 3µl Lipofectamine	34.07	19.58	14.49	-0.38	1.30
5pmol each siRNA 5µl Lipofectamine	34.72	20.04	14.68	-0.19	1.14
10pmol each siRNA 4µl Lipofectamine	N/A	19.86	14.48	-0.39	1.31
20pmol each siRNA 1.5µl Lipofectamine	34.34	20.58	-	-	-
20pmol each siRNA 3µl Lipofectamine	N/A	23.50	-	-	-
30pmol each siRNA 2µl Lipofectamine	N/A	23.26	-	-	-
30pmol each siRNA 5µl Lipofectamine	N/A	25.04	-	-	-
50pmol each siRNA 4µl Lipofectamine	N/A	24.68	-	-	-

Appendix 11:Raw relative population doubling data +/-O^6BG (Chapter 6).

Baseline = 240000 cells.

MNU -O^6BG 24 Rep A			
Dose (µg/ml)	**Number of cells**	**Population doubling (PD)**	**RPD (%)**
0	520000	1.12	105.34
DMSO	500000	1.06	100.00
0.00075	528000	1.14	107.42
0.001	461800	0.94	89.17
0.05	451600	0.91	86.13

MNU-O6BG 24hr RepB			
Dose (µg/ml)	**Number of cells**	**Population doubling (PD)**	**RPD (%)**
0	513800	1.10	99.59
DMSO	515400	1.10	100.00
0.00075	484600	1.01	91.94
0.001	475000	0.98	89.32
0.05	473400	0.98	88.88

MNU -O^6BG 48 Rep A			
Dose (µg/ml)	**Number of cells**	**Population doubling (PD)**	**RPD (%)**
0	870000	1.86	102.12
DMSO	847000	1.82	100.00
0.00075	712200	1.57	86.25
0.001	737600	1.62	89.03
0.05	711000	1.57	86.12

MNU-O6BG 48hr Rep B			
Dose (µg/ml)	**Number of cells**	**Population doubling (PD)**	**RPD (%)**
0	722200	1.59	100.61
DMSO	717400	1.58	100.00
0.00075	651000	1.44	91.13
0.001	629700	1.39	88.09
0.05	625000	1.38	87.41

MNU +O^6BG 24 Rep A			
Dose (µg/ml)	**Number of cells**	**Population doubling (PD)**	**RPD (%)**
O6BG-MNU	500000	1.06	96.87
O6BG+DMSO	567600	1.24	120.60
0.00075	487400	1.02	99.25
0.001	439000	0.87	84.60
0.05	435800	0.86	83.58
METH+DMSO	490000	1.03	100.00
Methanol	512000	1.09	106.15

MNU+O6BG24 RepB			
Dose (µg/ml)	**Number of cells**	**Population doubling (PD)**	**RPD (%)**
O6BG-MNU	500000	1.06	100.83
O6BG+DMSO	489200	1.03	94.33
0.00075	469600	0.97	88.91
0.001	442600	0.88	81.07
0.05	446800	0.90	82.32
METH+DMSO	510600	1.09	100.00
Methanol	497000	1.05	96.42

MNU +O^{6}BG 48 Rep A			
Dose (µg/ml)	**Number of cells**	**Population doubling (PD)**	**RPD (%)**
O6BG-MNU	819000	1.77	103.14
O6BG+DMSO	741000	1.63	92.68
0.00075	609400	1.34	76.61
0.001	662000	1.46	83.41
0.05	694000	1.53	87.29
METH+DMSO	810000	1.75	100.00
Methanol	789000	1.72	97.84

MNU +O^{6}BG 48 B			
Dose (µg/ml)	**Number of cells**	**Population doubling (PD)**	**RPD (%)**
O6BG-MNU	760000	1.66	100.23
O6BG+DMSO	744000	1.63	100.72
0.00075	724600	1.59	98.37
0.001	596800	1.31	81.09
0.05	560400	1.22	75.49
METH+DMSO	738000	1.62	100.00
Methanol	758000	1.66	102.38

Baseline=262500 cells.

MNU -O6BG Rep A 24hr count			
Dose (µg/ml)	**Number of cells**	**Population doubling (PD)**	**RPD (%)**
Meth+DMSO	660000	1.33	100.00
2	455000	0.79	59.66
4	470000	0.84	63.18
6	340000	0.37	28.06
8	350000	0.42	31.20
10	255000	-0.04	-3.14

MNU -O6BG Rep B 24hr count			
Dose (µg/ml)	**Number of cells**	**Population doubling (PD)**	**RPD (%)**
Meth+DMSO	475000	1.03	100.00
2	375000	0.69	66.79
4	400000	0.78	75.85
6	266000	0.19	18.54
8	246000	0.08	7.55
10	260000	0.16	15.33

MNU -O6BG 48 Rep A			
Dose (µg/ml)	**Number of cells**	**Population doubling (PD)**	**RPD (%)**
Meth+DMSO	825000	1.82	100.00
2	455000	0.96	52.91
4	315000	0.43	23.82
6	320000	0.46	25.06
8	260000	0.16	8.63
10	240000	0.04	2.30

MNU -O6BG 48 Rep B			
Dose (µg/ml)	**Number of cells**	**Population doubling (PD)**	**RPD (%)**
Meth+DMSO	750000	1.51	100.00
2	387500	0.56	37.10
4	305000	0.22	14.29
6	310000	0.24	15.84
8	290000	0.14	9.49
10	250000	-0.07	-4.65

MNU +O6BG Rep A 24hr post treatment			
Dose (µg/ml)	**Number of cells**	**Population doubling (PD)**	**RPD (%)**
Meth+DMSO	380000	0.70	100.00
2	305000	0.39	55.00
4	265000	0.18	26.23
6	180000	-0.37	-52.93
8	150000	-0.64	-90.25
10	190000	-0.30	-41.86

MNU +O6BG Rep B 24hr post treatment			
Dose (µg/ml)	**Number of cells**	**Population doubling (PD)**	**RPD (%)**
Meth+DMSO	480000	1.04	100.00
2	300000	0.36	34.92
4	330000	0.50	48.12
6	175000	-0.41	-39.71
8	150000	-0.64	-61.05
10	150000	-0.64	-61.05

MNU +O6BG 48Rep A			
Dose (µg/ml)	**Number of cells**	**Population doubling (PD)**	**RPD (%)**
Meth+DMSO	780000	1.57	100.00
2	250000	-0.07	-4.48
4	190000	-0.47	-29.68
6	157500	-0.74	-46.91
8	110000	-1.25	-79.87
10	100000	-1.39	-88.62

MNU +O6BG 48 Rep B			
Dose (µg/ml)	**Number of cells**	**Population doubling (PD)**	**RPD (%)**
Meth+DMSO	740000	1.50	100.00
2	225000	-0.22	-14.87
4	145000	-0.86	-57.27
6	135000	-0.96	-64.16
8	105000	-1.32	-88.41
10	75000	-1.81	-120.88

Appendix 12:Raw HPRT data (Chapter 6).

Replicate A	6-TG (selective conditions)		-6-TG (non-selective conditions)					
Dose MNU (µg/ml)	**Number of wells without colonies**	**Total number of wells scored**	**Number of wells without colonies**	**Total number of wells scored**	**Dilution Factor**	**Mutant Frequency (MF)**	**Average of replicates**	**Standard deviation**
0	560	600	3	480	0.0005	6.80E-06	1.00E-05	7.82E-06
Meth+DMSO	544	600	4	480	0.0005	1.02E-05	1.49E-05	5.85E-06
DMSO	567	600	4	480	0.0005	5.91E-06	1.33E-05	1.05E-05
Meth	512	600	4	480	0.0005	1.66E-05	1.86E-05	3.55E-06
0.00075	457	600	4	480	0.0005	2.84E-05	1.36E-05	1.28E-05
0.001	385	600	7	480	0.0005	5.25E-05	2.95E-05	2.00E-05
0.0025	427	600	12	480	0.0005	4.61E-05	3.10E-05	1.33E-05
0.005	419	600	14	480	0.0005	5.08E-05	3.29E-05	1.70E-05
0.0075	381	600	7	480	0.0005	5.37E-05	3.62E-05	1.60E-05
0.01	496	600	19	480	0.0005	2.95E-05	3.01E-05	1.76E-05
0.025	501	600	12	480	0.0005	2.44E-05	3.15E-05	2.81E-05
0.05	448	600	23	480	0.0005	4.81E-05	4.83E-05	1.95E-05
0.075	341	600	8	480	0.0005	6.90E-05	4.56E-05	2.11E-05

Rep B	6-TG (selective conditions)		-6-TG (non-selective conditions)			
Dose MNU (µg/ml)	Number of wells without colonies	Total number of wells scored	Number of wells without colonies	Total number of wells scored	Dilution Factor	Mutant Frequency (MF)
0	572	600	2	480	0.0005	4.36E-06
Meth+DMSO	552	600	20	480	0.0005	1.31E-05
DMSO	563	600	12	480	0.0005	8.63E-06
METH	548	600	31	480	0.0005	1.65E-05
0.00075	563	600	3	480	0.0005	6.27E-06
0.001	468	600	1	480	0.0005	2.01E-05
0.0025	452	600	2	480	0.0005	2.58E-05
0.005	505	600	3	480	0.0005	1.70E-05
0.0075	431	600	3	480	0.0005	3.26E-05
0.01	542	600	9	480	0.0005	1.28E-05
0.025	567	600	11	480	0.0005	7.49E-06
0.05	331	600	6	480	0.0005	6.79E-05
0.075	538	600	68	480	0.0005	2.79E-05
Rep C	6-TG (selective conditions)		-6-TG (non-selective conditions)			
Dose MNU (µg/ml)	Number of wells without colonies	Total number of wells scored	Number of wells without colonies	Total number of wells scored	Dilution Factor	Mutant Frequency (MF)
0	516	600	9	480	0.0005	1.90E-05
Meth+DMSO	531	600	28	480	0.0005	2.15E-05
DMSO	540	600	60	480	0.0005	2.53E-05
Meth	536	600	40	480	0.0005	2.27E-05
0.00075	576	600	17	480	0.0005	6.11E-06
0.001	510	600	3	480	0.0005	1.60E-05
0.0025	528	600	23	477	0.0005	2.11E-05
0.005	527	600	59	480	0.0005	3.09E-05
0.0075	478	600	3	480	0.0005	2.24E-05
0.01	529	600	129	480	0.0005	4.79E-05
0.025	494	600	101	479	0.0005	6.24E-05
0.05	547	600	97	480	0.0005	2.89E-05
0.075	495	600	43	480	0.0005	3.99E-05

Appendix 13:Raw HPRT plating efficiency data.

	Rep A		Rep B		Rep C				
Dose MNU (µg/ml)	**PE**	**RPE (%)**	**PE**	**RPE (%)**	**PE**	**RPE (%)**	**Average cell viability**	**Standard deviation**	**TTEST**
Untreated	441.77	-	478.75	-	324.26	-	-	-	-
0+O6BG	507.52	106.01	548.06	200.04	397.66	160.03	155.36	47.19	0.34
Meth+DMSO	478.75	108.37	317.81	66.38	284.16	87.63	87.46	20.99	0.51
DMSO	478.75	108.37	368.89	77.05	207.94	64.13	83.18	22.75	0.53
Meth	478.75	108.37	273.98	57.23	248.49	76.63	80.74	25.82	0.40
0.00075	478.75	100.00	507.52	159.69	334.06	117.56	125.75	30.68	0.74
0.001	422.79	88.31	617.38	194.26	507.52	178.60	153.73	57.19	0.24
0.0025	368.89	77.05	548.06	172.45	303.20	106.70	118.74	48.83	0.93
0.005	353.47	73.83	507.52	159.69	209.62	73.77	102.43	49.59	0.58
0.0075	422.79	88.31	507.52	159.69	507.52	178.60	142.20	47.62	0.30
0.01	322.93	67.45	397.66	125.13	131.40	46.24	79.61	40.82	0.23
0.025	368.89	77.05	377.59	118.81	155.66	54.78	83.55	32.51	0.26
0.05	303.83	63.46	438.20	137.88	159.91	56.27	85.87	45.19	0.29
0.075	409.43	85.52	195.43	61.49	241.26	84.90	77.31	13.70	0.17

Appendix 14:Fraction of unrepaired adducts (Chapter 6).

Dose MNU (µg/ml)	**MF -O^{6}BG**	**MF +O^{6}BG**	**Fraction of unrepaired lesions**
0.001	1.39E-05	2.95E-05	4.71E-01
0.0025	5.52E-06	3.10E-05	1.78E-01
0.005	8.92E-06	3.29E-05	2.71E-01
0.0075	1.03E-05	3.62E-05	2.84E-01
0.01	2.40E-05	3.01E-05	7.98E-01
0.025	3.79E-05	3.15E-05	1.21E+00
0.05	3.62E-05	4.83E-05	7.49E-01
0.075	5.15E-05	4.56E-05	1.13E+00

Rep B					
Dose MNU (µg/ml)	**Ct MGMT**	**Ct TBP**	**ΔCt**	**ΔΔCt**	**Fold change**
METH + DMSO	33.94	21.72	12.21	-0.78	1.71
0	34.11	22.01	12.10	-0.12	1.09
0.00075	33.96	21.66	12.30	0.09	0.94
0.0025	32.76	21.55	11.21	-1.00	2.01
0.0075	33.03	21.54	11.49	-0.73	1.65
0.01	33.57	21.98	11.58	-0.63	1.55
0.025	33.33	21.44	11.89	-0.32	1.25
0.05	33.52	21.75	11.77	-0.44	1.36
Rep C					
Dose MNU (µg/ml)	**Ct MGMT**	**Ct TBP**	**ΔCt**	**ΔΔCt**	**Fold change**
METH + DMSO	33.33	21.59	11.73	-0.30	1.23
0	34.50	21.79	12.71	0.98	0.51
0.00075	32.96	21.81	11.15	-0.58	1.50
0.0025	34.40	21.63	12.76	1.03	0.49

Appendix 15: Raw real time data +O^6BG (Chapter 6).

1 hour post MNU treatment

Rep A							
Dose MNU (µg/ml)	**Ct MGMT**	**Ct TBP**	**ΔCt**	**ΔΔCt**	**Fold change**	**Average**	**Standard deviation**
METH + DMSO	33.21	21.77	11.44	0.00	1.00	1.31	0.36
0	33.96	21.60	12.36	0.92	0.53	0.71	0.33
0.00075	33.75	22.28	11.47	0.03	0.98	1.14	0.31
0.0025	33.94	21.72	12.21	0.78	0.58	1.03	0.85
0.0075	33.94	21.47	12.47	1.04	0.49	0.85	0.69
0.01	33.55	22.62	10.93	-0.51	1.42	1.31	0.31
0.025	31.78	21.30	10.48	-0.95	1.94	1.24	0.70
0.05	33.93	21.31	12.62	1.18	0.44	0.75	0.52

0.0075	34.70	21.72	12.98	1.24	0.42
0.01	33.55	21.76	11.79	0.05	0.97
0.025	34.45	21.85	12.60	0.87	0.55
0.05	34.44	21.59	12.85	1.11	0.46

4hr post MNU treatment.

Rep A							
Treatment	**Ct MGMT**	**Ct TBP**	**ΔCt**	**ΔΔCt**	**Fold change**	**Average fold change**	**Standard deviation**
METH + DMSO	32.65	21.16	11.49	0.00	1.00	1.17	0.86
0	31.97	21.20	10.77	-0.72	1.65	1.23	0.36
0.00075	31.82	21.02	10.80	-0.69	1.61	1.86	1.38
0.0025	32.41	21.02	11.39	-0.09	1.07	1.03	0.44
0.0075	32.08	20.83	11.26	-0.23	1.17	1.65	0.95
0.01	31.72	21.86	9.86	-1.63	3.10	1.68	1.29
0.025	36.70	21.23	15.47	3.98	0.06	0.47	0.40
0.05	33.00	20.96	12.04	0.55	0.68	0.86	0.69

Rep B					
Treatment	**Ct MGMT**	**Ct TBP**	**ΔCt**	**ΔΔCt**	**Fold change**
METH + DMSO	33.76	21.20	12.56	-1.08	2.11
0	33.92	21.34	12.57	0.01	0.99
0.00075	31.70	20.87	10.82	-1.74	3.34
0.0025	32.88	20.84	12.03	-0.53	1.44
0.0075	31.97	20.86	11.10	-1.46	2.75
0.01	33.35	21.23	12.13	-0.43	1.35
0.025	33.79	21.03	12.76	0.20	0.87
0.05	32.76	20.89	11.86	-0.70	1.62

Rep C					
Treatment	**Ct MGMT**	**Ct TBP**	**ΔCt**	**ΔΔCt**	**Fold change**
METH + DMSO	31.09	20.88	10.21	1.27	0.41
0	31.44	21.30	10.14	-0.07	1.05
0.00075	31.78	20.87	10.91	0.70	0.62
0.0025	32.05	21.04	11.01	0.80	0.57
0.0075	30.95	20.80	10.15	-0.06	1.04
0.01	32.17	21.20	10.97	0.75	0.59
0.025	32.38	21.11	11.26	1.05	0.48
0.05	32.79	20.77	12.02	1.81	0.29

6hr post MNU treatment.

Treatment	Ct MGMT	Ct TBP	ΔCt	ΔΔCt	Fold change	Average fold change	Standard deviation
METH + DMSO	32.25	21.71	10.53	0.00	1.00	1.26	0.24
0	32.70	21.29	11.41	0.87	0.55	0.67	0.20
0.00075	34.06	21.32	12.75	2.22	0.22	0.78	0.72
0.0025	34.08	21.30	12.77	2.24	0.21	0.71	0.65
0.0075	32.52	21.14	11.37	0.84	0.56	0.73	0.19
0.01	32.26	21.39	10.87	0.34	0.79	0.89	0.26
0.025	33.48	21.06	12.43	1.89	0.27	0.46	0.18
0.05	32.88	20.79	12.09	1.55	0.34	0.85	0.46

Rep B

Treatment	Ct MGMT	Ct TBP	ΔCt	ΔΔCt	Fold change
METH + DMSO	32.67	21.75	10.92	-0.39	1.31
0	33.19	21.45	11.74	0.82	0.57
0.00075	32.84	21.00	11.84	0.92	0.53
0.0025	33.17	21.14	12.04	1.12	0.46
0.0075	32.23	21.20	11.03	0.11	0.93
0.01	32.01	21.33	10.68	-0.24	1.18
0.025	33.04	21.43	11.61	0.69	0.62
0.05	31.43	20.82	10.61	-0.31	1.24

Rep C

Treatment	Ct MGMT	Ct TBP	ΔCt	ΔΔCt	Fold change
METH + DMSO	32.51	21.43	11.08	-0.55	1.46
0	32.57	21.35	11.22	0.14	0.91
0.00075	31.57	21.16	10.41	-0.67	1.60
0.0025	31.73	21.18	10.55	-0.53	1.45
0.0075	32.68	21.11	11.58	0.50	0.71
0.01	32.80	21.18	11.62	0.54	0.69
0.025	33.43	21.33	12.10	1.02	0.49
0.05	32.14	21.04	11.10	0.02	0.99

24hr post treatment.

Rep A							
Treatment	**Ct MGMT**	**Ct TBP**	**ΔCt**	**ΔΔCt**	**Fold change**	**Average fold change**	**Standard deviation**
METH + DMSO	34.97	21.13	13.83	0.00	1.00	0.84	0.17
0	35.43	21.16	14.27	0.44	0.74	1.03	0.27
0.00075	34.56	21.04	13.52	-0.31	1.24	1.21	0.04
0.0025	35.55	21.91	13.64	-0.19	1.14	1.61	0.40
0.0075	34.96	21.38	13.58	-0.26	1.19	1.66	0.50
0.01	35.63	21.74	13.89	0.06	0.96	1.10	0.71
0.025	37.13	22.22	14.91	1.08	0.47	0.94	1.06
0.05	36.01	21.69	14.32	0.49	0.71	0.42	0.29

Rep B					
Treatment	**Ct MGMT**	**Ct TBP**	**ΔCt**	**ΔΔCt**	**Fold change**
METH + DMSO	34.56	21.34	13.22	0.61	0.65
0	34.00	20.88	13.12	-0.10	1.07
0.00075	34.79	21.79	13.00	-0.22	1.17
0.0025	34.04	21.69	12.35	-0.87	1.83
0.0075	34.43	22.34	12.09	-1.13	2.19
0.01	36.03	21.71	14.32	1.10	0.47
0.025	37.42	21.80	15.61	2.39	0.19
0.05	36.72	22.17	14.55	1.33	0.40

Rep C					
Treatment	**Ct MGMT**	**Ct TBP**	**ΔCt**	**ΔΔCt**	**Fold change**
METH + DMSO	34.49	20.86	13.62	0.21	0.86
0	34.12	20.85	13.28	-0.35	1.27
0.00075	34.46	21.12	13.35	-0.28	1.21
0.0025	34.60	21.86	12.73	-0.89	1.85
0.0075	35.06	22.11	12.95	-0.68	1.60
0.01	34.54	21.81	12.72	-0.90	1.87
0.025	34.21	21.69	12.52	-1.11	2.15
0.05	37.58	21.15	16.43	2.80	0.14

Appendix 16: Accepted abstract for poster at UKEMS 2009 and ICEM, 2009.

Comparison and validation of the micronucleus assay with and without cytochalasin in mammalian cell lines

Adam D. Thomas, Shareen H. Doak, Gareth J. Jenkins and George E. Johnson
Institute of Lie Sciences School of Medicine, Swansea University, Swansea SA2 8PP, UK

As a consequence of the reduced, refined and ultimate replacement of animal usage in genetic toxicology, more emphasis has been placed on in vitro assays. The in vitro micronucleus assay is one such test system, and we are working with a number of European laboratories to standardise and validate the assay, as recommended in the late 2007 version of the draft OECD Test Guideline 487. Cytochalasin B (CytoB) is used in the cytokinesis block micronucleus (CBMN) assay is widely used to assess chromosomal damage in cells that have undergone one cellular division. The micronucleus assay can also be carried out without CytoB in the non-CBMN assay, although this is less widely conducted due to lack of control of mitotic kinetics. In this communica- tion we compare these two methodologies by testing the known spindle poisons, vinblastine and diethylstilboestrol (DES) in both test systems in CHO cells. Relative population doubling (RPD), relative increase in cell count (RICC) and relative cell counts (RCC) were used in the non-CBMN assay and the replicative index (RI) was used in the CBMN assay. These measures were then compared and their implications for dose selection are highlighted. Notably, RI exaggerated toxicity and lead to a lower dose being selected to give 50% toxicity (vinblastine 0.7 lg/ml; DES 4lg/ml), possibly due to temporary mitotic block. RCC underestimated toxicity and lead to higher doses selected (vinblastine .2 lg/ml; DES .6 lg/ml). Failure to detect known genotoxins (so called false negatives) at doses selected using RPD is its main criticism for use, however, in the following report, I have shown this is not the case. This work supports the premise that RPD and RICC are appropriate measures for the non-CBMN assay in vitro. We are also using this information to help in our validation of both the CBMN and non-CBMN assays using the Metasystems Metafer automated system.

Comparison and Validation of the Micronucleus Assay with and without Cytochalasin B in Mammalian Cell Lines.

Adam D. Thomas[1], George E. Johnson, Shareen H. Doak and Gareth J. S. Jenkins.

School of Medicine, University of Wales Swansea, Singleton Park, Swansea.
[1]Presenting author.

Swansea University
Prifysgol Abertawe

EPSRC
Engineering and Physical Sciences Research Council

Introduction

Current micronucleus assay methodology is being standardised in a collaborative effort to ensure the reduction of false positive and false negative results. The different toxicity measures used to define the dose range for the micronucleus (Mn) assay without cytokinesis block are currently under scrutiny.

Such measures being RPD and RICC, are recommended in draft OECD guideline 487 for use in absence of Cytochalasin B (CytoB). They are known to produce very different results to more traditionally used cytotoxic end-points (RCC) and their influences are implicated in risk assessment.

Aim

Through quantification of Mn induction in response to Vinblastine we hope to validate the use of RPD and RICC for use in the Mn assay without cytokinesis block with implications in the Metasystems Metafer automated system.

Materials and Methods

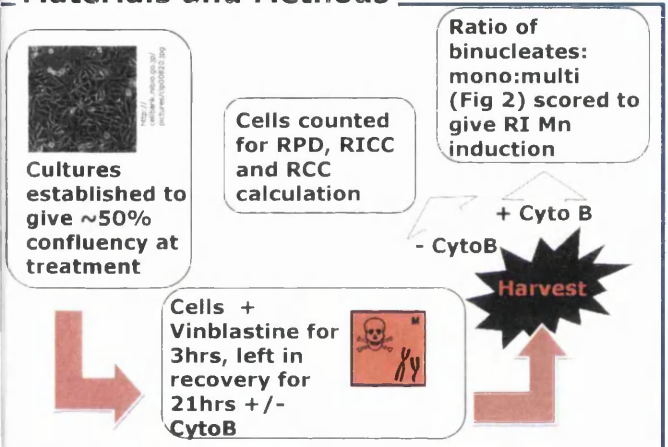

Figure 1. Schematic of the experimental design.

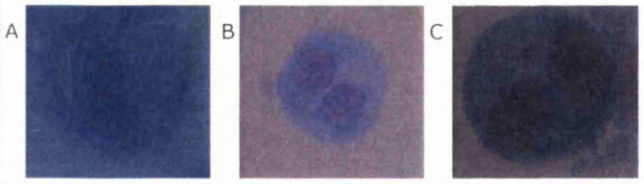

Figure 2. Chinese hamster CHO cells. **A**) Mononucleated, **B**) Binucleated **C**) Binucleate with micronucleus.

Chemical.
Vinblastine (from Covance, Harrogate, UK).
Chemotherapeutic and model aneugen, through inhibition of microtubule assembly. Active at 0.5-5µg/ml in DMSO.

Toxicity endpoints measured.
•Relative population doubling (RPD)
•Relative increase in cell count (RICC)
•Relative cell count (RCC)
•Replication Index (RI)

Results and Discussion

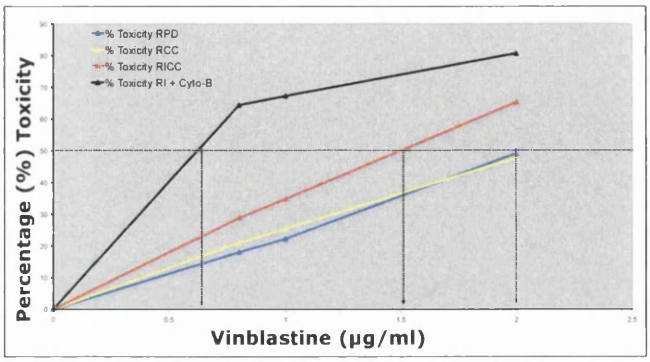

Figure 3. Illustration of the impact that different toxicity endpoints have on dose selection, giving the same extent of toxicity.
•RICC leads to higher doses selected and RI leads to lower doses selected compared to RPD for same extent of toxicity.

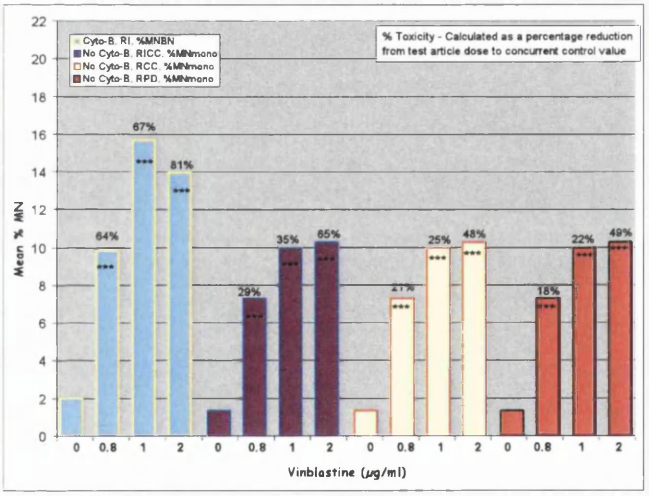

Figure 4. Mn induction with and without CytoB, coupled with toxicity using relevant toxicity endpoints.
*** Significant increase above control ($p<0.001$)

•There was a positive response at all doses selected by RPD, RCC, RICC and RI giving appropriate extent of toxicity.

Conclusions

•RI gives over exaggeration of toxicity through mitotic arrest, and leads to lower doses selected to give LD50.

•RPD, RICC and RCC adequately identify known aneugens as positive genotoxins and so could be used as a toxicity measure in non-CBMN assay.

•These results are in line with the rest of the collaborative group in showing that all of the toxicity measures are suitable and should be included in the OECD guideline 487.

Appendix 18: Accepted abstract for poster at UKEMS 2010.

Low dose exposure to MNU in Human Lymphoblastoid cell line AHH-1.

Adam D. Thomas, Gareth J. S. Jenkins, Shareen H. Doak and George E. Johnson.

Institute of Life Science, Swansea University, Swansea, UK, SA2 8PP.

Before pharmaceuticals are approved for human usage, their potential to cause point mutations and chromosome damage is assessed at increasing doses using *in vitro* cell culture systems and animal models. The resulting dose-response is a critical factor in establishing safe exposure limits. It has long been assumed that DNA reactive chemicals cause adverse effects at every dose. However, experimentation into the low dose region has revealed a threshold mechanism where, up to the threshold dose, DNA reactive chemicals can be tolerated without incurring more damage than that naturally occurring within the cell. MNU, a model alkylating agent has been shown to illicit DNA damage in a linear fashion even at low doses, whereas similar acting compounds MMS and EMS have been shown to have thresholds (1). In this study we find a putative threshold dose for point mutation induction at 0.00075μg/ml MNU when quantified through the HPRT assay in the AHH-1 Human Lymphoblastoid cell line. Sequence analysis of the resultant mutants will give mechanistic information regarding point mutation induction over this thresholded dose range. Through use of the Metasystems metafer software optimised for the micronucleus assay, we aim to evaluate MNUs ability to induce chromosome breakages over a wider dose range than previously tested. Further work will identify the mechanism of the threshold dose-response for genetic damage hypothesised to involve DNA repair of pre-mutagenic lesions.

References

Doak, S.H., Jenkins, G.J.S., Johnson, G.E., Quick, E., Parry, E. M. and Parry, J. M. (2007) Mechanistic Influences for Mutation Induction Curves after Exposure to DNA-Reactive Carcinogens. *Cancer Research.*, **67**:(8), 3904-3911,

Establishing a mutation spectrum for MNU over a threshold dose-response in AHH-1 Human cells.

Adam D. Thomas[1], George E. Johnson, Shareen H. Doak and Gareth J. S. Jenkins.

School of Medicine, University of Wales Swansea, Singleton Park, Swansea SA2 8PP.
[1]Presenting author.

Swansea University Prifysgol Abertawe

EPSRC Engineering and Physical Sciences Research Council

Introduction

•Experiments into the genotoxic potential of low dose exposures highlight a threshold dose response.

•Evidence is accumulating to suggest that alkylating agents are safe at low doses, where significant DNA damage was once thought to occur.

•Safe exposure levels have implications in drug development and chemotherapeutic cancer treatment.

•The cytoprotective mechanism responsible is currently under investigation.

•We are hypothesising that DNA repair removes alkylation damage **(Fig 1)** up until the threshold dose where these mechanisms become overwhelmed and mutation induction thereafter accrues in a liner fashion **(Fig 2)**.

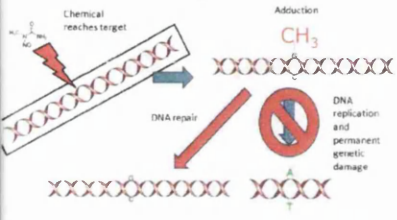

Figure 1 DNA repair as a bodyguard against alkylation damage. MNU induces O^6MeG that, if not repaired by MGMT, becomes replicated and fixed as GC-AT point mutations

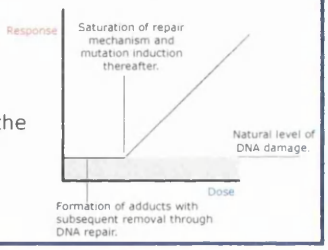

Figure 2 Incorporating the DNA repair hypothesis into the threshold dose-response.

Key research questions

Does MNU illicit a threshold dose-response in AHH-1 human cells using the HPRT point mutation assay? (previous data suggests not (Doak *et al, 2007)*.

Does the spectrum of point mutations induced by MNU change at doses below and above a threshold?

Materials and Methods

Mutations and small deletions quantified through the HPRT assay as previously detailed (Doak *et al*, 2007) and resulting mutants sequenced.

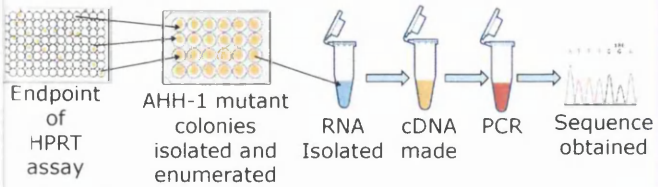

PCR strategy:

Two overlapping pairs of primers used for 83% gene coverage.

Results and Discussion

Figure 3 Low dose exposure to MNU in AHH-1 in the HPRT assay. Doses sequenced are circled in red.

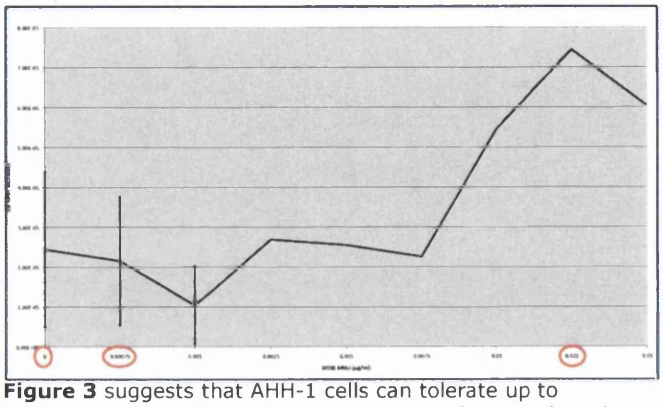

Figure 3 suggests that AHH-1 cells can tolerate up to 0.00075µg/ml MNU without incurring more damage than that occurring in the cell naturally.

Figure 4 proportions of GC to AT transitions at the respective doses of MNU.

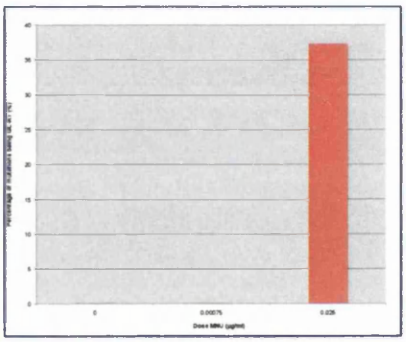

Mutants recovered at **0µg/ml** were found to contain a ~70bp deletion,

At **0.00075µg/ml** the predominance of mutants were A-T point mutations at the start codon,

0.025µg/ml MNU induced more GC-AT transitions (37%) than any other single mutational event.

The spectrum of mutations induced changes over the threshold dose response.

The proportion of GC-AT transitions, characteristic of MNU exposure, increase drastically once the threshold dose is surpassed.

Conclusions

We have found that AHH-1 human cells can tolerate low doses of MNU in the HPRT assay, the resistance, we believe is conveyed through DNA repair mechanisms.

Analysing the sequence at the HPRT locus reveals the spectrum of mutations induced by increasing concentrations of MNU.

MNU produces O^6MeG, a pre-mutagenic event that gives rise to GC-AT mutations unless it is repaired by MGMT. doses above the threshold saturate MGMT and so the proportions of GC-AT events increase thereafter.

Reference:
Doak *et al* (2007)

Appendix 20: Accepted abstract for oral presentation (UKEMS, 2011) and poster (EEMS, 2011)

Can O^6-Methylgaunine methyltransferase (MGMT) protect DNA from low doses of Methyl Nitrosourea?

Adam D. Thomas, Gareth J. S. Jenkins, Shareen H. Doak, Paul D. Lewis and George E. Johnson.
Institute of Life Science, College of Medicine, Swansea University, SA2 8P.

In the hope of decreasing the chance of human cancer and heritable genetic defects; pharmaceuticals and food products are tested for their ability to cause DNA damage. As a precaution, it has been assumed that chemicals known to induce DNA damage at high doses also damage DNA at low doses. This linear hypothesis, derived from extrapolation of high dose data, could prevent beneficial products from entering the market if shown to contain very low level of genotoxins.

Our laboratory has identified threshold dose-responses for model alkylating agents [methyl methanesulfonate (MMS) and ethyl methanesulfonate (EMS)] in the HPRT mutation assay (Doak *et al*, 2007). Since then there has been an accumulation of *in vitro* and *in vivo* data for certain DNA reactive compounds supporting the threshold hypothesis.

Nucleotide substitutions, quantified by the HPRT assay can be caused by the miscoding potential of O^6methylguanine (O^6MeG), a pre-mutagenic DNA adduct present in low amounts following exposure to these alkylating agents. It is repaired by Methylguanine methyl transferase (MGMT) before it causes GC-AT transitions, MGMT, is therefore predicted to protect DNA at low levels until it is saturated at the threshold dose and above. This is the hypothesised mechanism behind the mutagenic threshold dose response.

Doak *et al* (2007) showed that MNU did not have a threshold dose response. The following work reports a threshold dose-response with a NOEL of 0.0075μg/ml. We have inactivated MGMT by O^6benzylguanine and the mutation frequency at the NOEL increases from 9.22×10^{-6} to 5.37×10^{-5}. The HPRT locus has been sequenced to obtain the mutation spectra over the dose response. We have observed 12% GC-AT mutations sub-threshold compared to 33% above the threshold.

References

Doak, S.H., Jenkins. G.J.S., Johnson. G.E., Quick. E., Parry. E.M. and Parry. J.M. (2007) Mechanistic influences for Mutation Induction Curves Following Exposure to DNA-Reactive carcinogens. *Cancer Research.* **67**:1-8.

DNA repair as the mechanism in genotoxic thresholds

Adam D. Thomas, Gareth J. S. Jenkins, Shareen H. Doak, Paul D. Lewis and George E. Johnson.

College of Medicine, University of Wales Swansea, Singleton Park, Swansea SA2 8PP.

Swansea University Prifysgol Abertawe

EPSRC Engineering and Physical Sciences Research Council

Introduction

ethyl nitrosourea (MNU) and other kylating agents are DNA reactive enotoxins, assumed to be mutagenic, en at low doses (linear dose-response);

Pharmaceuticals with impurities assumed to have a linear dose-response are not approved for human use.

idence is accumulating suggesting at other alkylating agents (MMS) are not utagenic at low doses but exhibit a reshold dose-response (Doak *et al*, 2007);

However, MNU is 20 times more mutagenic than MMS (Baranek, 1990).

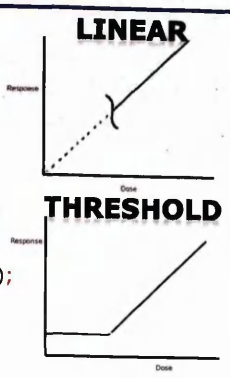

YPOTHESISED MECHANISM

We hypothesise that at low doses, NA repair mechanisms remove remutagenic DNA damage before it s fixed into mutations.

The repair mechanism involved depends on the chemical's mechanism f action (MOA)

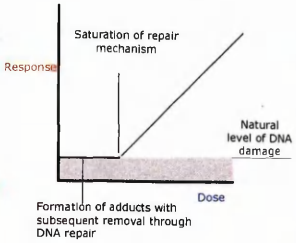

Figure 1. Incorporating the DNA repair hypothesis into the threshold dose-response.

OA OF MNU AND DNA REPAIR;

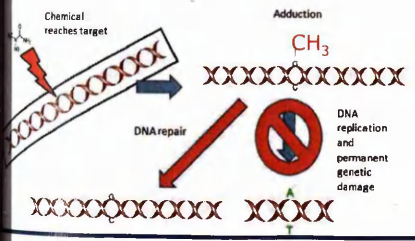

MNU induces O⁶methylguanine (O⁶MeG) a mutagenic adduct

MGMT repairs O⁶MeG which prevents GC→AT point mutations

1**MGMT** can only repair 1O⁶MeG

We predict **MGMT** saturation at high doses

Aims

Quantify mutations induced by low doses of MNU through the HPRT ssay.

Establish mutation spectra and quantify GC→AT mutations to entify mutations below and above the NOEL.

Inhibit MGMT and quantify GC→AT changes and MF at the NOEL.

Materials and Methods

Mutations were quantified through the HPRT assay as previously etailed (Doak *et al*, 2007) and the resulting mutants sequenced.

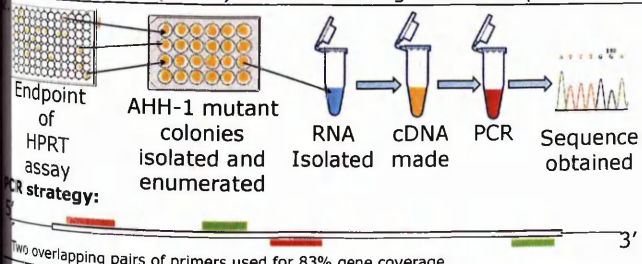

MGMT inhibition was achieved through 1hr pre-treatment with 0μM O⁶benzylguanine followed by HPRT assay and sequencing

eal-time PCR performed as detailed in Zair *et al*, (2011)

Results and Discussion

1. MNU THRESHOLD DOSE RESPONSE IN THE HPRT ASSAY

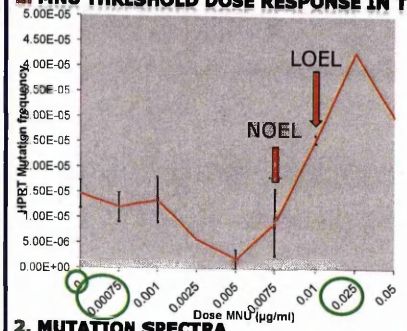

n=3360. Where stdev bars shown n=6720

The cell can tolerate up to 0.0075μg/ml without an increase in mutation frequency (MF) compared to the negative control

Green circles depicts doses selected for sequence analysis

2. MUTATION SPECTRA

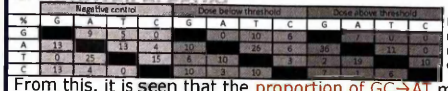

Each mutation as a proportion of total number found for each dose e.g. in negative control G→C mutation=13% of total.

From this, it is seen that the proportion of GC→AT mutations (attributed to O⁶MeG from MNU exposure) mimic the threshold dose response;

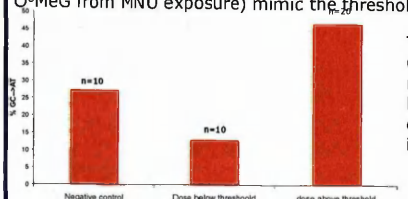

This highlights the role for O⁶MeG in threshold dose-response. Is it being repaired by MGMT at sub-threshold doses? Test this by MGMT inhibition

3. MGMT INHIBITION BY PRE-TREATMENT WITH O⁶BENZYLGUANINE

The effect of MGMT inhibition on percentage GC→AT mutations at the NOEL and Mutation frequency (MF);

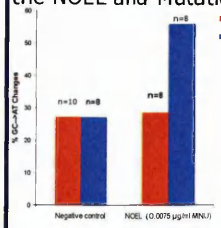

Loss of MGMT increases both the proportion of GC→AT changes and the mutation frequency at the NOEL

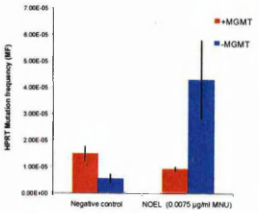

MGMT EXPRESSION OVER THRESHOLD DOSE-RESPONSE

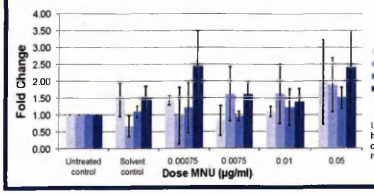

There is no increase in synthesis of new MGMT.

There is a finite amount within the cell and once it is used up it is not replaced and becomes SATURATED

Conclusions

1. The HPRT assay quantifies mutations. We observed that MNU elicits a NOEL at 0.0075μg/ml for mutation induction

2. Sequence analysis at the HPRT locus shows a marked increase in GC→AT changes above the NOEL. This mutation is attributed to methylation at guanine (O⁶MeG) which is repaired by MGMT.

3. Inhibition of MGMT increases MF and GC→AT at sub-threshold doses. This provides evidence that MGMT is the repair protein responsible for MNU threshold by repairing O⁶MeG, thereby preventing GC→AT changes at low doses but not at high doses.

References;
Doak *et al* (2007) *Cancer Res.* **67**;3904-3911
Zair *et al* (2011) *Toxicol. Sci.* **119** (2);346-358

Mutation Research 702 (2010) 189–192

Contents lists available at ScienceDirect

Mutation Research/Genetic Toxicology and Environmental Mutagenesis

journal homepage: www.elsevier.com/locate/gentox
Community address: www.elsevier.com/locate/mutres

Vinblastine and diethylstilboestrol tested in the *in vitro* mammalian cell micronucleus test (MNvit) at Swansea University UK in support of OECD draft Test Guideline 487

George E. Johnson*, Gareth J. Jenkins, Adam D. Thomas, Shareen H. Doak

DNA Damage Group, Institute of Life Science, School of Medicine, Swansea University, Swansea SA2 8PP, United Kingdom

ARTICLE INFO

Article history:
Received 23 July 2009
Accepted 27 July 2009
Available online 8 August 2009

Keywords:
Diethylstilboestrol
Cytotoxicity
In vitro micronucleus test
Vinblastine

ABSTRACT

The known aneugens vinblastine and diethylstilboestrol (DES) were tested in the *in vitro* micronucleus assay, with and without cytokinesis block in Chinese hamster CHO cells, at the laboratories of Swansea University, Swansea, UK. These experiments were carried out to determine the suitability of the cell death and cytostasis measures used in the assay, as recommended in the draft OECD Test Guideline 487, 2007. Both compounds were positive in the assay without cytokinesis block at concentrations giving approximately 50% or less cell death and cytostasis, using relative population doublings and relative increase in cell counts. Moreover, both compounds were positive in the assay with cytokinesis block at concentrations giving approximately 50% cell death and cytostasis, using replicative index. Vinblastine was also positive for mitotic slippage, causing micronuclei in mononucleate cells with cytokinesis block. Relative population doublings and relative increase in cell counts were appropriate measures of cell death and cytostasis for the non-cytokinesis block *in vitro* micronucleus assay. In the cytokinesis blocked micronucleus assay, replicative index and cytokinesis block proliferation index were suitable cell death and cytostasis measures.

1. Introduction

This investigation is part of an inter-laboratory exercise to assess the suitability of the cell death and cytostasis measures used in the *in vitro* micronucleus assay, as recommended in the draft OECD Test Guideline 487, 2007 [1]. The main aim was to establish whether relative population doubling (RPD) and relative increase in cell count (RICC) are appropriate [2].

In Swansea University we tested the known aneugens vinblastine and diethylstilboestrol (DES). Both compounds are mitotic spindle poisons and they were both tested in CHO cells in the presence and absence of cytokinesis block using cytochalasin-B (Cyto-B). RICC, RPD and relative cell counts (RCC) were used to measure cell death and cytostasis in the absence of cytokinesis block, while replicative index (RI) was used in the cytokinesis block micronucleus (CBMN) assay.

2. Materials and methods

Covance Laboratories Limited purchased and supplied the test chemicals for testing in the *in vitro* micronucleus assay in the presence and absence of Cyto-B.

2.1. Test chemicals

Vinblastine and DES were the test chemicals. Vinblastine was dissolved in dimethyl sulfoxide (DMSO) and DES was dissolved in 1% ethanol.

2.2. Cell line and culture conditions

Chinese hamster ovary (CHO) cells were obtained from HPACC (European Collection of Cell Cultures, Health Protection Agency, Porton Down, Salisbury, Wiltshire, UK). The expected karyotype was hypodiploid, modal no. 20, and the average cell doubling time was approximately 14–17 h. Cells were cultured in Ham's F12 (Gibco, Invitrogen UK), 2 mM glutamine (Gibco, Invitrogen UK) 10% foetal bovine serum (FBS, Sigma–Aldrich) and maintained at 37 °C in a humidified atmosphere of 5% CO_2 in air.

2.3. Treatment with test chemicals

Six-well treatment plates were set up that contained 5×10^4 cells/mL in each well, suspended in 3 mL culture medium, and these were treated with vinblastine for 3 h followed by 21 h growth, or with DES for 24 h. Test chemicals and solvents were added to the cell cultures at 1% (v/v). Each test agent concentration and solvent control was repeated, with at least duplicate treatment flasks being prepared for each test concentration. 3 μg/mL of Cyto-B was added to each treatment flask at the same time as the test chemical for DES treatment, and for the 21 h growth period for the vinblastine treatment in the CBMN assay. However, Cyto-B was omitted for the non-cytokinesis block method.

2.4. Preparation and scoring of slides for micronuclei determination

Microscope slides were prepared by spinning 1.5×10^4 cells onto their surface in a Cytospin (ThermoShandon; 200 rpm for 8 min). They were air dried, fixed in 90%

* Corresponding author. Tel.: +44 1792 295158.
E-mail address: g.johnson@swansea.ac.uk (G.E. Johnson).

1383-5718/$ – see front matter © 2009 Elsevier B.V. All rights reserved.
doi:10.1016/j.mrgentox.2009.07.014

hanol and stained with Giemsa (CAS number: 51811-82-6). Where possible, a of at least 1000 cell per replicate culture were examined for the presence of ctionuclei. Fisher's exact test was used to determine the significance of the com- ison between treated cultures and negative controls, using $p < 0.05$ or $p < 0.001$ re appropriate (Tables 1 and 2; Figs. 1 and 2).

Methods used to determine cell death and cytostasis in the absence of halasin-B

Methods were as described by Lorge et al. [3] and Kirkland [2], namely:

elative cell count (RCC)
RCC was determined as:

$$\frac{\text{final count treated cultures}}{\text{final count control cultures}} \times 100$$

elative increase in cell count (RICC)
RICC was determined as:

$$\frac{\text{increase in number of cells in treated cultures (final} - \text{starting)}}{\text{increases in number of cells in control cultures (final} - \text{starting)}} \times 100$$

elative population doubling (RPD)
RPD was determined as:

$$\frac{\text{number of population doublings in treated cultures}}{\text{number of population doublings in control cultures}} \times 100$$

ere

$$\text{pulation doubling} = \frac{[\log(\text{post-treatment cell number/initial cell number})]}{\log 2}$$

6. Method used to determine cell death and cytostasis in the presence of ochalasin-B

6.1. Replicative index (RI)
Method was described by Kirsch-Volders et al. [4].
RI was determined as:

$$\frac{\text{No. binucleated cells} + 2 \times \text{no. multinucleate cells})/\text{total number of cells treated cultures}}{\text{No. binucleated cells} + 2 \times \text{no. multinucleate cells})/\text{total number of cells control cultures}} \times 100$$

3. Results

3.1. Vinblastine

Results for vinblastine are shown in Table 1 and Fig. 1. Signif- increases in the number of micronucleated cells were seen concentrations giving approximately 30% or less cell death and yto- tasis as measured by RPD, RCC and RICC, when assessed using he non-blocked micronucleus assay. There were also significant ncreases in both the percentage of micronuclei in binucleate cells %MNBN) and in mononuclear cells (%MNMONO) at 64% cell death

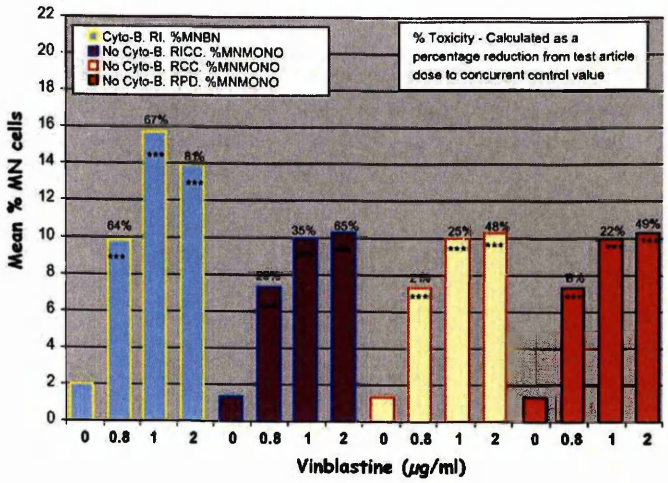

Fig. 1. Vinblastine: 3 + 21 h, -S-9, micronucleus data. Toxicity, cell death and cytostasis; RCC, relative cell count; RICC, relative increase in cell counts; RPD, relative population doubling; RI, replicative index; ***significant increase above control ($p < 0.001$).

and cytostasis, as measured by RI in the cytokinesis block method. When testing vinblastine in CHO cells, RICC and RI overestimated cell death and cytostasis.

3.2. Diethylstilboestrol (DES)

Results for DES are shown in Table 2 and Fig. 2. Significant increases in the number of micronucleated cells were seen at concentrations giving approximately 50% or less cell death and cytostasis as measured by RPD, RCC and RICC, when assessed using the non-cytokinesis blocked method. However, RICC overestimated cell death and cytostasis, and RCC underestimated cell death and cytostasis. There was also a significant increase in %MNBN but not

Table 1
inblastine, 3 + 21-h genotoxicity, cell death and cytostasis results.

Dose (µg/mL)	Day 1 replicate cell counts (×10⁵/mL)	Without Cyto-B				With Cyto-B		
		RPD	RCC	RICC	%MN MONO	RI	%MN BN	%MN MONO
0	1.43 1.35 1.58	0	0	0	1.35	0	2.01	1.47
0.8	1.09 1.21	18	21	29	7.29***	64	9.84***	3.51***
1	0.89 1.28	22	25	35	9.96***	67	15.72***	3.44***
2	0.72 0.80	49	48	65	10.28***	81	13.97***	5.05***

aseline 3.9133 × 10⁴/mL. RCC, relative cell count; RICC, relative increase in cell counts; RPD, relative population doubling; RI, replicative index (binucleates); MN, micronuclei; ONO, mononucleate cells; BN, binucleate cells; NS, not scored.
Significant increase above control ($p < 0.001$).

Table 2
DES, 24-h genotoxicity, cell death and cytostasis results.

Dose (μg/mL)	Day 1 replicate cell counts (×10⁴/mL)	Without Cyto-B				With Cyto-B		
		RPD	RCC	RICC	%MN/MONO	RI	%MN/BN	%MN/MONO
0	4.78 5.64 3.82 5.38	0	0	0	1.36	0	1.79	1.85
2	3.60 4.44	15	18	19	1.28	17	3.33***	0.73
3	4.30 4.32	20	12	25	2.06†	25	5.48***	1.71
4	3.89 3.65	39	23	47	2.87***	32	9.79***	2.10
8	1.07 1.59	NS	78	NS	3.89***	97	9.31***	2.05

Baseline = 2.5 × 10⁴/mL. RCC, relative cell count; RICC, relative increase in cell counts; RPD, relative population doubling; RI, replicative index (binucleates); MN, micronuclei; MONO, mononucleate cells; BN, binucleate cells; NS, not scored.
† $p = 0.05$.
*** Significant increase above control ($p < 0.001$).

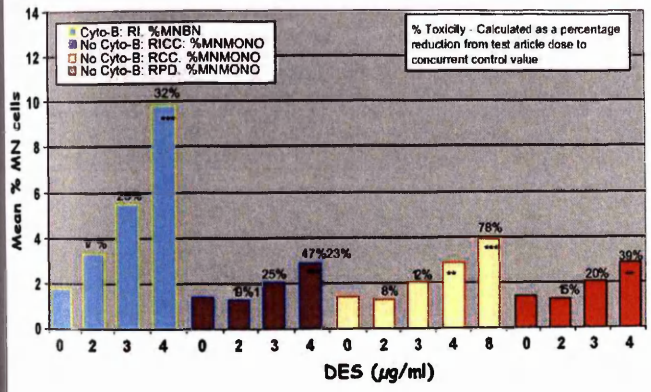

Fig. 2. DES: 24 h, -S-9, micronucleus data. Toxicity, cell death and cytostasis; RCC, relative cell count; RICC, relative increase in cell counts; RPD, relative population doubling; RI, replicative index; ***significant increase above control ($p < 0.001$).

%MNMONO at concentrations giving 50% or less cell death and cytostasis as measured by RI, in the cytokinesis block method.

4. Discussion

Both vinblastine and DES gave significant increases ($p < 0.001$) in micronucleated mononucleated cells at concentrations that produced approximately 50% cell death and cytostasis or less as calculated using RPD, RICC and RCC. Therefore, both vinblastine and DES were positive at an acceptable level of cell viability using any one of these measures of cell death and cytostasis, along with the non-cytokinesis block *in vitro* micronucleus assay. These data are also in line with previous publications which show that RCC generally underestimates cell death and cytostasis, and RICC generally overestimates cell death and cytostasis when the three measures are compared to one another [3,5].

The tests were carried out both with and without cytokinesis block in CHO cells, and both versions of the assay correctly identified vinblastine and DES as genotoxic chemicals. However for DES (Table 2, Fig. 2) the lower doses of 2 and 3 μg/mL were not significant for %MNMONO either with or without cytokinesis block, but were significant at 4 μg/mL without cytokinesis block. As %MNMONO with cytokinesis block are known to be a measure of mitotic slippage [6], these findings indicate that DES does not induce mitotic slippage in CHO cells at the concentrations tested. The low level of %MNMONO without cytokinesis block could also be due to the nature of the assays, as it has been previously stated that "the frequency of MN per cell in binucleate cells is twice that which would be observed in the resulting cells if one allowed the binucleate cell to complete cytokinesis" [7]. Therefore, when testing in the assay without cytokinesis block, "at least twice the number of mononucleate cells should be scored, to observe the same level of MN that would occur in binucleate cells scored in the assay with cytokinesis block" [7]. A further observation is with the RI following treatment with vinblastine, where the level of cell death and cytostasis is overestimated compared to the measures used in the assay without cytokinesis block. This is most likely because by vinblastine blocks mitosis through aberrant centrosomes [8] resulting in an artifactual high level of mononucleate cells compared to binucleate cells. There was also a high level of mitotic slippage induced vinblastine, as seen by significant levels of %MNMONO at each test concentration presented in Table 1 and Fig. 1.

Our findings show that RICC and RPD were appropriate measures of cell death and cytostasis for the non-cytokinesis blocked *in vitro* micronucleus assay when testing the model aneugens vinblastine and DES in CHO cells.

Conflict of interest

None declared.

Acknowledgements

The authors would like to thank Margaret Clatworthy for her excellent technical support during the course of this project.

Grant support: Engineering and Physical Research Council Doctoral Training Account (EPSRC-DTA) and Hoffman-La-Roche.

References

[1] OECD, OECD Guideline for the Testing of Chemicals Draft Proposal for a New Guideline 487: *In Vitro* Micronucleus Test, In Vitro Micronucleus Test, 2007.
[2] D.J. Kirkland, Evaluation of different cytotoxicity measures for the *in vitro* micronucleus test (MNVit): introduction to the collaborative trial, Mutat. Res. 702 (2010) 135–138.
[3] E. Lorge, M. Hayashi, S. Albertini, D. Kirkland, Comparison of different methods for an accurate assessment of cytotoxicity in the in vitro micronucleus test. I. Theoretical aspects, Mutat. Res. 655 (2008) 1–3.
[4] M. Kirsch-Volders, T. Sofuni, M. Aardema, S. Albertini, D. Eastmond, M. Fenech, J.M. Ishidate, S. Kirchner, E. Lorge, Corrigendum to "Report from the in vitro micronucleus assay working group" [Mutat. Res. 540 (2003) 153–163], Mutat. Res./Genet. Toxicol. Environ. Mutagen. 564 (2004) 97–100.

M.D. Fellows, M.R. O'Donovan, E. Lorge, D. Kirkland, Comparison of different methods for an accurate assessment of cytotoxicity in the in vitro micronucleus test. II. Practical aspects with toxic agents, Mutat. Res. 655 (2008) 4–21.
A. Elhajouji, C. Monica, M. Kirsch-Volders, Spindle poisons can induce polyploidy by mitotic slippage and micronucleate mononucleates in the cytokinesis-block assay, Mutagenesis 13 (1998) 193–198.
[7] M. Fenech, The advantages and disadvantages of the cytokinesis-block micronucleus method, Mutat. Res./Genet. Toxicol. Environ. Mutagen. 392 (1997) 11–18.
[8] M.A. Jordan, D. Thrower, Wilson L., Effects of vinblastine, podophyllotoxin and nocodazole on mitotic spindles. Implications for the role of microtubule dynamics in mitosis, J. Cell Sci. 102 (Pt 3) (1992) 401–416.

Glossary

Alkylating agents-A group of hazardous compounds in the environment. Upon reaction in aqueous solutions, or to DNA or proteins transfer an alkyl group (e.g. MNU).

Alkyl group-A functional group made of only carbon and hydrogen present on organic compounds e.g. Methyl CH_3.

Alkylation-A chemical reaction whereby an alkyl group replaces hydrogen of an organic structure.

Assay-a structured experiment.

Base substitution-A gene level mutation that changes the sequence of DNA by changing the nucleotide. The open reading frame is not affected. Can be caused by polymerase error.

DNA damage-Reversible chemical or physical modification to a nucleotide often affecting its base-pairing capabilities.

Hormesis (J-shaped)-A non-linear dose-response where low dose has the opposite effect to high dose. This can be observed as low dose benefit and high dose adversity.

HPRT assay-A genotoxicity assay used to quantify the number of HPRT mutants in a population at increasing concentrations of test chemical.

Methyl nitrosourea (MNU)-A mutagenic alkylating agent that causes comparatively more O^6Methylguanine than other alkylating agents.

Methylguanine methyltransferase (MGMT)-A DNA repair protein that removes methyl group from O^6MeG stocihimoetrically. Thereby preventing GC→AT changes. Following the abstraction of methyl group to an internal cysteine (cys145) target MGMT for proteolytic degradation.

Mutation-A permanent change to DNA e.g. **base substitution**, anueploidy or structural aberration

Mutation spectra-Identifying the kinds, frequency and location of mutations at a defined locus.

Non-linear dose-response-A dose response where response (e.g. mutant frequency) does not increase proprtinally with dose. e.g. **Threshold dose response** and **hormesis.**

N7-Methlyguanine (N7MeG)-A clastogenic and mutagenic adduct that is formed naturally in high levels and from alkylating exposure without adverse consequence. Severes as a biomarker of exposure to alkylating agents.

O^6Methylguanine-A miscoding adduct formed by MNU and, to a lesser extent, other alkylating agents. Causes GC→AT transitions.

Pre-mutagenic lesion-Reversible DNA damage that requires DNA replication to be fixed as permanent mutation.

Threshold dose response-A threshold in concentration needs to be exceeded for an increase in adverse response. Represented as a statistical NO(A)EL.

References.

Aardema, M. J., Barnett, B. C., Khambatta, Z., Reisinger, K., Ouedraogo-Arras, G., Faquet, B., Ginestet, A. C., Mun, G. C., Dahl, E. L., Hewitt, N. J., Corvi, R. & Curren, R. D. 2010. International prevalidation studies of the EpiDerm 3D human reconstructed skin micronucleus (RSMN) assay: transferability and reproducibility. *Mutat Res,* **701,** 123-31.

Aburatani, H. 2011. [Cancer genome analysis through next-generation sequencing]. *Gan To Kagaku Ryoho,* **38,** 1-6.

Adams, W. T. & Skopek, T. R. 1987. Statistical test for the comparison of samples from mutational spectra.*J Mol Biol.* **194(3)**:391-6.

Agency, E. P. 2005.

Ahn, J. & Lee., J. 2008. X Chromosome: X Inactivation. *Nature Education* **1**.

Aidoo, A., Morris, S. M. & Casciano, D. A. 1997. Development and utilization of the rat lymphocyte hprt mutation assay. *Mutat Res,* **387,** 69-88.

Albertini, R. J. 2001. HPRT mutations in humans: biomarkers for mechanistic studies. *Mutat Res,* **489,** 1-16.

Albertini, R. J., Nicklas, J. A. & O'neill, J. P. 1993. Somatic cell gene mutations in humans: biomarkers for genotoxicity. *Environ Health Perspect,* **101 Suppl 3,** 193-201.

Ames, B. N. 1979. Identifying environmental chemicals causing mutations and cancer. *Science,* **204,** 587-93.

Ames, B. N. 1989. Endogenous DNA damage as related to cancer and aging. *Mutat Res,* **214,** 41-6.

Ames, B. N. & Gold, L. S. 1991. Endogenous mutagens and the causes of aging and cancer. *Mutat Res,* **250,** 3-16.

Ammenheuser, M. M., Au, W. W., Whorton, E. B., Jr., Belli, J. A. & Ward, J. B., Jr. 1991. Comparison of hprt variant frequencies and chromosome aberration frequencies in lymphocytes from radiotherapy and chemotherapy patients: a prospective study. *Environ Mol Mutagen,* **18,** 126-35.

Anderson, D., Green, M. H., Mattern, I. E. & Godley, M. J. 1984. An international collaborative study of 'genetic drift' in Salmonella typhimurium strains used in the Ames test. *Mutat Res.* **130(1)**:1-10.

Anderson, T. J. & Burdon, R. H. 1970. N-methyl-N'-nitro-N-nitrosoguanidine: reactions of possible significance to biological activity with mammalian cells. *Cancer Res,* **30,** 1773-

81.

Androutsopoulos, V. P., Tsatsakis, A. M. & Spandidos, D. A. 2009. Cytochrome P450 CYP1A1: wider roles in cancer progression and prevention. *BMC Cancer,* **9,** 187.

Androutsos, G. 2006. The outstanding British surgeon Percivall Pott (1714-1789) and the first description of an occupational cancer. *J BUON,* **11,** 533-9.

Appleyard, R. C., Burkhardt, D., Ghosh, P., Read, R., Cake, M., Swain, M. V. & Murrell, G. A. 2003. Topographical analysis of the structural, biochemical and dynamic biomechanical properties of cartilage in an ovine model of osteoarthritis. *Osteoarthritis Cartilage,* **11,** 65-77.

Aquilina, G., Biondo, R., Dogliotti, E., Meuth, M. & Bignami, M. 1992. Expression of the endogenous O6-methylguanine-DNA-methyltransferase protects Chinese hamster ovary cells from spontaneous G:C to A:T transitions. *Cancer Res,* **52,** 6471-5.

Aquilina, G., Ceccotti, S., Martinelli, S., Hampson, R. & Bignami, M. 1998. N-(2-chloroethyl)-N'-cyclohexyl-N-nitrosourea sensitivity in mismatch repair-defective human cells. *Cancer Res,* **58,** 135-41.

Arlett, C. F., Turnbull, D., Harcourt, S. A., Lehmann, A. R. & Colella, C. M. 1975. A comparison of the 8-azaguanine and ouabain-resistance systems for the selection of induced mutant Chinese hamster cells. *Mutat Res,* **33,** 261-78.

Ashby, J. & Paton, D. 1993. The influence of chemical structure on the extent and sites of carcinogenesis for 522 rodent carcinogens and 55 different human carcinogen exposures. *Mutat Res,* **286,** 3-74.

Ashihara, H. & Suzuki, T. 2004. Distribution and biosynthesis of caffeine in plants. *Front Biosci,* **9,** 1864-76.

Au, W.W. 2007. Usefulness of biomarkers in population studies: from exposure to susceptibility and to prediction of cancer. *Int J Hyg Environ Health.* **210(3-4)**:239-46.

Aubrecht, J., Goad, M. E. & Schiestl, R. H. 1997. Tissue specific toxicities of the anticancer drug 6-thioguanine is dependent on the Hprt status in transgenic mice. *J Pharmacol Exp Ther,* **282,** 1102-8.

Ayi, T. C., Oh, H. K., Lee, T. K. & Li, B. F. 1994. A method for simultaneous identification of human active and active-site alkylated O6-methylguanine-DNA methyltransferase and

its possible application for monitoring human exposure to alkylating carcinogens. *Cancer Res,* **54,** 3726-31.

Bacolod, M. D., Johnson, S. P., Pegg, A. E., Dolan, M. E., Moschel, R. C., Bullock, N. S., Fang, Q., Colvin, O. M., Modrich, P., Bigner, D. D. & Friedman, H. S. 2004. Brain tumor cell lines resistant to O6-benzylguanine/1,3-bis(2-chloroethyl)-1-nitrosourea chemotherapy have O6-alkylguanine-DNA alkyltransferase mutations. *Mol Cancer Ther,* **3,** 1127-35.

Baillie, T. A., Cayen, M. N., Fouda, H., Gerson, R. J., Green, J. D., Grossman, S. J., Klunk, L. J., Leblanc, B., Perkins, D. G. & Shipley, L. A. 2002. Drug metabolites in safety testing. *Toxicol Appl Pharmacol,* **182,** 188-96.

Baker, M. S. & Topal, M. D. 1983. Reaction of dATP with N-methyl-N-nitrosourea in vitro. *J Biol Chem,* **258,** 9729-32.

Balajee, A. S. & Geard, C. R. 2004. Replication protein A and gamma-H2AX foci assembly is triggered by cellular response to DNA double-strand breaks. *Exp Cell Res,* 300, 320-34.

Banoub, J. H. & Limbach, P. A. 2009. In Mass Spectrometry of Nucleosides and Nucleic Acids .

Barros, C. S., Calabrese, B., Chamero, P., Roberts, A. J., Korzus, E., Lloyd, K., Stowers, L., Mayford, M., Halpain, S. & Muller, U. 2009. Impaired maturation of dendritic spines without disorganization of cortical cell layers in mice lacking NRG1/ErbB signaling in the central nervous system. *Proc Natl Acad Sci U S A,* **106,** 4507-12.

Bartsch, H., Nair, U., Risch, A., Rojas, M., Wikman, H. & Alexandrov, K. 2000. Genetic polymorphism of CYP genes, alone or in combination, as a risk modifier of tobacco-related cancers. *Cancer Epidemiol Biomarkers Prev,* **9,** 3-28.

Batts, E. D., Maisel, C., Kane, D., Liu, L., Fu, P., O'brien, T., Remick, S., Bahlis, N. & Gerson, S. L. 2007. O6-benzylguanine and BCNU in multiple myeloma: a phase II trial. *Cancer Chemother Pharmacol,* **60,** 415-21.

Becker, K., Dosch, J., Gregel, C. M., Martin, B. A. & Kaina, B. 1996. Targeted expression of human O(6)-methylguanine-DNA methyltransferase (MGMT) in transgenic mice protects against tumor initiation in two-stage skin carcinogenesis. *Cancer Res.* **56(14)**:3244-9.

Becker, K., Gregel, C., Fricke, C., Komitowski, D., Dosch, J. & Kaina, B. 2003. DNA repair protein MGMT protects against N-methyl-N-nitrosourea-induced conversion of benign into malignant tumors. *Carcinogenesis,* **24,** 541-6.

Beletskii, A. & Bhagwat, A. S. 1996. Transcription-induced mutations: increase in C to T mutations in the nontranscribed strand during transcription in Escherichia coli. *Proc Natl Acad Sci U S A,* **93,** 13919-24.

Benigni, R. & Bossa, C. 2008. Structure alerts for carcinogenicity, and the Salmonella assay system: a novel insight through the chemical relational databases technology. *Mutat Res,* **659,** 248-61.

Benigni, R., Palombo, F. & Dogliotti, E. 1992. Multivariate statistical analysis of mutational spectra of alkylating agents. *Mutat Res,* **267,** 77-88.

Beranek, D. T. 1990. Distribution of methyl and ethyl adducts following alkylation with monofunctional alkylating agents. *Mutation Research/Fundamental and Molecular Mechanisms of Mutagenesis,* **231,** 11-30.

Beranek, D. T., Heflich, R. H., Kodell, R. L., Morris, S. M. & Casciano, D. A. 1983. Correlation between specific DNA-methylation products and mutation induction at the HGPRT locus in Chinese hamster ovary cells. *Mutat Res,* **110,** 171-80.

Beranek, D. T., Weis, C. C. & Swenson, D. H. 1980. A comprehensive quantitative analysis of methylated and ethylated DNA using high pressure liquid chromatography. *Carcinogenesis,* **1,** 595-606.

Berg, S. L., Murry, D. J., Mccully, C. L., Godwin, K. & Balis, F. M. 1998. Pharmacokinetics of O6-benzylguanine and its active metabolite 8-oxo-O6-benzylguanine in plasma and cerebrospinal fluid after intrathecal administration of O6-benzylguanine in the nonhuman primate. *Clin Cancer Res,* **4,** 2891-4.

Berger, E. Y., Farber, S. J. & Earle, D. P., Jr. 1948. Comparison of the constant infusion and urine collection techniques for the measurement of renal function. *J Clin Invest,* **27,** 710-6.

Berger, E. Y., Farber, S. J., Earle, D. P. & Jackenthal, R. 1948. Comparison of the Constant Infusion and Urine Collection Techniques for the Measurement of Renal Function. *J Clin Invest,* **27,** 710-6.

Bernauer, U., Oberemm, A., Madle, S. & Gundert-Remy, U. 2005. The use of in vitro data in risk assessment. *Basic Clin Pharmacol Toxicol,* **96,** 176-81.

Bhat, P. V. & Lacroix, A. 1989. Metabolism of retinol and retinoic acid in N-methyl-N-nitrosourea-induced mammary carcinomas in rats. *Cancer Res,* **49,** 139-44.

Blakey, D., Galloway, S. M., Kirkland, D. J. & Macgregor, J. T. 2008. Regulatory aspects of genotoxicity testing: from hazard identification to risk assessment. *Mutat Res,* **657,** 84-90.

Blough, M. D., Zlatescu, M. C. & Cairncross, J. G. 2007. O6-methylguanine-DNA methyltransferase regulation by p53 in astrocytic cells. *Cancer Res,* **67,** 580-4.

Bobola, M. S., Berger, M. S., Ellenbogen, R. G., Roberts, T. S., Geyer, J. R. & Silber, J. R. 2001. O6-Methylguanine-DNA methyltransferase in pediatric primary brain tumors: relation to patient and tumor characteristics. *Clin Cancer Res,* **7,** 613-9.

Bobola, M. S., Blank, A., Berger, M. S. & Silber, J. R. 2007. O6-methylguanine-DNA methyltransferase deficiency in developing brain: implications for brain tumorigenesis. *DNA Repair (Amst),* **6,** 1127-33.

Bobola, M. S., Tseng, S. H., Blank, A., Berger, M. S. & Silber, J. R. 1996. Role of O6-methylguanine-DNA methyltransferase in resistance of human brain tumor cell lines to the clinically relevant methylating agents temozolomide and streptozotocin. *Clin Cancer Res,* **2,** 735-41.

Bocangel, D., Sengupta, S., Mitra, S. & Bhakat, K. K. 2009. p53-Mediated down-regulation of the human DNA repair gene O6-methylguanine-DNA methyltransferase (MGMT) via interaction with Sp1 transcription factor. *Anticancer Res,* **29,** 3741-50.

Boffetta, P. & Kogevinas, M. 1999. Introduction: Epidemiologic research and prevention of occupational cancer in Europe. *Environ Health Perspect,* **107 Suppl 2,** 229-31.

Bohgaki, T., Bohgaki, M. & Hakem, R. 2010. DNA double-strand break signaling and human disorders. *Genome Integr,* **1,** 15.

Boiteux, S. & Guillet, M. 2004. Abasic sites in DNA: repair and biological consequences in Saccharomyces cerevisiae. *DNA Repair (Amst),* **3,** 1-12.

Boldogh, I., Ramana, C. V., Chen, Z., Biswas, T., Hazra, T. K., Grosch, S., Grombacher, T., Mitra, S. & Kaina, B. 1998. Regulation of expression of the DNA repair gene O6-methylguanine-DNA methyltransferase via protein kinase C-mediated signaling. *Cancer Res,* **58,** 3950-6.

Bolt, H. M., Foth, H., Hengstler, J. G. & Degen, G. H. 2004. Carcinogenicity categorization of chemicals-new aspects to be considered in a European perspective. *Toxicol Lett,* **151,** 29-41.

Bol, S. A., van Steeg, H., Jansen, J. G., Van Oostrom, C., de Vries, A., de Groot, A. J., Tates, A. D., Vrieling, H., van Zeeland, A. A. & Mullenders, L. H. 1998. Elevated frequencies of benzo(a)pyrene-induced Hprt mutations in internal tissue of XPA-deficient mice. *Cancer Res.* **58(13)**:2850-6.

Boon, E. M., Ceres, D. M., Drummond, T. G., Hill, M. G. & Barton, J. K. 2000. Mutation detection by electrocatalysis at DNA-modified electrodes. *Nat Biotechnol,* **18,** 1096-100.

Bos, J. L. 1989. ras oncogenes in human cancer: a review. *Cancer Res,* **49,** 4682-9.

Boue, J., Boue, A. & Lazar, P. 1975. Retrospective and prospective epidemiological studies of 1500 karyotyped spontaneous human abortions. *Teratology,* **12,** 11-26.

Bouwens-Rombouts, A. G., Van Den Boogaard, M. J., Puig, J. G., Mateos, F. A., Hennekam, R. C. & Tilanus, M. G. 1993. Identification of two new nucleotide mutations (HPRTUtrecht and HPRTMadrid) in exon 3 of the human hypoxanthine-guanine phosphoribosyltransferase (HPRT) gene. *Hum Genet,* **91,** 451-4.

Boveri,T. 1914. *Zur Frage der Entsehung Maligner Tumouren.* Fisher, Jena, Germany.

Bradley, W. E., Gareau, J. L., Seifert, A. M. & Messing, K. 1987. Molecular characterization of 15 rearrangements among 90 human in vivo somatic mutants shows that deletions predominate. *Mol Cell Biol,* **7,** 956-60.

Brown, K., Buchmann, A. & Balmain, A. 1990. Carcinogen-induced mutations in the mouse c-Ha-ras gene provide evidence of multiple pathways for tumor progression. *Proc Natl Acad Sci U S A,* **87,** 538-42.

Brown, V. K., Robinson, J. & Stevenson, D. E. 1963. A Note on the Toxicity and Solvent Properties of Dimethyl Sulphoxide. *J Pharm Pharmacol,* **15,** 688-92.

Bryce, S. M., Avlasevich, S. L., Bemis, J. C., Phonethepswath, S. & Dertinger, S. D. 2010. Miniaturized flow cytometric in vitro micronucleus assay represents an efficient tool for comprehensively characterizing genotoxicity dose-response relationships. *Mutat Res,* **703,** 191-9.

Bugni, J. M., Meira, L. B. & Samson, L. D. 2009. Alkylation-induced colon tumorigenesis in mice deficient in the Mgmt and Msh6 proteins. *Oncogene,* **28,** 734-41.

Cabelof, D. C., Raffoul, J. J., Yanamadala, S., Guo, Z. & Heydari, A. R. 2002. Induction of DNA polymerase beta-dependent base excision repair in response to oxidative stress in vivo. *Carcinogenesis,* **23,** 1419-25.

Cairns, J. 1980. Efficiency of the adaptive response of Escherichia coli to alkylating agents. *Nature,* **286,** 176-8.

Calabrese, E. 2009. Hormesis, non-linearity, and risk communication. *Hum Exp Toxicol,* **28,** 5-6.

Calabrese, E. J. 2004. Hormesis: a revolution in toxicology, risk assessment and medicine. *EMBO Rep,* **5 Spec No,** S37-40.

Calabrese, E. J. 2005. Paradigm lost, paradigm found: the re-emergence of hormesis as a fundamental dose response model in the toxicological sciences. *Environ Pollut,* **138,** 379-411.

Calabrese, E. J. 2009. Hormesis: a conversation with a critic. *Environ Health Perspect,* **117,** 1339-43.

Calabrese, E. J. 2009. Getting the dose-response wrong: why hormesis became marginalized and the threshold model accepted. *Arch Toxicol,* **83,** 227-47.

Calabrese, E. J. 2009. The road to linearity: why linearity at low doses became the basis for carcinogen risk assessment. *Arch Toxicol,* **83,** 203-25.

Calabrese, E. J. & Baldwin, L. A. 2000. Radiation hormesis: its historical foundations as a biological hypothesis. *Hum Exp Toxicol,* **19,** 41-75.

Calabrese, E. J. & Baldwin, L. A. 2001. The frequency of U-shaped dose responses in the toxicological literature. *Toxicol Sci,* **62,** 330-8.

Calabrese, E. J. & Blain, R. 2005. The occurrence of hormetic dose responses in the toxicological literature, the hormesis database: an overview. *Toxicol Appl Pharmacol.* **202(3)**:289-301.

Calabrese, E. J., Stanek, E. J., 3rd & Nascarella, M. A. 2011. Evidence for hormesis in mutagenicity dose-response relationships. *Mutat Res,* **726,** 91-7.

Calabrese, E. J., Staudenmayer, J. W. & Stanek, E. J. 2006. Drug development and hormesis: changing conceptual understanding of the dose response creates new challenges and opportunities for more effective drugs. *Curr Opin Drug Discov Devel,* **9,** 117-23.

Calabrese, E. J., Staudenmayer, J. W., Stanek, E. J., 3rd & Hoffmann, G. R. 2006. Hormesis outperforms threshold model in National Cancer Institute antitumor drug screening database. *Toxicol Sci,* **94,** 368-78.

Calabrese, V., Cornelius, C., Dinkova-Kostova, A. T. & Calabrese, E. J. 2009. Vitagenes, cellular stress response, and acetylcarnitine: relevance to hormesis. *Biofactors,* **35,** 146-

60.

Cariello, N. F., Scott, J. K., Kat, A. G., Thilly, W. G. & Keohavong, P. 1988. Resolution of a missense mutant in human genomic DNA by denaturing gradient gel electrophoresis and direct sequencing using in vitro DNA amplification: HPRT Munich. *Am J Hum Genet,* **42,** 726-34.

Cariello, N. F. & Skopek, T. R. 1993. In vivo mutation at the human HPRT locus. *Trends Genet,* **9,** 322-6.

Cariello, N. F. & Skopek, T. R. 1993. Mutational analysis using denaturing gradient gel electrophoresis and PCR. *Mutat Res,* **288,** 103-12.

Cariello, N. F., Piegorsch, W. W., Adams, W. T. & Skopek, T. R. 1994. Computer program for the analysis of mutational spectra: application to p53 mutations. *Carcinogenesis.* **15(10)**:2281-5.

Cariello, N. F., Wilson, J. D., Britt, B. H., Wedd, D. J., Burlinson, B. & Gombar, V. 2002. Comparison of the computer programs DEREK and TOPKAT to predict bacterial mutagenicity. Deductive Estimate of Risk from Existing Knowledge. Toxicity Prediction by Komputer Assisted Technology. *Mutagenesis,* **17,** 321-9.

Casanova, M. & Heck Hd, A. 1987. Further studies of the metabolic incorporation and covalent binding of inhaled [3H]- and [14C]formaldehyde in Fischer-344 rats: effects of glutathione depletion. *Toxicol Appl Pharmacol,* **89,** 105-21.

Casciano, D. A., Aidoo, A., Chen, T., Mittelstaedt, R. A., Manjanatha, M. G. & Heflich, R. H. 1999. Hprt mutant frequency and molecular analysis of Hprt mutations in rats treated with mutagenic carcinogens. *Mutat Res,* **431,** 389-95.

Cathcart, R., Schwiers, E., Saul, R. L. & Ames, B. N. 1984. Thymine glycol and thymidine glycol in human and rat urine: a possible assay for oxidative DNA damage. *Proc Natl Acad Sci U S A,* **81,** 5633-7.

Cavalieri, E., Frenkel, K., Liehr, J. G., Rogan, E. & Roy, D. 2000. Estrogens as endogenous genotoxic agents--DNA adducts and mutations. *J Natl Cancer Inst Monogr,* 75-93.

Cavalieri, E., Frenkel, K., Liehr, J. G., Rogan, E. & Roy, D. 2000. Estrogens as endogenous genotoxic agents--DNA adducts and mutations. *J Natl Cancer Inst Monogr,* 75-93.

I. G. O. H. R. F. 2003.

Chao, M. R., Wang, C. J., Yang, H. H., Chang, L. W. & Hu, C. W. 2005. Rapid and

sensitive quantification of urinary N7-methylguanine by isotope-dilution liquid chromatography/electrospray ionization tandem mass spectrometry with on-line solid-phase extraction. *Rapid Commun Mass Spectrom.* **19(17)**:2427-32.

Chen, J. M., Zhang, Y. P., Moschel, R. C. & Ikenaga, M. 1993. Depletion of O6-methylguanine-DNA methyltransferase and potentiation of 1,3-bis(2-chloroethyl)-1-nitrosourea antitumor activity by O6-benzylguanine in vitro. *Carcinogenesis.* **14(5)**:1057-60.

Chen, G., Xu, Y., Xu, L., Zheng, Y., Steinberg, C. E. & Kettrup, A. 1998. Glutathione S-transferase activity in aquatic macrophytes with emphasis on habitat dependence. *Ecotoxicol Environ Saf,* **40,** 226-33.

Chen, T., Harrington-Brock, K. & Moore, M. M. 2002. Mutant frequency and mutational spectra in the Tk and Hprt genes of N-ethyl-N-nitrosourea-treated mouse lymphoma cellsdagger. *Environ Mol Mutagen,* **39,** 296-305.

Chen, T., Harrington-Brock, K. & Moore, M. M. 2002. Mutant frequency and mutational spectra in the Tk and Hprt genes of N-ethyl-N-nitrosourea-treated mouse lymphoma cellsdagger. *Environ Mol Mutagen,* **39,** 296-305.

Chen, T. & Li, E. 2004. Structure and function of eukaryotic DNA methyltransferases. *Curr Top Dev Biol,* **60,** 55-89.

Cheng, A., Magdaleno, S. & Vlassov, A. V. 2011. Optimization of transfection conditions and analysis of siRNA potency using real-time PCR. *Methods Mol Biol,* **764,** 199-213.

Cheshier, S. H., Morrison, S. J., Liao, X. & Weissman, I. L. 1999. *In vivo* proliferation and cell cycle kinetics of long-term self-renewing hematopoietic stem cells. *Proc Natl Acad Sci U S A.* **96(6)**: 3120–3125.

Chesis, P. L., Levin, D. E., Smith, M. T., Ernster, L. & Ames, B. N. 1984. Mutagenicity of quinones: pathways of metabolic activation and detoxification. *Proc Natl Acad Sci U S A,* **81,** 1696-700.

Chiang, S. Y., Swenberg, J. A., Weisman, W. H. & Skopek, T. R. 1997. Mutagenicity of vinyl chloride and its reactive metabolites, chloroethylene oxide and chloroacetaldehyde, in a metabolically competent human B-lymphoblastoid line. *Carcinogenesis.* **18(1)**:31-6.

Chiou, C. C., Chang, P. Y., Chan, E. C., Wu, T. L., Tsao, K. C. & Wu, J. T. 2003.

Urinary 8-hydroxydeoxyguanosine and its analogs as DNA marker of oxidative stress: development of an ELISA and measurement in both bladder and prostate cancers.*Clin Chim Acta.* **334(1-2)**:87-94.

Chung, Y. H., Youn, J., Choi, Y., Paik, D. J. & Cho, Y. J. 2001. Requirement of de novo protein synthesis for aminopterin-induced apoptosis in a mouse myeloma cell line. *Immunol Lett,* **77,** 127-31.

Claycamp, H. G. 1992. Phenol sensitization of DNA to subsequent oxidative damage in 8-hydroxyguanine assays. *Carcinogenesis,* **13,** 1289-92.

Coles, B. F. & Kadlubar, F. F. 2003. Detoxification of electrophilic compounds by glutathione S-transferase catalysis: determinants of individual response to chemical carcinogens and chemotherapeutic drugs? *Biofactors,* **17,** 115-30.

Colella, C. M., Rainaldi, G. & Piras, A. 1983. 8-Azaguanine versus 6-thioguanine: influence on frequency and expression time of induced HGPRT- mutations in Chinese hamster V79 cells. *Mutat Res.* **107(2)**:397-411.

Collins, A. R., Dusinska, M., Gedik, C. M. & Stetina, R. 1996. Oxidative damage to DNA: do we have a reliable biomarker? *Environ Health Perspect,* **104 Suppl 3,** 465-9.

Conolly, R. B. & Lutz, W. K. 2004. Nonmonotonic dose-response relationships: mechanistic basis, kinetic modeling, and implications for risk assessment. *Toxicol Sci,* **77,** 151-7.

Cooper, D. N. & Krawczak, M. 1990. The mutational spectrum of single base-pair substitutions causing human genetic disease: patterns and predictions. *Hum Genet,* **85,** 55-74.

Cooper, D. N. & Youssoufian, H. 1988. The CpG dinucleotide and human genetic disease. *Hum Genet,* **78,** 151-5.

Cooper, D. P., Griffin, K. A. & Povey, A. C. 1992. Immunoaffinity purification combined with 32P-postlabelling for the detection of O6-methylguanine in DNA from human tissues. *Carcinogenesis,* **13,** 469-75.

Corso, C. & Parry, E. M. 1999. The application of comparative genomic hybridization and fluorescence in situ hybridization to the characterization of genotoxicity screening tester strains AHH-1 and MCL-5. *Mutagenesis,* **14,** 417-26.

Corso, C. & Parry, J. M. 2004. Comparative genomic hybridization analysis of N-methyl-N'-nitrosoguanidine-induced rat gastrointestinal tumors discloses a cytogenetic fingerprint. *Environ Mol Mutagen,* **43,** 20-7.

Coulondre, C., Miller, J. H., Farabaugh, P. J. & Gilbert, W. 1978. Molecular basis of base substitution hotspots in Escherichia coli. *Nature,* **274,** 775-80.

Cox, C. 1987. Threshold dose-response models in toxicology. *Biometrics,* **43,** 511-23.

Crespi, C. L., Gonzalez, F. J., Steimel, D. T., Turner, T. R., Gelboin, H. V., Penman, B. W. & Langenbach, R. 1991. A metabolically competent human cell line expressing five cDNAs encoding procarcinogen-activating enzymes: application to mutagenicity testing. *Chem Res Toxicol,* **4,** 566-72.

Crespi, C. L. & Thilly, W. G. 1984. Assay for gene mutation in a human lymphoblast line, AHH-1, competent for xenobiotic metabolism. *Mutat Res,* **128,** 221-30.

Crone, T. M., Goodtzova, K., Edara, S. & Pegg, A. E. 1994. Mutations in human O6-alkylguanine-DNA alkyltransferase imparting resistance to O6-benzylguanine. *Cancer Res,* **54,** 6221-7.

Crone, T. M., Goodtzova, K. & Pegg, A. E. 1996. Amino acid residues affecting the activity and stability of human O6-alkylguanine-DNA alkyltransferase. *Mutat Res,* **363,** 15-25.

Crump, K. S., Hoel, D. G., Langley, C. H. & Peto, R. 1976. Fundamental carcinogenic processes and their implications for low dose risk assessment. *Cancer Res,* **36,** 2973-9.

Curry, J., Karnaoukhova, L., Guenette, G. C. & Glickman, B. W. 1999. Influence of sex, smoking and age on human hprt mutation frequencies and spectra. *Genetics,* **152,** 1065-77.

da Cruz, A. D., Glickman, B. W. 1997. Nature of mutation in the human hprt gene following in vivo exposure to ionizing radiation of cesium-137. *Environ Mol Mutagen.* **30(4)**:385-95.

Daley, G. Q., Van Etten, R. A. & Baltimore, D. 1990. Induction of chronic myelogenous leukemia in mice by the P210bcr/abl gene of the Philadelphia chromosome. *Science,* **247,** 824-30.

Daniels, D. S., Mol, C. D., Arvai, A. S., Kanugula, S., Pegg, A. E. & Tainer, J. A. 2000. Active and alkylated human AGT structures: a novel zinc site, inhibitor and extrahelical base binding. *EMBO J,* **19,** 1719-30.

Davies, M. J., Phillips, B. J. & Rumsby, P. C. 1993. Molecular analysis of mutations at the tk locus of L5178Y mouse-lymphoma cells induced by ethyl methanesulphonate and mitomycin C. *Mutat Res,* **290,** 145-53.

Davis, J. M. & Svendsgaard, D. J. 1990. U-shaped dose-response curves: their occurrence and implications for risk assessment. *J Toxicol Environ Health,* **30,** 71-83.

Davis, W., Hewer, A., Rajkowski, K. M., Meinl, W., Glatt, H. & Phillips, D. H. 2000. Sex differences in the activation of tamoxifen to DNA binding species in rat liver in vivo and in rat hepatocytes in vitro: role of sulfotransferase induction. *Cancer Res,* **60,** 2887-91.

De Bont, R. & Van Larebeke, N. 2004. Endogenous DNA damage in humans: a review of quantitative data. *Mutagenesis,* **19,** 169-85.

De Groot, A. J., Jansen, J. G., Van Valkenburg, C. F. & Van Zeeland, A. A. 1994. Molecular dosimetry of 7-alkyl- and O6-alkylguanine in DNA by electrochemical detection. *Mutat Res,* **307,** 61-6.

De Jong, P. J., Grosovsky, A. J. & Glickman, B. W. 1988. Spectrum of spontaneous mutation at the APRT locus of Chinese hamster ovary cells: an analysis at the DNA sequence level. *Proc Natl Acad Sci U S A,* **85,** 3499-503.

De Moura Gallo, C. V., Azevedo, E. S. M. G., De Moraes, E., Olivier, M. & Hainaut, P. 2005. TP53 mutations as biomarkers for cancer epidemiology in Latin America: current knowledge and perspectives. *Mutat Res,* **589,** 192-207.

Degawa, M., Stern, S. J., Martin, M. V., Guengerich, F. P., Fu, P. P., Ilett, K. F., Kaderlik, R. K. & Kadlubar, F. F. 1994. Metabolic activation and carcinogen-DNA adduct detection in human larynx. *Cancer Res,* **54,** 4915-9.

Della Puppa, A., Persano, L., Masi, G., Rampazzo, E., Sinigaglia, A., Pistollato, F., Denaro, L., Barzon, L., Palu, G., Basso, G., Scienza, R. & D'avella, D. 2012. MGMT expression and promoter methylation status may depend on the site of surgical sample collection within glioblastoma: a possible pitfall in stratification of patients? *J Neurooncol,* **106,** 33-41.

Demarini, D. M., Brockman, H. E., De Serres, F. J., Evans, H. H., Stankowski, L. F., Jr. & Hsie, A. W. 1989. Specific-locus mutations induced in eukaryotes (especially mammalian cells) by radiation and chemicals: a perspective. *Mutat Res,* **220,** 11-29.

Dempsey, J. L., Seshadri, R. S. & Morley, A. A. 1985. Increased mutation frequency following treatment with cancer chemotherapy. *Cancer Res,* **45,** 2873-7.

Diamond, L., Kruszewski, F. & Baird, W. M. 1982. Expression time for benzo[a]pyrene-induced 6-thioguanine-resistant mutations in V79 Chinese hamster cells. *Mutat Res,* **95,** 353-62.

Dijt, F. J., Fichtinger-Schepman, A. M., Berends, F. & Reedijk, J. 1988. Formation and repair of

cisplatin-induced adducts to DNA in cultured normal and repair-deficient human fibroblasts. *Cancer Res,* **48,** 6058-62.

Doak, S. H., Jenkins, G. J., Johnson, G. E., Quick, E., Parry, E. M. & Parry, J. M. 2007. Mechanistic influences for mutation induction curves after exposure to DNA-reactive carcinogens. *Cancer Res,* **67,** 3904-11.

Doak, S. H., Brusehafer, K., Dudley, E., Quick, E., Johnson, G., Newton, R. P. & Jenkins, G. J. 2008. No-observed effect levels are associated with up-regulation of MGMT following MMS exposure. *Mutat Res,* **648,** 9-14.

Dobrovolsky, V. N., Shaddock, J. G. & Heflich, R. H. 2005. Analysis of in vivo mutation in the hprt and tk genes of mouse lymphocytes. *Methods Mol Biol,* **291,** 133-44.

Dogliotti, E., Palombo, F., Kohfeldt, E. & Nehls, P. 1991. Recombinant shuttle vectors for studying mutagenesis in mammalian cells. *Prog Clin Biol Res,* **372,** 301-11.

Dogliotti, E., Palombo, F., Kohfeldt, E. & Nehls, P. 1991. Recombinant shuttle vectors for studying mutagenesis in mammalian cells. *Prog Clin Biol Res,* **372,** 301-11.

Dolan, M. E., Mitchell, R. B., Mummert, C., Moschel, R. C. & Pegg, A. E. 1991. Effect of O6-benzylguanine analogues on sensitivity of human tumor cells to the cytotoxic effects of alkylating agents. *Cancer Res,* **51,** 3367-72.

Dolan, M. E., Morimoto, K. & Pegg, A. E. 1985. Reduction of O6-alkylguanine-DNA alkyltransferase activity in HeLa cells treated with O6-alkylguanines. *Cancer Res,* **45,** 6413-7.

Dolan, M. E., Moschel, R. C. & Pegg, A. E. 1990. Depletion of mammalian O6-alkylguanine-DNA alkyltransferase activity by O6-benzylguanine provides a means to evaluate the role of this protein in protection against carcinogenic and therapeutic alkylating agents. *Proc Natl Acad Sci U S A,* **87,** 5368-72.

Dolan, M. E., Oplinger, M. & Pegg, A. E. 1988. Sequence specificity of guanine alkylation and repair. *Carcinogenesis,* **9,** 2139-43.

Doniger, J., Day, R. S. & Dipaolo, J. A. 1985. Quantitative assessment of the role of O6-methylguanine in the initiation of carcinogenesis by methylating agents. *Proc Natl Acad Sci U S A,* **82,** 421-5.

Donovan, P. & Smith, G. 2010. Mutagenicity of N-ethyl-N-nitrosourea, N-methyl-N-nitrosourea, methyl methanesulfonate and ethyl methanesulfonate in the developing

Syrian hamster fetus. *Mutat Res,* **699,** 55-7.

Dorman, B. P., Shimizu, N. & Ruddle, F. H. 1978. Genetic analysis of the human cell surface: antigenic marker for the human X chromosome in human-mouse hybrids. *Proc Natl Acad Sci U S A,* **75,** 2363-7.

Dragan, V. P., Vaughan, J., Jordan, V. C. & Pitot, H. C. 1995. Comparison of the effects of tamoxifen and toremifene on liver and kidney tumor promotion in female rats. *Carcinogenesis,* **16,** 2733-41.

Druckrey, H., Preussmann, R., Ivankovic, S. & Schmahl, D. 1967. [Organotropic carcinogenic effects of 65 various N-nitroso- compounds on BD rats]. *Z Krebsforsch,* **69,** 103-201.

Dumenco, L. L., Allay, E., Norton, K. & Gerson, S. L. 1993. The prevention of thymic lymphomas in transgenic mice by human O6-alkylguanine-DNA alkyltransferase. *Science,* **259,** 219-22.

Dunn WC, Foote RS, Hand RE Jr, Mitra S. 1986. Cell cycle-dependent modulation of O6-methylguanine-DNA methyltransferase in C3H/10T1/2 cells. *Carcinogenesis.* **7(5)**:807-12.

Duthie, S. J., Ross, M. & Collins, A. R. 1995. The influence of smoking and diet on the hypoxanthine phosphoribosyltransferase (hprt) mutant frequency in circulating T lymphocytes from a normal human population. *Mutat Res,* **331,** 55-64.

Edara, S., Kanugula, S., Goodtzova, K. & Pegg, A. E. 1996. Resistance of the human O6-alkylguanine-DNA alkyltransferase containing arginine at codon 160 to inactivation by O6-benzylguanine. *Cancer Res.* **56(24)**:5571-5.

Eder, E., Schuler, D. & Budiawan 1999. Cancer risk assessment for crotonaldehyde and 2-hexenal: an approach. *IARC Sci Publ,* 219-32.

Edwards, A., Voss, H., Rice, P., Civitello, A., Stegemann, J., Schwager, C., Zimmermann, J., Erfle, H., Caskey, C. T. & Ansorge, W. 1990. Automated DNA sequencing of the human HPRT locus. *Genomics,* **6,** 593-608.

Efrati, E., Tocco, G., Eritja, R., Wilson, S. H. & Goodman, M. F. 1997. Abasic translesion synthesis by DNA polymerase beta violates the "A-rule". Novel types of nucleotide incorporation by human DNA polymerase beta at an abasic lesion in different sequence contexts. *J Biol Chem,* **272,** 2559-69.

Ehrenberg, L. & Osterman-Golkar, S. 1980. Alkylation of macromolecules for detecting

mutagenic agents. *Teratog Carcinog Mutagen.* **1(1)**:105-27.

Eisenbrand, G., Pool-Zobel, B., Baker, V., Balls, M., Blaauboer, B. J., Boobis, A., Carere, A., Kevekordes, S., Lhuguenot, J. C., Pieters, R. & Kleiner, J. 2002. Methods of in vitro toxicology. *Food Chem Toxicol,* **40,** 193-236.

Elhajouji, A., Van Hummelen, P. & Kirsch-Volders, M. 1995. Indications for a threshold of chemically-induced aneuploidy in vitro in human lymphocytes. *Environ Mol Mutagen,* **26,** 292-304.

Emerit, I. & Cerutti, P. 1983. Clastogenic action of tumor promoter phorbol-12-myristate-13 acetate in mixed human leukocyte cultures. *Carcinogenesis,* **4,** 1313-6.

Engelbergs, J., Thomale, J. & Rajewsky, M. F. 2000. Role of DNA repair in carcinogen-induced ras mutation. *Mutat Res,* **450,** 139-53.

Engelward, B. P., Dreslin, A., Christensen, J., Huszar, D., Kurahara, C. & Samson, L. 1996. Repair-deficient 3-methyladenine DNA glycosylase homozygous mutant mouse cells have increased sensitivity to alkylation-induced chromosome damage and cell killing. *EMBO J,* **15,** 945-52.

Esteller, M. 2005. Aberrant DNA methylation as a cancer-inducing mechanism. *Annu Rev Pharmacol Toxicol,* **45,** 629-56.

Esteller, M. & Herman, J. G. 2002. Cancer as an epigenetic disease: DNA methylation and chromatin alterations in human tumours. *J Pathol,* **196,** 1-7.

Esteller, M., Risques, R. A., Toyota, M., Capella, G., Moreno, V., Peinado, M. A., Baylin, S. B. & Herman, J. G. 2001. Promoter hypermethylation of the DNA repair gene O(6)-methylguanine-DNA methyltransferase is associated with the presence of G:C to A:T transition mutations in p53 in human colorectal tumorigenesis. *Cancer Res,* **61,** 4689-92.

Esteller, M., Garcia-Foncillas, J., Andion, E., Goodman, S. N., Hidalgo, O. F., Vanaclocha, V., Baylin, S. B. & Herman, J. G. Inactivation of the DNA-repair gene MGMT and the clinical response of gliomas to alkylating agents. *N Engl J Med.* **343(19)**:1350-4.

Everhard, S., Kaloshi, G., Criniere, E., Benouaich-Amiel, A., Lejeune, J., Marie, Y., Sanson, M., Kujas, M., Mokhtari, K., Hoang-Xuan, K., Delattre, J. Y. & Thillet, J. 2006. MGMT methylation: a marker of response to temozolomide in low-grade gliomas. *Ann Neurol,* **60,** 740-3.

Everhard, S., Tost, J., El Abdalaoui, H., Criniere, E., Busato, F., Marie, Y., Gut, I. G., Sanson, M., Mokhtari, K., Laigle-Donadey, F., Hoang-Xuan, K., Delattre, J. Y. & Thillet, J. 2009. Identification of regions correlating MGMT promoter methylation and gene expression in glioblastomas. *Neuro Oncol,* **11,** 348-56.

Farber, S. & Diamond, L. K. 1948. Temporary remissions in acute leukemia in children produced by folic acid antagonist, 4-aminopteroyl-glutamic acid. *N Engl J Med,* **238,** 787-93.

Farmer, P. B. 2004. DNA and protein adducts as markers of genotoxicity. *Toxicol Lett,* **149,** 3-9.

Farmer, P. B. 2004. Exposure biomarkers for the study of toxicological impact on carcinogenic processes. *IARC Sci Publ,* 71-90.

Farmer, P. B. & Shuker, D. E. 1999. What is the significance of increases in background levels of carcinogen-derived protein and DNA adducts? Some considerations for incremental risk assessment. *Mutat Res,* **424,** 275-86.

Fedorov, Y., Anderson, E. M., Birmingham, A., Reynolds, A., Karpilow, J., Robinson, K., Leake, D., Marshall, W. S. & Khvorova, A. 2006. Off-target effects by siRNA can induce toxic phenotype. *RNA,* **12,** 1188-96.

Feinendegen, L. E. 2003. Relative implications of protective responses versus damage induction at low dose and low-dose-rate exposures, using the microdose approach. *Radiat Prot Dosimetry,* **104,** 337-46.

Feinendegen, L. E. 2005. Evidence for beneficial low level radiation effects and radiation hormesis. *Br J Radiol,* **78,** 3-7.

Fellows, M. D., O'donovan, M. R., Lorge, E. & Kirkland, D. 2008. Comparison of different methods for an accurate assessment of cytotoxicity in the in vitro micronucleus test. II: Practical aspects with toxic agents. *Mutat Res,* **655,** 4-21.

Fenwick, R. G. 1985. The HGPRT system, in Molecular Cell Genetics 1st Ed. (ed Gottesman, M.) *Wiley, New York,* , 333-73

Fichtinger-Schepman, A. M., Dijt, F. J., Bedford, P., Van Oosterom, A. T., Hill, B. T. & Berends, F. 1988. Induction and removal of cisplatin-DNA adducts in human cells in vivo and in vitro as measured by immunochemical techniques. *IARC Sci Publ,* 321-8.

Figure 1.1. Macro-mutations affecting chromosome structure including deletion (A), duplication (B), inversion (C) and translocation (D). Downloaded from

http://www.bioscience.org/2012/v4s/af/302/fulltext.asp?bframe=figures.htm&doi=yes on 28/8/2012.

Filipsson, A. F., Sand, S., Nilsson, J. & Victorin, K. 2003. The benchmark dose method--review of available models, and recommendations for application in health risk assessment. *Crit Rev Toxicol,* **33,** 505-42.

Finette, B. A., Homans, A. C., Rivers, J., Messier, T. & Albertini, R. J. 2001. Accumulation of somatic mutations in proliferating T cell clones from children treated for leukemia. *Leukemia,* **15,** 1898-905.

Fischer, S. J., Benson, L. M., Fauq, A., Naylor, S. & Windebank, A. J. 2008. Cisplatin and dimethyl sulfoxide react to form an adducted compound with reduced cytotoxicity and neurotoxicity. *Neurotoxicology,* **29,** 444-52.

Fishel, R., Lescoe, M. K., Rao, M. R., Copeland, N. G., Jenkins, N. A., Garber, J., Kane, M. & Kolodner, R. 1993. The human mutator gene homolog MSH2 and its association with hereditary nonpolyposis colon cancer. *Cell,* **75,** 1027-38.

Fontenelle, L. J. & Henderson, J. F. 1969. An enzymatic basis for the inability of erythrocytes to synthesize purine ribonucleotides de novo. *Biochim Biophys Acta,* **177,** 175-6.

Foote, R. S. & Mitra, S. 1984. Lack of induction of O6-methylguanine-DNA methyltransferase in mammalian cells treated with N-methyl-N'-nitro-N-nitrosoguanidine. *Carcinogenesis.* **5(2)**:277-81.

Fowler P, Whitwell J, Jeffrey L, Young J, Smith K, Kirkland D. 2010. Cadmium chloride, benzo[a]pyrene and cyclophosphamide tested in the in vitro mammalian cell micronucleus test (MNvit) in the human lymphoblastoid cell line TK6 at Covance laboratories, Harrogate UK in support of OECD draft Test Guideline 487.*Mutat Res.* **702(2)**:171-4.

Fowler, P., Smith, K., Young, J., Jeffrey, L., Kirkland, D., Pfuhler, S. & Carmichael, P. 2012a. Reduction of misleading ("false") positive results in mammalian cell genotoxicity assays. I. Choice of cell type. *Mutat Res,* **742,** 11-25.

Fowler P, Smith R, Smith K, Young J, Jeffrey L, Kirkland D, Pfuhler S, Carmichael P. 2012 Reduction of misleading ("false") positive results in mammalian cell genotoxicity assays. II. Importance of accurate toxicity measurement.*Mutat Res.* **747(1)**:104-17.

Fox, E. J., Beckman, R. A. & Loeb, L. A. 2010. Reply: Is There Any Genetic Instability in Human Cancer? *DNA Repair (Amst),* **9,** 859-60.

Freedman, H. J., Parker, N. B., Marinello, A. J., Gurtoo, H. L. & Minowada, J. 1979. Induction, inhibition, and biological properties of aryl hydrocarbon hydroxylase in a stable human B-lymphocyte cell line, RPMI-1788. *Cancer Res,* **39,** 4612-9.

Friedman, H. S., Kerby, T. & Calvert, H. 2000. Temozolomide and treatment of malignant glioma. *Clin Cancer Res,* **6,** 2585-97.

Fritz, G. & Kaina, B. 1992. Genomic differences between O6-methylguanine-DNA methyltransferase proficient (Mex+) and deficient (Mex-) cell lines: possible role of genetic and epigenetic changes in conversion of Mex+ into Mex. *Biochem Biophys Res Commun,* **183,** 1184-90.

Fritz, G., Tano, K., Mitra, S. & Kaina, B. 1991. Inducibility of the DNA repair gene encoding O6-methylguanine-DNA methyltransferase in mammalian cells by DNA-damaging treatments. *Mol Cell Biol,* **11,** 4660-8.

Frosina, G. 2009. DNA repair and resistance of gliomas to chemotherapy and radiotherapy. *Mol Cancer Res,* **7,** 989-99.

Fukuchi, M., Mineura, K., Kowada, M., Terashima, I. & Kohda, K. 1997. [Study on potentiation of nitrosourea-cytotoxicity by DNA repair enzyme inhibitors in human brain tumor cells]. *No To Shinkei,* **49,** 521-8.

Fukushima, S., Kinoshita, A., Puatanachokchai, R., Kushida, M., Wanibuchi, H. & Morimura K. 2005. Hormesis and dose-response-mediated mechanisms in carcinogenesis: evidence for a threshold in carcinogenicity of non-genotoxic carcinogens. *Carcinogenesis.* **26(11)**:1835-45.

Fukushima, S., Wanibuchi, H., Morimura, K., Wei, M., Nakae, D., Konishi, Y., Tsuda, H., Uehara, N., Imaida, K., Shirai, T., Tatematsu, M., Tsukamoto, T., Hirose, M., Furukawa, F., Wakabayashi, K. & Totsuka, Y. 2002. Lack of a dose-response relationship for carcinogenicity in the rat liver with low doses of 2-amino-3,8-dimethylimidazo[4,5-f]quinoxaline or N-nitrosodiethylamine. *Jpn J Cancer Res,* **93,** 1076-82.

Fuscoe, J. C., Fenwick, R. G., Jr., Ledbetter, D. H. & Caskey, C. T. 1983. Deletion and amplification of the HGPRT locus in Chinese hamster cells. *Mol Cell Biol,* **3,** 1086-96.

Galloway SM, Greenwood SK, Hill RB, Bradt CI, Bean CL. 1995. A role for mismatch

repair in production of chromosome aberrations by methylating agents in human cells.*Mutat Res.* **346(4)**:231-45.

Ganem, N. J., Storchova, Z. & Pellman, D. 2007. Tetraploidy, aneuploidy and cancer. *Curr Opin Genet Dev,* **17,** 157-62.

Gaylor, D. W., Lutz, W. K. & Conolly, R. B. 2004. Statistical analysis of nonmonotonic dose-response relationships: research design and analysis of nasal cell proliferation in rats exposed to formaldehyde. *Toxicol Sci,* **77,** 158-64.

Gehring, P. J. & Blau, G. E. 1978. Mechanisms of carcinogenesis: dose response. *J Environ Pathol Toxicol,* **1,** 163-79.

Geiman, T. M. & Robertson, K. D. 2002. Chromatin remodeling, histone modifications, and DNA methylation-how does it all fit together? *J Cell Biochem,* **87,** 117-25.

Georgiadis, P., Kaila, S., Makedonopoulou, P., Fthenou, E., Chatzi, L., Pletsa, V. & Kyrtopoulos, S. A. 2011. Development and validation of a new, sensitive immunochemical assay for O-methylguanine in DNA and its application in a population study. *Cancer Epidemiol Biomarkers Prev,* **20,** 82-90.

Georgiadis, P., Samoli, E., Kaila, S., Katsouyanni, K. & Kyrtopoulos, S. A. 2000. Ubiquitous presence of O6-methylguanine in human peripheral and cord blood DNA. *Cancer Epidemiol Biomarkers Prev,* **9,** 299-305.

Gerber, C. & Toelle, H. G. 2009. What happened: the chemistry side of the incident with EMS contamination in Viracept tablets. *Toxicol Lett,* **190,** 248-53.

Gerson, S. L. 1988. Regeneration of O6-alkylguanine-DNA alkyltransferase in human lymphocytes after nitrosourea exposure. *Cancer Res,* **48,** 5368-73.

Gerson, S. L. 2002. Clinical relevance of MGMT in the treatment of cancer. *J Clin Oncol,* **20,** 2388-99.

Gerson, S. L., Kaplan, S. L., Bruss, J. B., Le, V., Arellano, F. M., Hafkin, B. & Kuter, D. J. 2002. Hematologic effects of linezolid: summary of clinical experience. *Antimicrob Agents Chemother,* **46,** 2723-6.

Gerson, S. L., Zborowska, E., Norton, K., Gordon, N. H. & Willson, J. K. 1993. Synergistic efficacy of O6-benzylguanine and 1,3-bis(2-chloroethyl)-1-nitrosourea (BCNU) in a human colon cancer xenograft completely resistant to BCNU alone. *Biochem Pharmacol,* **45,** 483-91.

Glaab, W. E. & Tindall, K. R. 1997. Mutation rate at the hprt locus in human cancer cell lines with specific mismatch repair-gene defects. *Carcinogenesis,* **18,** 1-8.

Glaab, W. E., Tindall, K. R. & Skopek, T. R. 1999. Specificity of mutations induced by methyl methanesulfonate in mismatch repair-deficient human cancer cell lines. *Mutat Res,* **427,** 67-78.

Glassner, B. J., Weeda, G., Allan, J. M., Broekhof, J. L., Carls, N. H., Donker, I., Engelward, B. P., Hampson, R. J., Hersmus, R., Hickman, M. J., Roth, R. B., Warren, H. B., Wu, M. M., Hoeijmakers, J. H. & Samson, L. D. 1999. DNA repair methyltransferase (Mgmt) knockout mice are sensitive to the lethal effects of chemotherapeutic alkylating agents. *Mutagenesis,* **14,** 339-47.

Glassner, B. J., Weeda, G., Allan, J. M., Broekhof, J. L., Carls, N. H., Donker, I., Engelward, B. P., Hampson, R. J., Hersmus, R., Hickman, M. J., Roth, R. B., Warren, H. B., Wu, M. M., Hoeijmakers, J. H. & Samson, L. D. 1999. DNA repair methyltransferase (Mgmt) knockout mice are sensitive to the lethal effects of chemotherapeutic alkylating agents. *Mutagenesis,* **14,** 339-47.

Glazko, G. V., Babenko, V. N., Koonin, E. V. & Rogozin, I. B. 2006. Mutational hotspots in the TP53 gene and, possibly, other tumor suppressors evolve by positive selection. *Biol Direct,* **1,** 4.

Glickman, B. W., Horsfall, M. J., Gordon, A. J. & Burns, P. A. 1987. Nearest neighbor affects G:C to A:T transitions induced by alkylating agents. *Environ Health Perspect,* **76,** 29-32.

Glickman, M. H. & Ciechanover, A. 2002. The ubiquitin-proteasome proteolytic pathway: destruction for the sake of construction. *Physiol Rev,* **82,** 373-428.

Glover, R. P., Sweetman, G. M., Farmer, P. B. & Roberts, G. C. 1995. Sequencing of oligonucleotides using high performance liquid chromatography and electrospray mass spectrometry. *Rapid Commun Mass Spectrom,* **9,** 897-901.

Gocke, E., Ballantyne, M., Whitwell, J. & Muller, L. 2009. MNT and MutaMouse studies to define the in vivo dose response relations of the genotoxicity of EMS and ENU. *Toxicol Lett,* **190,** 286-97.

Gocke, E. & Muller, L. 2009. In vivo studies in the mouse to define a threshold for the genotoxicity of EMS and ENU. *Mutat Res,* **678,** 101-7.

Gocke, E. & Muller, L. 2009. In vivo studies in the mouse to define a threshold for the

genotoxicity of EMS and ENU. *Mutat Res,* **678,** 101-7.

Gocke, E., Muller, L. & Pfister, T. 2009. EMS in Viracept--initial ('traditional') assessment of risk to patients based on linear dose response relations. *Toxicol Lett,* **190,** 266-70.

Gocke, E. & Wall, M. 2009. In vivo genotoxicity of EMS: statistical assessment of the dose response curves. *Toxicol Lett,* **190,** 298-302.

Golding, T. B. B., C. Mcginnis, J. Müller, S. Rees, H. T. Rees, N.H. Farmer, P. B. Watson, W. P 1997. The mechanism of decomposition of N-methyl-N-nitrosourea (MNU) in water and a study of its reactions with 2′-deoxyguanosine, 2′-deoxyguanosine 5′-monophosphate and d(GTGCAC). *Tetrahedron,* **53,** 4063-82.

Goldmacher, V. S., Cuzick, R. A., Jr. & Thilly, W. G. 1986. Isolation and partial characterization of human cell mutants differing in sensitivity to killing and mutation by methylnitrosourea and N-methyl-N'-nitro-N-nitrosoguanidine. *J Biol Chem,* **261,** 12462-71.

Gollapudi BB, Johnson GE, Hernandez LG, Pottenger LH, Dearfield KL, Jeffrey AM, Julien E, Kim JH, Lovell DP, Macgregor JT, Moore MM, van Benthem J, White PA, Zeiger E, Thybaud V. 2012. Quantitative approaches for assessing dose-response relationships in genetic toxicology studies. *Environ Mol Mutagen.* DOI: 10.1002/em.21727

Goodwin, M. S. & Farber, M. S. 1948. The necessity for treatment of pregnant syphilitic women during every pregnancy. *Am J Syph Gonorrhea Vener Dis,* **32,** 409-17.

Graham, T. A. & Leedham, S. J. 2010. Field defects in DNA repair: is loss of MGMT an initial event in colorectal carcinogenesis? *Gut,* **59,** 1452-3.

Grombacher, T., Eichhorn, U. & Kaina, B. 1998. p53 is involved in regulation of the DNA repair gene O6-methylguanine-DNA methyltransferase (MGMT) by DNA damaging agents. *Oncogene,* **17,** 845-51.

Grombacher, T., Mitra, S. & Kaina, B. 1996. Induction of the alkyltransferase (MGMT) gene by DNA damaging agents and the glucocorticoid dexamethasone and comparison with the response of base excision repair genes. *Carcinogenesis,* **17,** 2329-36.

Groopman, J. D. & Kensler, T. W. 1999. The light at the end of the tunnel for chemical-specific biomarkers: daylight or headlight? *Carcinogenesis,* **20,** 1-11.

Grosovsky, A. J. & Little, J. B. 1983. Effect of growth rate on phenotypic expression of 6-

thioguanine resistance in human diploid fibroblasts. *Mutat Res,* **110,** 163-70.

Guengerich, F. P. 1992. Metabolic activation of carcinogens. *Pharmacol Ther,* **54,** 17-61.

Guess, H., Crump, K. & Peto, R. 1977. Uncertainty estimates for low-dose-rate extrapolations of animal carcinogenicity data. *Cancer Res,* **37,** 3475-83.

Guest, R. D. & Parry, J. M. 1999. P53 integrity in the genetically engineered mammalian cell lines AHH-1 and MCL-5. *Mutat Res,* **423,** 39-46.

Gunn, J. M., Clark, M. G., Knowles, S. E., Hopgood, M. F. & Ballard, F. J. 1977. Reduced rates of proteolysis in transformed cells. *Nature,* **266,** 58-60.

Gupta, R. C., Arif, J. M. & Gairola, C. G. 1999. Enhancement of pre-existing DNA adducts in rodents exposed to cigarette smoke. *Mutat Res,* **424,** 195-205.

Gupta, R. C. & Lutz, W. K. 1999. Background DNA damage for endogenous and unavoidable exogenous carcinogens: a basis for spontaneous cancer incidence? *Mutat Res,* **424,** 1-8.

Hallahan, D. E., Spriggs, D. R., Beckett, M. A., Kufe, D. W. & Weichselbaum, R. R. 1989. Increased tumor necrosis factor alpha mRNA after cellular exposure to ionizing radiation. *Proc Natl Acad Sci U S A,* **86,** 10104-7.

Hang, B. 2010. Formation and repair of tobacco carcinogen-derived bulky DNA adducts. *J Nucleic Acids,* **2010,** 709521.

Hansen, K. M., Ji, H. F., Wu, G., Datar, R., Cote, R., Majumdar, A. & Thundat, T. 2001. Cantilever-based optical deflection assay for discrimination of DNA single-nucleotide mismatches. *Anal Chem,* **73,** 1567-71.

Hansen, R. J., Nagasubramanian, R., Delaney, S. M., Samson, L. D. & Dolan, M. E. 2007. Role of O6-methylguanine-DNA methyltransferase in protecting from alkylating agent-induced toxicity and mutations in mice. *Carcinogenesis,* **28,** 1111-6.

Harbach, P. R., Mattano, S. S., Zimmer, D. M., Wang, Y. & Aaron, C. S. 1995. DNA sequence analysis of spontaneous hprt mutations arising in vivo in cynomolgus monkey T-lymphocytes. *Environ Mol Mutagen,* **26,** 218-25.

Harris, L. C., Remack, J. S., Houghton, P. J. & Brent, T. P. 1996. Wild-type p53 suppresses transcription of the human O6-methylguanine-DNA methyltransferase gene. *Cancer Res,* **56,** 2029-32.

Hawksworth, G. M. 1994. Advantages and disadvantages of using human cells for pharmacological and toxicological studies. *Hum Exp Toxicol,* **13,** 568-73.

Heacock, M. L., Stefanick, D. F., Horton, J. K. & Wilson, S. H. 2010. Alkylation DNA damage in combination with PARP inhibition results in formation of S-phase-dependent double-strand breaks. *DNA Repair (Amst),* **9,** 929-36.

Hebels, D. G., Brauers, K. J., Van Herwijnen, M. H., Georgiadis, P. A., Kyrtopoulos, S. A., Kleinjans, J. C. & De Kok, T. M. 2011. Time-series analysis of gene expression profiles induced by nitrosamides and nitrosamines elucidates modes of action underlying their genotoxicity in human colon cells. *Toxicol Lett,* **207,** 232-41.

Hebels, D. G., Briede, J. J., Khampang, R., Kleinjans, J. C. & De Kok, T. M. 2010. Radical mechanisms in nitrosamine- and nitrosamide-induced whole-genome gene expression modulations in Caco-2 cells. *Toxicol Sci,* **116,** 194-205.

Hebels, D. G., Jennen, D. G., Kleinjans, J. C. & De Kok, T. M. 2009. Molecular signatures of N-nitroso compounds in Caco-2 cells: implications for colon carcinogenesis. *Toxicol Sci,* 108, 290-300.

Hecht, S. S., McIntee, E. J., Cheng, G., Shi, Y., Villalta, P. W. & Wang M. 2001. New aspects of DNA adduct formation by the carcinogens crotonaldehyde and acetaldehyde. *Adv Exp Med Biol.* **500**:63-71.

Hegi, M. E., Diserens, A. C., Gorlia, T., Hamou, M. F., De Tribolet, N., Weller, M., Kros, J. M., Hainfellner, J. A., Mason, W., Mariani, L., Bromberg, J. E., Hau, P., Mirimanoff, R. O., Cairncross, J. G., Janzer, R. C. & Stupp, R. 2005. MGMT gene silencing and benefit from temozolomide in glioblastoma. *N Engl J Med,* **352,** 997-1003.

Heighway, J., Margison, G. P. & Santibanez-Koref, M. F. 2003. The alleles of the DNA repair gene O6-alkylguanine-DNA alkyltransferase are expressed at different levels in normal human lung tissue. *Carcinogenesis,* **24,** 1691-4.

Hein, D. W. 2002. Molecular genetics and function of NAT1 and NAT2: role in aromatic amine metabolism and carcinogenesis. *Mutat Res,* **506-507,** 65-77.

Hemminki, K. 1983. Nucleic acid adducts of chemical carcinogens and mutagens. *Arch Toxicol,* **52,** 249-85.

Henderson L, Albertini S, Aardema M. 2000. Thresholds in genotoxicity responses.*Mutat Res.* **464(1)**:123-8.

Herron, D. C. & Shank, R. C. 1981. In vivo kinetics of O6-methylguanine and 7-methylguanine formation and persistence in DNA of rats treated with symmetrical dimethylhydrazine.

Cancer Res, **41,** 3967-72.

Hickman, M. J. & Samson, L. D. 1999. Role of DNA mismatch repair and p53 in signaling induction of apoptosis by alkylating agents. *Proc Natl Acad Sci U S A,* **96,** 10764-9.

Hines, E. A., Jr. & Farber, E. M. 1948. The arterioles of the skin in essential hypertension. *J Lab Clin Med,* **33,** 1486.

Hirose, Y., Katayama, M., Stokoe, D., Haas-Kogan, D. A., Berger, M. S. & Pieper, R. O. 2003. The p38 mitogen-activated protein kinase pathway links the DNA mismatch repair system to the G2 checkpoint and to resistance to chemotherapeutic DNA-methylating agents. *Mol Cell Biol,* **23,** 8306-15.

Hirose, Y., Kreklau, E. L., Erickson, L. C., Berger, M. S. & Pieper, R. O. 2003. Delayed repletion of O6-methylguanine-DNA methyltransferase resulting in failure to protect the human glioblastoma cell line SF767 from temozolomide-induced cytotoxicity. *J Neurosurg,* **98,** 591-8.

Hodgkinson, A. & Eyre-Walker, A. 2011. Variation in the mutation rate across mammalian genomes. *Nat Rev Genet,* **12,** 756-66.

Hori, T., Haruta, S., Ueno, Y., Ishii, M. & Igarashi, Y. 2006. Direct comparison of single-strand conformation polymorphism (SSCP) and denaturing gradient gel electrophoresis (DGGE) to characterize a microbial community on the basis of 16S rRNA gene fragments. *J Microbiol Methods,* **66,** 165-9.

Hovig, E., Smith-Sorensen, B., Brogger, A. & Borresen, A. L. 1991. Constant denaturant gel electrophoresis, a modification of denaturing gradient gel electrophoresis, in mutation detection. *Mutat Res,* **262,** 63-71.

Hu, C. W., Chen, C. M., Ho, H. H. & Chao, M. R. 2012. Simultaneous quantification of methylated purines in DNA by isotope dilution LC-MS/MS coupled with automated solid-phase extraction. *Anal Bioanal Chem,* **402,** 1199-208.

Hudson, R. E., Bergthorsson, U. & Ochman, H. 2003. Transcription increases multiple spontaneous point mutations in Salmonella enterica. *Nucleic Acids Res,* **31,** 4517-22.

Huennekens, F. M., Bertino, J. R., Silber, R. & Gabrio, B. W. 1963. Antimetabolites in the Chemotherapy of Leukemia. *Exp Cell Res,* **24,** SUPPL9:441-61.

Ibeanu, G., Hartenstein, B., Dunn, W. C., Chang, L. Y., Hofmann, E., Coquerelle, T., Mitra, S. & Kaina, B. 1992. Overexpression of human DNA repair protein N-methylpurine-DNA

glycosylase results in the increased removal of N-methylpurines in DNA without a concomitant increase in resistance to alkylating agents in Chinese hamster ovary cells. *Carcinogenesis,* **13,** 1989-95.

Ide, H., Murayama, H., Sakamoto, S., Makino, K., Honda, K., Nakamuta, H., Sasaki, M. & Sugimoto, N. 1995. On the mechanism of preferential incorporation of dAMP at abasic sites in translesional DNA synthesis. Role of proofreading activity of DNA polymerase and thermodynamic characterization of model template-primers containing an abasic site. *Nucleic Acids Res,* **23,** 123-9.

Imai, Y., Oda, H., Nakatsuru, Y. & Ishikawa, T. 1995. A polymorphism at codon 160 of human O6-methylguanine-DNA methyltransferase gene in young patients with adult type cancers and functional assay. *Carcinogenesis,* **16,** 2441-5.

Ishibashi, T., Nakabeppu, Y. & Sekiguchi, M. 1994. Artificial control of nuclear translocation of DNA repair methyltransferase. *J Biol Chem,* **269,** 7645-50.

Jack, P. L. & Brookes, P. 1981. The distribution of benzo(a)pyrene DNA adducts in mammalian chromatin. *Nucleic Acids Res,* **9,** 5533-52.

Jackson, P. E., Cooper, D. P., Meyer, T. A., Wood, M., Povey, A. C. & Margison, G. P. 2000. Formation and persistence of O(6)-methylguanine in the mouse colon following treatment with 1,2-dimethylhydrazine as measured by an O(6)-alkylguanine-DNA alkyltransferase inactivation assay. *Toxicol Lett,* **115,** 205-12.

Jackson, S. P. 2002. Sensing and repairing DNA double-strand breaks. *Carcinogenesis,* **23,** 687-96.

Jefcoate, C. R., Liehr, J. G., Santen, R. J., Sutter, T. R., Yager, J. D., Yue, W., Santner, S. J., Tekmal, R., Demers, L., Pauley, R., Naftolin, F., Mor, G. & Berstein, L. 2000. Tissue-specific synthesis and oxidative metabolism of estrogens. *J Natl Cancer Inst Monogr*, 95-112.

Jenkins, G. J., Burlinson, B. & Parry, J. M. 2000. The polymerase inhibition assay: A methodology for the identification of DNA-damaging agents. *Mol Carcinog,* **27,** 289-97.

Jenkins, G. J., Doak, S. H., Johnson, G. E., Quick, E., Waters, E. M. & Parry, J. M. 2005. Do dose response thresholds exist for genotoxic alkylating agents? *Mutagenesis,* **20,** 389-98.

Jenkins, G. J., Takahashi, N. & Parry, J. M. 1999. A study of ENU-induced mutagenesis in the mouse using the restriction site mutation (RSM) assay. *Teratog Carcinog Mutagen,* **19,**

281-92.

Jenkins, G. J., Zair, Z., Johnson, G. E. & Doak, S. H. 2010. Genotoxic thresholds, DNA repair, and susceptibility in human populations. *Toxicology,* **278,** 305-10.

Jensen, D. E. 1983. Denitrosation as a determinant of nitrosocimetidine in vivo activity. *Cancer Res,* **43,** 5258-67.

Jinnah, H. A., De Gregorio, L., Harris, J. C., Nyhan, W. L. & O'Neill, J. P. 2000. The spectrum of inherited mutations causing HPRT deficiency: 75 new cases and a review of 196 previously reported cases. *Mutat Res.* **463(3)**:309-26.

Johnson, G. E., Doak, S. H., Griffiths, S. M., Quick, E. L., Skibinski, D. O., Zair, Z. M. & Jenkins, G. J. 2009. Non-linear dose-response of DNA-reactive genotoxins: recommendations for data analysis. *Mutat Res,* **678,** 95-100.

Johnson, G. E., Jenkins, G. J., Thomas, A. D. & Doak, S. H. 2010. Vinblastine and diethylstilboestrol tested in the in vitro mammalian cell micronucleus test (MNvit) at Swansea University UK in support of OECD draft Test Guideline 487. *Mutat Res,* **702,** 189-92.

Jolly, D. J., Okayama, H., Berg, P., Esty, A. C., Filpula, D., Bohlen, P., Johnson, G. G., Shively, J. E., Hunkapillar, T. & Friedmann, T. 1983. Isolation and characterization of a full-length expressible cDNA for human hypoxanthine phosphoribosyl transferase. *Proc Natl Acad Sci U S A,* **80,** 477-81.

Jones, P. A. & Baylin, S. B. 2002. The fundamental role of epigenetic events in cancer. *Nat Rev Genet,* **3,** 415-28.

Jump, D. B., Sudhakar, S., Tew, K. D. & Smulson, M. 1980. Probes to study the effect of methyl nitrosourea on ADP-ribosylation and chromatin structure at the subunit level. *Chem Biol Interact,* **30,** 35-51.

Kaina, B. 1982. Enhanced survival and reduced mutation and aberration frequencies induced in V79 chinese hamster cells pre-exposed to low levels of methylating agents. *Mutat Res,* **93,** 195-211.

Kaina, B. 1983. Cross-resistance studies with V79 Chinese hamster cells adapted to the mutagenic or clastogenic effect of N-methyl-N'-nitro-N-nitrosoguanidine. *Mutat Res,* **111,** 341-52.

Kaina, B. 1983. Studies on adaptation of V79 Chinese hamster cells to low doses of methylating

agents. *Carcinogenesis,* **4,** 1437-43.

Kaina, B., Christmann, M., Naumann, S. & Roos, W. P. 2007. MGMT: key node in the battle against genotoxicity, carcinogenicity and apoptosis induced by alkylating agents. *DNA Repair (Amst),* **6,** 1079-99.

Kaina, B., Fritz, G. & Coquerelle, T. 1991. Identification of human genes involved in repair and tolerance of DNA damage. *Radiat Environ Biophys,* **30,** 1-19.

Kaina, B., Fritz, G., Mitra, S. & Coquerelle T. 1991. Transfection and expression of human O6-methylguanine-DNA methyltransferase (MGMT) cDNA in Chinese hamster cells: the role of MGMT in protection against the genotoxic effects of alkylating agents. *Carcinogenesis.***12(10)**:1857-67.

Kaina, B., Heindorff, K. & Aurich, O. 1983. O6-methylguanine, but not N7-methylguanine or N3-methyladenine, induces gene mutations, sister-chromatid exchanges and chromosomal aberrations in Chinese hamster cells. *Mutat Res,* **108,** 279-92.

Kaina, B., Margison, G. P. & Christmann, M. 2010. Targeting O-methylguanine-DNA methyltransferase with specific inhibitors as a strategy in cancer therapy. *Cell Mol Life Sci,* **67,** 3663-81.

Kaina, B., Ziouta, A., Ochs, K. & Coquerelle, T. 1997. Chromosomal instability, reproductive cell death and apoptosis induced by O6-methylguanine in Mex-, Mex+ and methylation-tolerant mismatch repair compromised cells: facts and models. *Mutat Res,* **381,** 227-41.

Kaiser, J. 2003. Hormesis. Sipping from a poisoned chalice. *Science,* **302,** 376-9.

Kamranvar, S. A., Gruhne, B., Szeles, A. & Masucci, M. G. 2007. Epstein-Barr virus promotes genomic instability in Burkitt's lymphoma. *Oncogene,* **26,** 5115-23.

Kang, D. H., Rothman, N., Poirier, M. C., Greenberg, A., Hsu, C. H., Schwartz, B. S., Baser, M. E., Groopman, J. D., Weston, A. & Strickland, P. T. 1995. Interindividual differences in the concentration of 1-hydroxypyrene-glucuronide in urine and polycyclic aromatic hydrocarbon-DNA adducts in peripheral white blood cells after charbroiled beef consumption. *Carcinogenesis,* **16,** 1079-85.

Kato, K., Yamamura, E., Kawanishi, M., Yagi, T., Matsuda, T., Sugiyama, A. & Uno, Y. 2011. Application of the DNA adductome approach to assess the DNA-damaging capability of in vitro micronucleus test-positive compounds. *Mutat Res,* **721,** 21-6.

Kato, T., Natsume, A., Toda, H., Iwamizu, H., Sugita, T., Hachisu, R., Watanabe, R., Yuki, K.,

Motomura, K., Bankiewicz, K. & Wakabayashi, T. 2010. Efficient delivery of liposome-mediated MGMT-siRNA reinforces the cytotoxity of temozolomide in GBM-initiating cells. *Gene Ther,* **17,** 1363-71.

Katoh, T. 1995. [Application of molecular biology to occupational health field--the frequency of gene polymorphism of cytochrome P450 1A1 and glutathione S-transferase M1 in patients with lung, oral and urothelial cancer]. *J UOEH,* **17,** 271-8.

Kaur, T. B., Travaline, J. M., Gaughan, J. P., Richie, J. P., Jr., Stellman, S. D. & Lazarus, P. 2000. Role of polymorphisms in codons 143 and 160 of the O6-alkylguanine DNA alkyltransferase gene in lung cancer risk. *Cancer Epidemiol Biomarkers Prev,* **9,** 339-42.

Khaidakov, M. & Glickman, B. W. 1996. Possible factors leading to a misjudgement of mutant frequencies in HPRT assay. *Mutat Res,* **354,** 9-14.

Khaidakov, M., Young, D., Erfle, H., Mortimer, A., Voronkov, Y. & Glickman, B. W. 1997. Molecular analysis of mutations in T-lymphocytes from experienced Soviet cosmonauts. *Environ Mol Mutagen,* **30,** 21-30.

Kinoshita, A., Wanibuchi, H., Morimura, K., Wei, M., Shen, J., Imaoka, S., Funae, Y. & Fukushima, S. 2003. Phenobarbital at low dose exerts hormesis in rat hepatocarcinogenesis by reducing oxidative DNA damage, altering cell proliferation, apoptosis and gene expression. *Carcinogenesis,* **24,** 1389-99.

Kinsella, A. R., Smith, D. & Pickard, M. 1997. Resistance to chemotherapeutic antimetabolites: a function of salvage pathway involvement and cellular response to DNA damage. *Br J Cancer,* **75,** 935-45.

Kirkhus, B., Iversen, O. H. & Kristensen, A. 1987. Carcinogenic doses of methylnitrosourea induce dose response related delay in transit through S and G2 phases in mouse epidermis: a cell kinetic study. *Carcinogenesis,* **8,** 369-75.

Kirkland, D., Aardema, M., Henderson, L. & Muller, L. 2005. Evaluation of the ability of a battery of three in vitro genotoxicity tests to discriminate rodent carcinogens and non-carcinogens I. Sensitivity, specificity and relative predictivity. *Mutat Res,* **584,** 1-256.

Kirkland, D. J., Aardema, M., Banduhn, N., Carmichael, P., Fautz, R., Meunier, J. R. & Pfuhler, S. 2007. In vitro approaches to develop weight of evidence (WoE) and mode of action (MoA) discussions with positive in vitro genotoxicity results. *Mutagenesis,* **22,** 161-75.

Kirkland, D. & Fowler, P. 2010. Further analysis of Ames-negative rodent carcinogens that are

only genotoxic in mammalian cells in vitro at concentrations exceeding 1 mM, including retesting of compounds of concern. *Mutagenesis,* **25,** 539-53.

Kirkland, D. J. & Muller, L. 2000. Interpretation of the biological relevance of genotoxicity test results: the importance of thresholds. *Mutat Res,* **464,** 137-47.

Kirsch-Volders, M., Aardema, M. & Elhajouji, A. 2000. Concepts of threshold in mutagenesis and carcinogenesis. *Mutat Res,* **464,** 3-11.

Kirsch-Volders, M., Vanhauwaert, A., Eichenlaub-Ritter, U. & Decordier, I. 2003. Indirect mechanisms of genotoxicity. *Toxicol Lett,* **140-141,** 63-74.

Kitange, G. J., Carlson, B. L., Mladek, A. C., Decker, P. A., Schroeder, M. A., Wu, W., Grogan, P. T., Giannini, C., Ballman, K. V., Buckner, J. C., James, C. D. & Sarkaria, J. N. 2009. Evaluation of MGMT promoter methylation status and correlation with temozolomide response in orthotopic glioblastoma xenograft model. *J Neurooncol,* **92,** 23-31.

Kleihues, P. & Bucheler, J. 1977. Long-term persistence of O6-methylguanine in rat brain DNA. *Nature,* **269,** 625-6.

Klein, J. C., Bleeker, M. J., Roelen, H. C., Rafferty, J. A., Margison, G. P., Brugghe, H. F., Van Den Elst, H., Van Der Marel, G. A., Van Boom, J. H., Kriek, E. & Et Al. 1994. Role of nucleotide excision repair in processing of O4-alkylthymines in human cells. *J Biol Chem,* **269,** 25521-8.

Knudson, A. G., Jr. 1971. Mutation and cancer: statistical study of retinoblastoma. *Proc Natl Acad Sci U S A,* **68,** 820-3.

Koana, T., Takashima, Y., Okada, M. O., Ikehata, M., Miyakoshi, J. & Sakai, K. 2004. A threshold exists in the dose-response relationship for somatic mutation frequency induced by X irradiation of Drosophila. *Radiat Res,* **161,** 391-6.

Kohler, S. W., Provost, G. S., Fieck, A., Kretz, P. L., Bullock, W. O., Putman, D. L., Sorge, J. A. & Short, J. M. 1991. Analysis of spontaneous and induced mutations in transgenic mice using a lambda ZAP/lacI shuttle vector. *Environ Mol Mutagen,* **18,** 316-21.

Kokkinakis, D. M., Ahmed, M. M., Delgado, R., Fruitwala, M. M., Mohiuddin, M. & Albores-Saavedra, J. 1997. Role of O6-methylguanine-DNA methyltransferase in the resistance of pancreatic tumors to DNA alkylating agents. *Cancer Res,* **57,** 5360-8.

Kokoska, R. J., Mcculloch, S. D. & Kunkel, T. A. 2003. The efficiency and specificity of apurinic/apyrimidinic site bypass by human DNA polymerase eta and Sulfolobus

solfataricus Dpo4. *J Biol Chem,* **278,** 50537-45.

Kondo, N., Takahashi, A., Ono, K. & Ohnishi, T. 2010. DNA damage induced by alkylating agents and repair pathways. *J Nucleic Acids.* **2010**:543531.

Konduri, S. D., Ticku, J., Bobustuc, G. C., Sutphin, R. M., Colon, J., Isley, B., Bhakat, K. K., Srivenugopal, K. S. & Baker, C. H. 2009. Blockade of MGMT expression by O6 benzyl guanine leads to inhibition of pancreatic cancer growth and induction of apoptosis. *Clin Cancer Res,* **15,** 6087-95.

Korenberg, J. R. 1991. Down syndrome phenotypic mapping. *Prog Clin Biol Res,* **373,** 43-52.

Kulling, S. E. & Metzler, M. 1997. Induction of micronuclei, DNA strand breaks and HPRT mutations in cultured Chinese hamster V79 cells by the phytoestrogen coumoestrol. *Food Chem Toxicol,* **35,** 605-13.

Kuhnle, G. G. & Bingham, S. A. 2007. Dietary meat, endogenous nitrosation and colorectal cancer.*Biochem Soc Trans.* **35(5)**:1355-7.

Kyrtopoulos, S. A. 1998. O6-Alkylguanine-DNA alkyltransferase: influence on susceptibility to the genetic effects of alkylating agents. *Toxicol Lett,* **102-103,** 53-7.

Lafleur, M. V., Woldhuis, J. & Loman, H. 1981. Alkali-labile sites in biologically active DNA: comparison of radiation induced potential breaks and apurinic sites. *Int J Radiat Biol Relat Stud Phys Chem Med,* **39,** 113-8.

Lander, E. S., Linton, L. M., Birren, B., Nusbaum, C., Zody, M. C., Baldwin, J., Devon, K., Dewar, K., Doyle, M., Fitzhugh, W., Funke, R., Gage, D., Harris, K., Heaford, A., Howland, J., Kann, L., Lehoczky, J., Levine, R., Mcewan, P., Mckernan, K., Meldrim, J., Mesirov, J. P., Miranda, C., Morris, W., Naylor, J., Raymond, C., Rosetti, M., Santos, R., Sheridan, A., Sougnez, C., Stange-Thomann, N., Stojanovic, N., Subramanian, A., Wyman, D., Rogers, J., Sulston, J., Ainscough, R., Beck, S., Bentley, D., Burton, J., Clee, C., Carter, N., Coulson, A., Deadman, R., Deloukas, P., Dunham, A., Dunham, I., Durbin, R., French, L., Grafham, D., Gregory, S., Hubbard, T., Humphray, S., Hunt, A., Jones, M., Lloyd, C., Mcmurray, A., Matthews, L., Mercer, S., Milne, S., Mullikin, J. C., Mungall, A., Plumb, R., Ross, M., Shownkeen, R., Sims, S., Waterston, R. H., Wilson, R. K., Hillier, L. W., Mcpherson, J. D., Marra, M. A., Mardis, E. R., Fulton, L. A., Chinwalla, A. T., Pepin, K. H., Gish, W. R., Chissoe, S. L., Wendl, M. C., Delehaunty, K. D., Miner, T. L., Delehaunty, A., Kramer, J. B., Cook, L. L., Fulton, R. S., Johnson,

D. L., Minx, P. J., Clifton, S. W., Hawkins, T., Branscomb, E., Predki, P., Richardson, P., Wenning, S., Slezak, T., Doggett, N., Cheng, J. F., Olsen, A., Lucas, S., Elkin, C., Uberbacher, E., Frazier, M., et al. 2001. Initial sequencing and analysis of the human genome. *Nature,* **409,** 860-921.

Lau, S. K., Fan, R. Y., Ho, T. C., Wong, G. K., Tsang, A. K., Teng, J. L., Chen, W., Watt, R. M., Curreem, S. O., Tse, H., Yuen, K. Y. & Woo, P. C. 2011. Environmental adaptability and stress tolerance of Laribacter hongkongensis: a genome-wide analysis. *Cell Biosci,* **1,** 22.

Lavon, I., Fuchs, D., Zrihan, D., Efroni, G., Zelikovitch, B., Fellig, Y. & Siegal, T. 2007. Novel mechanism whereby nuclear factor kappaB mediates DNA damage repair through regulation of O(6)-methylguanine-DNA-methyltransferase. *Cancer Res,* **67,** 8952-9.

Lawley, P. D. & Thatcher, C. J. 1970. Methylation of deoxyribonucleic acid in cultured mammalian cells by N-methyl-N'-nitro-N-nitrosoguanidine. The influence of cellular thiol concentrations on the extent of methylation and the 6-oxygen atom of guanine as a site of methylation. *Biochem J,* **116,** 693-707.

Lawley, P. D. & Thatcher, C. J. 1970. Methylation of deoxyribonucleic acid in cultured mammalian cells by N-methyl-N'-nitro-N-nitrosoguanidine. The influence of cellular thiol concentrations on the extent of methylation and the 6-oxygen atom of guanine as a site of methylation. *Biochem J,* **116,** 693-707.

Lee, S. M., Rafferty, J. A., Elder, R. H., Fan, C. Y., Bromley, M., Harris, M., Thatcher, N., Potter, P. M., Altermatt, H. J., Perinat-Frey, T. & Et Al. 1992. Immunohistological examination of the inter- and intracellular distribution of O6-alkylguanine DNA-alkyltransferase in human liver and melanoma. *Br J Cancer,* **66,** 355-60.

Lehman, A. J. & Fitzhugh, O. G. 1953. 100-fold margin of safety. . *Quarterly Bulletin of the Association of Food and Drug Officials of the US,* **18,** 33–35.

Lehman-Mckeeman, L. 2010. Paracelsus and formaldehyde 2010: the dose to the target organ makes the poison. *Toxicol Sci,* **116,** 361-3.

Lehmann, A. R., Niimi, A., Ogi, T., Brown, S., Sabbioneda, S., Wing, J. F., Kannouche, P. L. & Green, C. M. 2007. Translesion synthesis: Y-family polymerases and the polymerase switch. *DNA Repair (Amst),* **6,** 891-9.

Leonhardt, E. A., Trinh, M., Chu, K. & Dewey, W. C. 1999. Evidence that most radiation-

induced HPRT mutants are generated directly by the initial radiation exposure. *Mutat Res,* **426,** 23-30.

Lewin, M. H., Bailey, N., Bandaletova, T., Bowman, R., Cross, A. J., Pollock, J., Shuker, D. E. & Bingham, S. A. 2006. Red meat enhances the colonic formation of the DNA adduct O6-carboxymethyl guanine: implications for colorectal cancer risk. *Cancer Res.* **66(3)**:1859-65.

Lewis, P. D., Manshian, B., Routledge, M. N., Scott, G. B. & Burns, P. A. 2008. Comparison of induced and cancer-associated mutational spectra using multivariate data analysis. *Carcinogenesis,* **29,** 772-8.

Lewis, P. D. & Parry, J. M. 2002. An exploratory analysis of multiple mutation spectra. *Mutat Res,* **518,** 163-80.

Li, D., Dragan, Y., Jordan, V. C., Wang, M. & Pitot, H. C. 1997. Effects of chronic administration of tamoxifen and toremifene on DNA adducts in rat liver, kidney, and uterus. *Cancer Res,* **57,** 1438-41.

Lichtenauer-Kaligis, E. G., Thijssen, J. C., Den Dulk, H., Van De Putte, P., Giphart-Gassler, M. & Tasseron-De Jong, J. G. 1995. Spontaneous mutation spectrum in the hprt gene in human lymphoblastoid TK6 cells. *Mutagenesis,* **10,** 137-43.

Liehr, J. G. 2000a. Is estradiol a genotoxic mutagenic carcinogen? *Endocr Rev,* **21,** 40-54.

Liehr, J. G. 2000. Role of DNA adducts in hormonal carcinogenesis. *Regul Toxicol Pharmacol,* **32,** 276-82.

Lightfoot, T. J., Skibola, C. F., Willett, E. V., Skibola, D. R., Allan, J. M., Coppede, F., Adamson, P. J., Morgan, G. J., Roman, E. & Smith, M. T. 2005. Risk of non-Hodgkin lymphoma associated with polymorphisms in folate-metabolizing genes.*Cancer Epidemiol Biomarkers Prev.***14(12)**:2999-3003.

Lindahl, T. & Nyberg, B. 1972. Rate of depurination of native deoxyribonucleic acid. *Biochemistry,* **11,** 3610-8.

Lindahl, T., Sedgwick, B., Sekiguchi, M. & Nakabeppu, Y. 1988. Regulation and expression of the adaptive response to alkylating agents. *Annu Rev Biochem,* **57,** 133-57.

Ling, Y. H., Chan, J. Y., Beattie, K. L. & Nelson, J. A. 1992. Consequences of 6-thioguanine incorporation into DNA on polymerase, ligase, and endonuclease reactions. *Mol Pharmacol,* **42,** 802-7.

Lister, R., Pelizzola, M., Dowen, R. H., Hawkins, R. D., Hon, G., Tonti-Filippini, J., Nery, J. R., Lee, L., Ye, Z., Ngo, Q. M., Edsall, L., Antosiewicz-Bourget, J., Stewart, R., Ruotti, V., Millar, A. H., Thomson, J. A., Ren, B. & Ecker, J. R. 2009. Human DNA methylomes at base resolution show widespread epigenomic differences. *Nature,* **462,** 315-22.

Liu, L. & Gerson, S. L. 2006. Targeted modulation of MGMT: clinical implications. *Clin Cancer Res,* **12,** 328-31.

Liu, L., Schwartz, S., Davis, B. M. & Gerson, S. L. 2002. Chemotherapy-induced O(6)-benzylguanine-resistant alkyltransferase mutations in mismatch-deficient colon cancer. *Cancer Res,* **62,** 3070-6.

Liu, L., Schwartz, S., Davis, B. M. & Gerson, S. L. 2002. Chemotherapy-induced O(6)-benzylguanine-resistant alkyltransferase mutations in mismatch-deficient colon cancer. *Cancer Res,* **62,** 3070-6.

Liu, S. X., Cao, J., An, H., Shun, H. M., Yang, L. J. & Liu, Y. 2003. Analysis of spontaneous, gamma ray- and ethylnitrosourea-induced hprt mutants in HL-60 cells with multiplex PCR. *World J Gastroenterol,* **9,** 578-83.

Livak, K. J. & Schmittgen, T. D. 2001. Analysis of relative gene expression data using real-time quantitative PCR and the 2(-Delta Delta C(T)) Method. *Methods,* **25,** 402-8.

Loeb, K. R. & Loeb, L. A. 2000. Significance of multiple mutations in cancer. *Carcinogenesis,* **21,** 379-85.

Loeb, L. A. 1989. Endogenous carcinogenesis: molecular oncology into the twenty-first century--presidential address. *Cancer Res,* **49,** 5489-96.

Loeb, L. A. 1991. Mutator phenotype may be required for multistage carcinogenesis. *Cancer Res,* **51,** 3075-9.

Loeb, L. A. & Preston, B. D. 1986. Mutagenesis by apurinic/apyrimidinic sites. *Annu Rev Genet,* **20,** 201-30.

Loft, S., Poulsen, H. E., Vistisen, K. & Knudsen, L. E. 1999. Increased urinary excretion of 8-oxo-2'-deoxyguanosine, a biomarker of oxidative DNA damage, in urban bus drivers. *Mutat Res.* **441(1)**:11-9.

Loktionova, N. A. & Pegg, A. E. 1996. Point mutations in human O6-alkylguanine-DNA alkyltransferase prevent the sensitization by O6-benzylguanine to killing by N,N'-bis (2-chloroethyl)-N-nitrosourea. *Cancer Res,* **56,** 1578-83.

Longhi, A., Pedrali, T., Raulli, P. & Speranza, R. 1984. [Fixed mydriasis in hemorrhagic shock treated with dopamine]. *Minerva Anestesiol,* **50,** 551-3.

Lorge, E., Lambert, C., Gervais, V., Becourt-Lhote, N., Delongeas, J. L. & Claude, N. 2007. Genetic toxicity assessment: employing the best science for human safety evaluation. Part II: Performances of the in vitro micronucleus test compared to the mouse lymphoma assay and the in vitro chromosome aberration assay. *Toxicol Sci,* **96,** 214-7.

Loveless, A. 1969. Possible relevance of O-6 alkylation of deoxyguanosine to the mutagenicity and carcinogenicity of nitrosamines and nitrosamides. *Nature,* **223,** 206-7.

Lovell, D. P. 2000. Dose-response and threshold-mediated mechanisms in mutagenesis: statistical models and study design. *Mutat Res,* **464,** 87-95.

Lovett, S. T. 2007. Polymerase switching in DNA replication. *Mol Cell,* **27,** 523-6.

Lu, K., Moeller, B., Doyle-Eisele, M., Mcdonald, J. & Swenberg, J. A. 2011. Molecular dosimetry of N2-hydroxymethyl-dG DNA adducts in rats exposed to formaldehyde. *Chem Res Toxicol,* **24,** 159-61.

Ludlum, D. B. 1970. The properties of 7-methylguanine-containing templates for ribonucleic acid polymerase. *J Biol Chem,* **245,** 477-82.

Luria, S. E. & Delbruck, M. 1943. Mutations of Bacteria from Virus Sensitivity to Virus Resistance. *Genetics,* **28,** 491-511.

Lutz, W. K. 1990. Dose-response relationship and low dose extrapolation in chemical carcinogenesis. *Carcinogenesis,* **11,** 1243-7.

Lutz, W. K. 1998. Dose-response relationships in chemical carcinogenesis: superposition of different mechanisms of action, resulting in linear-nonlinear curves, practical thresholds, J-shapes. *Mutat Res,* **405,** 117-24.

Lutz, W. K. & Lutz, R. W. 2009. Statistical model to estimate a threshold dose and its confidence limits for the analysis of sublinear dose-response relationships, exemplified for mutagenicity data. *Mutat Res,* **678,** 118-22.

Lynch, A., Harvey, J., Aylott, M., Nicholas, E., Burman, M., Siddiqui, A., Walker, S. & Rees, R. 2003. Investigations into the concept of a threshold for topoisomerase inhibitor-induced clastogenicity. *Mutagenesis,* **18,** 345-53.

Lynch, A. M., Giddings, A., Custer, L., Gleason, C., Henwood, A., Aylott, M. & Kenny, J. 2011. International Pig-a gene mutation assay trial (stage III): results with N-methyl-N-

nitrosourea. *Environ Mol Mutagen,* **52,** 699-710.

Maack, C. A., Silva, M. H., Petrakis, N. L., Lee, R. E. & Lyon, M. 1986. Procarcinogen activation by rat and human mammary extracts. *Carcinogenesis,* **7,** 899-905.

Mackay, W. J., Han, S. & Samson, L. D. 1994. DNA alkylation repair limits spontaneous base substitution mutations in Escherichia coli. *J Bacteriol,* **176,** 3224-30.

Madhani, H. D., Bohr, V. A. & Hanawalt, P. C. 1986. Differential DNA repair in transcriptionally active and inactive proto-oncogenes: c-abl and c-mos. *Cell,* **45,** 417-23.

Mah, M. C., Boldt, J., Culp, S. J., Maher, V. M. & Mccormick, J. J. 1991. Replication of acetylaminofluorene-adducted plasmids in human cells: spectrum of base substitutions and evidence of excision repair. *Proc Natl Acad Sci U S A,* **88,** 10193-7.

Mallet, C. R., Lu, Z. & Mazzeo, J. R. 2004. A study of ion suppression effects in electrospray ionization from mobile phase additives and solid-phase extracts. *Rapid Commun Mass Spectrom.* **18(1)**:49-58.

Mannan, A., Liu, C., Arsenault, P. R., Towler, M. J., Vail, D. R., Lorence, A. & Weathers, P. J. 2010. DMSO triggers the generation of ROS leading to an increase in artemisinin and dihydroartemisinic acid in Artemisia annua shoot cultures. *Plant Cell Rep.* **29(2)**:143-52.

Mariyama, M., Kishi, K., Nakamura, K., Obata, H. & Nishimura, S. 1989. Frequency and types of point mutation at the 12th codon of the c-Ki-ras gene found in pancreatic cancers from Japanese patients. *Jpn J Cancer Res,* **80,** 622-6.

Marsden, D. A., Jones, D. J., Britton, R. G., Ognibene, T., Ubick, E., Johnson, G. E., Farmer, P. B. & Brown, K. 2009. Dose-response relationships for N7-(2-hydroxyethyl)guanine induced by low-dose [14C]ethylene oxide: evidence for a novel mechanism of endogenous adduct formation. *Cancer Res,* **69,** 3052-9.

Mathison, B. H., Said, B. & Shank, R. C. 1993. Effect of 5-methylcytosine as a neighboring base on methylation of DNA guanine by N-methyl-N-nitrosourea. *Carcinogenesis,* **14,** 323-7.

Mccalla, D. R., Reuvers, A. & Kitai, R. 1968. Inactivation of biologically active N-methyl-N-nitroso compounds in aqueous solution: effect of various conditions of pH and illumination. *Can J Biochem,* **46,** 807-11.

McGinniss, M. J., Falta, M. T., Sullivan, L. M. & Albertini R. J. 1990. In vivo hprt

mutant frequencies in T-cells of normal human newborns.*Mutat Res.* **240(2)**:117-26.

Mcnamee, L. M. & Brodsky, M. H. 2009. p53-independent apoptosis limits DNA damage-induced aneuploidy. *Genetics,* **182,** 423-35.

Medcalf, A. S. & Lawley, P. D. 1981. Time course of O6-methylguanine removal from DNA of N-methyl-N-nitrosourea-treated human fibroblasts. *Nature,* **289,** 796-8.

Meikrantz, W., Bergom, M. A., Memisoglu, A. & Samson, L. 1998. O6-alkylguanine DNA lesions trigger apoptosis. *Carcinogenesis,* **19,** 369-72.

Melzer, M. S., Christian, R. T., Dooley, J. F., Schumann, B., Su, H. L. & Samuels S. 1983. Mutagenicity of cyanate, a decomposition product of MNU. *Mutat Res.* **116(3-4)**:281-7.

Metzker, M. L. 2010. Sequencing technologies - the next generation. *Nat Rev Genet,* **11,** 31-46.

Mhaskar, D. N., Chang, M. J., Hart, R. W. & D'Ambrosio, S. M. 1981. Analysis of alkylated sites at N-3 and N-7 positions of purines as an indicator for chemical carcinogens. *Cancer Res.* **41(1)**:223-9.

Middlemas, D. S., Stewart, C. F., Kirstein, M. N., Poquette, C., Friedman, H. S., Houghton, P. J. & Brent, T. P. 2000. Biochemical correlates of temozolomide sensitivity in pediatric solid tumor xenograft models. *Clin Cancer Res,* **6,** 998-1007.

Mikeska, T., Bock, C., El-Maarri, O., Hubner, A., Ehrentraut, D., Schramm, J., Felsberg, J., Kahl, P., Buttner, R., Pietsch, T. & Waha, A. 2007. Optimization of quantitative MGMT promoter methylation analysis using pyrosequencing and combined bisulfite restriction analysis. *J Mol Diagn,* **9,** 368-81.

Miller, J. A. & Miller, E. C. 1971. Chemical carcinogenesis: mechanisms and approaches to its control. *J Natl Cancer Inst,* **47,** V-XIV.

Mitra, S., Pal, B. C. & Foote, R. S. 1982. O6-methylguanine-DNA methyltransferase in wild-type and ada mutants of Escherichia coli. *J Bacteriol,* **152,** 534-7.

Mittelstaedt, R. A. & Heflich, R. H. 1994. Analysis of in vivo mutation in exon 8 of the rat hprt gene. *Mutat Res,* **311,** 139-48.

Mohr, L. C., Rodgers, J. K. & Silvestri, G. A. 2003. Glutathione S-transferase M1 polymorphism and the risk of lung cancer. *Anticancer Res,* **23,** 2111-24.

Mojas, N., Lopes, M. & Jiricny, J. 2007. Mismatch repair-dependent processing of methylation

damage gives rise to persistent single-stranded gaps in newly replicated DNA. *Genes Dev,* **21,** 3342-55.

Monroe, J. J., Kort, K. L., Miller, J. E., Marino, D. R. & Skopek, T. R. 1998. A comparative study of in vivo mutation assays: analysis of hprt, lacI, cII/cI and as mutational targets for N-nitroso-N-methylurea and benzo[a]pyrene in Big Blue mice. *Mutat Res,* **421,** 121-36.

Moore, D. H., Tucker, J. D., Jones, I. M., Langlois, R. G., Pleshanov, P., Vorobtsova, I. & Jensen R. 1997. A study of the effects of exposure on cleanup workers at the Chernobyl nuclear reactor accident using multiple end points. *Radiat Res.* **148(5)**:463-75.

Moore, P. & Strauss, B. S. 1979. Sites of inhibition of in vitro DNA synthesis in carcinogen- and UV-treated phi X174 DNA. *Nature,* **278,** 664-6.

Morgan, C. & Lewis, P. D. 2006. iMARS--mutation analysis reporting software: an analysis of spontaneous cII mutation spectra. *Mutat Res,* **603,** 15-26.

Morlan, J., Baker, J. & Sinicropi, D. 2009. Mutation detection by real-time PCR: a simple, robust and highly selective method. *PLoS One,* **4,** e4584.

Morris, S. M., Aidoo, A., Chen, J. J., Chou, M. W. & Casciano, D. A. 1999. Aflatoxin B1-induced Hprt mutations in splenic lymphocytes of Fischer 344 rats. Results of an intermittent feeding trial. *Mutat Res,* **423,** 33-8.

Morris, S. M., Domon, O. E., Mcgarrity, L. J., Chen, J. J., Manjanatha, M. G., Andrews, A. M., Aidoo, A. & Casciano, D. A. 1996. A role for apoptosis in the toxicity and mutagenicity of bleomycin in AHH-1 tk+/- human lymphoblastoid cells. *Mutat Res,* **357,** 143-65.

Morris, S. M. 2002. A role for p53 in the frequency and mechanism of mutation. *Mutat Res.* **511(1)**:45-62.

Mortier, K. A., Zhang, G. F., Van Peteghem, C. H. & Lambert, W. E. 2004. Adduct formation in quantitative bioanalysis: effect of ionization conditions on paclitaxel. *J Am Soc Mass Spectrom,* **15,** 585-92.

Moschel, R. C., Mcdougall, M. G., Dolan, M. E., Stine, L. & Pegg, A. E. 1992. Structural features of substituted purine derivatives compatible with depletion of human O6-alkylguanine-DNA alkyltransferase. *J Med Chem,* **35,** 4486-91.

Mukhtar, H., Das, M., Khan, W. A., Wang, Z. Y., Bik, D. P. & Bickers, D. R. 1988. Exceptional

activity of tannic acid among naturally occurring plant phenols in protecting against 7,12-dimethylbenz(a)anthracene-, benzo(a)pyrene-, 3-methylcholanthrene-, and N-methyl-N-nitrosourea-induced skin tumorigenesis in mice. *Cancer Res,* **48,** 2361-5.

Muller, L., Mauthe, R. J., Riley, C. M., Andino, M. M., Antonis, D. D., Beels, C., Degeorge, J., De Knaep, A. G., Ellison, D., Fagerland, J. A., Frank, R., Fritschel, B., Galloway, S., Harpur, E., Humfrey, C. D., Jacks, A. S., Jagota, N., Mackinnon, J., Mohan, G., Ness, D. K., O'donovan, M. R., Smith, M. D., Vudathala, G. & Yotti, L. 2006. A rationale for determining, testing, and controlling specific impurities in pharmaceuticals that possess potential for genotoxicity. *Regul Toxicol Pharmacol,* **44,** 198-211.

Muller, L. & Singer, T. 2009. EMS in Viracept--the course of events in 2007 and 2008 from the non-clinical safety point of view. *Toxicol Lett,* **190,** 243-7.

Muller, M., Belas, F. J., Blair, I. A. & Guengerich, F. P. 1997. Analysis of 1,N2-ethenoguanine and 5,6,7,9-tetrahydro-7-hydroxy-9-oxoimidazo[1,2-a]purine in DNA treated with 2-chlorooxirane by high performance liquid chromatography/electrospray mass spectrometry and comparison of amounts to other DNA adducts. *Chem Res Toxicol,* **10,** 242-7.

Murray, K. K. 1996. DNA sequencing by mass spectrometry. *J Mass Spectrom,* **31,** 1203-15.

Mustonen, R. & Hemminki, K. 1992. 7-Methylguanine levels in DNA of smokers' and non-smokers' total white blood cells, granulocytes and lymphocytes. *Carcinogenesis,* **13,** 1951-5.

Mutagenicity, C. O. 2000.

Mutagenicity, C. O. 2011.

Nakagawachi, T., Soejima, H., Urano, T., Zhao, W., Higashimoto, K., Satoh, Y., Matsukura, S., Kudo, S., Kitajima, Y., Harada, H., Furukawa, K., Matsuzaki, H., Emi, M., Nakabeppu, Y., Miyazaki, K., Sekiguchi, M. & Mukai, T. 2003. Silencing effect of CpG island hypermethylation and histone modifications on O6-methylguanine-DNA methyltransferase (MGMT) gene expression in human cancer. *Oncogene,* **22,** 8835-44.

Nakatsuru, Y., Matsukuma, S., Nemoto, N., Sugano, H., Sekiguchi, M. & Ishikawa, T. 1993. O6-methylguanine-DNA methyltransferase protects against nitrosamine-induced hepatocarcinogenesis. *Proc Natl Acad Sci U S A,* **90,** 6468-72.

Nakatsuru, Y., Matsukuma, S., Nemoto, N., Sugano, H., Sekiguchi, M. & Ishikawa, T. 1993.

O6-methylguanine-DNA methyltransferase protects against nitrosamine-induced hepatocarcinogenesis. *Proc Natl Acad Sci U S A,* **90,** 6468-72.

Nascarella, M. A., Stanek, E. J., 3rd, Hoffmann, G. R. & Calabrese, E. J. 2009. Quantification of hormesis in anticancer-agent dose-responses. *Dose Response,* **7,** 160-71.

Natsume, A., Ishii, D., Wakabayashi, T., Tsuno, T., Hatano, H., Mizuno, M. & Yoshida, J. 2005. IFN-beta down-regulates the expression of DNA repair gene MGMT and sensitizes resistant glioma cells to temozolomide. *Cancer Res,* **65,** 7573-9.

Natsume, A., Wakabayashi, T., Ishii, D., Maruta, H., Fujii, M., Shimato, S., Ito, M. & Yoshida, J. 2008. A combination of IFN-beta and temozolomide in human glioma xenograft models: implication of p53-mediated MGMT downregulation. *Cancer Chemother Pharmacol,* **61,** 653-9.

Nehls, P. & Rajewsky, M. F. 1985. Ethylation of nucleophilic sites in DNA by N-ethyl-N-nitrosourea depends on chromatin structure and ionic strength. *Mutat Res,* **150,** 13-21.

Nelson, J. A., Carpenter, J. W., Rose, L. M. & Adamson, D. J. 1975. Mechanisms of action of 6-thioguanine, 6-mercaptopurine, and 8-azaguanine. *Cancer Res,* **35,** 2872-8.

Newcomb, E. W., Bayona, W. & Pisharody, S. 1995. N-methylnitrosourea-induced Ki-ras codon 12 mutations: early events in mouse thymic lymphomas. *Mol Carcinog,* **13,** 89-95.

Nollau, P. & Wagener, C. 1997. Methods for detection of point mutations: performance and quality assessment. IFCC Scientific Division, Committee on Molecular Biology Techniques. *Clin Chem,* **43,** 1114-28.

Nusse, M. & Egner, H. J. 1984. Can nocodazole, an inhibitor of microtubule formation, be used to synchronize mammalian cells? Accumulation of cells in mitosis studied by two parametric flow cytometry using acridine orange and by DNA distribution analysis. *Cell Tissue Kinet,* **17,** 13-23.

O'Brien, V. & Brown, R. 2006. Signalling cell cycle arrest and cell death through the MMR System. *Carcinogenesis,* **27,** 682-92.

O'connor, P. J., Manning, F. C., Gordon, A. T., Billett, M. A., Cooper, D. P., Elder, R. H. & Margison, G. P. 2000. DNA repair: kinetics and thresholds. *Toxicol Pathol,* **28,** 375-81.

O'neill, J. P. 2000. DNA damage, DNA repair, cell proliferation, and DNA replication: how do gene mutations result? *Proc Natl Acad Sci U S A,* **97,** 11137-9.

O'neill, J. P., Rogan, P. K., Cariello, N. & Nicklas, J. A. 1998. Mutations that alter RNA splicing

of the human HPRT gene: a review of the spectrum. *Mutat Res,* **411,** 179-214.

Ohshima, M. & Ward, J. M. 1986. Dietary iodine deficiency as a tumor promoter and carcinogen in male F344/NCr rats. *Cancer Res,* **46,** 877-83.

Orita, M., Iwahana, H., Kanazawa, H., Hayashi, K. & Sekiya, T. 1989. Detection of polymorphisms of human DNA by gel electrophoresis as single-strand conformation polymorphisms. *Proc Natl Acad Sci U S A,* **86,** 2766-70.

Otteneder, M. & Lutz, W. K. 1999. Correlation of DNA adduct levels with tumor incidence: carcinogenic potency of DNA adducts. *Mutat Res,* **424,** 237-47.

Pai, G. S., Sprenkle, J. A., Do, T. T., Mareni, C. E. & Migeon, B. R. 1980. Localization of loci for hypoxanthine phosphoribosyltransferase and glucose-6-phosphate dehydrogenase and biochemical evidence of nonrandom X chromosome expression from studies of a human X-autosome translocation. *Proc Natl Acad Sci U S A,* **77,** 2810-3.

Palombo F, Bignami M, Dogliotti E. 1992. Non-phenotypic selection of N-methyl-N-nitrosourea-induced mutations in human cells. *Nucleic Acids Res.* **20(6)**:1349-54.

Palombo F, Kohfeldt E, Calcagnile A, Nehls P, Dogliotti E. 1992. N-methyl-N-nitrosourea-induced mutations in human cells. Effects of the transcriptional activity of the target gene. *J Mol Biol.* **223(3)**:587-94.

Parry, J. M., Fielder, R. J. & Mcdonald, A. 1994. Thresholds for aneuploidy-inducing chemicals. Advisory Committee on Mutagenicity of Chemicals in Food, Consumer Products and the Environment of the UK Department of Health. *Mutagenesis,* **9,** 503-4.

Patel, P. I., Nussbaum, R. L., Gramson, P. E., Ledbetter, D. H., Caskey, C. T. & Chinault, A. C. 1984. Organization of the HPRT gene and related sequences in the human genome. *Somat Cell Mol Genet.* **10(5)**:483-93.

Pedrali-Noy, G., Spadari, S., Miller-Faurès, A., Miller, A. O., Kruppa, J. & Koch, G. 1980. Synchronization of HeLa cell cultures by inhibition of DNA polymerase alpha with aphidicolin. *Nucleic Acids Res.* **8(2)**:377-87.

Peek, A. S. & Behlke, M. A. 2007. Design of active small interfering RNAs. *Curr Opin Mol Ther,* **9,** 110-8.

Pegg, A. E., Boosalis, M., Samson, L., Moschel, R. C., Byers, T. L., Swenn, K. & Dolan, M. E. 1993. Mechanism of inactivation of human O6-alkylguanine-DNA alkyltransferase by O6-benzylguanine. *Biochemistry,* **32,** 11998-2006.

Pegg, A. E. & Byers, T. L. 1992. Repair of DNA containing O6-alkylguanine. *FASEB J,* **6,** 2302-10.

Perera, F. P. 1991. Perspectives on the risk assessment for nongenotoxic carcinogens and tumor promoters. *Environ Health Perspect,* **94,** 231-5.

Perin-Roussel, O., Barat, N., Zajdela, F. & Perin, F. 1997. Tissue-specific differences in adduct formation by hepatocarcinogenic and sarcomatogenic derivatives of 7H-dibenzo[c,g]carbazole in mouse parenchymal and nonparenchymal liver cells. *Environ Mol Mutagen,* 29, 346-56.

Petruzzelli, S., Tavanti, L. M., Celi, A. & Giuntini, C. 1996. Detection of N7-methyldeoxyguanosine adducts in human pulmonary alveolar cells.*Am J Respir Cell Mol Biol.* **15(2)**:216-23.

Pfaffl, M. W. 2001. A new mathematical model for relative quantification in real-time RT-PCR. *Nucleic Acids Res,* **29,** e45.

Pfuhler, S., Fellows, M., Van Benthem, J., Corvi, R., Curren, R., Dearfield, K., Fowler, P., Frotschl, R., Elhajouji, A., Le Hegarat, L., Kasamatsu, T., Kojima, H., Ouedraogo, G., Scott, A. & Speit, G. 2011. In vitro genotoxicity test approaches with better predictivity: summary of an IWGT workshop. *Mutat Res,* **723,** 101-7.

Phear, G., Armstrong, W. & Meuth, M. 1989. Molecular basis of spontaneous mutation at the aprt locus of hamster cells. *J Mol Biol,* **209,** 577-82.

Phillips, D. H., Farmer, P. B., Beland, F. A., Nath, R. G., Poirier, M. C., Reddy, M. V. & Turteltaub, K. W. 2000. Methods of DNA adduct determination and their application to testing compounds for genotoxicity. *Environ Mol Mutagen.* **35(3)**:222-33.

Pieles, U., Zurcher, W., Schar, M. & Moser, H. E. 1993. Matrix-assisted laser desorption ionization time-of-flight mass spectrometry: a powerful tool for the mass and sequence analysis of natural and modified oligonucleotides. *Nucleic Acids Res,* **21,** 3191-6.

Pieper, R. O., Costello, J. F., Kroes, R. A., Futscher, B. W., Marathi, U. & Erickson, L. C. 1991. Direct correlation between methylation status and expression of the human O-6-methylguanine DNA methyltransferase gene. *Cancer Commun,* **3,** 241-53.

Pinsky, S. D., Lee, K. E. & Woolley, P. V., 3rd 1980. Uptake and binding of 1-methyl-1-nitrosourea (MNU) and 1-methyl-3-nitro-1-nitrosoguanidine (MNNG) by the isolated

guinea pig pancreas. *Carcinogenesis,* **1,** 567-75.

Pistoia, V., Nocera, A., Ghio, R., Minale, P. & Ferrarini, M. 1982. Phytohemagglutinin or pokeweed mitogen induction of in vitro colony formation by T-cells from patients with chronic lymphocytic leukemia. *J Natl Cancer Inst,* **68,** 233-7.

Poirier, M. C. & Yuspa, S. H. 1981. Detection and quantitation of acetylated and deacetylated N-2-fluorenylacetamide-DNA adducts by radioimmunoassay. *Natl Cancer Inst Monogr,* 211-6.

Poirier, V. J., Burgess, K. E., Adams, W. M. & Vail, D. M. 2004. Toxicity, dosage, and efficacy of vinorelbine (Navelbine) in dogs with spontaneous neoplasia. *J Vet Intern Med,* **18,** 536-9.

Posnick, L. M. & Samson, L. D. 1999. Influence of S-adenosylmethionine pool size on spontaneous mutation, dam methylation, and cell growth of Escherichia coli. *J Bacteriol,* **181,** 6756-62.

Pottenger, L. H., Becker, R. A., Moran, E. J. & Swenberg, J. A. 2011. Workshop report: identifying key issues underpinning the selection of linear or non-linear dose-response extrapolation for human health risk assessment of systemic toxicants. *Regul Toxicol Pharmacol,* **59,** 503-10.

Pottenger, L. H. & Gollapudi, B. B. 2009. A case for a new paradigm in genetic toxicology testing. *Mutat Res,* **678,** 148-51.

Pottenger, L. H., Schisler, M. R., Zhang, F., Bartels, M. J., Fontaine, D. D., Mcfadden, L. G. & Gollapudi, B. 2009. Dose-response and operational thresholds/NOAELs for in vitro mutagenic effects from DNA-reactive mutagens, MMS and MNU. *Mutat Res,* **678,** 138-47.

Pozniak, A., Muller, L., Salgo, M., Jones, J. K., Larson, P. & Tweats, D. 2009. Elevated ethyl methanesulfonate (EMS) in nelfinavir mesylate (Viracept, Roche): overview. *AIDS Res Ther,* **6,** 18.

Puig, J. G., Torres, R. J., Mateos, F. A., Ramos, T. H., Arcas, J. M., Buño, A. S. & O'Neill, P. 2001. The spectrum of hypoxanthine-guanine phosphoribosyltransferase (HPRT) deficiency. Clinical experience based on 22 patients from 18 Spanish families. *Medicine (Baltimore).* **80(2)**:102-12.

Pullman, A. & Pullman, B. 1981. Molecular electrostatic potential of the nucleic acids. *Q Rev*

Biophys, **14,** 289-380.

Quinn, J. A., Jiang, S. X., Carter, J., Reardon, D. A., Desjardins, A., Vredenburgh, J. J., Rich, J. N., Gururangan, S., Friedman, A. H., Bigner, D. D., Sampson, J. H., Mclendon, R. E., Herndon, J. E., 2nd, Threatt, S. & Friedman, H. S. 2009. Phase II trial of Gliadel plus O6-benzylguanine in adults with recurrent glioblastoma multiforme. *Clin Cancer Res,* **15,** 1064-8.

Quiros, S., Roos, W. P. & Kaina, B. 2010. Processing of O6-methylguanine into DNA double-strand breaks requires two rounds of replication whereas apoptosis is also induced in subsequent cell cycles. *Cell Cycle,* **9,** 168-78.

Rabik, C. A., Njoku, M. C. & Dolan, M. E. 2006. Inactivation of O6-alkylguanine DNA alkyltransferase as a means to enhance chemotherapy. *Cancer Treat Rev,* **32,** 261-76.

Rafferty, J. A., Clarke, A. R., Sellappan, D., Koref, M. S., Frayling, I. M. & Margison, G. P. 1996. Induction of murine O6-alkylguanine-DNA-alkyltransferase in response to ionising radiation is p53 gene dose dependent. *Oncogene,* **12,** 693-7.

Randerath, K., Reddy, M. V. & Gupta, R. C. 1981. 32P-labeling test for DNA damage. *Proc Natl Acad Sci U S A,* **78,** 6126-9.

Rasimas, J. J., Pegg, A. E. & Fried, M. G. 2003. DNA-binding mechanism of O6-alkylguanine-DNA alkyltransferase. Effects of protein and DNA alkylation on complex stability. *J Biol Chem,* **278,** 7973-80.

Ratnasinghe, D., Tangrea, J. A., Andersen, M. R., Barrett, M. J., Virtamo, J., Taylor, P. R. & Albanes, D. 2000. Glutathione peroxidase codon 198 polymorphism variant increases lung cancer risk. *Cancer Res,* **60,** 6381-3.

Ravanat, J. L., Duretz, B., Guiller, A., Douki, T. & Cadet, J. 1998. Isotope dilution high-performance liquid chromatography-electrospray tandem mass spectrometry assay for the measurement of 8-oxo-7,8-dihydro-2'-deoxyguanosine in biological samples. *J Chromatogr B Biomed Sci Appl,* **715,** 349-56.

Raveh, D. & Huberman, E. 1983. A microtiter plate assay for the selection of 6-thioguanine-resistant mutants in Chinese hamster V79 cells in the presence of phorbol-12-myristate-13-acetate. *Mutat Res,* **113,** 499-506.

Razin, A. & Cedar, H. 1991. DNA methylation and gene expression. *Microbiol Rev,* **55,** 451-8.

Recio, L., Simpson, D., Cochrane, J., Liber, H. & Skopek, T. R. 1990. Molecular analysis of

hprt mutants induced by 2-cyanoethylene oxide in human lymphoblastoid cells. *Mutat Res,* **242,** 195-208.

Reinhard, J., Eichhorn, U., Wiessler, M. & Kaina, B. 2001. Inactivation of O(6)-methylguanine-DNA methyltransferase by glucose-conjugated inhibitors. *Int J Cancer,* **93,** 373-9.

Remington, M., Chtchetinin, J., Ancheta, K., Nghiemphu, P. L., Cloughesy, T. & Lai, A. 2009. The L84F polymorphic variant of human O6-methylguanine-DNA methyltransferase alters stability in U87MG glioma cells but not temozolomide sensitivity. *Neuro Oncol,* **11,** 22-32.

Rideout, W. M., 3rd, Coetzee, G. A., Olumi, A. F. & Jones, P. A. 1990. 5-Methylcytosine as an endogenous mutagen in the human LDL receptor and p53 genes. *Science,* **249,** 1288-90.

Riscoe, M. K., Brouns, M. C. & Fitchen, J. H. 1989. Purine metabolism as a target for leukemia chemotherapy. *Blood Rev,* **3,** 162-73.

Romach, E., Moore, J., Rummel, S. & Richie, E. 1994. Influence of sex and carcinogen treatment protocol on tumor latency and frequency of K-ras mutations in N-methyl-N-nitrosourea-induced lymphomas. *Carcinogenesis,* **15,** 2275-80.

Roos, W., Baumgartner, M. & Kaina, B. 2004. Apoptosis triggered by DNA damage O6-methylguanine in human lymphocytes requires DNA replication and is mediated by p53 and Fas/CD95/Apo-1. *Oncogene,* **23,** 359-67.

Roos, W. P., Nikolova, T., Quiros, S., Naumann, S. C., Kiedron, O., Zdzienicka, M. Z. & Kaina, B. 2009. Brca2/Xrcc2 dependent HR, but not NHEJ, is required for protection against O(6)-methylguanine triggered apoptosis, DSBs and chromosomal aberrations by a process leading to SCEs. *DNA Repair (Amst),* **8,** 72-86.

Roos, W. P., Nikolova, T., Quiros, S., Naumann, S. C., Kiedron, O., Zdzienicka, M. Z. & Kaina, B. 2009. Brca2/Xrcc2 dependent HR, but not NHEJ, is required for protection against O(6)-methylguanine triggered apoptosis, DSBs and chromosomal aberrations by a process leading to SCEs. *DNA Repair (Amst),* **8,** 72-86.

Rosati, S. F., Williams, R. F., Nunnally, L. C., Mcgee, M. C., Sims, T. L., Tracey, L., Zhou, J., Fan, M., Ng, C. Y., Nathwani, A. C., Stewart, C. F., Pfeffer, L. M. & Davidoff, A. M. 2008. IFN-beta sensitizes neuroblastoma to the antitumor activity of temozolomide by modulating O6-methylguanine DNA methyltransferase expression. *Mol Cancer Ther,* **7,** 3852-8.

Rossiter, B. J. & Caskey, C. T. 1995. Presymptomatic testing for genetic diseases of later life. Pharmacoepidemiological considerations. *Drugs Aging,* **7,** 117-30.

Rossiter, B. J. F. a. C., C.T. 1990. Molecular scanning methods of mutation detection *J. Biol. Chem* **265**.

Rozman, K. K. 2005. Hormesis and risk assessment. *Hum Exp Toxicol,* **24,** 255-7.

Rydberg, B. & Lindahl, T. 1982. Nonenzymatic methylation of DNA by the intracellular methyl group donor S-adenosyl-L-methionine is a potentially mutagenic reaction. *EMBO J,* **1,** 211-6.

Sandercock, L. E., Hahn, J. N., Li, L., Luchman, H. A., Giesbrecht, J. L., Peterson, L. A. & Jirik, F. R. 2008. Mgmt deficiency alters the in vivo mutational spectrum of tissues exposed to the tobacco carcinogen 4-(methylnitrosamino)-1-(3-pyridyl)-1-butanone (NNK). *Carcinogenesis,* **29,** 866-74.

Sandercock, L. E., Kwok, M. C., Luchman, H. A., Mark, S. C., Giesbrecht, J. L., Samson, L. D. & Jirik, F. R. 2004. Mutational-reporter transgenes rescued from mice lacking either Mgmt, or both Mgmt and Msh6 suggest that O6-alkylguanine-induced miscoding does not contribute to the spontaneous mutational spectrum. *Oncogene,* **23,** 5931-40.

Sandrini, J. Z., Trindade, G. S., Nery, L. E. & Marins, L. F. 2009. Time-course expression of DNA repair-related genes in hepatocytes of zebrafish (Danio rerio) after UV-B exposure. *Photochem Photobiol,* **85,** 220-6.

Schaaper, R. M., Kunkel, T. A. & Loeb, L. A. 1983. Infidelity of DNA synthesis associated with bypass of apurinic sites. *Proc Natl Acad Sci U S A,* **80,** 487-91.

Schneiderman, M. A., Decouflé, P., Brown. C. C., 1979. THRESHOLDS FOR ENVIRONMENTAL CANCER: BIOLOGIC AND STATISTICAL CONSIDERATIONS. *Annals of the New York Academy of Sciences,* **329,** 92-130.

Schorr, S., Schneider, S., Lammens, K., Hopfner, K. P. & Carell, T. 2010. Mechanism of replication blocking and bypass of Y-family polymerase {eta} by bulky acetylaminofluorene DNA adducts. *Proc Natl Acad Sci U S A,* **107,** 20720-5.

Schroering, A. G., Kothandapani, A., Patrick, S. M., Kaliyaperumal, S., Sharma, V. P. & Williams, K. J. 2009. Prolonged cell cycle response of HeLa cells to low-level alkylation exposure. *Cancer Res,* **69,** 6307-14.

Schuster, S. C. 2008. Next-generation sequencing transforms today's biology. *Nat Methods,* **5,**

16-8.

Scott, B. R. 2008. It's time for a new low-dose-radiation risk assessment paradigm--one that acknowledges hormesis. *Dose Response,* **6,** 333-51.

Seager, A. L., Shah, U. K., Mikhail, J. M., Nelson, B. C., Marquis, B. J., Doak, S. H., Johnson, G. E., Griffiths, S. M., Carmichael, P. L., Scott, S. J., Scott, A. D. & Jenkins, G. J. 2012. Pro-oxidant induced DNA damage in human lymphoblastoid cells: homeostatic mechanisms of genotoxic tolerance. *Toxicol Sci.* **128(2)**:387-97.

Sega, G. A., Wolfe, K. W. & Owens, J. G. 1981. A comparison of the molecular action of an SN1-type methylating agent, methyl nitrosourea and an SN2-type methylating agent, methyl methanesulfonate, in the germ cells of male mice. *Chem Biol Interact,* **33,** 253-69.

Seitan, V. C., Hao, B., Tachibana-Konwalski, K., Lavagnolli, T., Mira-Bontenbal, H., Brown, K. E., Teng, G., Carroll, T., Terry, A., Horan, K., Marks, H., Adams, D. J., Schatz, D. G., Aragon, L., Fisher, A. G., Krangel, M. S., Nasmyth, K. & Merkenschlager, M. 2011. A role for cohesin in T-cell-receptor rearrangement and thymocyte differentiation. *Nature,* **476,** 467-71.

Shah, N., Lin, B., Sibenaller, Z., Ryken, T., Lee, H., Yoon, J. G., Rostad, S. & Foltz, G. 2011. Comprehensive analysis of MGMT promoter methylation: correlation with MGMT expression and clinical response in GBM. *PLoS One,* **6**.

Shane, B. S., Smith-Dunn, D. L., deBoer, J. G., Glickman, B. W. & Cunningham, M. L. 2000. Subchronic administration of phenobarbital alters the mutation spectrum of lacI in the livers of Big Blue transgenic mice. *Mutat Res.* **448(1)**:69-80.

Shen, J. C., Rideout, W. M., 3rd & Jones, P. A. 1992. High frequency mutagenesis by a DNA methyltransferase. *Cell,* **71,** 1073-80.

Shen, L., Kondo, Y., Rosner, G. L., Xiao, L., Hernandez, N. S., Vilaythong, J., Houlihan, P. S., Krouse, R. S., Prasad, A. R., Einspahr, J. G., Buckmeier, J., Alberts, D. S., Hamilton, S. R. & Issa, J. P. 2005. MGMT promoter methylation and field defect in sporadic colorectal cancer. *J Natl Cancer Inst,* **97,** 1330-8.

Shibata, D. & Lieber, M. R. 2010. Is there any genetic instability in human cancer? *DNA Repair (Amst),* **9,** 858; discussion 59-60.

Shields, P. G., Povey, A. C., Wilson, V. L., Weston, A. & Harris, C. C. 1990. Combined high-performance liquid chromatography/32P-postlabeling assay of N7-methyldeoxyguanosine. *Cancer Res,* **50,** 6580-4.

Shiraishi, A., Sakumi, K. & Sekiguchi, M. 2000. Increased susceptibility to chemotherapeutic alkylating agents of mice deficient in DNA repair methyltransferase. *Carcinogenesis,* **21,** 1879-83.

Shrivastav, N., Li, D. & Essigmann, J. M. 2010. Chemical biology of mutagenesis and DNA repair: cellular responses to DNA alkylation. *Carcinogenesis,* **31,** 59-70.

Shtygasheva, A. A., Belousova, E. A., Rechkunova, N. I., Lebedeva, N. A. & Lavrik, O. I. 2008. DNA polymerases beta and lambda as potential participants of TLS during genomic DNA replication on the lagging strand. *Biochemistry (Mosc).* **73(11)**:1207-13.

Shuker, D. E. & Bartsch, H. 1994. Detection of human exposure to carcinogens by measurement of alkyl-DNA adducts using immunoaffinity clean-up in combination with gas chromatography-mass spectrometry and other methods of quantitation. *Mutat Res,* **313,** 263-8.

Shupe, T. & Sell, S. 2004. Low hepatic glutathione S-transferase and increased hepatic DNA adduction contribute to increased tumorigenicity of aflatoxin B1 in newborn and partially hepatectomized mice. *Toxicol Lett,* **148,** 1-9.

Simpson, D., Crosby, R. M. & Skopek, T. R. 1988. A method for specific cloning and sequencing of human hprt cDNA for mutation analysis. *Biochem Biophys Res Commun,* **151,** 487-92.

Singer, B. 1985. In vivo formation and persistence of modified nucleosides resulting from alkylating agents. *Environ Health Perspect,* **62,** 41-8.

Singer, B., Chavez, F., Spengler, S. J., Kusmierek, J. T., Mendelman, L. & Goodman, M. F. 1989. Comparison of polymerase insertion and extension kinetics of a series of O2-alkyldeoxythymidine triphosphates and O4-methyldeoxythymidine triphosphate. *Biochemistry,* **28,** 1478-83.

Singh, R. & Farmer, P. B. 2006. Liquid chromatography-electrospray ionization-mass spectrometry: the future of DNA adduct detection. *Carcinogenesis,* **27,** 178-96.

Singh, R., Kaur, B. & Farmer, P. B. 2005. Detection of DNA damage derived from a direct

acting ethylating agent present in cigarette smoke by use of liquid chromatography-tandem mass spectrometry. *Chem Res Toxicol,* **18,** 249-56.

Singh, R., Silva Elipe, M. V., Pearson, P. G., Arison, B. H., Wong, B. K., White, R., Yu, X., Burgey, C. S., Lin, J. H. & Baillie, T. A. 2003. Metabolic activation of a pyrazinone-containing thrombin inhibitor. Evidence for novel biotransformation involving pyrazinone ring oxidation, rearrangement, and covalent binding to proteins. *Chem Res Toxicol,* **16,** 198-207.

Sklar, R. & Strauss, B. 1981. Removal of O6-methylguanine from DNA of normal and xeroderma pigmentosum-derived lymphoblastoid lines. *Nature,* **289,** 417-20.

Skopek, T. R., Kort, K. L. & Marino, D. R. 1995. Relative sensitivity of the endogenous hprt gene and lacI transgene in ENU-treated Big Blue B6C3F1 mice. *Environ Mol Mutagen,* **26,** 9-15.

Sledziewska-Gojska, E. & Torzewska, D. 1997. Different repair of O6-methylguanine occurring in DNA modified by MMS in vivo or in vitro. *Mutat Res,* **383,** 31-7.

Sleno, L. & Volmer, D. A. 2004. Ion activation methods for tandem mass spectrometry. *J Mass Spectrom,* **39,** 1091-112.

Slob, W. 1999. Thresholds in Toxicology and Risk Assessment. *International Journal of Toxicology,* **18,** 259-68.

Song, F. 2011. "Cross-talk" in scheduled multiple reaction monitoring caused by in-source fragmentation in herbicide screening with liquid chromatography electrospray tandem mass spectrometry. *J Agric Food Chem,* **59,** 4361-4.

Sonich-Mullin C, F. R., Wiltse J, Baetcke K, Dempsey J, Fenner-Crisp P, Grant D, Hartley M, Knaap a, Kroese D, Mangelsdorf I, Meek E, Rice Jm, Younes M; 2001. IPCS conceptual framework for evaluating a mode of action for chemical carcinogenesis. *Regul Toxicol Pharmacol.,* **34,** 146-52.

Sorg, U. R., Kleff, V., Fanaei, S., Schumann, A., Moellmann, M., Opalka, B., Thomale, J. & Moritz, T. 2007. O6-methylguanine-DNA-methyltransferase (MGMT) gene therapy targeting haematopoietic stem cells: studies addressing safety issues. *DNA Repair (Amst),* **6,** 1197-209.

Souliotis, V. L., Boussiotis, V. A., Pangalis, G. A. & Kyrtopoulos, S. A. 1991. In vivo formation and repair of O6-methylguanine in human leukocyte DNA after intravenous exposure to

dacarbazine. *Carcinogenesis,* **12,** 285-8.

Souliotis, V. L. & Kyrtopoulos, S. A. 1989. A novel, sensitive assay for O6-methyl- and O6-ethylguanine in DNA, based on repair by the enzyme O6-alkylguanine-DNA-alkyltransferase in competition with an oligonucleotide containing O6-methylguanine. *Cancer Res,* **49,** 6997-7001.

Souliotis, V. L., Valavanis, C., Boussiotis, V. A., Pangalis, G. A. & Kyrtopoulos, S. A. 1996. Comparative study of the formation and repair of O6-methylguanine in humans and rodents treated with dacarbazine. *Carcinogenesis,* **17,** 725-32.

Speit G, A. H., Crebelli R, Henderson L, Kirsch-Volders M, Madle S, Parry Jm, Sarrif Am, Vrijhof H. 2000. Thresholds in genetic toxicology - concluding remarks. *Mutat Res,* **464,** 149-53.

Spratt, T. E., Zydowsky, T. M. & Floss, H. G. 1997. Stereochemistry of the in vitro and in vivo methylation of DNA by (R)- and (S)-N-[2H1,3H]methyl-N-nitrosourea and (R)- and (S)-N-nitroso-N-[2H1,3H]methyl-N-methylamine. *Chem Res Toxicol,* **10,** 1412-9.

Srivenugopal, K. S., Yuan, X. H., Friedman, H. S. & Ali-Osman, F. 1996. Ubiquitination-dependent proteolysis of O6-methylguanine-DNA methyltransferase in human and murine tumor cells following inactivation with O6-benzylguanine or 1,3-bis(2-chloroethyl)-1-nitrosourea. *Biochemistry,* **35,** 1328-34.

Steen, A. M., Meyer, K. G. & Recio L. 1997. Characterization of hprt mutations following 1,2-epoxy-3-butene exposure of human TK6 cells. *Mutagenesis.* **12(5)**:359-64.

Stefanov, B., Ribarov, S., Kainakchieva, R., Georgieva, I. & Benchev, I. 1982. [Effect of tocopherol on the hematological indices in lead poisoning]. *Gig Sanit,* 64-5.

Stern, S. J., Degawa, M., Martin, M. V., Guengerich, F. P., Kaderlik, R. K., Ilett, K. F., Breau, R., Mcghee, M., Montague, D., Lyn-Cook, B. & Et Al. 1993. Metabolic activation, DNA adducts, and H-ras mutations in human neoplastic and non-neoplastic laryngeal tissue. *J Cell Biochem Suppl,* **17F,** 129-37.

Stout, J. T. & Caskey, C. T. 1985. HPRT: gene structure, expression, and mutation. *Annu Rev Genet.* **19**:127-48.

Strickland, P. T. & Boyle, J. M. 1984. Immunoassay of carcinogen-modified DNA. *Prog Nucleic Acid Res Mol Biol,* **31,** 1-58.

Su, X., Robelek, R., Wu, Y., Wang, G. & Knoll, W. 2004. Detection of point mutation and

insertion mutations in DNA using a quartz crystal microbalance and MutS, a mismatch binding protein. *Anal Chem,* **76,** 489-94.

Sukumar, S. 1989. ras oncogenes in chemical carcinogenesis. *Curr Top Microbiol Immunol,* **148,** 93-114.

Sussman, H. E., Olivero, O. A., Meng, Q., Pietras, S. M., Poirier, M. C., O'Neill, J. P., Finette, B. A., Bauer, M. J. & Walker, V. E. 1999. Genotoxicity of 3'-azido-3'-deoxythymidine in the human lymphoblastoid cell line, TK6: relationships between DNA incorporation, mutant frequency, and spectrum of deletion mutations in HPRT.*Mutat Res.* **429(2)**:249-59.

Suter, W., Brennand, J., Mcmillan, S. & Fox, M. 1980. Relative mutagenicity of antineoplastic drugs and other alkylating agents in V79 Chinese hamster cells, independence of cytotoxic and mutagenic responses. *Mutat Res,* **73,** 171-81.

Suzen, S., Jenkins, G. J. & Parry, J. M. 1998. Application of the restriction site mutation technique to N-methyl-N-nitrosourea-induced mutations in the rat. *Teratog Carcinog Mutagen,* **18,** 171-82.

Swain, G. C., Scott. B.C. 1953. Quantitative Correlation of Relative Rates. Comparison of Hydroxide Ion with Other Nucleophilic Reagents toward Alkyl Halides, Esters, Epoxides and Acyl Halides. *J. Am. Chem. Soc,* **75,** 141-7.

Swann, P. F. 1968. The rate of breakdown of methyl methanesulphonate, dimethyl sulphate and N-methyl-N-nitrosourea in the rat. *Biochem J,* **110,** 49-52.

Swann, P. F. & Magee, P. N. 1968. Nitrosamine-induced carcinogenesis. The alklylation of nucleic acids of the rat by N-methyl-N-nitrosourea, dimethylnitrosamine, dimethyl sulphate and methyl methanesulphonate. *Biochem J,* **110,** 39-47.

Swenberg, J. A., Koestner, A., Wechsler, W., Brunden, M. N. & Abe, H. 1975. Differential oncogenic effects of methylnitrosourea. *J Natl Cancer Inst,* **54,** 89-96.

Swenberg, J. A., La, D. K., Scheller, N. A. & Wu, K. Y. 1995. Dose-response relationships for carcinogens. *Toxicol Lett,* **82-83,** 751-6.

Swenberg, J. A., Lu, K., Moeller, B. C., Gao, L., Upton, P. B., Nakamura, J. & Starr, T. B. 2011. Endogenous versus exogenous DNA adducts: their role in carcinogenesis, epidemiology, and risk assessment. *Toxicol Sci,* **120 Suppl 1,** S130-45.

Swenberg, J. A., Richardson, F. C., Boucheron, J. A., Deal, F. H., Belinsky, S. A., Charbonneau,

M. & Short, B. G. 1987. High- to low-dose extrapolation: critical determinants involved in the dose response of carcinogenic substances. *Environ Health Perspect,* **76,** 57-63.

Swenberg JA, Fryar-Tita E, Jeong YC, Boysen G, Starr T, Walker VE, Albertini RJ. 2008. Biomarkers in toxicology and risk assessment: informing critical dose-response relationships.*Chem Res Toxicol.* **21(1)**:253-65.

Swenson, D. H. & Lawley, P. D. 1978. Alkylation of deoxyribonucleic acid by carcinogens dimethyl sulphate, ethyl methanesulphonate, N-ethyl-N-nitrosourea and N-methyl-N-nitrosourea. Relative reactivity of the phosphodiester site thymidylyl(3'-5')thymidine. *Biochem J,* **171,** 575-87.

Talaska, G., Jaeger, M., Reilman, R., Collins, T. & Warshawsky, D. 1996. Chronic, topical exposure to benzo[a]pyrene induces relatively high steady-state levels of DNA adducts in target tissues and alters kinetics of adduct loss. *Proc Natl Acad Sci U S A,* **93,** 7789-93.

Talaska, G., Jaeger, M., Reilman, R., Collins, T. & Warshawsky, D. 1996. Chronic, topical exposure to benzo[a]pyrene induces relatively high steady-state levels of DNA adducts in target tissues and alters kinetics of adduct loss. *Proc Natl Acad Sci U S A,* **93,** 7789-93.

Tano, K., Shiota, S., Collier, J., Foote, R. S. & Mitra, S. 1990. Isolation and structural characterization of a cDNA clone encoding the human DNA repair protein for O6-alkylguanine. *Proc Natl Acad Sci U S A,* **87,** 686-90.

Teng, Y., Bennett, M., Evans, K. E., Zhuang-Jackson, H., Higgs, A., Reed, S. H. & Waters, R. 2011. A novel method for the genome-wide high resolution analysis of DNA damage. *Nucleic Acids Res,* **39,** e10.

Tennant, R. W. 1987. Issues in biochemical applications to risk assessment: are short-term tests predictive of in vivo tumorigenicity? *Environ Health Perspect,* **76,** 163-7.

Terry, M. B., Gammon, M. D., Zhang, F. F., Eng, S. M., Sagiv, S. K., Paykin, A. B., Wang, Q., Hayes, S., Teitelbaum, S. L., Neugut, A. I. & Santella, R. M. 2004. Polymorphism in the DNA repair gene XPD, polycyclic aromatic hydrocarbon-DNA adducts, cigarette smoking, and breast cancer risk. *Cancer Epidemiol Biomarkers Prev,* **13,** 2053-8.

Thybaud, V., Aardema, M., Casciano, D., Dellarco, V., Embry, M. R., Gollapudi, B. B., Hayashi, M., Holsapple, M. P., Jacobson-Kram, D., Kasper, P., Macgregor, J. T. & Rees,

R. 2007. Relevance and follow-up of positive results in in vitro genetic toxicity assays: an ILSI-HESI initiative. *Mutat Res,* **633,** 67-79.

Tippin, B., Pham, P. & Goodman, M. F. 2004. Error-prone replication for better or worse. *Trends Microbiol,* **12,** 288-95.

Tomita-Mitchell, A., Ling, L. L., Glover, C. L., Goodluck-Griffith, J. & Thilly, W. G. 2003. The mutational spectrum of the HPRT gene from human T cells in vivo shares a significant concordant set of hot spots with MNNG-treated human cells. *Cancer Res,* **63,** 5793-8.

Tomita-Mitchell, A., Ling, L. L., Glover, C. L., Goodluck-Griffith, J. & Thilly, W. G. 2003. The mutational spectrum of the HPRT gene from human T cells in vivo shares a significant concordant set of hot spots with MNNG-treated human cells. *Cancer Res,* **63,** 5793-8.

Tong, C., Fazio, M. & Williams, G. M. 1980. Cell cycle-specific mutagenesis at the hypoxanthine phosphoribosyltransferase locus in adult rat liver epithelial cells. *Proc Natl Acad Sci U S A,* **77,** 7377-9.

Tornqvist, M. 1988. Search for unknown adducts: increase of sensitivity through preselection by biochemical parameters. *IARC Sci Publ,* 378-83.

Tosal, L., Comendador, M. A. & Sierra, L. M. 1998. N-ethyl-N-nitrosourea predominantly induces mutations at AT base pairs in pre-meiotic germ cells of Drosophila males. *Mutagenesis,* **13,** 375-80.

Trezl, L., Park, K. S., Kim, S. & Paik, W. K. 1987. Studies on in vitro S-methylation of naturally occurring thiol compounds with N-methyl-N-nitrosourea and methyl methanesulfonate. *Environ Res,* **43,** 417-26.

Tricker, A. R. 1997. N-nitroso compounds and man: sources of exposure, endogenous formation and occurrence in body fluids. *Eur J Cancer Prev,* **6,** 226-68.

Tsubura, A., Lai, Y. C., Miki, H., Sasaki, T., Uehara, N., Yuri, T. & Yoshizawa, K. 2011. Review: Animal models of N-Methyl-N-nitrosourea-induced mammary cancer and retinal degeneration with special emphasis on therapeutic trials. *In Vivo,* **25,** 11-22.

Tsurusawa, M., Niwa, M., Katano, N. & Fujimoto, T. 1990. Methotrexate cytotoxicity as related to irreversible S phase arrest in mouse L1210 leukemia cells. *Jpn J Cancer Res,* **81,** 85-90.

Tsuzuki, T., Sakumi, K., Shiraishi, A., Kawate, H., Igarashi, H., Iwakuma, T., Tominaga, Y., Zhang, S., Shimizu, S. & Ishikawa, T. 1996. Targeted disruption of the DNA repair

methyltransferase gene renders mice hypersensitive to alkylating agent. *Carcinogenesis,* **17,** 1215-20.

Tubiana, M., Feinendegen, L. E., Yang, C. & Kaminski, J. M. 2009. The linear no-threshold relationship is inconsistent with radiation biologic and experimental data. *Radiology,* **251,** 13-22.

Tudek, B., Boiteux, S. & Laval, J. 1992. Biological properties of imidazole ring-opened N7-methylguanine in M13mp18 phage DNA. *Nucleic Acids Res,* **20,** 3079-84.

Turteltaub, K. W., Felton, J. S., Gledhill, B. L., Vogel, J. S., Southon, J. R., Caffee, M. W., Finkel, R. C., Nelson, D. E., Proctor, I. D. & Davis, J. C. 1990. Accelerator mass spectrometry in biomedical dosimetry: relationship between low-level exposure and covalent binding of heterocyclic amine carcinogens to DNA. *Proc Natl Acad Sci U S A,* **87,** 5288-92.

Tweats, D. J., Scott, A. D., Westmoreland, C. & Carmichael, P. L. 2007. Determination of genetic toxicity and potential carcinogenicity in vitro--challenges post the Seventh Amendment to the European Cosmetics Directive. *Mutagenesis,* **22,** 5-13.

Ueno, T., Ko, S. H., Grubbs, E., Yoshimoto, Y., Augustine, C., Abdel-Wahab, Z., Cheng, T. Y., Abdel-Wahab, O. I., Pruitt, S. K., Friedman, H. S. & Tyler, D. S. 2006. Modulation of chemotherapy resistance in regional therapy: a novel therapeutic approach to advanced extremity melanoma using intra-arterial temozolomide in combination with systemic O6-benzylguanine. *Mol Cancer Ther,* **5,** 732-8.

Ugazio, G., Koch, R. R. & Recknagel, R. O. 1972. Mechanism of protection against carbon tetrachloride by prior carbon tetrachloride administration. *Exp Mol Pathol,* **16,** 281-5.

Van Diggelen, O. P., Donahue, T. F. & Shin, S. I. 1979. Basis for differential cellular sensitivity to 8-azaguanine and 6-thioguanine. *J Cell Physiol,* **98,** 59-71.

Van Zeeland, A. A., De Groot, A. J., Mohn, G. R., Van Steeg, H., Van Oostrom, C., Van Duijn-Goedhart, A. M., Mullenders, L. F. & Jansen, J. G. 2008. Reduced methylation-induced mutagenesis in rat splenocytes in vivo by sub-chronic low dose exposure to N-metyl-N-nitrosourea. *Mutat Res,* **640,** 131-8.

Van Zeeland, A. A., Mohn, G. R., Mullenders, L. H., Natarajan, A. T., Nivard, M., Simons, J. W., Venema, J., Vogel, E. W., Vrieling, H., Zdzienicka, M. Z. & Et Al. 1989. Relationship between DNA-adduct formation, DNA repair, mutation frequency and

mutation spectra. *Ann Ist Super Sanita,* **25,** 223-8.

Verbeek, B., Southgate, T. D., Gilham, D. E. & Margison, G. P. 2008. O6-Methylguanine-DNA methyltransferase inactivation and chemotherapy. *Br Med Bull,* **85,** 17-33.

Vernole, P., Pepponi, R. & D'atri, S. 2003. Role of mismatch repair in the induction of chromosomal aberrations and sister chromatid exchanges in cells treated with different chemotherapeutic agents. *Cancer Chemother Pharmacol,* **52,** 185-92.

Vickers, T. J., Murta, S. M., Mandell, M. A. & Beverley, S. M. 2009. The enzymes of the 10-formyl-tetrahydrofolate synthetic pathway are found exclusively in the cytosol of the trypanosomatid parasite Leishmania major. *Mol Biochem Parasitol.* **166(2)**:142-52.

Villani, G., Hubscher, U., Gironis, N., Parkkinen, S., Pospiech, H., Shevelev, I., Di Cicco, G., Markkanen, E., Syvaoja, J. E. & Tanguy Le Gac, N. 2011. In vitro gap-directed translesion DNA synthesis of an abasic site involving human DNA polymerases epsilon, lambda, and beta. *J Biol Chem,* **286,** 32094-104.

Vos, J. M. & Rommelaere, J. 1987. Replication of DNA containing apurinic sites in human and mouse cells probed with parvoviruses MVM and H-1. *Mol Cell Biol,* **7,** 2620-4.

Waddell, W. J. 2005. Dose thresholds should exist for chemical carcinogens. *Toxicol Sci,* **85,** 1064-5.

Waddell, W. J., Fukushima, S. & Williams, G. M. 2006. Concordance of thresholds for carcinogenicity of N-nitrosodiethylamine. *Arch Toxicol,* **80,** 305-9.

Wagner, L. M., Mclendon, R. E., Yoon, K. J., Weiss, B. D., Billups, C. A. & Danks, M. K. 2007. Targeting methylguanine-DNA methyltransferase in the treatment of neuroblastoma. *Clin Cancer Res,* **13,** 5418-25.

Walder, L. & Lutzelschwab, R. 1984. Effects of 12-O-tetradecanoylphorbol-13-acetate (TPA), retinoic acid and diazepam on intercellular communication in a monolayer of rat liver epithelial cells. *Exp Cell Res,* **152,** 66-76.

Walmsley, R. M. 2008. GADD45a-GFP GreenScreen HC genotoxicity screening assay. *Expert Opin Drug Metab Toxicol,* **4,** 827-35.

Warren, W., Crathorn, A. R. & Shooter, K. V. 1979. The stability of methylated purines and of methylphosphotriesters in the DNA of V79 cells after treatment with N-methyl-N-nitrosourea. *Biochim Biophys Acta,* **563,** 82-8.

Wedge, S. R. & Newlands, E. S. 1996. O6-benzylguanine enhances the sensitivity of a glioma xenograft with low O6-alkylguanine-DNA alkyltransferase activity to temozolomide and BCNU. *Br J Cancer,* **73,** 1049-52.

Wedge, S. R., Porteous, J. K. & Newlands, E. S. 1997. Effect of single and multiple administration of an O6-benzylguanine/temozolomide combination: an evaluation in a human melanoma xenograft model. *Cancer Chemother Pharmacol,* **40,** 266-72.

Williams, M., Rainville, I. R. & Nicklas, J. A. 2002. Use of inverse PCR to amplify and sequence breakpoints of HPRT deletion and translocation mutations. *Environ Mol Mutagen,* **39,** 22-32.

Wirtz, S., Nagel, G., Eshkind, L., Neurath, M. F., Samson, L. D. & Kaina, B. 2010. Both base excision repair and O6-methylguanine-DNA methyltransferase protect against methylation-induced colon carcinogenesis. *Carcinogenesis,* **31,** 2111-7.

Wiseman, H. & Halliwell, B. 1996. Damage to DNA by reactive oxygen and nitrogen species: role in inflammatory disease and progression to cancer. *Biochem J,* **313 (Pt 1),** 17-29.

Winter, J., Nyskohus, L., Young, G. P., Hu, Y., Conlon, M. A., Bird, A. R., Topping, D. L., Le, Leu, R. K. 2011. Inhibition by resistant starch of red meat-induced promutagenic adducts in mouse colon. *Cancer Prev Res (Phila).* **4(11)**:1920-8.

Whitwell J, Fowler P, Allars S, Jenner K, Lloyd M, Wood D, Smith K, Young J, Jeffrey L, Kirkland D. 2010. 2-Aminoanthracene, 5-fluorouracil, colchicine, benzo[a]pyrene, cadmium chloride and cytosine arabinoside tested in the in vitro mammalian cell micronucleus test (MNvit) in Chinese hamster ovary (CHO) cells at Covance Laboratories, Harrogate UK in support of OECD draft Test Guideline 487.*Mutat Res* **702(2)**:237-47.

Wogan, G. N., Hecht, S. S., Felton, J. S., Conney, A. H. & Loeb, L. A. 2004. Environmental and chemical carcinogenesis. *Semin Cancer Biol,* **14,** 473-86.

Wood, D. A. 1969. New concepts in cancer control. Preventable and avoidable cancer. *Calif Med,* **111,** 313-6.

Woolley, P. V., 3rd & Pinsky, S. D. 1981. Binding of N-nitroso carcinogens in pancreatic tissue. *Cancer,* **47,** 1485-9.

Xiao, W. & Samson, L. 1993. In vivo evidence for endogenous DNA alkylation damage as a source of spontaneous mutation in eukaryotic cells. *Proc Natl Acad Sci U S A,* **90,** 2117-

21.

Xu-Welliver, M. & Pegg, A. E. 2000. Point mutations at multiple sites including highly conserved amino acids maintain activity, but render O6-alkylguanine-DNA alkyltransferase insensitive to O6-benzylguanine. *Biochem J,* **347,** 519-26.

Xu-Welliver, M. & Pegg, A. E. 2002. Degradation of the alkylated form of the DNA repair protein, O(6)-alkylguanine-DNA alkyltransferase. *Carcinogenesis,* **23,** 823-30.

Yan, T., Berry, S. E., Desai, A. B. & Kinsella, T. J. 2003. DNA mismatch repair (MMR) mediates 6-thioguanine genotoxicity by introducing single-strand breaks to signal a G2-M arrest in MMR-proficient RKO cells. *Clin Cancer Res,* **9,** 2327-34.

Yang, J. L., Lee, P. C., Lin, S. R. & Lin, J. G. 1994. Comparison of mutation spectra induced by N-ethyl-N-nitrosourea in the hprt gene of Mer+ and Mer- diploid human fibroblasts. *Carcinogenesis,* **15,** 939-45.

Yang, T. P., Stout, J. T., Konecki, D. S., Patel, P. I., Alford, R. L. & Caskey, C. T. 1988. Spontaneous reversion of novel Lesch-Nyhan mutation by HPRT gene rearrangement. *Somat Cell Mol Genet,* **14,** 293-303.

Yu, Z. W. & Quinn, P. J. 1994. Dimethyl sulphoxide: a review of its applications in cell biology. *Biosci Rep.* **14(6)**:259-81.

Yoshioka, K., Yoshioka, Y. & Hsieh, P. 2006. ATR kinase activation mediated by MutSalpha and MutLalpha in response to cytotoxic O6-methylguanine adducts. *Mol Cell,* **22,** 501-10.

Zaidi, N. H., Liu, L. & Gerson, S. L. 1996. Quantitative immunohistochemical estimates of O6-alkylguanine-DNA alkyltransferase expression in normal and malignant human colon. *Clin Cancer Res,* **2,** 577-84.

Zair, Z. M., Jenkins, G. J., Doak, S. H., Singh, R., Brown, K. & Johnson, G. E. 2011. N-methylpurine DNA glycosylase plays a pivotal role in the threshold response of ethyl methanesulfonate-induced chromosome damage. *Toxicol Sci,* **119,** 346-58.

Zhang, L. H. & Jenssen, D. 1991. Site specificity of N-methyl-N-nitrosourea-induced transition mutations in the hprt gene. *Carcinogenesis,* **12,** 1903-9.

Zhang, L. H., Vrieling, H., Van Zeeland, A. A. & Jenssen, D. 1992. Spectrum of spontaneously occurring mutations in the hprt gene of V79 Chinese hamster cells. *J Mol Biol,* **223,** 627-35.

Zhao, C., Georgellis, A., Flato, S., Palmberg, L., Thunberg, E. & Hemminki, K. 1997. DNA adducts in human nasal mucosa and white blood cells from smokers and non-smokers. *Carcinogenesis.* **18(11)**:2205-8.

Zhen, W., Evans, M. K., Haggerty, C. M. & Bohr, V. A. 1993. Deficient gene specific repair of cisplatin-induced lesions in Xeroderma pigmentosum and Fanconi's anemia cell lines. *Carcinogenesis,* **14,** 919-24.

Zito, R. 2001. Low doses and thresholds in genotoxicity: from theories to experiments. *J Exp Clin Cancer Res,* **20,** 315-25.